7.º CONGRESO INTERNACIONAL DE CORROSIÓN MARINA E INCRUSTACIONES

7th INTERNATIONAL CONGRESS ON MARINE CORROSION AND FOULING

7ème CONGRES INTERNATIONAL DE LA CORROSION MARINE ET DES SALISSURES

UNIVERSIDAD POLITÉCNICA
Valencia, 7-11 Noviembre, 1988
ESPAÑA

SECCIÓN I

Corrosión marina
Corrosion marine
Corrosion marine

The unpublished manuscripts have been reproduced as received from the authors. The Scientific Committee takes not responsability for any error or omission.

Las ponencias no han sido publicadas y están reproducidas tal y como se han recibido de sus autores. El Comité Científico no se responsabiliza de cualquier error u omisión.

SESSION I Corrosion Marine
Thursday 10th November

CORROSION DE ARMADURAS EN HORMIGONES EN CONTACTO CON AGUA DE MAR:
EL EFECTO DE LA GALVANIZACION Y EL USO DE NITRITOS COMO INHIBIDOR
C Andrade, C Alonso, S Goni and J A Gonzalez

COMPORTAMIENTO FRENTE A LA CORROSION MARINA DE RECUBRIMIENTOS DE NIQUEL DEPOSITADO POR VIA QUIMICA Y POR VIA ELECTROLITICA
E Julve

COMPORTAMIENTO ELECTROQUIMICO DE UNA ALEACION Cu:Ni EN AGUA DE MAR CONTAMINADA CON SULFUROS
Maria del Carmen Leiro and Bianca M Rosales

USO DE LAMINAS DE FLUORURO DE POLIVINILO APLICADAS EN FRIO PARA LA PROTECCION SUPERFICIAL DE ACEROS AL CARBONO EN AMBIENTES MARINOS
P Merino, X R Novoa, M Izquierdo and L Espada

COMPORTEMENT DE QUELQUES ALLIAGES CU-ZN A LA CORROSION
Emanuele D Mor

PROTECCION CATODICA DEL INTERIOR DE UNSISTEMA DE TUBERIAS DE AGUA DE REFRIGERACION
J Ladera, E Cucarella and M A Guillen

PINTURA MARINAS PARA BUQUES. RESULTADOS DE INVESTIGACIONES
M Morcillo, S Gimenez, J Simancas, J Antunano and A Monje

OBSERVATIONS ON THE CATHODIC PROTECTION OF STEEL IN BIOLOGICALLY ACTIVE SEAWATER
R G J Edyvean, C J Hutchinson and N J Silk

A CONTRIBUTION TO THE DEFINITION OF A QUALIFICATION PROCEDURE FOR APPLICATION OF STAINLESS STEELS IN SEAWATER
J M Krougman and F P IJaseling

THE CORROSION AND PROTECTION OF STEEL PIPE PILES IN NATURAL SEAWATER
Kiyoshi Katawaki, Tatsuo Asama and Kazuyuki Doi

A COMPARATIVE STUDY OF THE CuNi30Fe ELECTROCHEMICAL BEHAVIOUR IN SEA WATER AND DIFFERENT CHOLORIDE SALINE SOLUTION TO ASSESS THE EFFECT OF MICROFOULING SETTLEMENT
M F L de Mele, G Brankevich and M A Videla

CORROSION DE ARMADURAS EN HORMIGONES EN CONTACTO CON AGUA DE MAR: EL EFECTO DE LA GALVANIZACION Y EL USO DE NITRITOS COMO INHIBIDOR.

C. Andrade, C. Alonso, S. Goñi (Instituto "Eduardo Torroja" de la Construcción y del Cemento del CSIC - Madrid - España)

y J.A. González (Centro Nacional de Investigaciones Metalúrgicas del CSIC - Madrid - España).

ABSTRACT

In marine environments, chlorides penetrate into concrete structures generating the corrosion of reinforcements. In this paper results up to 5,5 years are presented on corrosion rates of reinforcements (measured by means of Polarization Resistance technique) embedded in different concrete qualites and with 0,5-1,5-2,5-4 and 7,5 cm of cover, immersed in natural sea water. Galvanized rebars and $NaNO_2$ were also used as suplementary protection method.

INTRODUCCION

El ataque de las armaduras de hormigones situados en ambientes marinos es conocido desde hace muchos años, si bien los costos de las reparaciones no eran tan preocupantes como en la actualidad, en la que ha aumentado espectacularmente el parque construído en las zonas costeras en los últimos 30 años.

Las medidas de protección preventiva para evitar deterioros prematuros, cuando se han tomado, han incidido generalmente en una mejora de la calidad del bormigón (1) (2) (3) (4) y del recubrimiento de las armaduras, así como en un control más severo de las reglas de cálculo para reducir la anchura de las fisuras. Sin embargo, aún en hormigones de buena calidad, cuando el hormigón está en medios marinos, es sólo cuestión de tiempo que los cloruros alcancen la armadura y ésta comience a corroerse (5), por lo que es necesario investigar sobre métodos de protección adicionales que permitan alargar todavía más la vida en servicio de aquellos tipos de estructuras cuyo costo relativo de construcción lo haga aconsejable.

Varios son los métodos de protección adicional que se pueden utilizar contra la corrosión de las armaduras, y muchos son los trabajos que se publican en la actualidad (6) (7) (8), debido a las implicaciones económicas de las reparaciones. En el presente trabajo dos son los métodos que se comparan: galvanización de armaduras y empleo de nitrito sódico como inhibidor añadido al agua de amasado.

TECNICA EXPERIMENTAL

Materiales

Para los ensayos se fabricaron probetas de hormigón de 15 x 20 x 10 cm de dimensiones, que tenían embebidos redondos de 8 mm de diámetro, con espesores de recubrimiento de: 0,5-1,5-2,5-4 y 7,5 cm. La probeta se muestra en la fotografía nº 1 y en el esquema de la figura 2. Para forzar a que el agua de mar penetre sólo por las superficies anterior y posterior (la distancia de los paramentos laterales a las armaduras es de 2,5 cm) se recubrieron las superficies laterales, superior e inferior, con una resina epoxi y luego con una capa de cera vegetal. De esta forma la penetración de los cloruros sólo es posible por las dos superficies extremas de la probeta.

Los redondos que se embebieron fueron protegidos con una cinta aislante en su extremo inferior y en la zona de interfase hormigón/aire, de tal forma que el área expuesta al ataque fue de 23 cm^2.

El hormigón se fabricó con dos proporciones de cemento en kg por m^3 de hormigón de 300 y 400 kg/m^3. Cada una de estas dosificaciones se amasó con dos relaciones de a/c de tal forma que el escurrimiento en el cono de Abrams fue de 1 cm y 14-15 cm. En el caso en que se añadió el inhibidor al agua de amasado se utilizó un 2% de $NaNO_2$ en relación al peso de cemento en el caso de la dosificación menos fluída (2 cm de cono) y con 300 y 400 kg de cemento/m^3 de hormigón.

En el caso de las armaduras galvanizadas, el galvanizado se realizó por inmersión en caliente a 450°C, obteniéndose una capa de grosor variable entre 60 y 100 µm. De las dos series de armaduras que contenía cada probeta, una se ensayó galvanizada y la otra de acero desnudo.

Todas las variables se ensayaron por duplicado, de tal forma que los valores que se expresan en los gráficos son la media aritmética de 2 ó 4 medidas (probetas con nitritos).

Las probetas, una vez fabricadas, se curaron durante 60 días, pasados los cuales se introdujeron en agua dulce durante unos 15 días más y cuando ya se encontraban saturadas de agua se introdujeron hasta 3-4 cm de su borde superior en agua de mar natural en una balsa de conservación situada en el Instituto de Ciencias del Mar de Barcelona, perteneciente al CSIC.

La salinidad media del agua es de 38 gr/l, la temperatura oscila entre 14°C en invierno y 24°C en verano, y el contenido medio de oxígeno es de 5 ppm. El agua se renueva todos los meses.

Técnica de medida

Para seguir la evolución de la velocidad de corrosión con el tiempo, se utilizó en todos los casos la determinación de la Resistencia de Polarización, R_p. La intensidad de corrosión, I_{corr}, se calculó mediante la fórmula de Stern, al igual que en anteriores trabajos (9), utilizando un valor de la constante B de 26 mV. Los potenciales se midieron en todos los casos frente a un electrodo de calomelanos saturado.

RESULTADOS

En las figuras 3 y 4 se muestran unos ejemplos de la evolución de los potenciales de corrosión y de la intensidad de corrosión de aceros desnudos para los casos de 300 y 400 kg/m^3 de hormigón de consistencia fluída. En los gráficos sólo se muestran los resultados para recubrimientos de 1,5 (línea de trazos) y 7,5 (línea continua).

Puede comprobarse que los redondos muestran un primer período con E_{corr} en valores que indican pasivación e I_{corr} inferiores a 0,1 $\mu A/cm^2$. El primer redondo que se activa (alrededor de los 100 días, de los cuales 75 fueron de curado) es el embebido en hormigón de 300 kg y con 1,5 cm de espesor de recubrimiento. Los embebidos a 7,5 cm se activaron aproximadamente al mismo tiempo en ambas calidades de hormigón (alrededor de 800 días). Una vez despasivados ($I_{corr} \simeq$ 0,1-0,2 $\mu A/cm^2$), las intensidades de corrosión van creciendo paulatinamente, situándose los valores máximos medidos hasta el momento entre 50 y 100 $\mu A/cm^2$.

En las figuras 5, 6 y 7 se han resumido los valores de I_{corr} para todas las variables ensayadas, para las edades de 3 y 5 años y medio.

En cuanto a la calidad del hormigón, se comprueba que una mayor cantidad de cemento es beneficiosa si la relación a/c es baja (cono 1 cm), ya que para las probetas con cono de 14-15 cm se apreciа una mejoría en los resultados a 3 años, que desaparece para los resultados a 5 años y medio.

Las armaduras galvanizadas presentan I_{corr} inferiores que las de acero desnudo. Esta diferencia es menos notable en el hormigón de peor calidad (mayor relación a/c) que en el de 400 kg y cono de 1 cm. En cambio las probetas que contienen nitritos presentan un claro mejor comportamiento para edades similares, ya que los redondos situados a 4 cm permanecen todavía en la zona de pasividad a los 5 años y medio.

Las probetas no muestran en su exterior ninguna fisura y únicamente aparecen manchas de óxido marrón en la cara más cercana a los redondos con 0,5 cm de recubrimiento.

DISCUSION

Las condiciones de conservación de estas probetas no pueden considerarse muy agresivas, ya que no están sometidas a variaciones del nivel del agua y los redondos están prácticamente sumergidos, por lo que el acceso de oxígeno, sin estar impedido, no es el más favorable para provocar elevadas velocidades de corrosión. Sin embargo puede comprobarse en los resultados obtenidos que redondos situados incluso a 7,5 cm de profundidad (recubrimientos entre 4 y 7,5 cm son los recomendados en distintos códigos para plataformas off-shore de hormigón) se activan al cabo de un período de tiempo mucho más corto que la vida en servicio nominal (alrededor de 50 años) que se espera de las construcciones de hormigón armado.

Esta realidad de la despasivación temprana del acero de las armaduras situadas en ambientes marinos debe llevar a insistir en la importancia de una cuidadosa puesta en obra del hormigón, que asegure para éste una gran impermeabilidad, así como la necesidad de prever en el proyecto cantidades de cemento y espesores de recubrimiento relativamente elevados.

Estas precauciones se deberían tomar no sólo en construcciones singulares como las obras públicas, sino también en viviendas y en edificaciones, que en general se tiene tendencia a cuidar menos, pero que en ocasiones están sometidas a situaciones a veces incluso más agresivas, ya que los cloruros pueden penetrar mucho más deprisa cuando se encuentran suspendidos en las gotitas de agua en climas húmedos y calurosos (penetran por fuerzas capilares), situación habitual en las zonas costeras del ámbito mediterráneo donde se dan condiciones de "niebla" de elevada salinidad. En cambio la penetración de los cloruros por difusión simple, como en el caso de las probetas aquí ensayadas, es comparativamente bastante más lento.

De los dos métodos de protección adicional ensayados, a la edad última considerada (5 años y medio), parece claramente más ventajoso el empleo de nitritos añadidos al agua de amasado, si bien es necesario esperar tiempos más largos para extraer conclusiones más definitivas, ya que el galvanizado en general se corroe actuando como ánodo de sacrificio, de tal forma que mientras no desaparece la capa galvanizada, el ataque al acero base no es demasiado intenso, por lo que las velocidades de corrosión que se están midiendo pueden ser todavía las de disolución de la capa galvanizada.

Por otra parte, los valores de intensidad de corrosión medidos en las probetas con nitritos para espesores de recu-

brimiento inferiores a 2,5 cm, aunque menores a los de probetas sin inhibidor, indican que los redondos se han ya activado, por lo que, aunque mejoran el comportamiento del acero alargando su vida útil, sin embargo no representan tampoco una solución definitiva al problema.

CONCLUSIONES

De los resultados obtenidos hasta el momento las conclusiones provisionales que se pueden extraer son:

1ª) La penetración de cloruros en el hormigón mediante difusión es un proceso relativamente rápido, de tal forma que los redondos de acero desnudo se encuentran despasivados a edades de 5 años y medio, excepto para espesores de recubrimiento superiores a 4 cm y elevadas calidades del hormigón (400 kg cemento/m^3 de hormigón y consistencia seca).

2ª) La galvanización de las armaduras resulta algo favorable cuando se utilizan elevadas calidades de hormigón.

3ª) La adición de nitrito sódico al agua de amasado supone una clara disminución de las intensidades de corrosión medidas cuando los espesores de recubrimiento son superiores a 2,5 cm.

AGRADECIMIENTOS

Los autores agradecen a los Dres. Enrique Arias y Pedro Arté, del Instituto de Ciencias del Mar de Barcelona (CSIC), su inestimable colaboración en el mantenimiento del ensayo. También agradecen a la Comisión Asesora de Investigación Científica y Técnica (CAICYT) de España la financiación de la investigación.

REFERENCIAS

(1) FIP Recommendations.- Design and Construction of concrete sea structures.- 4th Ed. (1985).

(2) DIN 1045.- Concrete and Reinforced Concrete. (Dic. 1978).

(3) American Concrete Institute.- ACI.- Manual of Concrete Practice. (1988).

(4) British Standard 8110.- Structural use of concrete. (1985).

(5) O.E. GJØRV.- Matériaux et Constructions.- Rilem. Vol 2, nº 12 (1969). 467-476.

(6) H.C. Schell y D.G. Manning.- NACE. Corrosion-85. Paper nº 263.- Boston.- March. (1985).

(7) J.T. Lundquist, A.M. Rosenberg y J.M. Gaidis.- Materials Performance.- March. (1979). 36.

(8) C. Andrade, G. Jáuregui y J.A. González.- 7th Int. Cong. of Metallic Corrosion.- Mainz. (1981). 1372-1377.

(9) C. Andrade, V. Castelo, C. Alonso y J.A. González.- Corrosion Effect of Stray Currents and the Techniques for evaluating Corrosion of Rebars in Concrete.- ASTM-STP-906.- V. Chacker Ed. (1986). 43-63.

Fig.1

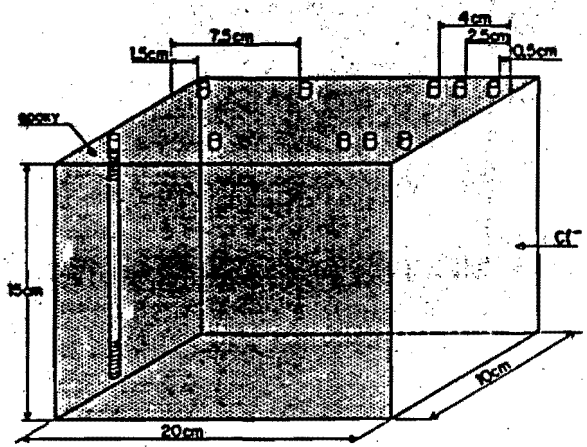

Fig.2

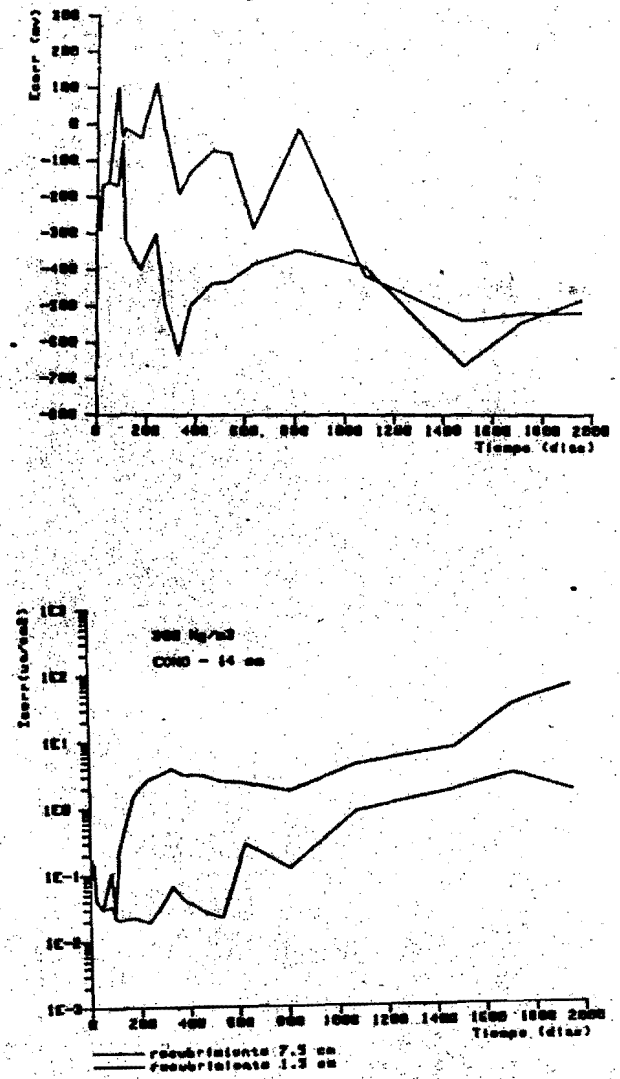
Ecorr (mv)
Tiempo (días)
300 Kg/m3
CONC - 14 cm
Icorr(us/cm2)
recubrimiento 7.5 cm
recubrimiento 1.5 cm

Fig 3

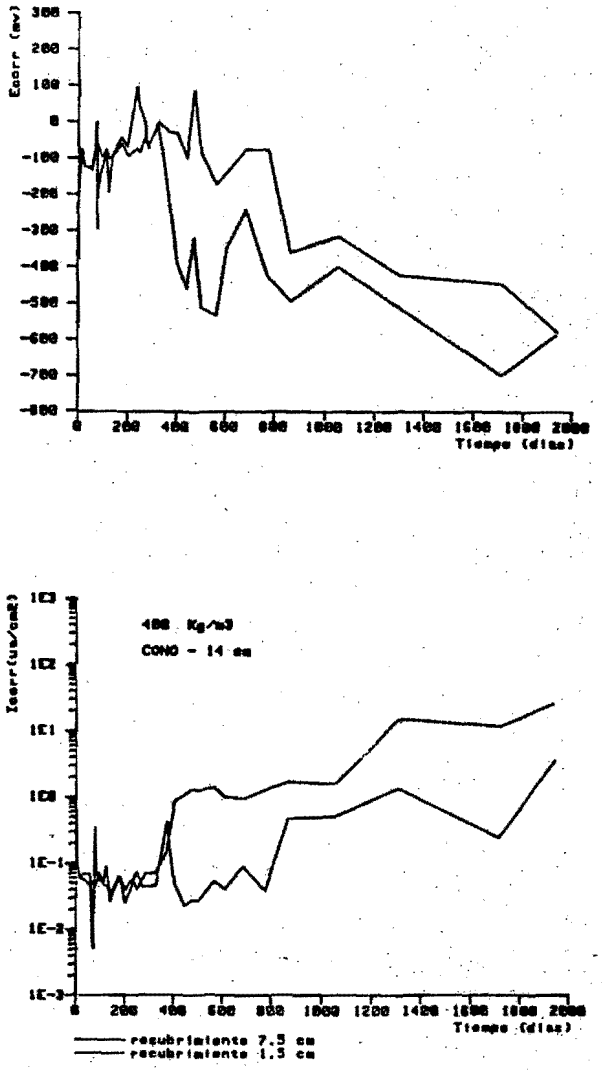
Ecorr (mv)
Tiempo (días)
400 Kg/m3
CONC - 14 cm
Icorr(us/cm2)
recubrimiento 7.5 cm
recubrimiento 1.5 cm

Fig 4

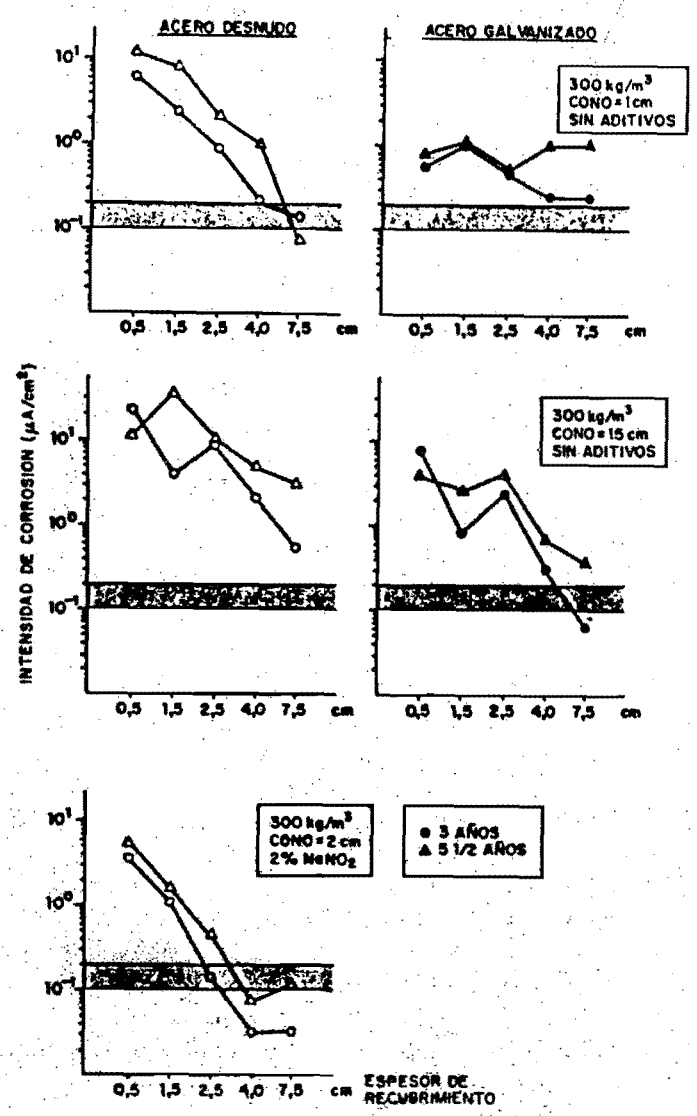
ACERO DESNUDO
ACERO GALVANIZADO
300 kg/m³
CONO = 1 cm
SIN ADITIVOS
300 kg/m³
CONO = 1.5 cm
SIN ADITIVOS
300 kg/m³
CONO = 2 cm
2% NaNO₂
● 3 AÑOS
▲ 5 1/2 AÑOS
INTENSIDAD DE CORROSION (μA/cm²)
0,5 1,5 2,5 4,0 7,5 cm
ESPESOR DE RECUBRIMIENTO

Fig. 5

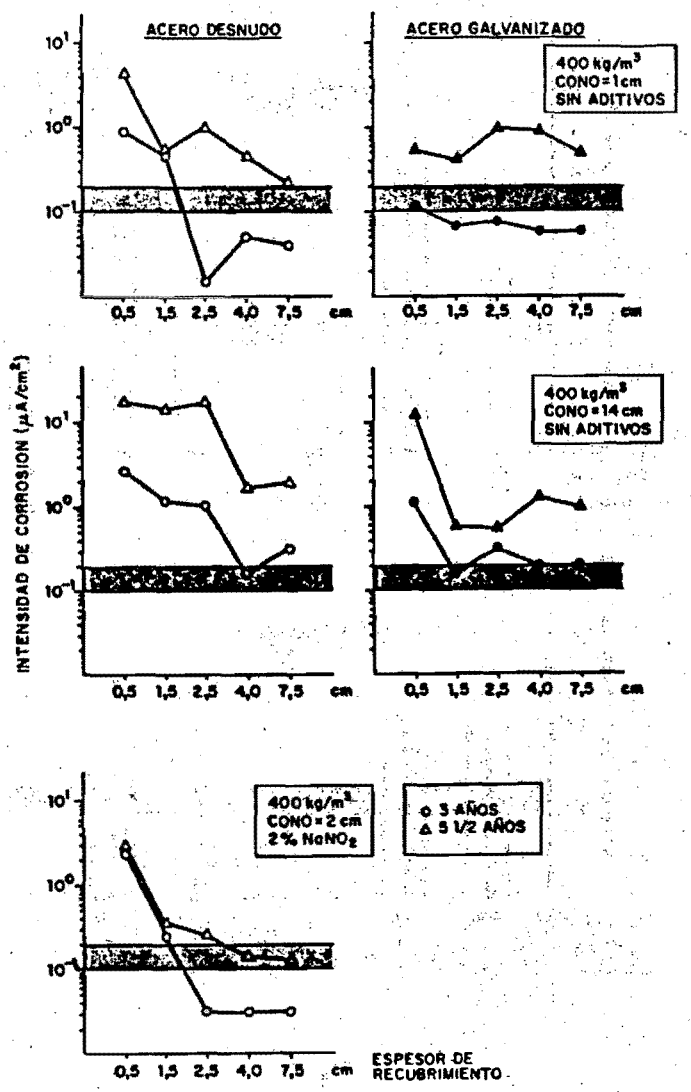
ACERO DESNUDO
ACERO GALVANIZADO
400 kg/m³
CONO = 1 cm
SIN ADITIVOS
400 kg/m³
CONO = 1.4 cm
SIN ADITIVOS
400 kg/m³
CONO = 2 cm
2% NaNO₂
○ 3 AÑOS
△ 5 1/2 AÑOS
INTENSIDAD DE CORROSION (μA/cm²)
0,5 1,5 2,5 4,0 7,5 cm
ESPESOR DE RECUBRIMIENTO

Fig. 6

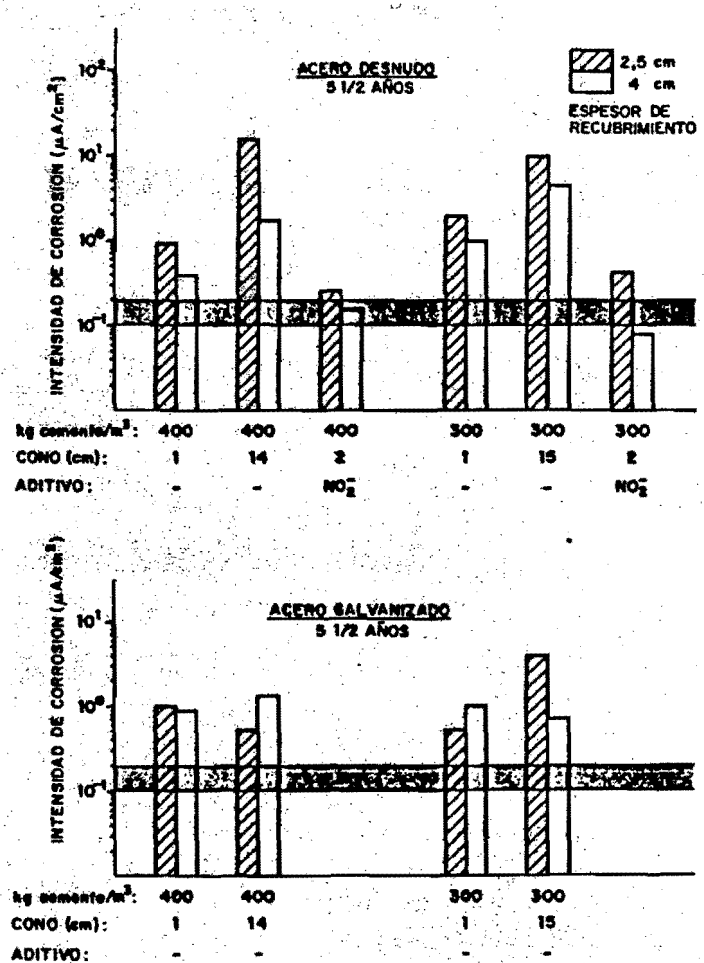
ACERO DESNUDO
5 1/2 AÑOS
2,5 cm
4 cm
ESPESOR DE RECUBRIMIENTO
INTENSIDAD DE CORROSION (μA/cm²)
10²
10¹
10⁰
10⁻¹
kg cemento/m³: 400 400 400 300 300 300
CONO (cm): 1 14 2 1 15 2
ADITIVO: - - NO₂⁻ - - NO₂⁻
ACERO GALVANIZADO
5 1/2 AÑOS
INTENSIDAD DE CORROSION (μA/cm²)
10¹
10⁰
10⁻¹
kg cemento/m³: 400 400 300 300
CONO (cm): 1 14 1 15
ADITIVO: - - - -

Fig. 7

COMPORTAMIENTO FRENTE A LA CORROSION MARINA DE RECUBRIMIENTOS DE NIQUEL DEPOSITADOS POR VIA QUIMICA Y POR VIA ELECTROLITICA

E. JULVE

Departamento de Química.Facultad de Ciencias
Universidad Autónoma de Barcelona. Bellaterra

ABSTRACT

There are relatively few reports on corrosion resistance of electroless nickel deposits and electrolytic nickel deposits in industrial-marine enviroments. In this study,the corrosion behaviour of both types of nickel coatings has been evaluated for three-months,six-months,12-months and 18-months of outdoor exposure in a sea side site.The nickel thickness of coatings and it composition have been correlated with it corrosion resistance.

INTRODUCCION

La corrosión de los metales,especialmente aceros,en un ambiente marino reviste la máxima importancia en la economía de un país,sobre todo en aquellos que poseen una gran extensión de costa,como es el caso de España. Por ello,a los metales se les suele proteger con películas,de mayor ó menor espesor,de recubrimientos de tipo orgánico ó de tipo metálico, que aislen al metal-base de su medio exterior agresivo. De entre los recubrimientos metálicos más utilizados para la protección de los aceros,destacan los de cinc,cadmio,estaño y niquel. Los recubrimientos de niquel se han utilizado,de modo especial,por ser a la vez protectores y decorativos.Tradicionalmente se han aplicado por vía electrolítica.Ahora bien,desde hace unos pocos años,la película de niquel se deposita sobre el metal a proteger por via química,mediante un proceso de reducción,dando lugar a una estructura diferente a la propia del niquel electrolítico.

Los recubrimientos de niquel electrodepositados han sido bastante estudiados en lo que se refiere a su comportamiento en ambientes interiores ó en ambientes exteriores no demasiado agresivos,correspondientes especialmente a zonas urbanas o rurales,pero han sido poco estudiados en lo que se refiere a ambientes marinos y marino-costeros industriales.Por otra parte,apenas existe información acerca del comportamiento de los recubrimientos de niquel obtenidos por via química(sin corriente) en ambientes urbanos y rurales, y menos en lo que respecta a atmósferas marino-costeras industriales,llevando como polucionantes a cloruros y al dióxido de azufre.En lo que se refiere a nuestro pais,no existe ningún dato referente a la resistencia frente a la corrosión ambiental marino-industrial de ambos tipos de recubrimientos de niquel.

En el presente trabajo se expone el comportamiento,en un clima marino-costero industrial catalán,de recubrimientos de niquel electrodepositado y de recubrimientos de niquel obtenido por via química(sin corriente).Ambos recubrimientos fueron depositados sobre probetas de acero dulce y para obtener esos recubrimientos se partió de un baño electrolítico de niquel llevando agentes de adición de tipo orgánico en el primer caso y de un baño llevando hipofosfito como agente reductor en el segundo caso.Se ha estudiado el comportamiento de ambos tipos de recubrimiento de niquel ,con diferentes espesores,durante un periodo total de 18 meses,comparándose el progreso de la corrosión en los mismos en distintos períodos de tiempo.Al propio tiempo,el progreso de la corrosión de estas probetas se comparó con la corrosión observada en probetas de acero dulce desnudo sometidas a las mismas condiciones de ensayo.

PARTE EXPERIMENTAL

Preparación de las probetas de niquel y evaluación de la corrosión

Se prepararon dos series de probetas,convenientemente

identificadas.La primera serie(A)correspondía a probetas de acero llevando un recubrimiento de niquel electrodepositado y la segunda serie(B)correspondía a probetas de acero llevando un recubrimiento de niquel depositado por via química(sin corriente).Ambas series se subdividieron en dos subseries(A-1 y A-2 y B-1 y B-2) según llevaran un recubrimiento de niquel de 6 µm ó de 12 µm de espesor. Las probetas que se utilizaron eran de acero dulce,de dimensiones:100 × 50 × 0,5 mm.La composición de este acero era la siguiente: C:0,04%,Si:0,05%,Mn: 0,35%,P:<0,02%,S:<0,02%,Ni:<0,01%,Cr:<0,05% y Cu:<0,05%. Las probetas,antes de ser recubiertas con los dos diferentes tipos de niquel,fueron pulidas con papel abrasivo del nº 800, desoxidadas por inmersión durante unos minutos en HCl al 10% y desengrasadas con pasta de cal de Viena(dolomita tostada). Después de enjuagadas en agua corriente y luego en agua destilada,fueron tratadas en el correspondiente baño para ser recubiertas con niquel,con espesores de 6 ó 12 µm,según los casos.

La composición de los baños de niquel utilizados:electrolítico y químico(sin corriente)ylas condiciones operatorias y caracteristicas de cada uno de ellos se exponen en la Tabla I.

Las probetas,una vez recubiertas con niquel y debidamente identificadas,se dispusieron,con una inclinación de 45°respecto a la horizontal,sobre un bastidor de ensayo orientado hacia el Sur(3). Una vez transcurridos los períodos de exposición al clima marino-costero industrial programados(tres meses,seis meses,doce meses y dieciocho meses) ,estas probetas niqueladas se retiraron del bastidor de ensayo y se evaluó su corrosión.

La evaluación se realizó de dos maneras:por estimación mediante el sistema ASTM(4) y mediante estimación por pérdida de peso(5)(6). Por el primer procedimiento cada probeta niquelada se evaluó inmediatamente después de la exposición,expresándose la corrosión observada mediante un "número de clasificación"(Rating Number).Este número está definido por la división del área corroida en diez grados:desde el grado 0 al grado 10.En esta evaluación hemos introducido una leve

Tabla I. Composición de los baños de niquel ,condiciones operatorias y caracteristicas de los mismos.

BAÑO ELECTROLITICO (1)	BAÑO QUIMICO (2)
$NiSO_4.7H_2O$ ..... 240 g/l	$NiSO_4.6H_2O$..... 28 g/l
$NiCl_2.6H_2O$ ..... 50 g/l	$NaH_2PO_2.H_2O$ ..... 30 g/l
H_3BO_3 ..... 40 g/l	Acido láctico(88%).... 25ml/l
Abrillantador Primario 1,5 g/l	Acido propiónico..... 5 g/l
Abrillantador Secundar.0,5 g/l	Acido succínico 15ml/l
Agente ductilizante... 1,5 g/l	$Pb(NO_3)_2$ .....0,002 g/l
Agente "anti-pitting". 1,0 g/l	
pH : 3,8-4,0	pH : 5,5
T : 55-60 ºC	T : 88 ± 2 ºC
Dens. corriente : 0,055 A/cm^2	
Anodo : niquel electrolítico	
Relac.ánodo/cátodo: 1,5/1	
Agitación catódica: 6 m/min.	
Distancia ánodo/catodo:8-10 cm	
Velocidad deposición: 1,1µm/min	Velocidad deposición:15µm/h

variación en esta clasificación,consistente en incluir los grados 9,75 , 9,5 y 9,25 entre el grado 10 y el grado 9. Un número de clasificación ó grado 10 significa que no se ha observado corrosión,es decir,que corresponde a un 0% de área corroida,mientras que un número de clasificación ó grado 0 corresponde al 50-100% de área corroida.Un número de clasificación ó grado comprendido entre 9,75 y 9 corresponde a un 0,01 -0,10% de área corroida.Este número de clasificación ó razón numérica corresponde a una función logarítmica del % de área corroida.En la tabla II se expresan los números de clasificación ASTM correspondientes al % de área corroida.

Por el segundo procedimiento de evaluación,cada probeta niquelada se limpió y se pesó antes y después de la exposición,expresándose la corrosión ,en cada período de tiempo,en -

forma de "pérdida de peso"(en $g.dm^{-2}$).Los productos de corrosión se separaron tratando las probetas niqueladas expuestas con una disolución de ácido fosfórico al 10%(vol.),conteniendo como inhibidor 0,1% de alil-tiourea(tiosinamina),a una temperatura de 50°C y durante un tiempo de 30 minutos,enjuagando y secando después esas probetas antes de pesarlas.

Tabla II. Número de clasificación ASTM según el área corroida

NUMERO DE CLASIFICACION ASTM	% DE AREA CORROIDA
10	0
9	0,0 - 0,10
8	0,10 - 0,25
7	0,25 - 0,5
6	0,5 - 1,0
5	1,0 - 2,5
4	2,5 - 5,0
3	5,0 - 10
2	10 - 25
1	25 - 50
0	50 - 100

Determinación de cloruros y dióxido de azufre

Los cloruros atmosféricos se captaron mediante el método de la "probeta de ángulo" ó "teja",al descubierto,utilizando una superficie total útil de 600 cm^2.Esta "teja" se orientó al Sur y se situó a 50 cm del suelo,según la normativa(7).Cada mes se realizó la recogida de cloruros,los cuales se valoraron mediante el método volumétrico de Mohr,expresándose el contenido de ellos en forma de $mgNaCl.m^{-2}.dia^{-1}$.

El dióxido de azufre atmosférico se captó mediante un cilindro de plástico duro,sobre el cual se colocó tela impregnada con pasta de dióxido de plomo,el cual absorbe el dióxido de azufre y lo transforma en sulfato(8).Este cilindro captador se instaló en el interior de una casta de tipo metereológico, con circulación libre de aire ambiental.Cada mes se renovó el cilindro y los sulfatos se determinaron por análisis gravimétrico,expresándose el contenido de dióxido de azufre en forma de mg $SO_3.m^{-2}.dia^{-1}$.

Preparación de las probetas de acero desnudo testigo

Para el estudio del progreso de la corrosión en el acero desnudo se utilizaron probetas testigo,constituidas por chapitas de acero dulce,de dimensiones:100 × 40 × 3 mm.Estas probetas,convenientemente identificadas y preparadas(desoxidadas, pulidas y desengrasadas),se colocaron,después de pesadas,en el mismo bastidor y con la misma orientación que las probetas niqueladas.Una vez transcurrido el periodo de exposición programado,se retiraron del bastidor,se limpiaron de productos de corrosión presentes(por tratamiento en una disolución acuosa de HCl al 50%,conteniendo 1 g/l de tiourea como inhibidor) y,una vez secas,se volvieron a pesar,expresándose la corrosión en cada período de tiempo en forma de "pérdida de peso"(en g/dm^{-2}).

Ubicacion de la estación y duración de los ensayos

Para el estudio de la corrosión en una atmósfera marino-costera industrial se eligió una localidad que,al propio tiempo que ambiente marino existiera en ella una destacada actividad industrial,existiendo por tanto en su atmósfera dióxido de azufre en apreciable cuantía.La localidad elegida fué la ciudad de Badalona,situada en la zona costera norte próxima a Barcelona,situándose la estación de ensayo a unos 150 metros de la línea del mar. La duración experimental de este estudio ha sido de 18 meses:desde comienzos de Enero de 1986 hasta finales de Junio de 1987.

RESULTADOS Y DISCUSION

Corrosión en las probetas niqueladas

Los resultados correspondientes al comportamiento de las probetas de la serie A,llevando niquel depositado electrolíticamente, y de las probetas de la serie B,llevando niquel depositado por via química,para un período de exposición de 3 meses

de 6 meses y de 18 meses,se exponen en las Figuras 1 y 2,en las Figuras 3 y 4 y en las Figuras 5 y 6,respectivamente.La corrosión observada se expresa en las figuras con número impar mediante el "número de clasificación"ASTM y en las figuras con número par mediante la "pérdida de peso"(en $g.dm^{-2}$).

Del examen de estas seis figuras se desprende que,en todos los casos,como era de esperar,la corrosión de las probetas niqueladas llevando un espesor de 12 µm ha sido menor que la de las probetas llevando un espesor de 6 µm.Por otra parte,se desprende que,en todos los períodos de exposición,las probetas de la serie B (llevando niquel químico) han presentado una mayor resistencia a la corrosión atmosférica que las probetas de la serie A (llevando niquel electrodepositado). Cabe atribuir este comportamiento al hecho de que el depósito de niquel químico(sin corriente) obtenido a partir del baño precedentemente citado y en las condiciones asimismo citadas (2),es,en realidad,una aleación niquel-fósforo(con un contenido en P del 10%).Esta aleación está exenta de poros y parece ser que posee una estructura amorfa,todo lo cual le confiere unas caracteristicas más nobles que las propias del depósito de niquel electrolítico(exento de fósforo) obtenido a partir del baño electrolítico anteriormente citado(1).

Para las probetas niqueladas químicamente(sin corriente) llevando un espesor de 6 µm,el "número de clasificación"ASTM fué de 9,5 a 9,75 para un período de exposición de 3 meses, de 9,5 para un período de exposición de 6 meses,de 8,5 para un período de exposición de 12 meses y de 7 para un período de exposición de 18 meses. Para las probetas niqueladasquímicamente(sin corriente)llevando un espesor de 12 µm,el "número de clasificación"ASTM fué de 9,75 a 10 para un período de exposición de 3 meses,de 9,75 para un período de exposición de 6 meses,de 9 para un período de exposición de 12 meses y de 7,5 para un período de exposición de 18 meses.

Para las probetas niqueladas electrolíticamente,con espesores de 6 µm y de 12 µm,los "números de clasificación"ASTM fueron,respectivamente,de 7 y 8 para un período de exposición de 3 meses,de 6 y 7 para un período de exposición de 6 meses, de aproximadamente 4 y aproximadamente 5 para un período de exposición de 12 meses y de 2 y 3 para un período de exposición de 18 meses.

Cuando la corrosión se expresó en forma de "pérdida de peso" los resultados obtenidos fueron análogos a los citados, como se puede observar en las figuras 2,4 y 6.

En todas las probetas el grado de corrosión varió según cual fuera el mes y la estación del año en que se expusieron. Asi,según se puede observar en las figuras 1 y 2,la corrosión fué más intensa durante el período de Abril a Junio y de Julio a Septiembre(casi coincidentes con la estaciones primavera y verano) que durante el período Enero a Marzo y Octubre a Diciembre(casi coincidentes con la estaciones invierno y otoño).

Corrosión en las probetas de acero desnudo

Los resultados de corrosión obtenidos para las probetas testigo,de acero dulce,sometidas a las mismas condiciones de ensayo que las probetas niqueladas,se exponen en la Fig.7.

Como en ella se puede observar,la corrosión en estas probetas fué más intensa en losmeses de Marzo,Abril,Mayo,Junio y Julio(casi coincidentes con las estaciones del año:primavera y verano) que en los meses de Enero,Febrero,Septiembre,Noviembre y Diciembre(casi coincidentes con las estaciones del año: invierno y otoño). Coincide este hecho con el observado en las probetas llevando recubrimiento de niquel químico y de niquel electrolítico.

Por otra parte,cabe indicar que el ataque de la corrosión es mucho mayor en el acero desnudo que en el acero recubierto con niquel,sea químico ó electrolítico.Asi,mientras que el valor medio de la corrosión anual del acero desnudo fué de 6 $g.dm^{-2}$,para el acero niquelado electrolíticamente ese valor fué de 0,18 $g.dm^{-2}$ (para 6 µm de espesor) y de 0,13 $g.dm^{-2}$ (para 12 µm de espesor) y para el acero niquelado químicamente ese valor fué todavía menor: de 0,05 $g.dm^{-2}$(para 6 µm de espesor) y de 0,03 $g.dm^{-2}$(para 12 µm de espesor).

Influencia de los cloruros y del dióxido de azufre.

Las concentraciones de los contaminantes:cloruro y SO_2

(expresadas como NaCl y SO_2)presentes en la atmósfera en que se realizó el ensayo, se exponen,respectivamente,en las Figuras 8 y 9.

Como en la primera de ellas se puede observar,las mayores concentraciones de cloruros se encontraron en los meses de Marzo,Abril,Mayo,Junio,Julio y Agosto(correspondientes a las estaciones:primavera y verano) y las menores concentraciones se encontraron enlos meses de Septiembre,Octubre,Noviembre, Diciembre,Enero y Febrero(correspondientes a las estaciones: otoño e invierno).Esta mayor concentración de cloruros,aceleradores de la corrosión,en los meses de primavera y verano(ayudado sinérgicamente por la presencia en algunos de esos meses de una elevada concentración de dióxido de azufre) explicaría el mayor ataque de la corrosión observado durante esos períodos de tiempo en las probetas de acero desnudo y en las de acero niquelado,a lo que contribuirían,además,las altas temperaturas propias de esas épocas del año.Al existir valores medios de la humedad relativa del aire muy semejantes entre el período primavera-verano y el período otoño-invierno en la localidad donde se ha realizado el ensayo, este factor climático parece que no es diferenciador en este caso,como puede serlo en otras localidades donde exista una pronunciada diferénciaen los valores de humedad relativa en los mencionados períodos.

BIBLIOGRAFIA

(1) JULVE,E.,Rev.Iberoamer.Corros.y Protecc.,17;Nº 6,393(1986).

(2) JULVE,E.,Rev.Iberoamer.Corros.y Protecc.,(en prensa).

(3) FELIU,S.;VICTORI,L.,JULVE,E. et alters,Rev.Iberoamer.Corros.y Protecc.,15,nº 3,11(1984).

(4) Proc.Amer.Soc.Testing Materials,49,226(1949).

(5) CHAMPION,F.A.,"Corrosion Testing Procedures",Chapman and Hall,London(1964).

(6) JULVE,E.,Quim.e Indust.,26,nº1,4(1980).

(7) NORMA ALEMANA DIN 50907-1952.

(8) NORMA BRITANICA BS 1747,Part 4,1969.

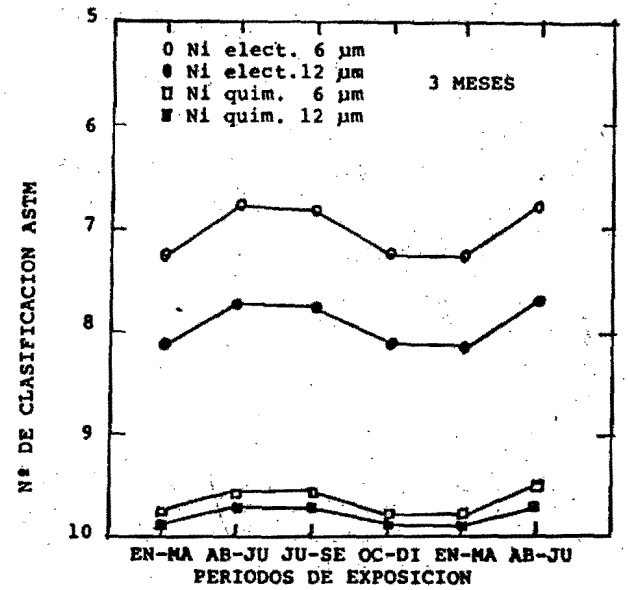

FIG.1

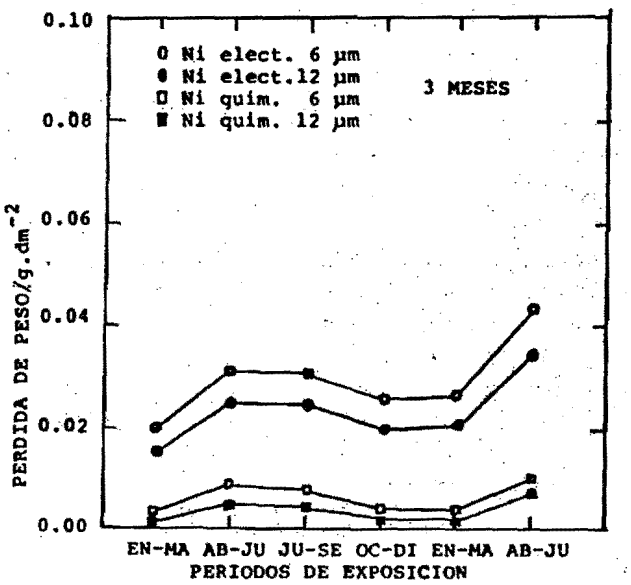

FIG.2

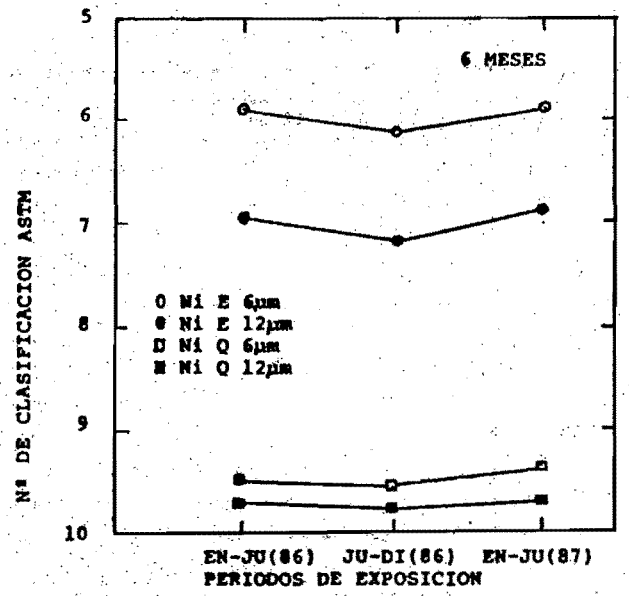

FIG.3

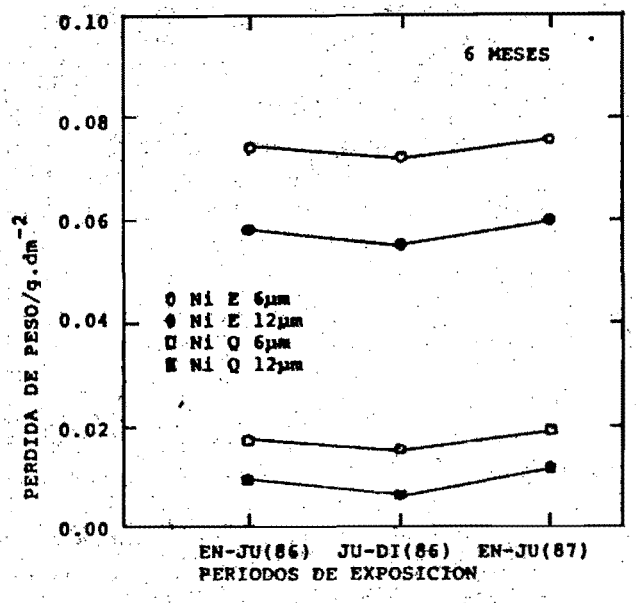

FIG.4

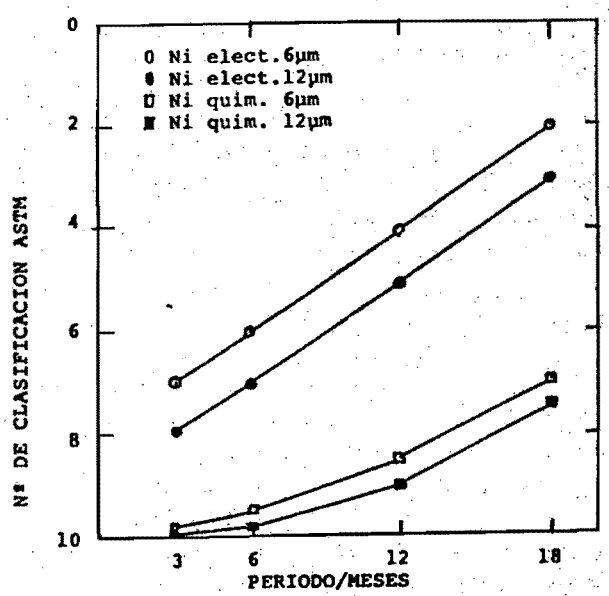

FIG.5

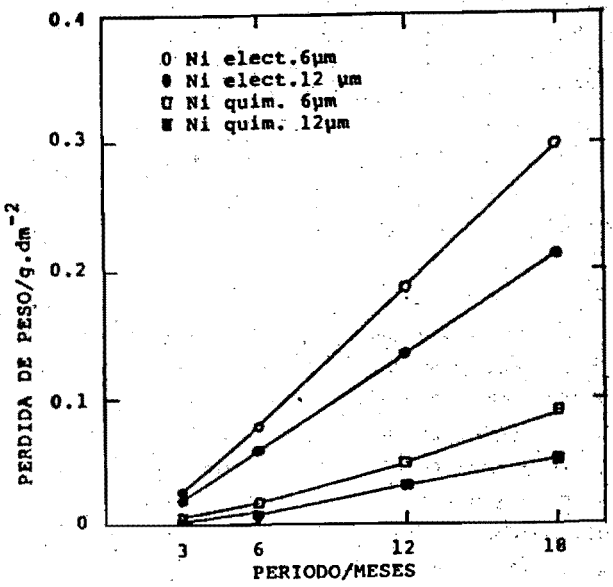

FIG.6

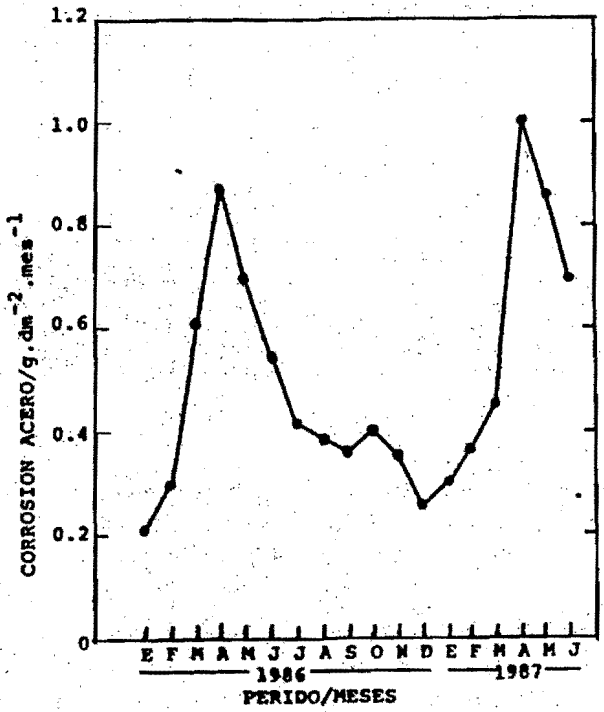
1.2
1.0
0.8
0.6
0.4
0.2
0
CORROSION ACERO/g.dm^{-2}.mes^{-1}
E F M A M J J A S O N D E F M A M J
1986
1987
PERIDO/MESES

FIG.7

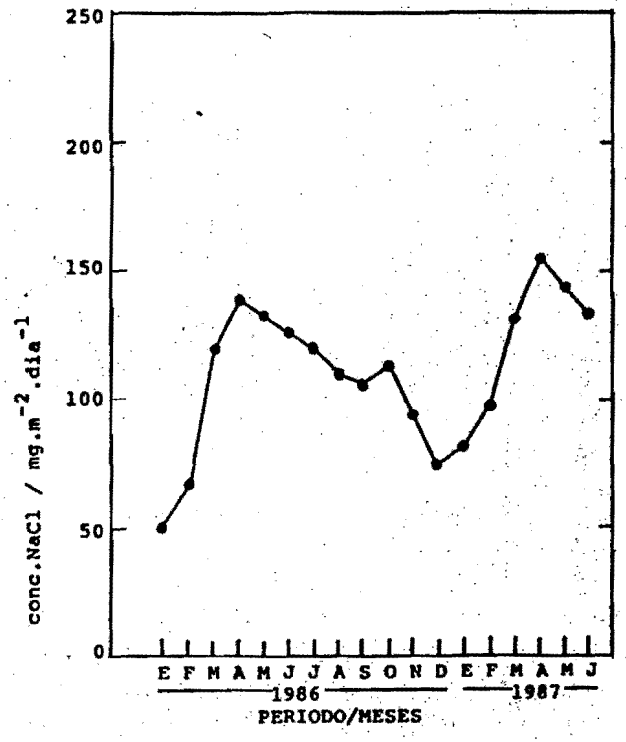
250
200
150
100
50
0
conc.NaCl / mg.m^{-2}.dia^{-1}
E F M A M J J A S O N D E F M A M J
1986
1987
PERIODO/MESES

FIG.8

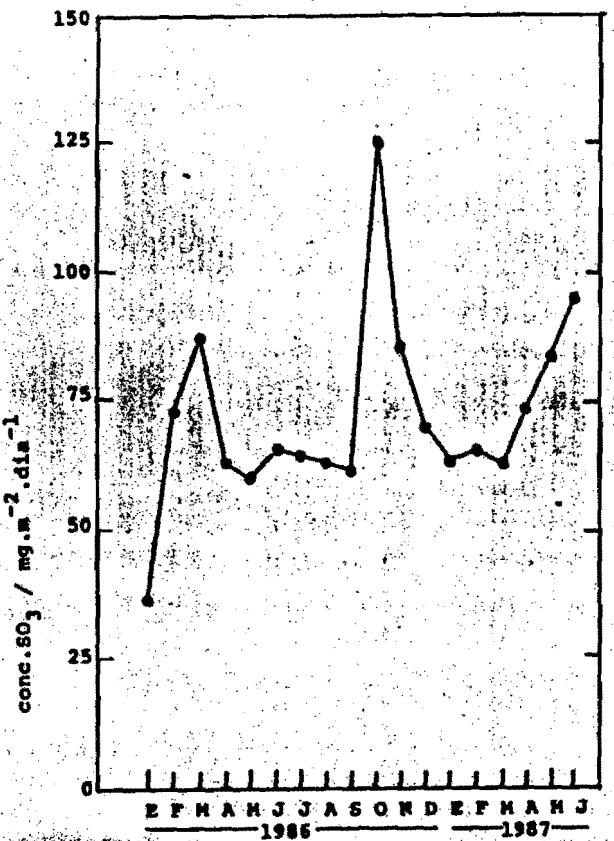
150
125
100
75
50
25
0
conc.SO_3 / mg.m^{-2}.dia^{-1}
E F M A M J J A S O N D E F M A M J
1986
1987
PERIODO/MESES

FIG.9

COMPORTAMIENTO ELECTROQUIMICO DE UNA ALEACION Cu:Ni EN AGUA DE MAR CONTAMINADA CON SULFUROS

María del Carmen LEIRO y Blanca M. ROSALES*
CEICOR - CITEFA/CONICET - Zufriategui 4380 - (1603) Villa Martelli - BUENOS AIRES - ARGENTINA

ABSTRACT

The corrosion resistence of a Cu:Ni 70:30 alloy in sea water was determined in the presence and the absence of sulfide to analize the effect of the anion. Electrochemical tests were performed in 3.4% w/v solutions of NaCl with and without addition of Na_2S at a concentration 10^{-3} M. Immersion tests were used to characterize the corrosion products grown in the different conditions. The results showed a protective effect associated to the cuprous sulfide formed when the microbial metabolite was additioned to the sea water only in the absence of oxygen.

INTRODUCCION

Las aleaciones de Cu-Ni, cuyo contenido en Ni varía entre 5 y 30%, han tenido en la última década nuevas aplicaciones en la industria naval ya que ofrecen ventajas prácticas y económicas sobre las de base Fe utilizadas hasta el momento[1].

En los barcos de acero convencionales, el costo de la corrosión e incrustación marina es muy elevado y además el aumento de la rugosidad del casco incrementa el consumo de combustible hasta en un 10%, dependiendo del tiempo que media entre cada limpieza. El placado con aleaciones de Cu:Ni reduce estos inconvenientes, en parte debido a que el Cu tiene características anti-incrustantes y en condiciones normales estas aleaciones tienen una velocidad de corrosión menor que el acero.

Otra aplicación de estas aleaciones es en cañerías y tubos de intercambiadores y condensadores por los cuales circula agua de mar.

Como consecuencia de la creciente difusión en el empleo de estos materiales, diversos autores estudiaron su comportamiento frente a la corrosión. Encontraron que su resistencia disminuye en agua de mar en presencia de contaminantes como $S^{=}$ producido por la reducción metabólica del sulfato por bacterias sulfato-reductoras. Se realizaron ensayos de aleaciones Cu:Ni en equipos de diversos diseños con circulación de fluido y se determinó mediante medidas de pérdidas de peso[2,3,4,5] la influencia de la velocidad de flujo y de la concentración del ión $S^{=}$ en la resistencia a la corrosión.

En base a ensayos electroquímicos realizados en soluciones acuosas de NaCl al 3% se observó que la curva de polarización anódica de la aleación Cu:Ni 70:30 presenta tres zonas en las cuales se forman distintos productos de corrosión constituídos principalmente por compuestos de Cu[6].

B. C. Syrett[7] reprodujo el fenómeno de corrosión en condiciones de flujo, para luego realizar un estudio de las superficies atacadas utilizando voltametría cíclica y microscopía electrónica de barrido, concluyendo que la composición de los productos de corrosión es distinta según el medio que se utilice y propone un mecanismo de corrosión que depende de la historia de los medios a los que estuvo expuesta la aleación. Encontró además, que el sulfuro, en ausencia de oxígeno, no es el causante directo del incremento de la velocidad de corrosión aún bajo condiciones adversas de flujo, resultado que fue confirmado por otros autores[8]. Del estudio realizado por D. D. Mc Donald y col.[9,10] sobre la acción del oxígeno y el sulfuro en la corrosión de estas aleaciones, se concluye que podría existir un efecto sinérgico entre ambos.

En el presente trabajo se analiza el comportamiento de la aleación Cu:Ni 70:30 mediante técnicas electroquímicas y medidas de pérdidas de peso. Se relacionan los resultados anteriores con la composición y estructura de los productos de corrosión formados, determinados mediante rayos X y microscopía electrónica de barrido con microsonda acoplada, respectivamente.

EXPERIMENTAL

Se prepararon probetas de la aleación Cu:Ni 70:30. Se incluyeron en resina epoxi dejando un área expuesta de unos 0,5 cm^2 y se las pulió hasta 0,25 µm. Los electrolitos utilizados fueron solución de NaCl

---

* Investigadora del CONICET.

3,4% w/v con agregado de Na_2S en una concentración de 1 x 10^{-3} M y sin agregado del peluente.

Se realizaron curvas de polarización potenciocinéticas, utilizando un potenciostato Tacussel PRT-20-2X con un Servovit 13 como generador de barrido, aplicándose una velocidad de 10 mV.min.$^{-1}$. Se empleó una celda electroquímica convencional de vidrio Pyrex, electrodo de referencia de calomel saturado, a través de un capilar de Luggin, y contraelectrodo de Pt. Los resultados son promedios de triplicados.

Las curvas anódicas se hicieron desareando las soluciones mediante burbujeo de N_2 99,99% y las catódicas saturando los medios con aire y con agitación magnética, todas a temperatura ambiente.

Luego de los ensayos anódicos y de inmersión, las muestras se analizaron con un microscopio electrónico de barrido (MEB) Philips 505 con EDAX 9100, determinándose mediante difracción de rayos X, la composición de los productos formados.

RESULTADOS

Ensayos electroquímicos

Se trazaron curvas de polarización (Fig. 1), de la aleación Cu:Ni 70:30 en solución de NaCl con y sin agregado de Na_2S. En el ensayo simulando agua de mar contaminada se suma al efecto del electrolito, el del sulfuro correspondiente a los metabolitos originados por los microorganismos capaces de proliferar en el medio.

Análisis Morfológico y EDAX

Se aplicó microscopía electrónica de barrido sobre muestras sometidas a polarizaciones anódicas y catódicas como puede observarse en las Figs. 2 y 3. Se realizaron determinaciones con EDAX sobre los productos de corrosión formados durante las polarizaciones en soluciones conteniendo $S^{=}$ y sobre los dos tipos de segundas fases observados en la aleación (Fig. 2) asociados al ataque anódico.

Ensayos de inmersión

En la siguiente tabla se reúnen las pérdidas de peso de las probetas sumergidas en agua de mar natural y sintética con adición de Na_2S en laboratorio. Durante el ensayo de 30 días se mantuvo la saturación en oxígeno mediante burbujeo de aire.

MEDIO	Agua de Mar	NaCl 3,4%	NaCl 3,4% + Na_2S 10^{-3} M
$[\frac{\Delta P}{mg/cm^2.año}]$	1,8 ± 0,6	2,7 ± 0,8	50 ± 2

Análisis mediante difracción de rayos X

El rango de pasividad, observado durante las polarizaciones anódicas de la aleación en soluciones con $S^{=}$ se asoció a la formación de una película protectora de productos de corrosión, cuya composición se determinó mediante difracción de rayos X. Los análisis se efectuaron sobre muestras sometidas a pulsos anódicos de polarización a -400 mVcs, potencial correspondiente a la región de pasividad de la curva b) de la Fig. 1.

En la curva a) de la misma figura se observa una estrecha zona de pasividad a + 100 mVcs y un máximo en la corriente a - 30 mVcs. Por ello, se analizaron en idénticas condiciones los productos de corrosión formados en solución de NaCl en ausencia de $S^{=}$ luego de pulsos a + 100 y -30 mVcs. En todos los casos el principal compuesto cristalino encontrado fue $Cu_2(OH)_3Cl$ (paratacamita).

En medios que contienen $S^{=}$ se detectaron películas negras de sulfuros cuproso y cúprico de bajo grado de cristalinidad, sobre la subyacente de oxicloruro verde.

Los resultados de inmersión en presencia de oxígeno evidencian, por el contrario, que la solución de NaCl es algo más agresiva a la aleación que el agua de mar natural y que se produce un gran incremento en la pérdida de peso por la adición de $S^{=}$. El efecto del $S^{=}$ es entonces contrario, en presencia y en ausencia de oxígeno.

CONCLUSIONES

De los resultados obtenidos en los ensayos de la aleación Cu:Ni

70:30 en agua de mar natural y sintética, se concluye que en presencia de $S^{=}$ se forma un delgado film color negro de sulfuros de cobre de baja cristalinidad encima de la película de óxidos de Cu. El crecimiento del doble film en ausencia de oxígeno incrementa el carácter protector del óxido formado en agua de mar pura, pero decrece mucho su poder pasivante en presencia de oxígeno.

BIBLIOGRAFIA

1. B. B. Moreton y T. J. Glover, Proceedings 5th. Int. Congress on Marine Corrosion and Fouling, p. 267-278. España (1980).
2. J. P. Gudas y H. P. Hack, Corrosion, Vol. 35, N° 2, p. 67-72, (1979).
3. J. P. Gudas y H. P. Hack, Corrosion, Vol. 35, N° 6, p. 259-265, (1979).
4. A. Abu-Safiah, Proceedings 6th. International Congress on Marine Corrosion and Fouling, p. 539-555, Grecia (1984).
5. T. S. Lee, H. P. Hack y D. G. Tipton, Proceedings 5th. International Congress on Marine Corrosion and Fouling. p. 274-291, España (1980).
6. J. Crousier, L. Pardessus y J. P. Crousier, Proceedings 9th. International Congress on Metallic Corrosion, p. 526-528, Canada (1984).
7. Barry C. Syrett, Corrosion Science, Vol. 21, N° 3, p. 187-209, (1981).
8. Y. Kalpana, T. R. Jayaraman y A. Prabhakara Rao, Proceedings 6th. European Symposium on Corrosion Inhibitors, p. 579-611, Italia (1985).
9. D. D. Mc Donald, B. C. Syrett y S. S. Wing, Corrosion, Vol. 34, N° 9, (1978).
10. D. D. Mc Donald, B. C. Syrett y S. S. WIng, Corrosion, Vol, 35, N° 8, (1979).

FIG. 1 POLARIZACION DE LA ALEACION Cu-Ni 70-30 EN :
a) NaCl 3,4% w/v b) NaCl 3,4% w/v + 1 x 10^{-3} M Na_2S

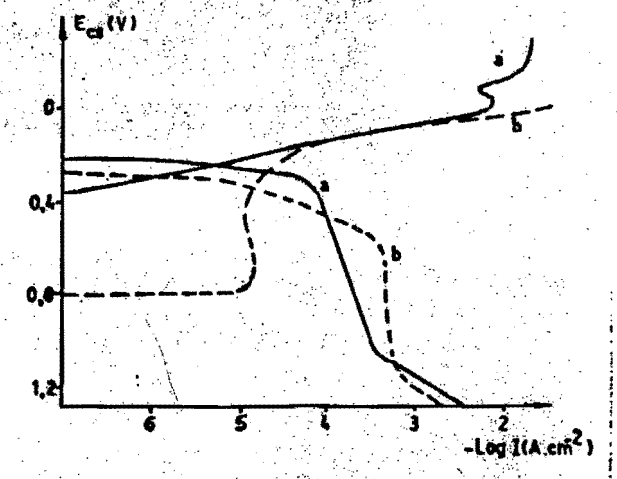

FIG. 2 MEB DE LA ALEACION LUEGO DE LAS POLARIZACIONES DE FIG. 1 CURVAS a)

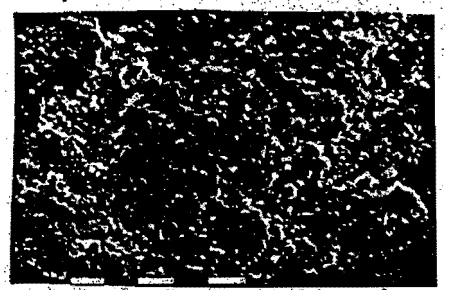

a)Aspecto de la superficie luego de polarizar hasta + 50 mV_{cs}

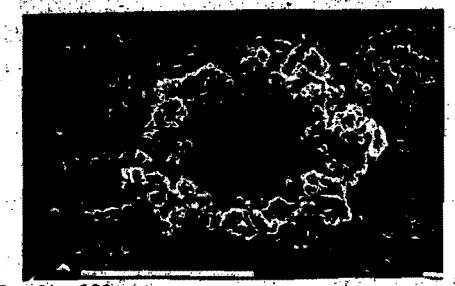

Escala: 100 µm

b) Hasta + 500 mV_{cs}

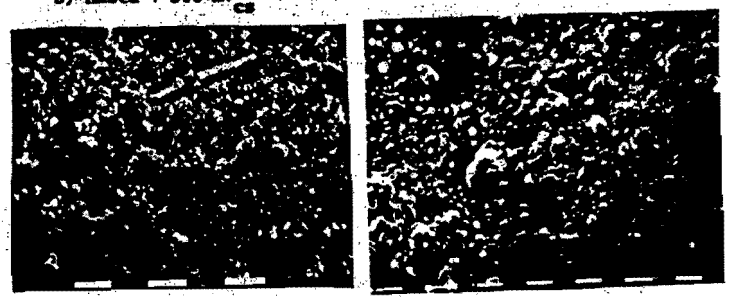

Escala: 10 µm

c) Hasta + 500 mV_{cs}

d) Pulso + 160 mV_{cs}

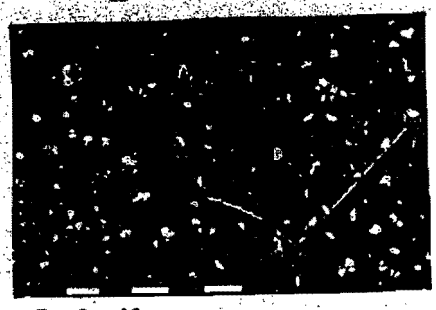

Escala: 10 µm

e) Luego de curva catódica en O_2

EDAX SOBRE LOS DOS TIPOS DE SEGUNDAS FASES DE LA ALEACION, DE DE FIGS. 2 b y c. Puntos: alargadas. Línea llena: redondas

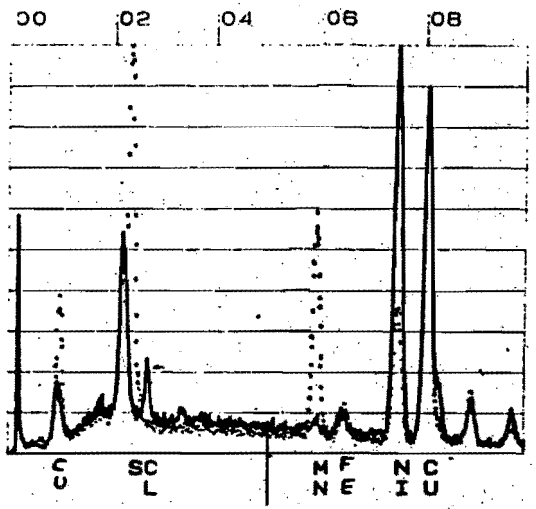

FIG. 3 MEB DE LA ALEACION LUEGO DE LAS POLARIZACIONES DE FIG. 1 b)

a) Hasta + 50mV_{cs}

Escala: 10 µm

Escala: 0,1 mm

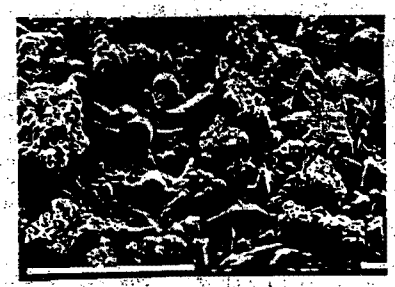

Escala: 0,1 mm

Escala: 10 µm

EDAX SOBRE PRODUCTOS DE CORROSION DE FOTOS ANTERIORES

Puntos: sobre esferas

Linea llena: sobre prismas triangulares

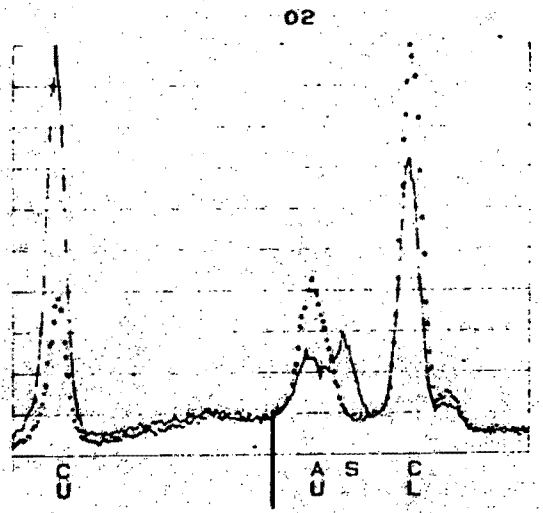

b) Pulsos: a +200 mV_{cs}

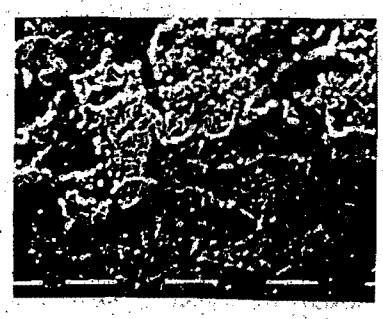

Escala: 10µm

Pulsos a -300 mV_{cs}

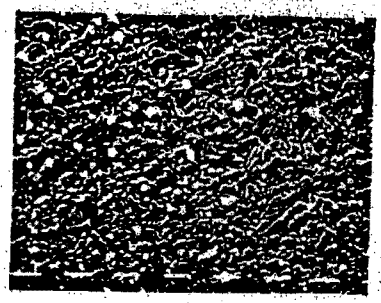

Escala: 10µm

USO DE LAMINAS DE FLUORURO DE POLIVINILO APLICADAS EN FRIO PARA LA PROTECCION SUPERFICIAL DE ACEROS AL CARBONO EN AMBIENTES MARINOS.

P. Merino*, X.R.Nóvoa**, M.Izquierdo** y L.Espada**

* Departamento de Ingeniería Mecánica y Ciencia de Materiales.

** Departamento de Ingeniería Química.

E.T.S. de Ingenieros Industriales (Universidad de Santiago de Compostela), Apartado 62, 36200 - VIGO

ESPAÑA.

ABSTRACT/RESUMEN

Test specimens of low carbon steels covered by the cold application of a white film of polyvinyl fluorure (PVF) with 45 micrometers thickness, were exposed to three types of environment conditions, in accelerated testing, in order to know whether this system ensures the protection of the surface treated against the marine weather. The results show that at 200 hours of exposition in climatic chamber already presents an initiation of oxide points on the steel surface, and at 2000 hours of exposition, all the steel surface was covered by an uniform localized corrosion products for the test specimens exposed to the three types of environment conditions.

INTRODUCCION Y OBJETIVOS

El objetivo de este estudio fue el de comprobar, mediante ensayos acelerados de laboratorio, el comportamiento como sistema de resistencia pasiva, de láminas de fluoruro de polivinilo aplicadas en frío a superficies de acero al carbono sin alear, con el fin de que la superficie tratada se convierta en inherte, física,química y fotoquimicamente, cuando esté, o bien sumergida en agua de mar o expuesta a condiciones marinas severas, tales como las que soportan, por ejemplo,las superestructuras de acero de los barcos durante su navegación.

El fluoruro de polivinilo (PVF) es un polímero que contiene átomos de fluor, que se ha extendido longitudinal y transversalmente durante su fabricación, para formar una especie de parrilla enrejada, lo que le debe conferir,al menos en teoría, unas excelentes propiedades como barrera, así como un alto grado de resistencia a la abrasión y a la fisuración, características estas últimas que necesariamente deben acompañar a la primera para asegurar su durabilidad. Sin embargo, en este trabajo, estas dos últimas propiedades no han sido estudiadas, al menos de una forma directa.

DESCRIPCION DEL TRABAJO EXPERIMENTAL

Todos los ensayos realizados fueron ensayos acelerados de laboratorio. Se utilizó lámina blanca de PVF de 45 micrometros de espesor, con la que se recubrieron totalmente probetas rectangulares de acero al carbono sin alear, tipo Naval A, de dimensiones 100x50 mm y 1 mm de espesor nominal. Todas las superficies metálicas estaban exentas de óxido y, antes de la aplicación de la lámina de PVF, las probetas fueron desengrasadas con tricloroetileno y acetona, lavadas con agua limpia y después cuidadosamente secadas.

No se aplicó ninguna capa intermedia de protección entre la superficie metálica y el PVF, tal como por ejemplo, fosfato cristalino con objeto de realizar los ensayos en las condiciones más desfavorables.

La aplicación del PVF sobre las probetas se hizo de tal forma, que en las zonas de solape, éste fuese al menos de 5 mm de anchura.

Se realizaron los siguientes ensayos, utilizando siempre en cada uno de ellos, probetas por triplicado:

a) Ensayos de cámara climática.
   Todas las probetas fueron sometidas durante las 100 primeras horas de exposición a una temperatura de 45ºC y una humedad relativa de del 85%. Después la cámara se reguló a unas condiciones constantes de 30ºC y una humedad relativa de 85%. Se sacaron y ensayaron probetas por triplicado, después de 200, 500, 1500 y 2000 horas de exposición dentro de la cámara.

b) Ensayos en cámara de niebla salina.
   Se utilizó una cámara de niebla salina de 0,2 cm^3 de capacidad neta, que cumple las normas ASTM -B-117-85 "Standard Method of Salt Spray (Fog) Testing" y BS-5466 "Method of Corrosion Testing of Metallic Coatings (Salt Spray, Acetic acid Salt Spray and Copper acelerated Salt Spray Test)".Se emplearon las condiciones de operación indicadas en la tabla I, que por estudios anteriores realizados en el Departamento de Ingeniería Química, se demostró que eran las más severas obtenibles con esta cámara (1).

   Se fueron sacando muestras por triplicado, después de 200,500, 1000, 1500 y 2000 horas de exposición en el interior de la cámara.

c) Ensayos de inmersión.
   Se sumergieron las probetas en agua de mar artificial preparada según la norma ASTM D.1141, a una temperatura de 30±0,5ºC. Se hizo pasar aire a través de la disolución para conseguir una saturación de oxígeno, cuya concentración resultante fue de 6,3 ppm.

   Se fueron sacando muestras por triplicado después de 200, 500, 1000, 1500 y 2000 horas de inmersión.

Sobre todas y cada una de las probetas sometidas a las condiciones de laboratorio encuadradas en los tipos a), b) y c) se realizaron los siguientes exámenes:

1.- Examen del posible deterioro de las propiedades físicas de las láminas de PVF después de la exposición.
Se estudió mediante este examen la posible variación del brillo especular, dureza, espesor, flexibilidad y adherencia de las láminas. Los resultados obtenidos fueron comparados con los de probetas preparadas de forma idéntica pero, no sometidas a las condiciones de exposición a), b) o c).

El brillo especulsr se midió de acuerdo con la norma UNE 48-026-80, utilizando una geometría de luz incidente de 85º.

El espesor de la película de PVF se midió mediante métodos electromagnéticos no destructivos, de acuerdo con UNE 48-031.

Para determinar la dureza superficial de la capa protectora se utilizó un péndulo Persoz, de acuerdo con las normas INTA 160225 y UNE 48-024-80.

La medida de la flexibilidad de las láminas de PVF, se realizó mediante ensayos de plegado de acuerdo con UNE 48-032-80.

2.- Medidas de impedancia electroquímica. Se utilizó la misma técnica empleada ya con éxito para el análisis del comportamiento de metales pintados ante la corrosión (2 y 3).

3.- Examen visual de la superficie de acero de cada probeta, mediante lupa a 19 aumentos, después de levantar la lámina de PVF, para comprobar la presencia de trazas de óxido.

4.- Estudio microscópico de la superficie del acero de cada probeta para estudiar la profundidad del ataque de óxido, mediante seccionado de la zona en donde se presentó el ataque (4).

RESULTADOS EXPERIMENTALES

Variación en las propiedades físicas de las láminas de PVF después de la exposición.

Después de 200 horas de exposición en cada uno de los ambientes ensayados, no se observó ninguna disminución del brillo especular. Lo mismo ocurrió con el espesor de las láminas de PVF y su capacidad de plegado que denotó ausencia de agrietamientos hasta con mandril de diámetro 3 mm. Sin embargo la degradación de las láminas de PVF se manifiesta en los ensayos de dureza y adherencia.

En la tabla II se muestran los resultados obtenidos en la medida de la dureza de las láminas de PVF después de 2000 horas de exposición, observándose un significativo aumento con respecto a las probetas patrones, sobre todo en las probetas expuestas en la cámara climáticas. Los resultados mostrados corresponden a los valores mínimo y máximo obtenidos, y entre paréntesis se indica también el valor medio.

La tabla III recoge los resultados del ensayo de adherencia antes y después de ser sometidas las probetas a los distintos medios agresivos. En realidad este ensayo sólo mide la pérdida de poder de fijación del adhesivo empleado para unir las láminas al material base.

Medidas de impedancia electroquímica

En la tabla IV se muestran los resultados obtenidos al realizar sobre las probetas ya expuestas, medidas de impedancia electroquímica con corriente alterna.

Puede observarse que hasta 500 horas de exposición en cualquiera de los medios agresivos lo único que se produce es un incremento significativo del ángulo de pérdida (tag δ) ó desviación con respecto a un componente ideal capacitivo. La única excepción a este aumento generalizado a 500 horas corresponde a los ensayos en cámara climática.

A partir de las 1000 horas de exposición, empiezan a presentarse arcos capacitivos, y en algún caso, como el de las probetas expuestas a la cámara climática durante 1500 horas, hasta tres arcos capacitivos. La obtención en el ensayo de un arco de alta frecuencia mide la presencia relativa de la cantidad de óxido sobre la superficie metálica de la probeta, de tal forma que una mayor resistencia óhmica asociada a la máxima alta frecuencia significa la presencia de una mayor cantidad de óxido. La resistencia óhmica asociada a las bajas frecuencias es un indicativo del comportamiento del film de PVF, por lo que a mayor resistencia óhmica asociada a la máxima baja frecuencia le corresponde un mejor comportamiento de la lámina (5).

La figura nº1 muestra de forma gráfica el comportamiento de las probetas a partir de las 1000 horas de exposición. Se observa como a 1000 horas, el ensayo de impedancia registra la presencia de óxido por debajo de la lámina de PVF en las probetas sometidas a la cámara de niebla salina, y a partir de las 1500 horas también se registra esta presencia en las probetas sometidas a la cámara climática y a inmersión en agua de mar. La misma figura también muestra el mejor comportamiento relativo de la lámina de PVF en inmersión en agua de mar que en los otros dos ensayos, tanto porque los valores de la resistencia óhmica son mayores a bajas frecuencias como porque la variación de la misma es menor, tal como se muestra en la pendiente de la recta.

Examen visual de la superficie de acero después de levantar la lámina de PVF.

La tabla V muestra los resultados después del examen con lupa de 19 aumentos de la superficie de acero que había estado cubierta por la lámina de PVF durante los ensayos de exposición a los tres tipos de medios. Puede observarse que ya a 200 horas de exposición en cámara climática hay indicios de iniciación de puntos de óxido, y que en general a partir de las 1500 horas estos puntos de óxido son más o menos generalizados por toda la superficie. Es importante notar también la aparición de líneas contínuas de óxido coincidiendo con las zonas de empalme de las láminas de PVF, lo que podría indicar la necesidad de realizar un mayor solape de la lámina en los empalmes.

Las figuras 2 y 3 muestran la presencia de puntos de óxido sobre la superficie del acero de las probetas después de estar sometidas a 1500 horas en cámara de niebla salina y a 200 horas en inmersión en agua de mar, respectivamente.

Estudio microscópico de las zonas con óxido.

El estudio realizado por seccionado de las zonas donde aparecieron puntos de óxido, revela que esta oxidación fue en todos los ca

sos totalmente superficial y sin penetrar en el material.

CONCLUSIONES

Los resultados de los ensayos realizados sobre láminas blancas de PVF utilizadas como elementos protectores ante la corrosión de superficies de acero, muestran que ya después de 200 horas de exposición se producen indicios de existencia de puntos de óxido por debajo de la capa protectora, lo que indica que el electrólito ha penetrado a través de la capa de PVF, bien por un proceso osmótico o por poros o microgrietas que se producen o existen previamente en el material. La presencia de líneas contínuas de óxido en los empalmes de las láminas indica la necesidad de un solape superior al ensayado, pero en cualquier caso, son zonas críticas a vigilar en el empleo industrial de este producto . Existe una buena correspondencia entre los resultados obtenidos por inspección visual de la superficie metálica , una vez eliminada la capa de PVF, y los obtenidos mediante examen por impedancia electroquímica de corriente alterna , aunque este último método es especialmente sensitivo a partir de las 1000 horas de exposición.

El comportamiento de las láminas de PVF es mejor en los ensayos de inmersión en agua de mar, que en las atmóferas de cámara de niebla salina o en cámara climática.

Por último, cabe destacar la baja degradación sufrida en las propiedades físicas de la lámina de PVF después de estar sometida a los distintos grados y tipos de exposición, especialmente en el mantenimiento de su brillo y flexibilidad.

BIBLIOGRAFIA

1) J.C. GONZALEZ. "Ensayos de Corrosión por pulverización salina para aceros de bajo contenido en carbono". Tesina de licenciatura. Facultad de Ciencias Químicas. Universidad de Santiago de Compostela. 1985: 64.

2) G.W. EALTER. "A review of impedance plot methods used for corrosion performance analysis of painted metals". Corros. Sc. 26, 9. 1986: 681-704.

3) K. HLADKY, L.M. CALLOW y J.L. DAWSON. "Corrosion rates from impedance measurements: an introduction". Br. Corrosion Journal. Vol. 15. No. 1. 1980.

4) AMERICAN SOCIETY FOR TESTING AND MATERIALS. "Rec. Practice for Examination and Evaluation of Pitting Corrosion. ASTM Standard G-46-76). Annual Book of ASTM Standards. Philadelphia, Pa.1987.

5) F.MANSFELD, M.W. KENDIG y S. TSAI. "Evaluation of Corrosion - behavior of coated metals with ac impedance measurements". Corrosion, Vol. 38, No. 9, 1982.

TITULOS Y PIES DE TABLAS Y FIGURAS

TABLA I : Condiciones de operación de la cámara de niebla salina.

TABLA II : Variación de la dureza de las láminas de PVF después de expuestas 2000 horas.

TABLA III : Variación de la sdherencia de las láminas de PVF después de expuestas 2000 horas.

TABLA IV : Medidas de impedancia electroquímica.

TABLA V : Examen visual mediante lupa de aumento de la superficie del acero después de la exposición.

Figura 1 : Comportamiento de las probetas a partir de 1000 horas exposición, mediante medidas de impedancia electroquímica. a) A altas frecuencias, b) A bajas frecuencias.

Figura 2 : Presencia de puntos de óxido sobre la superficie del acero después de estar sometida la probeta en cámara de niebla salina durante 1500 horas.

Figura 3 : Presencia de puntos de óxido sobre la superficie del acero, después de estar sometida la probeta en inmersión en agua de mar durante 2000 horas (x19).

TABLA I.- CONDICIONES DE OPERACION DE LA CAMARA DE NIEBLA SALINA

CARACTERISTICAS DEL MEDIO AGRESIVO	Sal	ClNa con impurezas < 0.2%
	Agua	Destilada
	Concentración de la solución	10 grs/litro
	Acidez de la solución a la temperatura de operación ..	$6.5 < pH < 7.2$
TEMPERATURA DE LA SOLUCION		30°C
PRESION DE PULVERIZACION		1 - 1.5 Kg/cm^2
VELOCIDAD DE PRODUCCION DE NIEBLA SALINA		1 - 2 ml/hora.
SECUENCIA DE PULVERIZACION		10 minutos/hora

TABLA II .- VARIACION DE LA DUREZA DE LAS LAMINAS DE PVF DESPUES DE EXPUESTAS 2000 HORAS.

DUREZA (En segundos Persoz)			
SIN EXPONER (Probetas patrón)	CAMARA CLIMATICA	CAMARA DE NIEBLA SALINA	INMERSION EN AGUA DE MAR
33-42 (39.7)	46-52 (48.5)	46-47 (46.5)	40-41 (40.5)

TABLA III.- VARIACION DE LA ADHERENCIA DE LAS LAMINAS DE PVF DESPUES DE EXPUESTAS 2000 HORAS

Adherencia ($Kg.cm^{-2}$)			
Sin exponer (Probetas patrón)	CAMARA CLIMATICA	CAMARA DE NIEBLA SALINA	INMERSION EN AGUA DE MAR
18	10	10	10

TABLA IV.- MEDIDAS DE IMPEDANCIA ELECTROQUIMICA

HORAS DE EXPOSICION	TIPO DE EXPOSICION		
	CAMARA CLIMATICA	CAMARA DE NIEBLA SALINA	INMERSION
200	tg δ = 0.31	tg δ = 0.24	tg δ = 0.08
500	tg δ = 0.14	tg δ = 0.38	tg δ = 0.42
1000	----	(Dos arcos capacitivos) Wmáx = 228 Hz R = 0.8M Ohm.cm^{+2} C = 50 μF. cm^{+2} Wmáx = 72 Hz R = 6.5M Ohm.cm^{+2} C = 50 μF.cm^{-2}	Wmáx = 1.3 KH_2 R = 6.15M Ohm.cm^{+2} C = 39 μF.cm^{-2}
1500	(tres arcos capacitivos) Wmáx = 15.8 KHz R = 0.22M Ohm.cm^{+2} C = 0.24 μF.cm^{-2} Wmáx = 158 Hz R = 1.68M Ohm.cm^{2} C = 0.6 μF.cm^{-2} Wmáx $\lesssim$ 1Hz R = sin resolver	(Dos arcos capacitivos) Wmáx = 21.97 KHz R = 0.074MOhm.cm^{+2} C = 0.25 μF.cm^{-2} Wmáx = 3.52 KHz R = 0.12M ohm.cm^{+2} C = 0.5 μF.cm^{-2}	(Dos arcos capacitivos) Wmáx > 10 KHz R = 0.070MOhm.cm^{+2} C = 1.18 μF.cm^{-2} W máx $\simeq$ 900 Hz R = 5.7M Ohm.cm^{-2} C = 0.70 μF.cm^{-2}
2000	Wmáx = 55 MHz R = 0.8K Ohm. cm^{2} C = 12 μF. cm^{-2} Wmáx = 96 Hz R = 40 KOhmcm^{2} C = 41 μF. cm^{-2}	(Dos arcos capacitivos) WMáx = 30 KHz R = 0.97K Ohm.cm^{2} C = 39 μF.cm^{-2} Wmáx = 0.16 Hz R = 14 KOhm.cm^{2} C = 1.3 μF.cm^{-2}	(Dos arcos capacitivos) Wmáx = 5.9 KHz R = 0.012M Ohm.cm^{2} C = 3.06 μF.cm^{-2} Wmáx = 305 Hz R = 97 KOhm. cm^{2} C = 5.36 μF.cm^{-2}

TABLA V .- EXAMEN VISUAL MEDIANTE LUPA DE AUMENTO DE LA SUPERFICIE DEL ACERO DESPUES DE LA EXPOSICION

HORAS DE EXPOSICION	TIPO DE EXPOSICION		
	CAMARA CLIMATICA	CAMARA DE NIEBLA SALINA	INMERSION
200	Iniciación de puntos de óxido. Línea de óxido en el empalme de las láminas	No hay indicación de óxidos	No hay indicación de óxidos
500	Iniciación de puntos de óxido. Línea de óxido en el empalme de las láminas	Iniciación de puntos de óxido. Línea de óxido en el empalme de las láminas.	No hay indicación de óxidos.
1000		Puntos de óxido aislados. Línea de óxido en el empalme de la lámina.	No hay indicación de óxido. Línea de óxido en el empalme de la lámina.
1500	Puntos de óxido uniformemente distribuidos por toda la superficie	Puntos de óxido aislados de mayor tamaño que a 1000 horas.	Iniciación de puntos de óxido aislados.
2000	Puntos de óxido uniformemente distribuidos por toda la superficie y de mayor dimensión que a 1500 horas.	Puntos de óxido aislados de tamaño similar y distribución que a 1500 horas.	Puntos de óxido uniformemente distribuidos por toda la superficie, de muy pequeño tamaño.

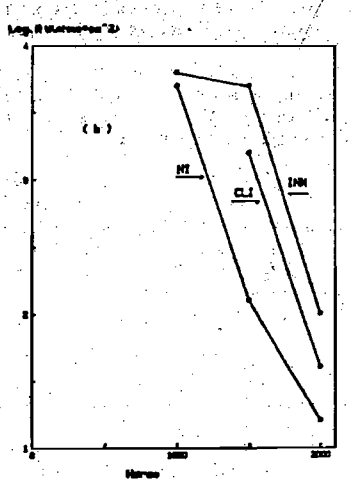

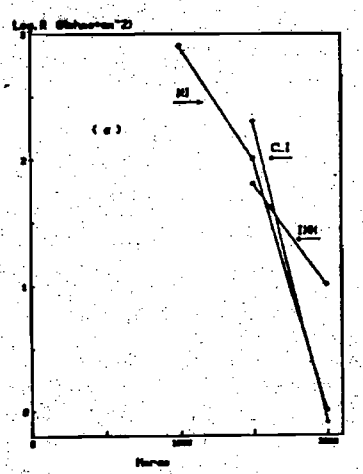

Fig. 1 .- Comportamiento de las probetas a partir de 1000 horas de exposición, mediante medidas de impedancia electroquímica. a) A altas frecuencias, b) a bajas frecuencias.

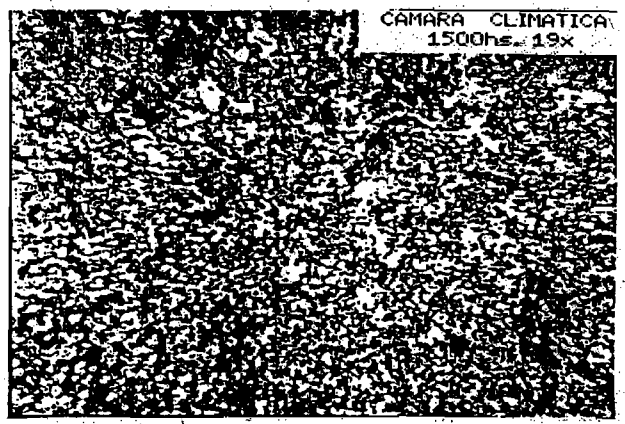

Fig. 2 .- Presencia de puntos de óxido sobre la superficie del acero después de estar sometida la probeta en cámara de niebla salina durante 1500 horas.

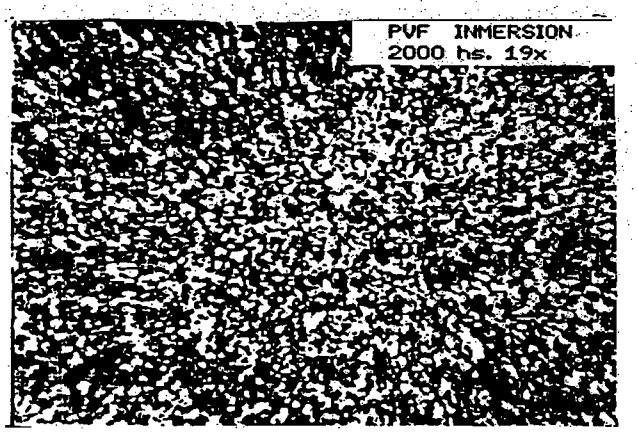

Fig. 3 .- Presencia de puntos de óxido sobre la superficie del acero, después de estar sometida la probeta en inmersión en agua de mar durante 2000 horas (x19).

COMPORTEMENT DE QUELQUES ALLIAGES CU-ZN A LA CORROSION DANS L'EAU DE MER.

Emanuele D. MOR

ELECTROCHIMIE - UNIVERSITE' de GENES - ITALIE

RESUME

L'addition d'Al (2,2%) ou d'Sn (1,12%) aux laitons α (70 Cu - 30 Zn) empêche leur corrosion en eau de mer calme à 40°C.
L'effet inhibiteur pour les laiton à l'Al influence le processus tant anodique que cathodique, ce qui est dû à la formation d'un film d'oxydation avec ségrégation en surface de composés d'Al et Mg qui présentent un effet de passivation synergique en réduisant la porosité du film d'oxydation et en empêchant la formation d'acidité locale qui entraîne la corrosion localisée.
L'effet d'inhibition de l'étain semble principalement dû à la diminution de la vitesse de réduction du processus cathodique à cause de la formation d'un film d'oxydes d'étain, qui se réduisent moins que les composés du cuivre.

SUMMARY

The addition of Al (2,2%) or Sn (1,12%) to the α brass alloys inhibits their corrosion in non stirred seawater at 40°C.
For Al brass the inhibiting effect influences both the cathodic and the anodic process and this is due to the formation of an oxidated film with segregation on the surface of Al and Mg compounds that have a synergistic passivation effect by decreasing the porosity of the oxidation layer and avoiding to formation of local acidity leading to localized corrosion.
The inhibiting effect of Sn seems to be mainly due to the decreased rate of the cathodic reduction process, because a layer of Sn oxides, that are less reduced with respect of the Cu compounds, is formed.

INTRODUCTION

The addition of small amounts of some elements Al or Sn $\leq$ 2% to Cu-Zn alloys increases their resistance to generalized corrosion in sea water (1-2).

The presence of Sn in OTS/70 alloys (admiralty brass) according to some authors seems to affect the microstructure (3), the number of defects (4) or the segregation of the alloy; according to other, however, it causes changes in the properties of the passivation film forming on the alloy (5).

The addition of Al to the Cu-Zn alloy (aluminum brass) seems to influence the composition and the passivating effect of the oxidation layer formed during the corrosive process (6-7) rather than the microstructure of the alloy. Different hypotesis are reported on the composition of this oxidation layer. According to some workers, Al is present under the form of an oxide, coprecipitated with the copper oxide in a structure of Me^{++} - M^{+++} hydroxides (7) or under the form of hydrated oxide coprecipitated with $Mg(OH)_2$.

According to Castle (8-9) aluminum is present in the corrosion products under the unique form of Al and Mg oxycarbonate (hydrotalcite). Previously published researches (10-11) showed that aluminum is present under two different forms: a compound (oxide or oxidrate) where Al is the unique cation, and a double salt coprecipitated with a bivalent metal (Mg) that exhibits with Al a synergistic action in the protection against corrosion.

In order to verify if the presence of some alloying elements influences the corrosion kinetics of α brass it seemed advisable to compare the behaviour of different alloys, one of which did not contain Sn and Al, while the other respectively contained 1,12% of Sn and 2,2% of Al.

Experimental

Copper-zinc alloys specimens (Table 1) annealed at 600°C in argon atmosphere for 2 hours, were slowly cooled (for 12 hours) to room temperature, polished with emery paper 600 and washed with CCl_4 before being immersed in seawater at pH 8.2 at the temperature of 40°C.

The corrosive solution was not stirred during the specimens treatment.

The weight loss measurements were carried out by using rectangular specimens (4x1. 84x0.1 cm) with exposure time of 24, 48, 120, 240 and 360 hours and was obtained by adding to the amounts of Copper and Zinc solubilized during the specimens exposure the amounts of the same metals still adhering to the specimen surface under the form of corrosion products.

The corrosion products adhering to the metal surface were examined by X-rays diffractometry, with a C.G.R. instrument by using the CuK α line (14 mA, 50 KV).

The chemical analysis was carried out after treatment of the corroded specimens with a suitable series of specific solvents (aqueous solutions of glycine, NH_4OH etc.) that permitted the selective dissolution of the various corrosion products by leaving rather unchanged the metallic matrix. (12)

The cations (Cu^+, Cu^{++}, Al^{+++}, Sn^{++}, Mg^{++}, Na^+) and anions (Cl^-, CO_3^{--}, SO_4^{--}) solubilized during the selective attack were determined by various analitical techniques (flame atomization and graphite furnace AAS, ionic chromatography, gas chromatography of the evolved CO_2 for analysis of the carbonates).

Electrochemical tests were performed by using cylindrical specimens (1.9 cm diam., 0.5 cm thick) embedded in epoxy resin. On specimens immersed for 2 and 360 hours in the corrosive solution, potentiodynamic polarization experiments were carried out with scanning speed of 250 mV/h, obtaining the corrosion density current (i_{corr}) and the polarization resistance (Rp).

At regular intervals during the exposure time, measurements of the free corrosion potential with respect of the standard calomel electrode (S.C.E.) were made.

Results and discussion

The weight loss values (Fig. 1) show that the average corrosion rate of the aluminum containing alloy is neatly lower than the corrosion rate of the other alloys within the entire exposure time. This is confirmed by the i_{corr} and R_p^{-1} values (Table 2), calculated from the Tafel straight lines obtained from the potentiodynamic plots made on the specimens after two hours (Fig. 2) and 360 hours (Fig. 3) of exposure.

The smaller corrodibility of aluminum brass is due, almost for short immersion times, to the decrease of the anodic process owing to the formation, at potential values between -250 and -220 mV (SCE), of a film probably formed by copper and Al compounds that inhibit the anodic process in the -150 and -80 mV (SCE) range.

The oxidation layer, whose presence is seen by anodic polarization, should inhibit the anodic process in the free corrosion because its formation potential (-250 to -220 mV) is near to the equilibrium potential of aluminum brass (about -280 mV). For long immersion times, (360 hours, see Fig. 3 and Table 2) aluminum brass shows both anodic and cathodic inhibition with respect of the other two tested alloys, that exhibit a quite similar behaviour.

The cathodic reduction mechanism is the same for all the tested alloys, because the slopes of the Tafel straight lines do not appreciably change and the small peaks of the cathodic side of the polarization plots are in the same range of potential (-400 to -500 mV) and may correspond to the $Cu^{++} \rightleftarrows Cu^+ + e^-$ transition of the bivalent copper compounds, that takes place in the range between -350 and -450 mV (13).

The SEM examination (x 1500 enlargement) of the metal matrix of the specimens after dissolution of the corrosion products showed the different behaviour of the corrosive attack of the three alloys. The corrosion of the Al containing alloy is uniform (see Fig. 4a) without preferential dissolution.

The two alloys OTS/70 and Cu-Zn 70/30 show localized corrosion phenomena with preferential dissolution. Figs. 4b and 4c show dezincification plugs of the alloys after 360 hours.

The dezincification tendency of OTS/70 and Cu-Zn 70/30 alloys is confirmed by the results of chemical analysis, that permits a dezincification factor, F_Z, shown in Fig. 5 as a function of the exposure time, to be calculated by the

$$F_z = \frac{Zn_{exp.}}{Cu_{exp.}} \times \frac{Cu_{th}}{Zn_{th}}$$

where Zn_{exp} and Cu_{exp} are the amounts (ug cm^{-2}) of oxidated copper and zinc experimentally measured as the sum of the solubilized amounts and of those adhering to the specimens (under the form of corrosion products), and Zn_{th} and Cu_{th} are the percentages of the two metals in the original alloy.

The smaller average corrosion rate of aluminum brass and the absence of localized corrosion may depend (10-11) on the composition and structure of the oxidation layer, where Al compounds, coming from the dissolution of the alloy, and Mg compounds, coming from seawater, have a synergistic passivating effect (Table 3). Al compounds decrease the porosity of the corrosion products layer and Mg compounds provide a solid reserve against development of local acidity.

The physico-chemical properties and the behaviour of the oxidation layer on aluminum brass are therefore different from these of the corrosion products of the other alloys, notwithstanding the main components are the same (Tables 4,5,6).

The low porosity of the oxidation layer on aluminum brass may enhance the concentration of the metal/oxide interface of Cu^+ ions, whose diffusion through the oxidation layer is inhibited and that are precipitated into the film as Cu_2O, as soon as its solubility product is reached.

The Cu^+/Cu^{++} ratio changes as a function of the exposition time for the different alloys (Fig. 5) showing that Cu^+ is the prevailing ionic species in the aluminum brass corrosion products and that Cu^{++} is predominant in other two alloys. The formation of bivalent copper compounds, due to oxidation in the corrosive solution of Cu^+ ions diffusing through the passivation film, takes place on the oxide-solution interface by sedimentation of successive layer of precipitated corrosion products. The formation of Cu^+ compounds takes place on the metal/oxide interface and the film grows from the inner face, the oxidation films are also permeated by the Zn^{++} ions, whose concentration in the oxidated layer is inversely correlated with the film permeability and with the concentration of Cu^+ ions.

This is confirmed by the behaviour of the Cu^+/Zn^{++} ratio as a function of the exposure time (Fig. 6).

The Cu/Zn and OTS/70 alloys have the same composition, except for the addition of 1.12% Sn to the latter, and yield the same corrosion products with similar concentration but the corrosion rate of Cu/Zn is about twice that of OTS/70.

The average concentration of Sn in the corrosion products (Table 4) is low and does not appreciably differ from that found in the alloy.

In the corrosion products, Sn is oxidized and with a valence different from 2, because it is not dissolved by the glycine that solubilizes the bivalent compounds.

The potentiodynamic plots for specimens corroded 360 hours (Fig. 3) show that the inhibiting effects is due to a small decrease of the cathodic process rate, in the potential interval close to the free corrosion potential, where the cathodic reduction current is mainly due to the reduction of the oxidation products of the base metals.

Conclusions

The addition of Sn or Al has an inhibiting effect on the average corrosion rate of the α brass alloys, but the mechanisms due to the two metals are different.

For aluminum brass the inhibition influences both the anodic and the cathodic process and is due to the segregation on the surface of the oxidated layer of Al and Mg compounds that have a synergistic passivation action, by decreasing the porosity of the oxidation film and inhibiting both the localized corrosion and the selective dissolution of Zn.

The inhibiting effect of Sn seems to be mainly due to the decrease of the cathodic reduction process.

References

1. - Taylor A.H. : J. Electrochem. Soc. 1971, 118, 834
2. - Heidersbach R.H. : Corrosion 1968, 24, 38
3. - Pugh E.N.-Craig J.V.-Sedkris A.J.: Paper presented at the International Conference on Fundamental Aspects of Stress Corrosion Cracking - Ohio State University - Columbus Ohio - September 1967.
4. - Delouze L. - Dervythere A.: Acta Metall 1967, 15, 727
5. - Hoar T.P. - Booker C.J.L.: Corros. Sci. 1965, 5, 821
6. - Thomas G.J. - Price L.E.: Nature 1938, 141, 8310
7. - Sury P. - Oswald H.R.: Corros. Sci. 1970, 12, 77
8. - Castle J.E. - Parvizi M.S.: Proc. Conf. of Copper Alloys in Marine Environments seminar - Paper n. 10 Copper Development Association 1985.
9. - Castle J.E. - Epler D.C.: Inst. Corros. Sci./Inst. Chem. Eng. Conference on Progress in the prevention of Fouling in Industrial Plant. University of Nottingham U.K. 1-3 April 1981
10. - Epler D.C. - Castle J.E.: Corrosion 1979, 35, 10, 451
11. - Castle J.E. - Parvizi M.S.: Corrosion Prev. and Control 1986, 33,1,5
12. - Mor E.D. - Beccaria A.M.:Proc. 3rd Intern.Congr. on Marine Corrosion and Fouling - Washington 1972, 427.
13. - Shams El Din A.M. - Abd En Wahab F.M.: Corros. Sci. 1977, 11, 49.

TABLE I

Composition of the used copper alloys samples (weight percent.)

Alloy	Cu	Sn	Al	Pb	As	P	Ni	Fe	Zn
Cu - Zn	70.3	0.001	0.002	0.008	0.020	0.0015	0.002	0.005	bal
OTS/70	70.61	1.12	0.002	0.001	0.024	0.001	0.020	0.006	bal
Al brass	77.22	0.005	2.20	0.005	0.024	0.001	0.002	0.006	bal

TABLE 2

Tafel slopes, corrosion density current, polarization conductance and corrosion potential of copper alloys in sea water.

Alloys	Exposure h	β_a mV/dec	β_c mV/dec	i_{corr} $\mu A.cm^{-2}$	R_p^{-1} $\mu A.V^{-1}\ cm^{-2}$	E_{corr} mV (SCE)
Al brass	2	31.4	- 27	0.399	63	- 300
	360	59.9	-160	0.076	4	- 287
CTS/70	2	62.8	- 78.7	1.240	82	- 304
	360	64.6	-131	0.250	13	- 289
Cu/Zn 70/30	2	43.9	- 54	5.75	237	- 278
	360	36.7	-108	0.305	26	- 254

TABLE 3

Chemical analysis of aluminum brass corrosion products in sea water.

The values of the various elements ($\mu g.cm^{-2}$) are averaged of 3 determinations values.

t h	Cu^{++}	Cu^{+}	Zn^{++}	Al^{+++} glic.	Al^{+++} ox	Mg^{++}	Cl^{-} glic.	Cl^{-} NH_4OH	CO_3^{--}	SO_4^{--}
48	24.7	17.0	14.7	0.65	0.42	0.49	0.94	5.5	0.94	2.58
90	15.1	42.1	14.8	0.74	0.81	0.52	1.00	1.1	0.82	2.62
120	17.5	28.9	15.6	0.76	0.46	0.56	1.40	1.1	1.53	3.70
240	18.0	39.9	17.6	1.00	0.57	0.65	0.16	0.4	1.77	4.07

TABLE 4

Chemical analysis of OT5/70 corrosion products in sea water.

The values of the various elements ($\mu g.cm^{-2}$) are averaged of 3 determinations values.

t h	Cu^{++}	Cu^{+}	Zn^{++}	Sn^{++}	Mg^{++}	Cl^{-} glic.	Cl^{-} NH_4OH	SO_4^{--}	CO_3^{--}
24	1.53	0.39	2.04	0.029	0.63	0.7	0.10	2.35	0.71
48	1.64	0.39	3.48	0.030	0.49	1.63	0.05	7.40	0.74
90	5.85	0.26	6.61	0.030	0.71	1.83	—	6.74	0.66
120	4.52	0.31	46.96	0.82	0.96	2.60	—	9.79	1.09
240	10.66	0.26	64.38	0.85	0.81	0.60	—	5.67	0.82
360	23.01	0.31	110.91	1.82	1.28	0.60	—	3.91	1.26

TABLE 5

Chemical analysis of Cu-Zn 70/30 corrosion products in sea water.

The values of the various elements ($\mu g.cm^{-2}$) are averaged of 3 determinations values.

t h	Cu^{++}	Cu^{+}	Zn^{++}	Mg^{++}	CO_3^{--}	Cl^{-}	SO_4^{--}
6	10.84	1.01	18.99	0.53	0.30	0.4	1.42
28	6.48	3.54	22.48	0.61	0.61	1.3	2.52
66	17.34	4.14	54.07	1.61	0.90	1.5	3.50
90	11.77	4.50	76.84	5.88	20.2	2.2	6.50
118	21.79	4.48	93.71	5.00	20.2	3.0	6.52
241	52.05	5.17	191.00	4.86	10.7	4.5	8.20
364	43.08	6.37	200.00	5.00	12.21	6.7	8.78

TABLE 6

X Ray diffractometric analysis of copper alloys corrosion products after 360 h exposure in sea water.

Alloy	Identified compounds
Al brass	$CuCO_3.Cu(OH)_2$ 10-399; Cu(OH)Cl 23-1063; CuO 5-661; Cu_2O 5-667; $Mg_6Al_2CO_3(OH)_{16}.4H_2O$ 14-191 22-700; AlO(OH) 20-364
OTS/70	Cu_2O (5-667); Cu_2O (5-661); $CuCO_3.Cu(OH)_2$ 10-399;
Cu-Zn 70/30	$Cu_2(OH)_3Cl$ 2-146; CuO 5-661; Cu_2O 5-667; $CuCO_3.Cu(OH)_2$ 10-399

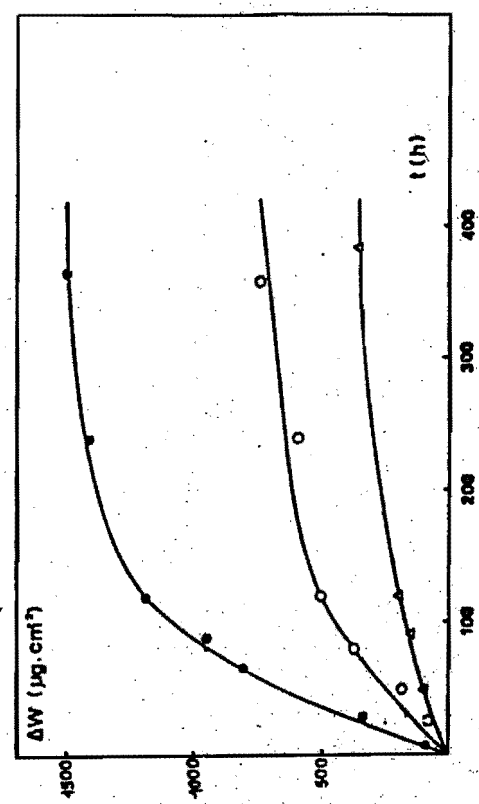

Fig. 1 - Weight loss of copper alloys specimens in sea water at 40°C
●-● Cu-Zn 70/30; o-o OTS/70; Δ-Δ Al brass.

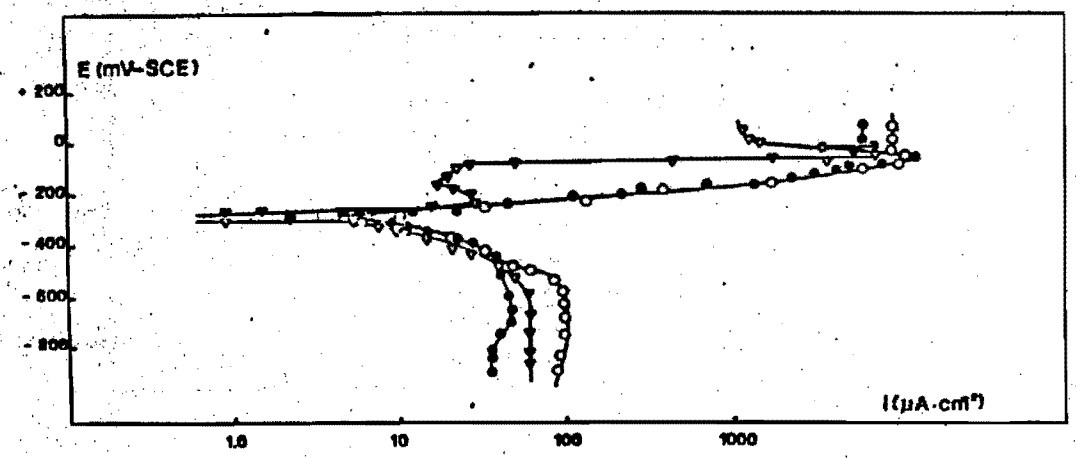

Fig 2 – Polarization curves of copper alloys after 2h of exposure time in sea water
o–o Cu Zn 70-30; e–e OTS/70; Δ–Δ Al brass.

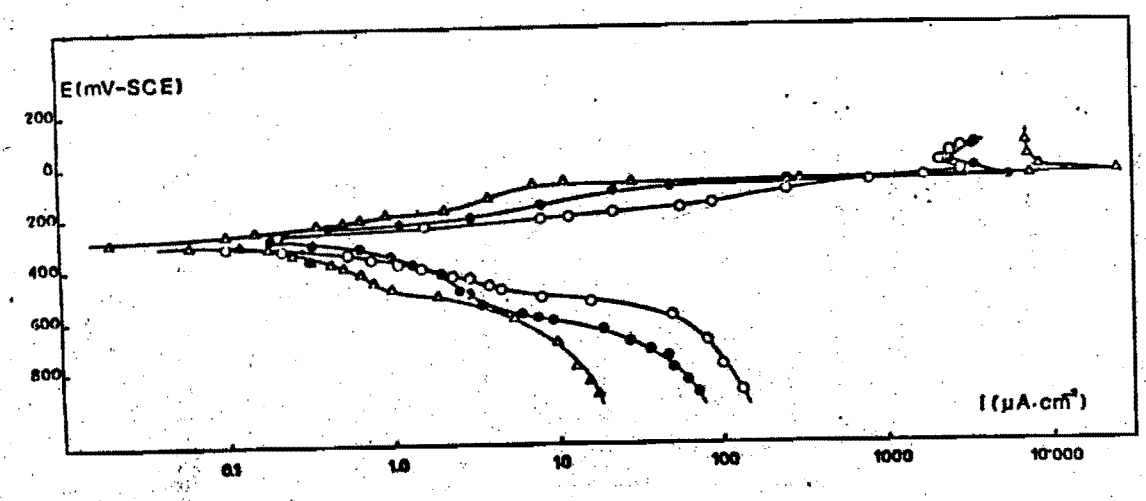

Fig.3 Polarization curves of copper alloys after each of exposure time in sea water
o–o Cu Zn 70/30; e–e OTS/70; Δ–Δ Al brass.

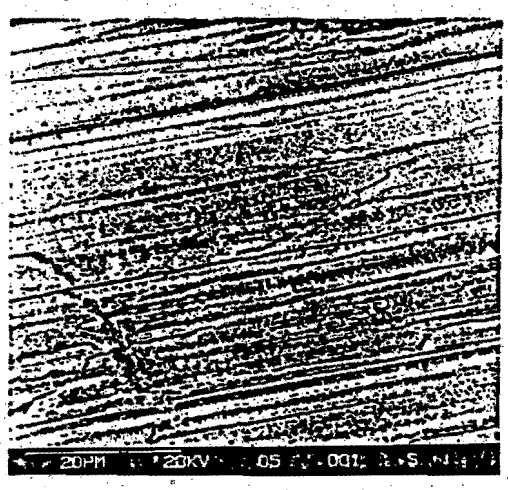

a

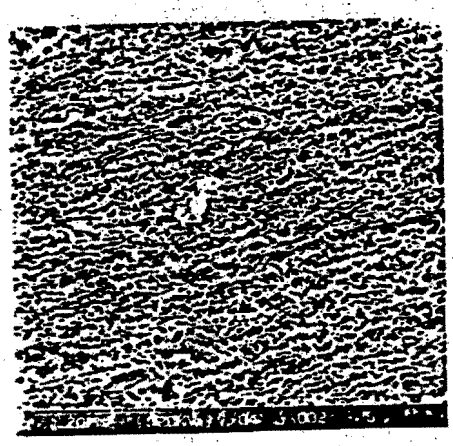

b

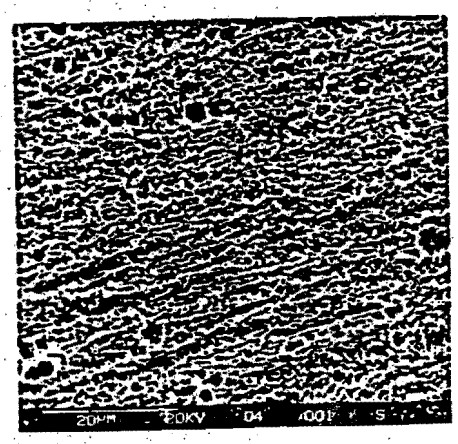

c

Fig. 4 - Surface appearance of Al brass (4a), OTS/70 (4b) and Cu-Zn 70/30 (4c) corroded in sea water at 40°C.

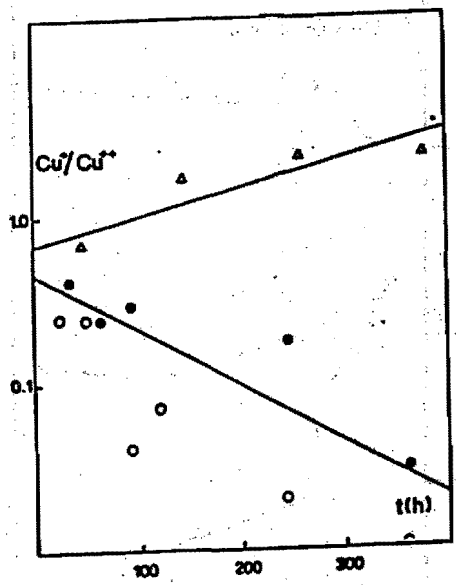

Fig.5 Cu^{+}/Cu^{++} ratio in the corrosion products of •-• Cu/Zn 70/30; ○-○ OTS/70 and ▲-▲ Al brass in sea water

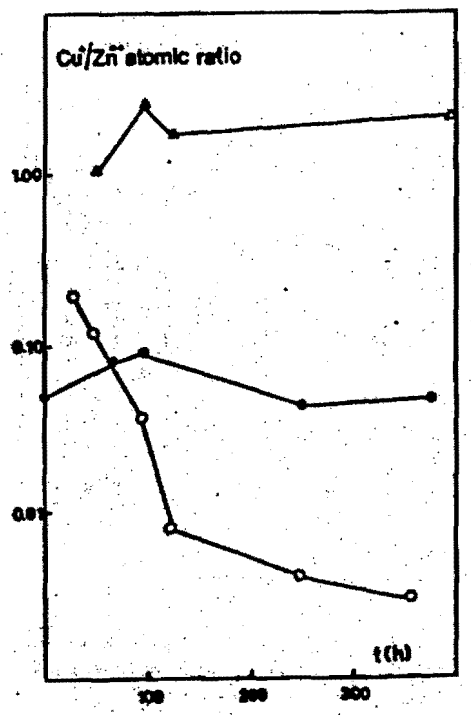

Fig. 8 Cu/Zn atomic ratio in the corrosion products of o-o Cu-Zn 70/30;o-o CT 3/8 and — Al brass in sea water

PROTECCION CATODICA DEL INTERIOR DE UN SISTEMA DE TUBERIAS DE AGUA DE REFRIGERACIÓN

Por J. Ladera*; E. Cucarella** y M.A. Guillén***

1. INTRODUCCION

La protección catódica técnica que puede aplicarse para la protección de cualquier metal en contacto con un electrolito, es muy conocida en sus aplicaciones en la protección de estructuras marinas, depósitos y tuberías enterradas por el exterior, etc. Sin embargo su aplicación al interior de tuberías, la experiencia es más reducida.

En tuberías de gran diámetro es posible la utilización de ánodos de sacrificio, pudiéndose asegurar una vida de los ánodos lo suficientemente dilatada que justifique económicamente el sistema. En tuberías de diámetro pequeños: solo el sistema de corriente impresa es aplicable.

Para la realización de la protección catódica mediante corriente impresa del interior de un tubo se utilizan, en general, ánodos de titanio platinado en forma de lanza. El ánodo, o electrodo dispersor de corriente, atraviesa de forma perpendicular la pared de tubo al cual se sujeta mediante una cabeza que se rosca a un manguito roscado, previamente soldado al tubo. Hay que resaltar la información que a este respecto facilita J.H.MORGAN (1) según el diámetro de los tubos habrá que colocar un ánodo de lanza cada 2, 3, 20 metros, lo que hacía muy costoso el sistema así como complicada la instalación. Si la tubería estaba bién revestida por el interior, la separación entre ánodo puede llegar a alcanzar los 50 metros, en comparación a los 4,5 metros que requeriría una tubería desnuda. La Fig. 1 ilustra sobre todas estas circunstancias que consideramos que son de interés.

(*) (**) Ford España, s.A. - ALMUSAFES (Valencia)

(***) Instituto Español de Corrosión y Protección - MADRID

TABLA I

Características fisico-químicas del agua de refrigeración.

pH	7,6
Resistividad	715 Ω x cm.
Dureza total (TH)	65,8° F
T.A.C.	27,5° F
Calcio (Ca^{2+})	155,0 mg Cl
Magnesio (Mg^{2+})	65,9 "
Sodio (Na^{+})	95,4 "
Potasio (K^{+})	3,0 "
Cloruros (Cl^{-})	177,5 "
Nitratos (NO_3^{-})	66,0 "
Sulfatos (SO_4)	28,0 "
Bicarbonatos (HCO_3^{-})	335,3 "
Silice (SiO_2)	16,5 "

F.L. LAQUE (2) operando con un tubo de 900 mm. de diámetro y situando un ánodo de magnesio en su centro atribuyó la propagación de la protección a la formación de una capa calcárea aislante, la evolución del potencial fue un proceso lento que duró alrededor de cinco semanas.

Hay que señalar finalmente, el interesante trabajo realizado por D.J. TIGHE-FORD y J.N. Mc Grath (3) que encuentran, en un estudio realizado a escala de laboratorio, utilizando tubos de 1 metro sin circulación de agua, de cobre y de acero suave, de 38 y 27 mm. de diámetro, que el potencial en función del tiempo se desarrolla por el interior de los tubos.

Con esta breve introducción queremos hacer ver, que hasta hace poco tiempo, se podia considerar como inviable la protección catódica del interior de un tubo, ya que sólo se conseguia la protección de unos pocos metros a partir de los electrodos dispersores de corriente.

En el trabajo que se va a exponer iniciado en Noviembre de 1983, se va a ver con resultados en trabajo real y a lo largo de casi 5 años, como se extiende la protección a lo largo de muchos metros a partir del electrodo/ dispersor de corriente.

2. PARTE EXPERIMENTAL

Los circuitos de refrigeración de los robots de soldadura de la planta de Ford en Almusafes (Valencia) están constituidos por unas tuberias de impulsión y retorno en acero y un diámetro de 250 mm. El óxido que se produce en la corrosión interior de los tubos, arrastrado por el agua, obstruye los circuitos de refrigeración de los robots ocasionando graves problemas. Las características del agua de refrigeración se agrupan en la Tabla I.

Este agua tiene un componente salino alto lo que se traduce en una resistividad baja. La concentración de calcio/ y bicarbonatos hace pensar en que pueda ser incrustante, es decir, que sea capaz de formar una capa calcárea que recubra interiormente el tubo. Si así fuera este recubrimiento tendría un gran interés a efectos de la protección catódica.

Este agua era tratada con inhibidores, verificándose mediante un simple ensayo de medida de pérdida de peso, que/ el agua tratada daba lugar a los mismos problemas de corrosión que el agua sin tratar, por lo que se tomó la decisión de cortar la adición de inhibidores y montar en plan experimental en un tramo de 100 m. de tuberia de la planta de/ carrocerias un sistema de protección catódica por corriente impresa.

2.1. INSTALACION DEL SISTEMA DE PROTECCION CATODICA POR CORRIENTE IMPRESA.

Como indica la figura 2, inicialmente se montó un sistema de protección catódica por corriente impresa tradicional. Como electrodo dispersor de corriente se utilizó alambre de titanio platino. Este alambre estaba platinado a intervalos de 10 mm. cada 100 mm. y unos separadores en material plastico aseguraban un correcto aislamiento del alambre frente al tubo. Se cubrian asi 84 metros de tuberia. Se establecieron unos electrodos de referencia como control montados de forma permamente, estos electrodos son de cinc puro, su situación se esquematiza en la figura 2. En la parte central se preparo un injerto de 200 mm., por el que se introdujo el alambre de Ti-Pt y en su tapa se fijaron los alambres y se hizo la inyección de corriente. Se colocó tambien un purgador automático con objeto de eliminar el aire o gases que se pudieran producir.

Como rectificador se utilizó uno que permite una salida de 15A de corriente rectificada a 12V. La regulación del voltaje se realiza mediante un autotransformador de forma/ continua.

2.2 PUESTA EN MARCHA.

Cada tramo de 42 metros lineales tienen una superficie/ a proteger de 33 m^2. Dada la fuerte corrosión que tienen los tubos por su interior, aparecen con alguna frecuencia/ poros y perforaciones, se tomó la decisión de aplicar una/ densidad de corriente de 125 mA/m^2. Según esto la intensidad total que se necesita por tramo es de 4 Amperios.

Se activó el alambre de la izquierda aplicando en él -- los 8 amperios, que se consiguieron a 6V y seguidamente se procedió a medir el potencial en todos los electrodos de referencia, tanto en los que correspondian a ese alambre,- como al del otro que estaba sin activar.

El resultado obtenido fue sorprendente ya que de forma/ inmediata se conseguia la protección no sólo en la zona -- del electrodo de referencia que estaba dentro del radio de acción del alambre de Ti-Pt, cosa totalmente normal, sino en los otros dos que correspondian al alambre de Ti-Pt todavía sin activar, el más alejado se encuentra a 44 metros de la zona más próxima del alambre activado. Todo esto ocurria en la dirección del flujo, ya que en contra de él, a/ tan sólo 1 metro de distancia, la zona del electrodo de referencia 3 queda sin protección.

Estos resultados motivaron a que se siguiera trabajando con solo este alambre, acabando finalmente por recuperar el alambre no activado y situarlo en la zona de retorno, tal y como se indica en la figura 3. El electrodo de referencia 1 bis fue tambien trasladado al otro tramo.

En el retorno la experiencia fue la misma por lo que vamos a tratar solamente los resultados de la impulsión.

3. RESULTADOS

Ante el gran volumen de resultados obtenidos, se ha tratado de conseguir unos valores medios orientativos de la evolución del potencial en función del tiempo expresado en horas. La Tabla II agrupa todos estos resultados, que han/ sido representados en la figura 4.

A la vista de la figura 4 se ve que en la zona influenciada por el alambre de Ti-Pt de forma directa existe una/ sobreprotección elevada llegandose a alcanzar potenciales/ con respecto al electrodo de referncia de cinc de -1000 mV (el potencial de protección con respecto a este electrodo/ es de + 220 mV) el potencial de protección se consigue de/ forma instantanea. Se observa que cuando la intensidad pasa de 9 a 6 Amperios el potencial sigue subiendo, siendo muy fuerte la polarización. Seguidamente, se inicia un punto de inflexión en el que el potencial comienza a descender aún a una intensidad de corriente más elevada 9 Amperios, lo cual puede indicar que las circunstancias experimentales, como oxígeno disuelto en el agua, temperatura, velocidad de flujo pueden variar y generar una corrosión más intensa que puede requerir unas densidades de corriente mucho más elevadas.

Dada la excesiva polarización en esta zona se redujo a 7 Amperios la intensidad cayendo el potencial a un valor de + 86 mV; teniendo en cuenta que las otras curvas a penas se modificaban con estos descensos de intensidad, se redujo esta a 4 Amperios, consiguiendo que a este valor el potencial se estabilice en los 3 puntos de medida y que el punto 3, el que está a 1 metro del alambre de Ti-Pt pero en contra -

TABLA II

Valores medios de intensidad de corriente y potenciales medidos en los 3 puntos de control frente al electrodo de referencia de Zn puro. Se dan los tiempos totales y parciales de intensidad y potencial.

INTENSIDAD (A)	TIEMPO (HORAS)	POTENCIALES ER 1	ER 2	ER 3	OBSERVACIONES
0	0	+ 506	+ 484	+ 567	Si paso de corriente.
8	3	+ 296	+ 86	+ 354	
8	24	+ 113	- 15	+ 300	
8	120	+ 96	- 100	+ 393	Tiempo parcial 120 h.
9	850	+ 110	- 223	+ 324	Tiempo parcial 730 h.
6	1500	+ 124	- 459	+ 486	Tiempo parcial 6650 h.
6	2200	+ 173	- 675	+ 435	
6	3000	+ 188	- 877	+ 447	
6	3700	+ 158	- 999	+ 488	
6	4500	+ 127	- 954	+ 493	
6	5200	+ 159	- 834	+ 432	
6	7500	+ 175	-1050	+ 370	
9	10000	+ 200	-1130	+ 380	Tiempo parcial 2500 h.
7	13500	+ 300	- 513	+ 280	Tiempo parcial 9500 h.
7	16500	+ 179	+ 86	+ 154	
7	19000	+ 200	+ 162	+ 218	
4	24000	+ 137	+ 108	+ 140	Tiempo parcial 5000 h.

del flujo pasase la frontera del nivel de protección.

La zona fuera de la acción del alambre de Ti-Pt y concretamente el punto más alejado, que es el punto 1 de medida, situado a 200 diámetros (50 metros) de la inyección de corriente, a las 72 horas estaba perfectamente protegido y así permanece sin que las variaciones de intensidad/ le afecten en nada significativo (Tabla II), el potencial a lo largo del tiempo ha permanecido practicamente constante.

El punto 3, el situado más cerca de la inyección de corriente, pero en contra corriente del flujo, ha tenido un potencial bastante constante pero siempre por debajo del/ nivel de protección. Las variaciones de intensidad tampoco parecen afectarle, excepto si estas son bajas, con 4 - Amperios se ha conseguido pasar el potencial a un buen nivel de protección (+ 140 mV) donde permanece despues de - varios miles de horas.

La velocidad de flujo del sistema de refrigeración es/ de 0,5 m/s y a esta velocidad, suponemos que más o menos/ constante dentro de un trabajo industrial, esta actuando/ la protección catódica. Ahora bien, era interesante conocer las variaciones que podia experimentar el potencial -- con èl agua estática. Para esto, se han aprovechado los momentos en que por razones de fabricación las bombas estaban paradas y por tanto no habia circulación de agua. La/ Tabla III agrupa los resultados obtenidos a lo largo de 8 paradas de las bombas, los intervalos de las paradas han/ sido siempre de 2 - 3 dias.

Se puede ver, que en general, en los puntos 1 y 2, en/ algún caso se acentua la polarización y en otros baja ligeramente, pero permanecen en los niveles altos de protección. El punto 3, por el contrario el estancamiento del - agua le favorece, así como las intensidades bajas de co-- rriente. Con 2 Amperios se obtiene un potencial de + 188mV,

TABLA III

Evolución del potencial en cada uno de los tres puntos de control en los periodos de tiempo en que no hay circulación de agua/ por estar las bombas paradas.

INTENSIDAD (A)	BOMBAS	POTENCIAL ER 1	ER 2	ER 3	OBSERVACIONES
8	marcha	+ 79	-343	+294	Intervalo del 16-18/12/83.
8	parada	+214	-248	+310	
8	marcha	+131	-370	+310	
8	marcha	+100	-220	+450	Intervalo 31/12/ 83 a 2/1/84.
2	parada	+106	-240	+188	
8	marcha	+ 92	-453	+504	
9	marcha	+118	-463	+500	Intervalo 7/1/ 84 a 9/1/84.
7,6	parada	+109	-190	+164	
8	marcha	+170	-430	+510	
7	marcha	+158	-528	+556	Intervalo 14/1/ 84 a 16/1/84.
7	parada	+160	-720	+521	
6,5	marcha	+132	-539	+555	
5	marcha	+135	-612	+376	Intevalo 10/2/ 84 a 12/2/84.
5,4	parada	+144	-630	+354	
5	marcha	+172	-654	+397	
6,7	marcha	+199	-1048	+466	Intervalo 24/3/ 84 a 26/3/84.
5,2	parada	+152	- 83	+256	
6	marcha	+157	-1112	+425	
7	marcha	+110	-865	+472	Intervalo 7/4/ 84 a 9/4/84.
7	parada	+113	-840	+483	
7	marcha	+141	-834	+418	
9	marcha	+181	-1463	+445	Intervalo 30/4/ 84 a 2/5/84.
8,4	parada	-146	+205	-227	
9	marcha	+190	-1410	+475	

partiendo de un potencial de corrosión de + 450 mV.

En un acero desnudo, si se corta el paso de corriente, la polarización debe de caer bruscamente, a no ser que sobre la superficie catódica se hayan podido formar recubrimientos calcáreos por la elevación del pH en la interfase metal-solución. La composición del agua con contenidos altos de HCO_3^- y Ca^{2+}, hacia pensar en la formación de estos depósitos calcáreos sobre todo en la zona de influencia del alambre de Ti-Pt, la rápida caida del potencial que pasa de -1400 a + 140 mV, hace pensar que estos recubrimientos no se han formado o si lo han hecho presentan una porosidad alta. Debido a la elevada polarización el potencial se estabiliza durante las 50 horas que permanece cortada la corriente sin llegar a entrar en niveles de corrosión.

En el punto 1, cuya polarización esta a niveles bastante ajustados de protección, el potencial pasa de + 160 mV (protección) a + 430 mV (corrosión) permaneciendo en corrosión durante todo el corte de corriente.

En el punto 3, con este corte de corriente se observa, que apenas el acero en esta zona está polarizado por el paso de corriente; el corte apenas le afecta y la caida de potencial es muy pequeña de + 420 mV a + 480 mV se eleva un poco el nivel de corrosión.

Cuando se reestablece la inyección de corriente el potencial en el punto 2 subre rápidamente pasando en 60 horas a - 850 mV, otra vez a valores de sobreprotección. En este mismo espacio de tiempo la curva correspondiente al/ potencial del punto 1 evoluciona y pasa de nuevo al nivel de protección y finalmente la curva correspondiente al punto 3 recupera la pequeña caida de tensión que experimentó y sigue evolucionando por debajo de los niveles de protección.

Se puede concluir este ensayo indicando que la fuerte caida de tensión que experimenta la tuberia cuando se suspende la inyección de corriente parece indicar que no hay/ formación de capas pasivantes o si las hubiera eran su acción protectora es muy pequeña.

En la actualidad la densidad de corriente que se está aplicando es de 60 mA/m^2, consiguiendose tal y como muestra la figura 4 un potencial uniforme en los tres puntos y todos en nivel de protección comprendido entre + 100 mV y + 200 mV.

4. DISCUSION

Se ha visto en todo lo expuesto anteriormente que el potencial se desplaza a lo largo de los tubos, como mínimo a 200 diámetros desde el punto de inyección de corriente. Varias son las causas que pueden intervenir en este proceso.

4.1 DESPOSITOS CALCAREOS

F. Laque (2) en ensayos de protecicón catódica interior de tuberías con ánodos de magnesio atribuyó el desplazamiento del potencial a la formación de una capa calcárea en la pared interior de los tubos. El mecanismo de formación de esta capa va siempre ligado a la elevación del pH en la interfase metal-solución, lo que normalmente ocurre en el cátodo por la reducción del oxigeno, por un lado, y la reducción de iones H^+ por otro.

Los estudios realizados por B.J. Tighe-Ford y J.N. McGrath (3) muestran que no existe diferencia en los resultados de los ensayos cuando se usa una solucion de NaCl al 3%, o agua de mar, lo cual parece indicar que en el interior de los tubos pueda no haber elevación del pH y, por tanto, reducción de oxigeno y, por tanto, no puede haber formación de depósitos calcáreos. Indudablemente si se formara capa calcárea se tenía

que manifestar en el potencial, lo cual, sin duda, consiguio F. Laque con su ánodo de magnesio, por eso resalta en su trabajo la capa aislante de "cal catódica".

En el presente trabajo las características del agua (Tabla I) podían hacer pensar en la formación de "cal catódica", sin embargo, teniendo en cuenta la exponencial caída de potencial que tiene lugar cuando se corta el paso de corriente (fig. 5) hace pensar que ni en la zona de mayor polarización, que es la que recibe directamente la inyección de corriente ha habido formación de depósitos calcáreos, o estos son tan porosos que su acción protectora es prácticamente nula.

4.2 TRANSPORTE IONICO Y MOLECULAR

Pueden existir películas protectoras distintas de los recubrimientos calcáreos, tales como las dobles capas electroquímicas formadas en la interfase metal-solución. En la zona comprendida entre las dos fases conductoras se originan diferencias de potencial. En el sistema metal-solución la ordenación de particulas cargadas es función de los iones presentes en la interfase y de los efectos de atracción o repulsión a que están sometidos. La ordenación estructural de la interfase metal-solución, denominada doble capa electroquímica, permite explicar el comportamiento cinético de los procesos de electrodo, ya que la velocidad de la reacción electródica var con el potencial de la interfase y depende del número de especies electroactivas presentes en dicha zona.

El transporte de materia se origina al modificar alguna de las condiciones de equilibrio del sistema. Cuando la temperatura, la presión o la densidad no es la misma en todos los punt de la solución o existe alguna fuerza mecánica se origina un movimiento del líquido que se denomina convección. Si existe una diferencia de potencial eléctrico entre puntos distintos del electrolito, cuando este contiene iones se produce el transporte por migración de los iones en dirección del campo. Finalmente, cuando existe un gradiente de concentración en el seno del electrolito, se origina el transporte de materia por

difusión.

El campo eléctrico que crea la protección catódica pensamos que origina una migración de iones importante que da lugar a la formación de dobles capas electroquímicas que dan lugar a sustanciales modificaciones del potencial. La exponencial caída del potencial cuando se interrumpe el paso de corriente, parece indicar que cuando el campo eléctrico deja de actuar, la película formada por la doble capa en la superficie catódica se rompe modificándose rápidamente el potencial, lo cual hace suponer que esta doble capa puede jugar un papel importante en la protección catódica y sobre todo en su extensión fuera de las zonas de inyección de corriente. Cuando el campo eléctrico se restituye el potencial, al cabo de un cierto tiempo (Fig. 5), vuelve a sus valores primitivos, lo que puede estar relacionado con la reconstrucción de la doble capa.

En el transporte molecular es el O_2 el elemento que juega un papel más importante. Va a existir un gradiente de concentración entre su contenido en la interfase metal-solución y en el seno de la disolución. Esto motivará un desplazamiento por difusión de estas moléculas hacia la superficie catódica. En medios neutros el O_2 juega un importante papel ya que se reduce en la superficie catódica según la reacción:

$$O_2 + 2H_2O + 4\,\theta \longrightarrow 4OH^-$$

alcalinizando la interfase metal-solución. Esta alcalinización puede, en determinadas aguas, producir la precipitación de $CaCO_3$ o simplemente puede llevar al acero a la zona de pasivación, siempre y cuando se alcancen los valores de pH adecuadas.

En los estudios de D.C. Tighe-Ford y J.N. McGrath (3) encuentran que el desplazamiento del potencial por el interior de los tubos es tanto más rápido cuando más reducido es el suministro de O_2 a la superficie catódica, incrementándose en zonas profundas o en aquellas que han sido desaireadas con gas inerte.

Teniendo en cuenta lo que acabamos de exponer, se ve que hasta el momento se establecen hipótesis para tratar de explicar estos hechos reales, pero falta la programación de un trabajo completo y ordenado en el que se estudien las muchas variables que, de hecho, intervienen en este fenómeno. Este trabajo, por su importancia técnica y económica, se está ya llevando a efecto.

5. CONCLUSIONES

1.- como en cualquier proceso de polarización el tiempo juega un papel importante.

2.- El potencial de protección se extiende en la dirección del flujo a una distancia de 200 diametros (aprox. 50 metros) fuera de la zona de inyección de corriente, en un intervalo de tiempo de 72 horas.

3.- A un metro de distancia de la zona de inyección de corriente en contra de la dirección de flujo no se logra el potencial de protección.

4.- Con el agua estática en la zona de inyección de corriente y en la más alejada, no se observan variaciones apreciables. Sin embargo, se detecta una mejora notable en el punto separado un metro en contra de la dirección del flujo que pasa a nivel de protección.

5.- Cuando se corta el paso de corriente de protección catódica, el potencial cae de forma exponencial. En la zona bajo la acción directa de la protección catódica, la polarización se mantiene a nivel de protección durante las 50 horas que permanece cortada la corriente. En el punto más alejado pasa rápidamente a nivel de corrosion y el que está en corrosión apenas sufre variación, lo que indica que la polarización apenas le ha afectado.

Estas circunstancias hacen pensar que no hay formación de recubrimientos calcáreos o que estos son muy porosos

y que el potencial que se extiende a lo largo de los tubos fuera de la zona de inyección de corriente, pueda estar bajo el influjo de la posible doble capa electroquímica que crea el campo eléctrico generado con la protección catódica. Esta doble capa se rompe al cesar el campo eléctrico y puede contribuir a la caída brusca del valor del potencial a niveles de corrosión.

6.- Rebajando a la mitad la densidad de corriente de protección (60 mA/m^2), se logra pasar en regimen de flujo a potencial de protección el punto situado a un metro de la inyección de corriente, situándose los valores de potneical en los 3 puntos entre +100 y +200 mV con respecto al electrodo de referencia de Zn puro.

7.- La velocidad de difusión del O_2 y su reducción en la superficie catódica, parecen jugar un papel importante pero contradictorio, lo que motiva el programar nuevas investigaciones para aclarar el mecanismo de actuación.

8.- Esta aportación a la protección catódica interior de tuberías pensamos que aporta datos de gran itnerés técnico y económico.

9.- Durante los 5 años que lleva funcionando el sistema de protección catódica por corriente impresa no han vuelto a aparecer ni poros ni perforaciones en las tuberías, no solo en la zona que recibe directamente la protección sino en las otras fuera del alcance durecto de las mismas.

REFERENCIAS

(1) MORGAN, J.H.- Protection Cathodique. Dunod Paris (1966) pags. 297 a 308.

(2) LAQUE, F.L.- Marine Corrosión, Causes and Prevention.- J. Wiley & Sons, NY, 1975, pags. 104 - 109

(3) TIGHE, D.J. y GRATH, J.N.- Analysis of the time-dependent development of cathodic Protection Withim Pipes. Comunicaciones 6º Congreso Internacional de Corrosión Marina e Inscrustaciones. Atenas, 5-8 Septiembre 1984 (Grecia).

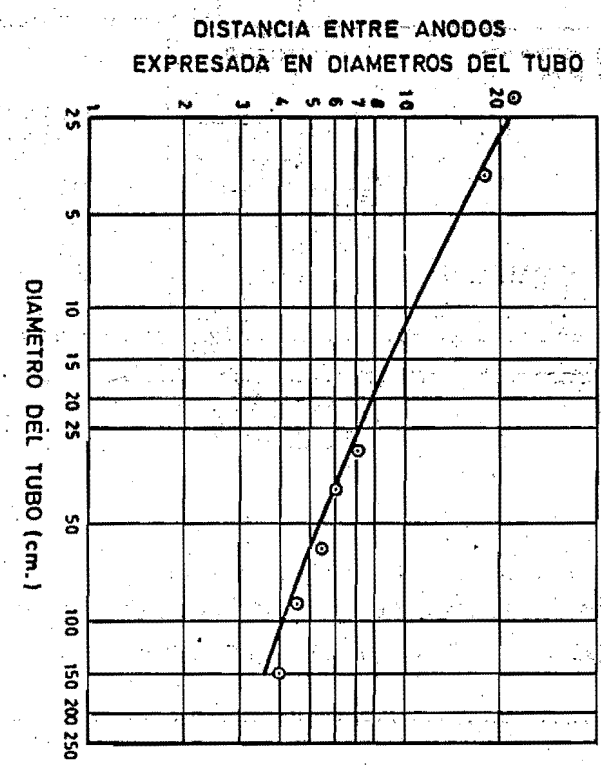

FIG.—1

SEPARACION MAXIMA ENTRE ANODOS EN TUBOS DESNUDOS DE DIFERENTES DIAMETROS POR LOS QUE CIRCULA AGUA DE MAR.

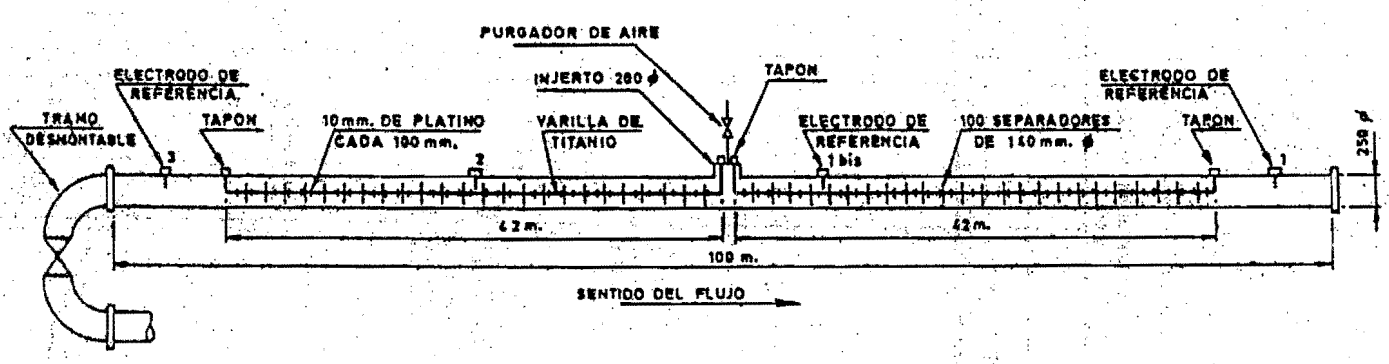

FIG.- 2

DISPOSICION INICIAL DEL SISTEMA DE PROTECCION CATODICA POR CORRIENTE IMPRESA DE 1 TRAMO DE TUBERIA DE 100 m. DE LONGITUD Y 250 mm. DE DIAMETRO. VELOCIDAD DE FLUJO 0,5 m/s.; PRESION DE TRABAJO 2,8 kg/cm^2.

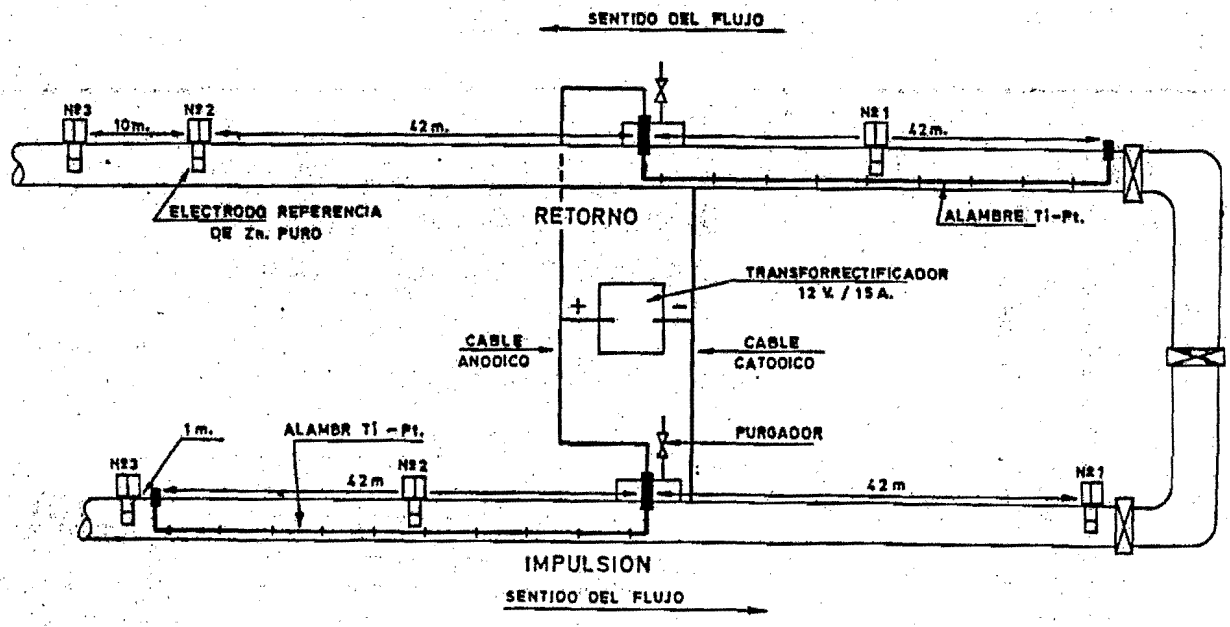

FIG.–3

ESQUEMA ACTUAL DEL SISTEMA DE PROTECCIÓN CATÓDICA POR CORRIENTE IMPRESA DE 2 TRAMOS DE TUBERIA DE 100 m. DE LONGITUD Y 250 mm. DE DIAMETRO. VELOCIDAD DE FLUJO 0,5 m/s., PRESION DE TRABAJO 2,8 kg/cm^2.

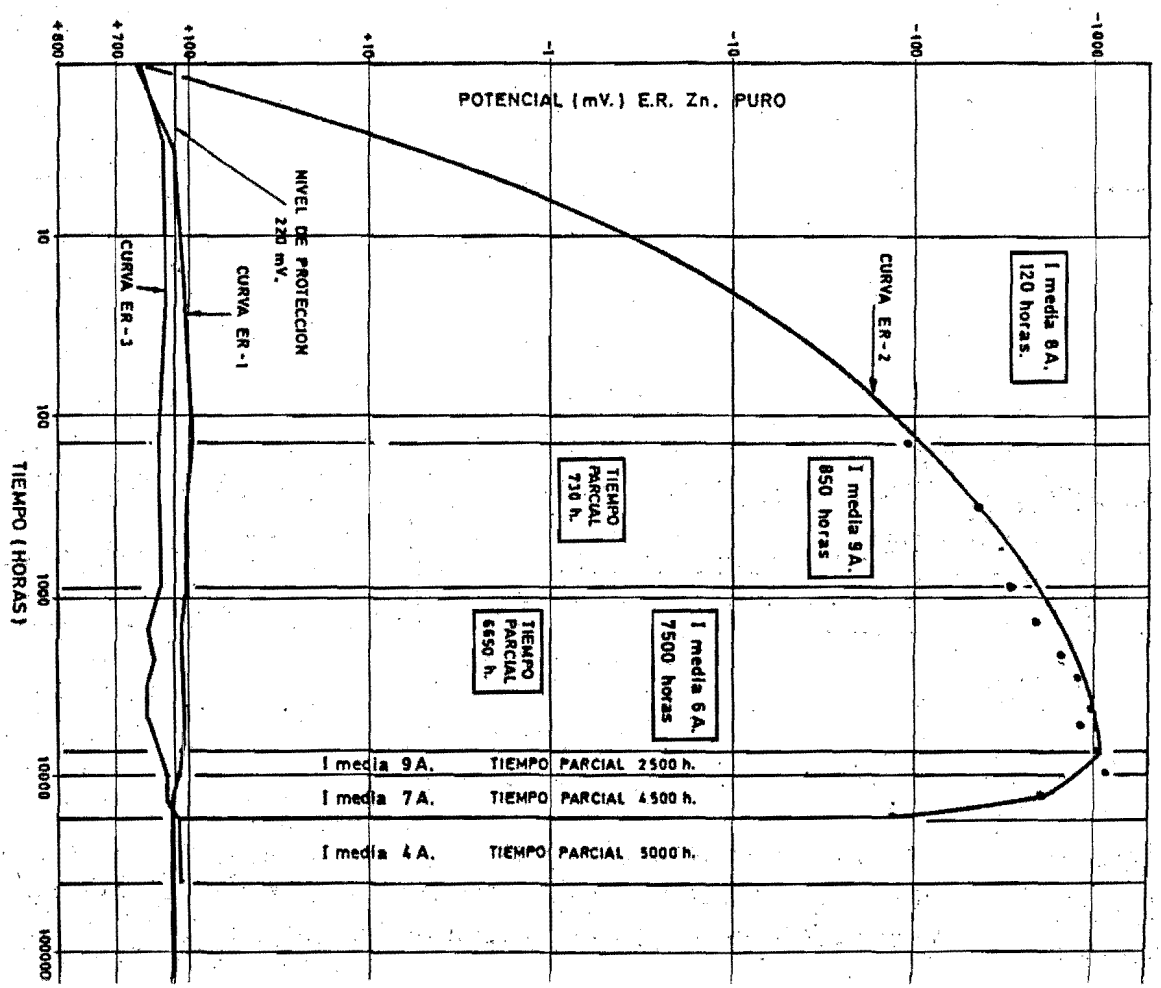

FIG.–4

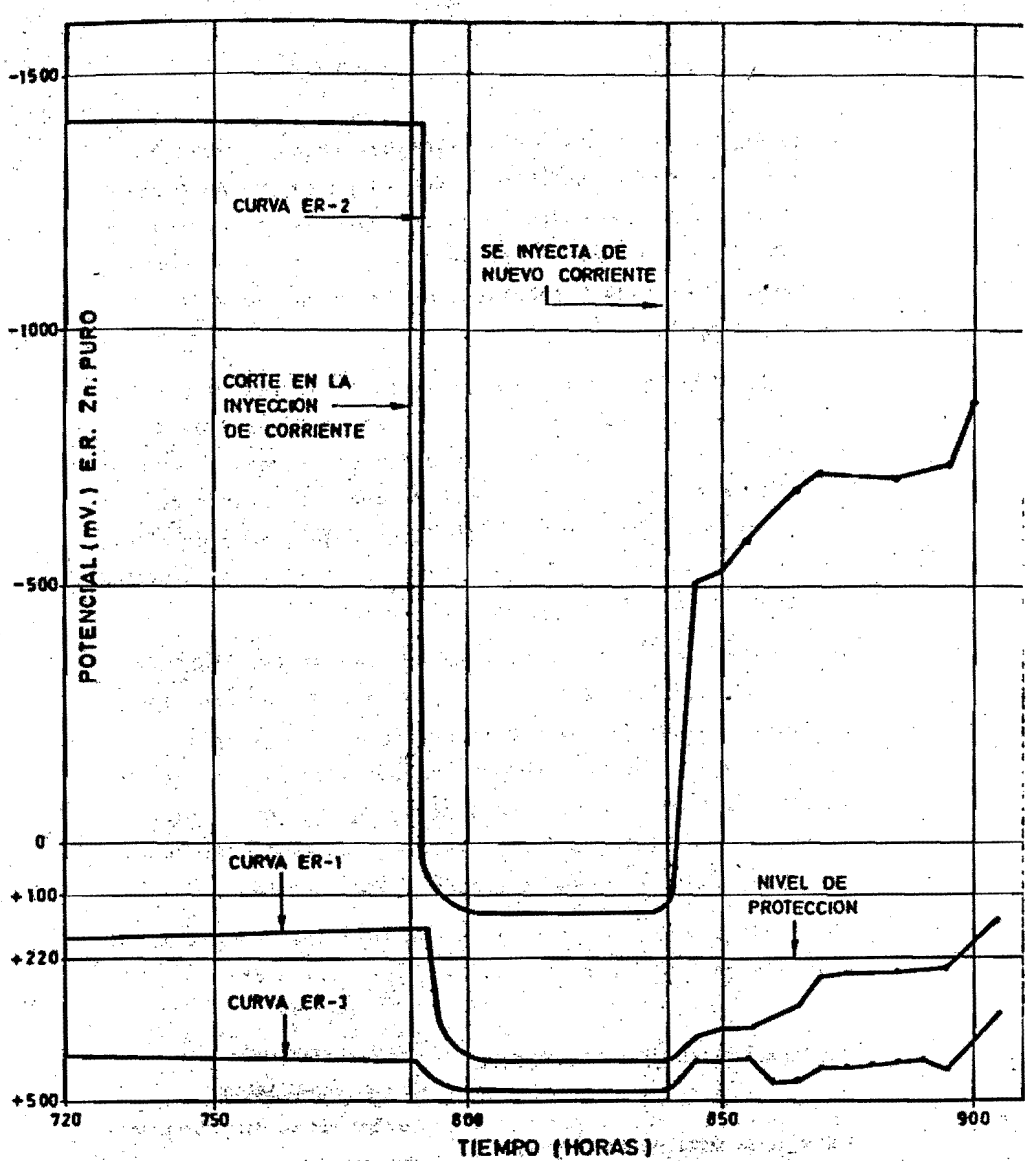

FIG.- 5

CURVAS DE DESPOLARIZACION EN EL MOMENTO DE CORTE DE LA INYECCION DE CORRIENTE Y DE REESTABLECIMIENTO DE LA POLARIZACION AL INYECTAR DE NUEVO.

PINTURAS MARINAS PARA BUQUES. RESULTADOS DE INVESTIGACIONES

M. Morcillo, S. Giménez, J. Simancas, J. Antuñano* y A. Monje**
Centro Nacional de investigaciones Metalúrgicas. 28040-Madrid.
*Astilleros Españoles, S.A. Factoría de Sestao. Sestao (Vizcaya)
**Astilleros Españoles, S.A. Factoría de Puerto Real. P. Real (Cádiz)

ABSTRACT

Unfortunately, premature failures in marine paint systems is a frequent problem in the shipping industry.

In the research different stages involved in the ship's construction are simulated.

The more significant variables in the anticorrosive behaviour of marine paint systems were the following: a) salt contamination at the steel/paint interface, b) unproperly cleaning of weathered shop-primer and c) high levels of cathodic protection.

INTRODUCCION

Es opinión generalizada que la inmensa mayoría de los fallos prematuros de los recubrimientos de pintura surgen al no haberse puesto en práctica ciertos requisitos básicos relativos a la preparación de superficie del substrato metálico sobre el que se va a aplicar posteriormente el esquema de pintura, métodos y condiciones de aplicación de la pintura e inadecuada integración de los trabajos de pintado en la planificación general de la construcción del buque.

Hoy en día, en el pintado en construcción naval se diferencian dos etapas en la preparación de superficies:

a) la primaria, relativa a la limpieza de las chapas de acero (desnudas) que han estado expuestas durante cierto tiempo a la atmósfera, en los parques de materialdel astillero. Los diferentes grados de limpieza de estas superficies vienen señalados en la norma sueca SIS 055900-1967.

b) la secundaria, relativa a la limpieza de las chapas de acero recubiertas con el shop-primer y que sufren distinto tipo de agresiones (quemaduras, soldadura, acción de la atmósfera salina, etc.) durante el periodo de construcción del buque. Los diferentes grados de limpieza de estas superficies vienen señalados en la norma japonesa JSRA (SPSS)-1975.

En esta investigación se han tratado de simular las distintas etapas por las que pasan las chapas de acero procedentes de los trenes de laminación en caliente de la acería, y que al llegar al astillero quedan sometidas al proceso de construcción del buque, para durante la vida en servicio de éste, estar integrando el casco en sus distintas zonas de exposición: fondos, flotación y obra muerta.

En el estudio se analizan en profundidad los efectos de diversas variables, agrupadas del siguiente modo:

	VARIABLE
PREPARACION PRIMARIA DE SUPERFICIE	Grado de chorreado
	Contaminación salina
	Envejecimiento del shop-primer
PREPARACION SECUNDARIA DE SUPERFICIE	Limpieza del shop-primer envejecido

CONDICIONES DE APLICACION DEL ESQUEMA DE PINTURA	Presencia de humedad sobre la superficie a pintar
	Tiempo de repintado
	Vida de la mezcla (pinturas de dos componentes)

En otra serie de ensayos se analiza separadamente el efecto de la protección catódica en el comportamiento de sistemas marinos de pintura.

DISEÑO EXPERIMENTAL

Las probetas, de dimensiones 125 x 250 mm, se prepararon a partir de chapas de acero suave laminado en caliente de 3 mm de espesor.

Una serie de probetas estuvo expuesta durante aproximadamente 3 meses en una atmósfera rural exenta de contaminantes atmosféricos del tipo SO_2 o cloruros.

En la Tabla I se expone el plan experimental general en el que se detallan las variables del estudio, así como los niveles de actuación de cada una de ellas.

Grado de chorreado. Los diferentes grados de limpieza se obtuvieron por chorreado centrífugo con granalla esférica del tipo S-280, variando el tiempo de tratamiento. La rugosidad final obtenida fue intermedia entre Sh 3 y Sh 4 (Keane-Tator, Surface Profile Comparator).

Contaminación salina. Los distintos niveles de contaminación se obtuvieron aplicando cantidades variables de soluciones en agua y metanol de NaCl y $FeSO_4 \cdot 7 H_2O$, con la ayuda de una varilla de vidrio. Posteriormente las probetas se introducían durante un cierto tiempo en una

estufa de laboratorio, a 40-50ºC, para evitar al máximo la formación de herrumbre.

Envejecimiento del Shop-Primer. En la investigación se consideran dos tipos de shop-primer: a) del tipo epoxi-óxido de hierro y b) del tipo epoxi-cinc, de uso común en construcción naval. A fines de comparación de resultados a una serie de probetas no les fue aplicado shop-primer. El espesor medio de película seca de ambas imprimaciones fue de 30-40 µm aproximadamente.

Para simular la condición FO de las normas japonesas SPSS del J.S.R.A., las superficies, una vez imprimadas, fueron sometidas a un proceso de quemado con la ayuda de un soplete de soldadura oxi-acetilénica. Las probetas se mantenían durante cierto tiempo (~ 10 seg) a la acción de la llama y se retiraban cuando el metal alcanzaba la temperatura de 350ºC, momento en que se producía el cambio de color en las marcas realizadas sobre las probetas con un lápiz Themochrom de la marca Faber-Castell.

Al ensayo de envejecimiento en cámara de niebla salina se sometieron posteriormente las series de probetas imprimadas que habrían sufrido el proceso de quemado, juntamente con otras series de probetas donde la imprimación se presentaba intacta. Las probetas se retiraron de la cámara a las 300 horas de ensayo tiempo que coincidía aproximadamente con el grado 7 de oxidación (ASTM D610) en las probetas imprimadas con el shop-primer del tipo epoxi-óxido de hierro.

Limpieza del shop-primer envejecido. Se consideraron 3 grados de limpieza en las probetas imprimadas y envejecidas:

a) lavado con agua y cepillo de cerdas de nylon, b) lavado y cepillado mecánico Pt 2 (SSPS, JSRA) y c) chorreado muy ligero S_s (SSPC, JSRA).

Presencia de humedad sobre la superficie a pintar (C.M.)

En una serie de probetas las pinturas se aplicaron en las condiciones normales de laboratorio, en tanto que en otra la superficie de la probeta presentaba una ligera capa de humedad, anterior a la aplicación de la primera capa de pintura del esquema. La presencia de esta capa acuosa se realizó pasando por la superficie de la probeta una esponja, algo humedecida, inmediatamente antes de la aplicación del recubrimiento de pintura.

Tiempo de repintado (T.R.) La aplicación de la segunda capa del esquema de pintura se realizó según las siguientes instrucciones

T.R. 1: el especificado por el fabricante de pintura
T.R. 2: la mitad del tiempo mínimo
T.R. 3: 15 días

Posteriores capas del esquema se aplicaron siguiendo las instrucciones dictadas por el fabricante de la pintura en cuestión.

Vida de la mezcla (V.M.) Tratándose de pinturas de dos componentes, se han preparado series de probetas de acuerdo con los siguientes niveles de actuación de esta variable

V.M. 1: ½ hr. después de haber realizado la mezcla
V.M. 2: 24 hrs. " " " "

En la Tabla II se exponen los sistemas de pintura aplicados en función de las condiciones de exposición a que iban a estar sometidas las probetas de ensayo en las balsas de experimentación. En la Fig. 1 se ofrece una vista panorámica de la balsa de ensayos. Los ensayos se llevaron a cabo en El Abra (Vizcaya) y Puerto Real (Cádiz).

Teniendo en cuenta el elevado número de variables que comprende esta investigación, un estudio sistemático que incluyera todas las variables así como todos los niveles de actuación de cada una de ellas hubiese supuesto preparar un número excesivo de probetas, teniendo en cuenta las limitaciones de espacio de la balsa experimental. Por ello, el diseño experimental que se ha realizado ha consistido en el estudio por separado de cada una de las variables mencionadas, a base de bloques de ensayos, haciendo intervenir en cada bloque a aquellas otras variables más relacionadas con la variable objeto de estudio. Lo mencionado queda ilustrado en las Figs 2 a 4 a base de círculos (blancos y negros) y cruces.

Los círculos señalan las variables que son objeto de estudio en cada bloque de ensayos, así como los niveles de actuación de cada variable, en tanto que las cruces indican las condiciones comunes para las restantes variables que no son objeto de estudio en ese bloque experimental.

Para estudiar el efecto de la protección catódica se prepararon probetas de 150 x 75 x 2 mm, que una vez chorreadas al grado ASa 3 se les aplicó una imprimación del tipo shop-primer epoxi-óxido de hierro (20 µm) y una pintura de acabado brea-epoxi o clorocaucho (180-230 µm) de diversos

fabricantes de pintura. Las probetas en una de sus caras presentaban una zona circular de 17 mm de diámetro sin pintura.

Los ensayos se llevaron a cabo en agua de mar artificial (ASTM D 1141) y un sistema electrónico independiente para cada probeta permitía aplicar el potencial de protección requerido. Se consideraron 2 niveles de protección catódica: -0,85 V y -1,20 V con relación al electrodo de referencia de Ag/AgCl. Como testigos a fin de comparación de resultados una serie de probetas estuvo expuesta a corrosión libre en agua de mar.

Resultados

Periódicamente se realizaron inspecciones del estado que presentaban las probetas de ensayo. En las inspecciones se anotaba el grado de oxidación de la superficie pintada y el grado de ampollamiento del recubrimiento de pintura.

En las probetas expuestas a la acción de la atmósfera marina (Fig. 4) el deterioro se manifiesta principalmente por la aparición de puntos de óxido en la superficie de la pintura. La valoración del grado de oxidación se realizó de acuerdo con la norma ASTM D-610, en la que "10" significa ausencia de puntos de oxidación y "0" que la superficie aparece completamente oxidada. En este artículo únicamente reseñamos que un sistema de pintura empieza a fallar (círculo negro) cuando el grado de oxidación alcanza un valor de 8 o valores inferiores.

En las probetas expuestas en inmersión parcial o permanente (Figs. 3 y 2) el deterioro se manifiesta principalmente

por la aparición de ampollas en la superficie de la pintura. La valoración del grado de ampollamiento se ha realizado de acuerdo con la norma ASTM D-714 con la que se evaluan la frecuencia de aparición y tamaño de las ampollas. En este artículo únicamente reseñamos que un sistema de pintura empieza a fallar (círculo negro) cuando la frecuencia de aparición es del tipo M (medio), MD (medio-densa) o D (denso).

Tampoco se considera fallo de un sistema de pintura cuando el deterioro se localiza únicamente en los bordes de la probeta de ensayo, ni cuando el ampollamiento corresponde a la película de pintura antiincrustante, que se aplicó de modo idéntico a todas las probetas expuestas en inmersión para impedir la incrustación biológica, pero no para su estudio en sí.

Los resultados que exponemos en esta comunicación (Fig. 2 a 4) corresponden a un tiempo de experimentación de 4 años en las condiciones descritas, reflejándose únicamente las tendencias observadas y sin profundizar mediante un análisis más riguroso de la graduación de efectos en las distintas variables estudiadas.

En la Fig. 5 se exponen los resultados obtenidos al estudiar el efecto de la protección catódica. En las pruebas a corrosión libre en agua de mar (sin protección catódica) los ensayos duraron 12 meses, en tanto que en las pruebas en que se aplicó un potencial de protección catódica, los ensayos tuvieron una duración de 50-60 días.

DISCUSION

Abordaremos la discusión de los resultados experimentales

obtenidos en función de cada tipo de exposición y de las variables objeto de estudio.

EXPOSICION ATMOSFERICA (Fig. 4)

Grado de chorreado. Si bien este efecto únicamente se estudió en dos sistemas (11 y 13), no se observa ningún efecto negativo en los niveles de actuación considerados para esta variable.

Contaminación salina. Con relación a la contaminación por NaCl únicamente en el caso del sistema 10, y siempre y cuando no se aplique shop-primer antes del esquema, se observa un efecto negativo por la presencia del contaminante NaCl a su nivel superior (100 mg/m^2). Respecto al contaminante $FeSO_4$ todos los sistemas ensayados se muestran sensibles a la presencia de este contaminante en la intercara metal/pintura, particularmente a concentraciones superiores a 500 mg/m^2, independientemente de la aplicación o no del shop-primer.

Limpieza secundaria del shop-primer envejecido. En todos los sistemas la limpieza del shop-primer del tipo epoxi-óxido de hierro, envejecido, únicamente mediante agua y cepillo de cerdas de nylon, se presenta insuficiente. El shop-primer epoxi-cinc parece, en cambio, tolerar este tipo de agresiones.

Condiciones de aplicación. Todos los sistemas toleran las desviaciones ensayadas con relación a la buena práctica durante la aplicación de los recubrimientos de pintura.

INMERSION PARCIAL (Fig. 3)

En la Fig.3 se observa que el sistema 9 muestra siempre deterioros, con independencia de la variable en estudio, lo que nos hace pensar que es el propio esquema de pintura, al espesor considerado, el que no resiste las condiciones de exposición.

Grado de chorreado. No se observa en los dos sistemas (7 y 8) donde se llevó a cabo el estudio de esta variable ningún efecto negativo en los niveles de actuación considerados.

Contaminación salina. El sistema 7 muestra sensibilidad a la presencia de los contaminantes NaCl o $FeSO_4$ en la intercara metal/pintura, independientemente del shop-primer aplicado, en tanto que el sistema 8 se muestra insensible a esta variable.

Limpieza secundaria del shop-primer envejecido. La limpieza con agua del shop-primer epoxi-óxido de hierro envejecido por la acción de la niebla salina se presenta como insuficiente en el caso del sistema 7, mientras que el shop-primer de epoxi-cinc tolera este tipo de agresión.

El sistema 8, en cambio, tolera el citado envejecimiento independientemente del shop-primer aplicado.

Condiciones de aplicación. Los sistemas 7 y 8 toleran las desviaciones ensayadas con relación a la buena práctica durante la aplicación de los recubrimientos de pintura.

INMERSION PERMANENTE (Fig. 2)

En la Fig. 2 se observa que el sistema 5 muestra fallos

con independencia de la variable en estudio, lo que nos hace pensar que es el propio esquema de pintura el que no resiste las condiciones de exposición.

Grado de chorreado. Los sistemas 1 y 6 se muestran insensibles a las variaciones de preparación primaria de superficie consideradas. Todo lo contrario sucede en el sistema 4, independientemente del shop-primer aplicado. En los sistemas 2 y 3 el efecto de esta variable se acusa únicamente frente a determinadas situaciones. Así, en el sistema 2 el efecto negativo de la variable se presenta siempre que el shop-primer no sea del tipo epoxi-cinc, y en el sistema 3 el efecto se presenta cuando no existe capa de imprimación y las preparaciones superficiales son aquellas que conducen a menores grados de limpieza (3 y 5).

Contaminación salina Los resultados experimentales obtenidos con relación al estudio de esta variable sugieren una cierta interacción entre las variables grado de chorreado y contaminación salina, en el sentido que la presencia de cierta herrumbre (grado 5 de chorreado) puede exaltar el efecto de una contaminación salina en la intercara metal/pintura, efecto que por si mismo no hubiese tenido lugar. Este es el caso del sistema 1 frente a una contaminación elevada de sulfato o del sistema 3 frente a concentraciones elevadas de ambos contaminantes o del sistema 4 frente a cualquier contaminación de las ensayadas.

En el sistema 2 resulta decisiva la intervención del shop-primer. Así el esquema, cuando no existe imprimación, no tolera contaminación alguna, independientemente del grado

de limpieza por chorreado que consideremos; cuando el shop-primer es del tipo epoxi-óxido de hierro únicamente se observan efectos negativos en el peor de los grados de limpieza (5) y frente a concentraciones elevadas de contaminante, apareciendo de nuevo el efecto sinérgico comentado anteriormente.

El esquema 6 tolera la presencia de contaminación salina independientemente del shop-primer aplicado.

Limpieza secundaria del shop-primer envejecido De todos los esquemas ensayados, los sistemas 2 y 6 se presentan como muy sensibles al efecto del envejecimiento del shop-primer y posterior limpieza. En el primero de ellos, independientemente del tipo de shop-primer, ninguna de las limpiezas consideradas consigue paliar el efecto del envejecimiento. En el sistema 6 el deterioro únicamente se presenta cuando el shop-primer es del tipo epoxi-óxido de hierro.

En los restantes sistemas, exceptuando claro está el sistema 5, del que por las causas ya comentadas no pueden analizarse los efectos, unicamente se observa un efecto negativo en la menor de las limpiezas consideradas; este efecto se presenta en los sistemas 1 y 3 cuando el shop-primer es del tipo epoxi-óxido de hierro y en el sistema 4 con ambos shop-primer.

EFECTO DE LA PROTECCION CATODICA (Fig. 5)

El deterioro, en forma de ampollamientos, del sistema de pintura se localiza en la vecindad del área desnuda (ventana o zona sin pintar) permaneciendo por lo general en

perfecto estado el resto de la superficie de ensayo. Ello es debido al fenómeno de deslaminación catódica que ocurre en la proximidad de zonas sin pintura.

Al observar la Fig. 5 se aprecia que un potencial catódico de -1,20 V. obviamente acelera los procesos de deterioro del recubrimiento, en particular tratándose de los sistemas de clorocaucho. También se observa en líneas generales un mejor comportamiento de los recubrimientos de brea-epoxi con relación a los del tipo clorocaucho.

Queda asimismo bien patente la gran diversidad de comportamientos en pinturas que aunque pertenezcan a un mismo tipo genérico, su formulación puede diferir notablemente.

CONCLUSIONES

En la investigación se pone de manifiesto la importancia relativa de las distintas variables consideradas. En términos generales, las variables con mayor influencia en el comportamiento de los esquemas de pintura fueron:

- la presencia de concentraciones elevadas de contaminación salina en la intercara metal/pintura.
- el envejecimiento del shop-primer sin una adecuada limpieza posterior.
- un potencial catódico elevado.

TABLA I. PLAN EXPERIMENTAL GENERAL

Preparación primaria de superficie		Shop-Primer (SP)	Preparación secundaria de superficie		Condiciones de aplicación		
Grado de limpieza	Contaminación salina		Envejecimiento del Shop-Primer	Tipo de limpieza	Presencia de humedad (CM)	Tiempo de repintado (TR)	Vida de la mezcla (VM)
	Sin contaminación (0)						
	$\frac{NaCl}{5\ mg/m^2}$ (1)						
ASa 3 (1)	10 " (2)	Sin shop-primer(6)	(1): Presencia de zonas quemadas + exposición a la niebla salina	Lavado con agua (1)			
ASa 2½ (2)	25 " (3)						
ASa 2 (3)	100 " (4)	Epoxi-óxido de(1) hierro		Cepillado manual (2)	Sí (2)	.El especificado por el fabricante(1)	30 min(1)
					No (1)	La mitad del tiempo mínimo (2)	
	$\frac{FeSO_4}{500\ mg/m^2}$ (5)		(2): Exposición a la niebla salina	Chorreado ligero (3)			24 hrs(2)
BSa 2½ (4)		Epoxi-cinc (2)				15 días (3)	
BSa 2 (5)	1000 " (6)						
	2500 " (7)						

Los números entre paréntesis indican la clave utilizada para la confección de las Figs. 2 a 4.

TABLA II.- Características de los sistemas de pintura aplicados.

Tipo de exposición	Sistema de pintura		Espesor total (µm)
	Clave*	Tipo Genérico	
Inmersión total	1	Clorocaucho pigmentado con aluminio (Fabricante 1)	150
	2	Clorocaucho sin pigmentar con aluminio (Fabricante 1)	100
	3	Clorocaucho pigmentado con aluminio (Fabricante 2)	120
	4	Clorocaucho sin pigmentar con aluminio (Fabricante 2)	120
	5	Alquitrán-epoxi	125
	6	Alquitrán-vinílico	160
Inmersión parcial	7	Clorocaucho pigmentado con aluminio	120
	8	Clorocaucho sin pigmentar con aluminio	140
	9	Epoxi puro	100
Atmosférica	10	Alcídico	115
	11	Clorocaucho sin pigmentar con aluminio	125
	12	Clorocaucho sin pigmentar con aluminio/acabado acrílico	110
	13	Vinílica/alcídica	100

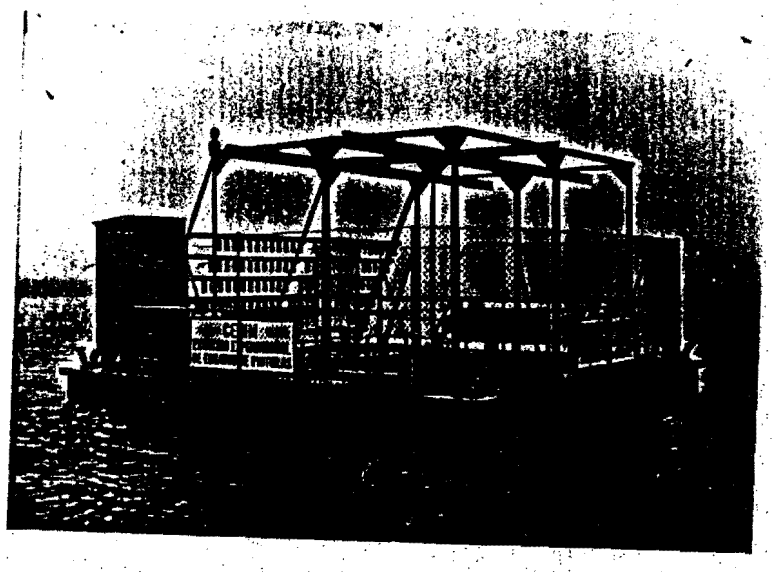

Fig. 1.- .Vista de la balsa experimental para ensayos de pinturas en agua de mar.

Fig. 2.- Resumen de los resultados experimentales correspondientes a los sistemas de pintura expuestos a inmersión permanente en agua de mar.

EXPOSICION : INMERSION PERMANENTE

TIPO DE PINTURA	EFECTO	LIMPIEZA PRIMARIA														SHOP PRIMER (SP)			LIMP. SECUND.					CONDICIONES APLICACION							
		GRADO DE CHORREADO					CONTAMINACION SALINA												ENVEJ. SP		LIMPIEZA SP			C.M.		T.R.			V.M.	
		1	2	3	4	5	0	1	2	3	4	5	6	7		0	1	2	1	2	1	2	3	1	2	1	2	3	1	2
1	G. Chorreado	○	○	○	●	○	x									○	●	○						x		x				
	Cont. salina	○				●	○	○	○	○	○	○	○	●	●	○	●							x		x				
	Limpieza SP	x					x									●	○	●	●	○	○	x		x						
	Cond. aplicac		○		○		x									○	○	○						○	○	○	○	○	○	
2	G. Chorreado	●	●	●	●	●	x									●	●	○						x		x				
	Cont. salina	●				●	●	●	●	●	●	●	●	●	●									x		x				
	" "	○				●	○	○	○	●	○	○	●			●								x		x				
	" "	○				○	○	○	○	○	○	○	○				○							x		x				
	Limpieza SP	x					x									●	●	●	●	●	●	●	●	x		x				
	Cond. aplicac		●		●		x									●	●	●						●	●	●	●	●	●	
3	G. chorreado	○	○	●	○	●	x									●	○	○						x		x				
	Cont. salina	○				●	○	○	○	○	●	○	●	●	●	●	○							x		x				
	Limpieza SP	x					x									●	○		●	●	○	○	x		x					
	Cond. aplicac		●		●		x									●	●	○						●	●	●	●	●	●	
4	G. chorreado	●	●	●	●	●	x									●	●	●						x		x				
	Cont. salina	○				●	●	●	●	●	●	●	●	●	●	●	●	●						x		x				
	Limpieza SP	x					x									●	●		●	●	○	○	x		x					
	Cond. aplicac		●		●		x									●	●	●						●	●	●	●	●	●	
5	G. chorreado	●	●	●	●	●	x									●	●	●						x		x				
	Cont. salina	●				●	●	●	●	●	●	●	●	●	●	●	●	●						x		x				
	Limpieza SP	x					x									●	●	●	●	●	●	●	●	x		x				
	Cond. aplicac		●		●		x									●	●	●						●	●	●	●	●	●	●
6	G. chorreado	○	○	○	○	○	x									○	○	○						x		x				
	Cont. salina	○				○	○	○	○	○	○	○	○	○	○	○	○	○						x		x				
	Limpieza SP	x					x									●	○	●	●	●	●	●	x		x					
	Cond. aplicac		○		○		x									○	○	○						○	○	○	○	○	○	

○ SIN EFECTO

● EFECTO NEGATIVO

x CONDICION COMUN EN EL ESTUDIO DEL EFECTO INDICADO

Fig. 3.- Resumen de los resultados experimentales correspondientes a los sistemas de pintura expuestos a inmersión parcial en agua de mar.

EXPOSICION : INMERSION PARCIAL

TIPO DE PINTURA	EFECTO	LIMPIEZA PRIMARIA														SHOP PRIMER (SP)			LIMP. SECUND.					CONDICIONES APLICACION							
		GRADO DE CHORREADO					CONTAMINACION SALINA												ENVEJ. SP		LIMPIEZA SP			C.M.		T.R.			V.M.	
		1	2	3	4	5	0	1	2	3	4	5	6	7		0	1	2	1	2	1	2	3	1	2	1	2	3	1	2
7	G. chorreado	○	○	○	○	○	x									○	○	○						x		x				
	Cont. salina	x					○	○	●	●	●	●	●	●		●	●	●						x		x				
	Limpieza SP	x					x										●	○		●	●	○	○	x		x				
	Cond. aplicación		x				x									○	●	○						○	●	●	○	○	●	
8	G. chorreado	○	○	○	○	○	x									○	○	○						x		x				
	Cond. salina	x					○	○	○	○	○	○	○	○		○	○	○						x		x				
	Limpieza SP	x					x										○	○		○	○	○	○	x		x				
	Cond. aplicación		x				x									○	○	○						○	○	○	○	○	○	
9	Cont. salina	x					●	●	●	●	●	●	●	●		●	●	●						x		x				
	Limpieza SP	x					x										●	●	●		●	●	●	x		x				
	Cond. aplicación		x				x									●	●	●						●	●	●	●	●	●	●

○ SIN EFECTO

● EFECTO NEGATIVO

x CONDICION COMUN EN EL ESTUDIO DEL EFECTO INDICADO

Fig. 4.- Resumen de los resultados experimentales correspondientes a los sistemas de pintura expuestos a la atmósfera marina.

EXPOSICION : ATMOSFERICA

TIPO DE PINTURA	EFECTO	LIMPIEZA PRIMARIA													SHOP PRIMER (SP)			LIMP. SECUND.					CONDICIONES APLICACION							
		GRADO DE CHORREADO					CONTAMINACION SALINA											ENVEJ. SP		LIMPIEZA SP			C.M.		T.R.			V.M.	
		1	2	3	4	5	0	1	2	3	4	5	6	7	0	1	2	1	2	1	2	3	1	2	1	2	3	1	2
10	Cont. salina	x					○	○	○	○	●	○	○	●	●	○	○						x		x				
	Limpieza SP	x					x									●	○	●	○	●	○	○	x		x				
	Cond. aplicación		x				x								○	○	●						○	●	●	○	○	●	
11	G. chorreado	○	○	○	○	○	x								○	○	○						x		x				
	Cont. salina	x					○	○	○	○	○	●	●	●	●	●	●						x		x				
	Limpieza SP	x					x									●	○		●	●	○	○	x		x				
	Cond. aplicación		x				x								○	○	○						○	○	○	○	○	○	
12	Cont. salina	x					○	○	○	○	○	○	●	●	●	●	●						x		x				
	Limpieza SP	x					x									●	○		●	●	○	○	x		x				
	Cond. aplicación		x				x								○	○	○						○	○	○	○	○	○	
13	G. chorreado	○	○	○	○	○	x								○	○	○						x		x				
	Cont. salina	x					○	○	○	○	○	○	●	●	●	●	●						x		x				
	Limpieza SP	x					x									●	○	●	○	●	○	○	x		x				
	Cond. aplicación		x				x								○	○	○						○	○	○	○	○	○	

○ SIN EFECTO

● EFECTO NEGATIVO

x CONDICION COMUN EN EL ESTUDIO DEL EFECTO INDICADO

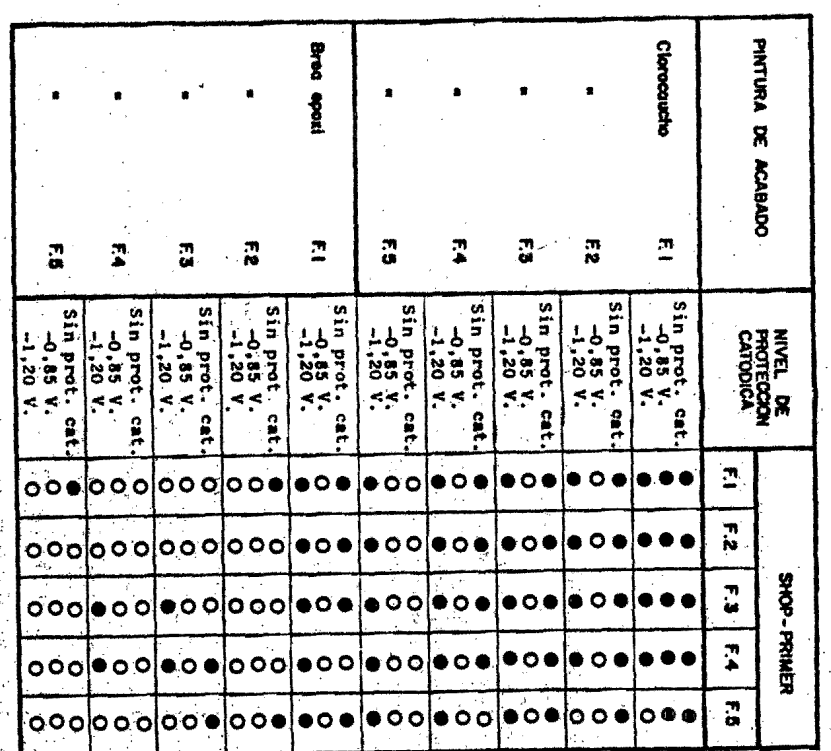

Fig. 5.- Resumen de los resultados experimentales correspondientes a los ensayos de protección catódica.

OBSERVATIONS ON THE CATHODIC PROTECTION OF STEEL IN BIOLOGICALLY ACTIVE SEAWATER

R.G.J.EDYVEAN, C.J.HUTCHINSON & N.J.SILK

SCHOOL OF MATERIALS, DIVISION OF METALS,
UNIVERSITY OF SHEFFIELD,
MAPPIN ST. SHEFFIELD S1 3JD. UK.

ABSTRACT

Cathodic protection of steel in seawater results in the formation of calcareous scales on the metal surface. Such scales can be both beneficial; in protecting the metal and detrimental; for example in heat exchanger systems. The structure of scale is modified by chemical and physical conditions at the metal surface including the presence of organic material. Data are presented showing initial current density changes, and scale compositions formed in seawater with various levels of organic loading. The results are discussed in the light of comparing experimental data using artificial seawater with real environments.

INTRODUCTION

Calcareous scales are an important factor in the protection of steel in seawater by cathodic protection. They can be both beneficial, in protecting the metal and reducing the current density required for adequate protection, and detrimental, for example in reducing the efficiency of heat exchanger systems or causing the disbondment of paint films. The deposits are produced as a direct consequence of cathodic reaction and form due to the high pH generated at the protected metal surface causing the solubility product of inorganic salts in seawater to be exceeded. Previous work has suggested that artificial seawater has markedly different effects than natural seawater on both the corrosion (Thomas et.al) and the scale formed in the cathodic protection (Edyvean 1984) of steel and that this is largely due to the organic content of the water (Chave and Suess 1970; Kitano and Hood,1965). Many corrosion and cathodic protection experiments are carried out in artificial seawater and this, together with the fact that there are large variations in the organic loading of seawater, means that any effects of organics are important in interpreting and extrapolating laboratory experimental results to a real situation.

Calcareous deposits on protected steel in seawater are principally calcium and magnesium hydroxides and carbonates, although they often contain other ions. The physical and chemical nature of the scale is important in determining its characteristics, for example its "throwing power" or electrical insulation properties, the stability of the cathodic protection system and the protection afforded by the scale should the protective current be cut off for some reason, where the scale acts as a physical barrier to the flux of dissolved oxygen to the cathode, reducing the corrosion reaction.

The reaction at the cathode in the cathodic protection is the formation of hydroxyl ions and hence an increase in the pH immediately adjacent to the cathode surface. pH values as high as 11.5 have been recorded (Hartt, et.al.1984).

The scales that form tend to be carbonates of calcium or magnesium or both:-

$$Ca^{++} + CO_3^{--} = CaCO_3 \text{ (ppt)}$$

$$Mg^{++} + CO_3^{--} = MgCO_3 \text{ (ppt)}$$

$$Ca^{++} + Mg^{++} + 2CO_3^{--} = CaCO_3.MgCO_3 \text{ (ppt)}$$

Calcium carbonate deposits are [illegible]

crystal forms aragonite and calcite. Magnesium carbonate (magnesite) and the mixed magnesium/calcium carbonate (dolomite) also form.

The thickness of scales has been found to increase linearly with time, at least initially (Wolfson and Hartt, 1981; Edyvean, 1984) and scales several centimetres thick can be found on offshore structures, especially where the metal surface is hot (e.g. on hot risers carrying hot oil from the seabed to the platform).

This work was designed as an initial study of the cathodic protection requirements and nature of calcareous scale in artificial, natural and heavily organically loaded seawater environments.

MATERIALS AND METHODS

Test specimens.

Mild steel (0.026%C, 0.004%S, 0.005% P, <0.02%Si, 0.340% Mn) test specimens of dimensions 80x25x1.5mm. were cut from strip, drilled to allow the passage of a support rod and electrical connection, sand-blasted with 20-40 grit to give a clean uniform finish and degreased in alcohol. The conection between the wire and the specimen was isolated with a sealant to prevent galvanic action and the specimens were suspended in the electrolyte on glass rods. For each experiment eight specimens were connected to one pole of a potentiostat so as to act as cathodes, the circuit being completed by graphite anodes connected to the other pole. Current was measured using a high impedance digital ammeter and potential (against a saturated calomel reference electrode) using a zero resistance voltmeter. Each system was set up at a

potential of -1.00V. The apparatus so arranded that pairs of specimens were exposed at different depths from the top to the bottom of 30 litre plastic experimental tanks (60 cm).

Short Term Experiments.

Three sets of experiments were carried out, all using artificial seawater (at 18°C +/- 2°C) containing NaCl, $CaSO_4$ $MgCl_2$ and $MgSO_4$ (to BS) as the electrolyte. Variations were made in the surface condition of the cathode specimens and in additions to the electrolyte. These were designed to reflect, in a uniform way, high organic environments, either on the metal surface or in the electrolyte. The first two series of experiments involved coating the cathode specimens with an agar gel to which various additions had been made. For the first series of experiments (series A) the gel was made using 30g/litre of agar powder in deionised water with the following additions:-

A1 Agar gel + 5g l^{-1} KCl.

A2 Agar gel + 10g l^{-1} KCl.

A3 Agar gel + 15g l^{-1} KCl.

A4 Agar gel + 20g l^{-1} KCl.

For the second series of experiments (series B) the gel was made using 30g/litre of agar powder dissolved in the following:-

B1 DEIONISED WATER

B2 ARTIFICIAL SEAWATER

B3 NATURAL SEAWATER

In all cases the average thickness of the gell was between 1 and 1.5mm.

For the third series of experiments (series C) no coating gel was used, instead organic material (Agar in solution) was added to the artificial seawater electrolyte in the following

concentrations:-

C1 0.25 g l^{-1} Agar

C2 0.50 g l^{-1} Agar

C3 1.00 g l^{-1} Agar

C4 2.00 g l^{-1} Agar

In each experiment the current density required to maintain a potential of -1.0 V (vs SCE) was automatically logged over the first 20 minutes on immersion of the specimens. The data was stored on a micro computer for later evaluation.

Long Term Experiments.

A series of experiments was carried out over 90 days in three different seawater environments to determine the effect of environment on the nature of the scale that forms on cathodically protected steel. The environments used were natural seawater over estuarine mud, (from the Humber estuary on the east coast of England); decomposing algal material in seawater, giving a reducing environment very high in organic material and bacterial metabolites (e.g. hydrogen sulphide) and thirdly, aerated artificial seawater. These three environments will be referred to as natural seawater, high organic seawater and artificial seawater.

Steel specimens were exposed in each environment at a potential of -1.0V (SCE). After 90 days the specimens were removed and the nature of the scales was determined using x-ray powder diffraction on finely ground material using copper Ka radiation with a wavelength of 1.5405nm.

RESULTS

Short Term Experiments

Current densities were monitored over the first 20 minutes following immersion of the specimens in the test environments. Typical results from the three series of experiments are shown in figures 1 and 2. For comparison between data a line of best fit was drawn through the first two minutes of each set of data using a computer program. The slopes of these lines, given in Tables 1, 2 and 3 provide a useful comparison between experiments. The tables also give the current density after 15 minutes.

TABLE 1

EXPERIMENTAL SERIES A

EXPERIMENT.	GEL.	INITIAL SLOPE.	CURRENT DENSITY AT 15MIN ($mA\ cm^{-2}$)
A1	Agar+5g l^{-1} KCl	-16.98.	0.353
A2	Agar+5g l^{-1} KCl	-17.36.	0.323
A3	Agar+5g l^{-1} KCl	-19.96.	0.306
A4	Agar+5g l^{-1} KCl	-24.12.	0.382

TABLE 2

EXPERIMENTAL SERIES B

EXPERIMENT.	GEL.	INITIAL SLOPE.	CURRENT DENSITY AT 15MIN ($mA\ cm^{-2}$)
B1	DEIONISED WATER .	-20.81	0.429
B2	ARTIFICIAL SEAWATER	-24.82	0.488
B3	NATURAL SEAWATER.	-27.84	0.531

TABLE 3

EXPERIMENTAL SERIES C

EXPERIMENT.	ADDITION TO ELECTROLYTE	INITIAL SLOPE.	CURRENT DENSITY AT 15MIN ($mA\ cm^{-2}$)
A1	$0.25g\ l^{-1}$ Agar	-21.28	1.118
A2	$0.50g\ l^{-1}$ Agar	-20.04	1.086
A3	$1.00g\ l^{-1}$ Agar	-18.07	0.912
A4	$2.00g\ l^{-1}$ Agar	-16.02	1.611

Average figures for each of the three series of experiments are given in Table 4 below.

TABLE 4

EXPERIMENTAL SERIES	AVERAGE CURRENT DENSITY
CONTROL	$0.995\ mA\ cm^{-2}$
SERIES A	$0.341\ mA\ cm^{-2}$
SERIES B	$0.483\ mA\ cm^{-2}$
SERIES C	$1.210\ mA\ cm^{-2}$

Long Term Experiments

A visual examination of the specimens after 90 days exposure gave the following results:-

Specimens from the natural seawater showed dark cream/grey scales with those on the specimens buried in mud being much thinner than those from the water.

Specimens exposed to the high organic reducing environment had blackened scales with large white crystals on their surfaces.

Specimens from the stirred artificial seawater showed varying thicknesses of a cream/white scale.

X-ray diffraction of the scales showed little difference within each environment due to depth of water and, for comparison between the environments, three specimens, taken from different

TABLE 5

DIFFRACTION PEAKS OBSERVED IN THE THREE SEAWATER REGIMES

	APPROXIMATE RELATIVE HEIGHT OF THE PEAK					
PEAK DESIGNATION	A	B	C	D	E	F
ARTIFICIAL SEAWATER	60%	20%	0%	100%	0%	10%
NATURAL SEAWATER	60%	0%	60%	100%	20%	50%
HIGH ORGANIC SEAWATER	0%	0%	60%	0%	20%	0%

TABLE 6

CARBONATE MINERALS OBSERVED IN THE SCALE DEPOSITS

	APPROXIMATE PROPORTION OF VARIOUS MINERALS			
ENVIRONMENT	ARAGONITE	CALCITE	DOLOMITE	MAGNESITE
ARTIFICIAL SEAWATER	25%	40%	30%	5%
NATURAL SEAWATER	0%	80%	0%	20%
HIGH ORGANIC SEAWATER	0%	60%	35%	5%

depths in each environment were selected and their scales ground together. The X-ray diffraction traces were found to be unique for each environment. To emphasise the differences random major peaks have been tabulated in Table 5. It is apparent from the table that the compounds giving rise to peaks C and E are only formed in natural seawater, the compound giving rise to peak B is only found in artificial seawater and that some compounds (A,B,D and F) are not found in organic rich reducing environments.

An analysis of the traces for carbonate minerals gave the results shown in Table 6. Calcite is the most abundant allotrope deposited in all the environments. Calcite, Dolomite, Aragonite

and a little magnesite were found in the artificial seawater. Only Calcite and magnesite were found in the natural seawater and mainly calcite and dolomite were found in the organically rich reducing environment. Aragonite was only found in the artificial (organic free) seawater environment.

While the x-ray diffraction peaks could be resolved for allotropes of carbonates some of the other peaks present could not be identified with certainty. However, sodium chloride and iron oxides are typical "contaminating" peaks.

DISCUSSION

The electrochemical reactions that occur at the surface of cathodically protected steel are considerably modified by a biologically active environment. Such an environment, results in a complex interface between the metal and the electrolyte.

The formation of calcareous scales in seawater is due to the high pH caused by the cathodic reduction reaction. However, the current density, and hence pH, over the metal surface will fall as the scale builds up. Thus the scale is the result of a complex sequence of initial and subsequent reactions at a range of pH and current densities. The nature of the first formed "bonding layer", is important to the integrity of the subsequent scale, which is more controlled by factors in the environment. These influences include the ratio of inorganic ions, the rate of crystallisation, pH, temperature and the presence of inorganic solutes (Kitano et.al.,1975).

Although the short term experiments are not entirely consistant they do show some interesting trends related to the organic and ionic conditions at the metal surface. The slope, and this the reaction rate at the surface leading to lower current demand, increases with increasing potassium chloride in the surface coating (Table 1) and decreases with increasing agar in the electrolyte (Table 3). This may indicate the role organic molecules have in slowing down precipitation processes (see below). However, these slopes are not reflected in the current densities found after 15 minutes. In fact, in Experimental series B the current density after 15 minutes in directly contradictory to what may be expected from thesteepness of the slopes.

Comparisons between experimental series are invalid due to the obvious sensitivity of each run to slight variations in experimental technique. However, experiment B2 does fit with experimental series C. The results for series B show trends are opposite to what might be expected in that the system with some organic content (natural seawater) gives the steepest slope (but the highest current density after 15 minutes). This reflects both the inorganic complexity, which results in a rapid surface reaction and the influence of organics, (slowing precipitation?) in natural seawater.

In the longer term experiments, the presence of organics produces a considerable effect. There are obvious differences, shown in Tables 5 and 6, in the crystallographic nature of the scales formed in different environments. It is interesting to note the major differences between artificial and natural seawater and then to note the considerable effect high organic loading has on the nature of the scale, reducing the calcite and magnesite and increasing the proportion of dolomite when compared to natural seawater. In fact in terms of the calcium/magnesium minerals, with the exception of aragonite, the high organic seawater is more akin to artificial seawater than natural seawater in its effect.

Hartt et.al.(1984) report that scale composition is a function of current density and that in laboratory systems at low current densities calcium carbonate is favoured while the magnesium content increases with increasing current densities (Klass, 1958). A higher potential will also produces a less coherent scale (Marette et.al.1963). Edyvean (1984) has shown a layered structure of scales formed in flowing seawater with high magnesium compounds, such as magnesium hydroxide and carbonate nearest the surface and then, as the current density and hence the ph drops, calcium carbonates further away from the surface. The influences determining which polymorph of calcium carbonate deposits are complex. In seawater, if precipitation is rapid, aragonite will deposit due to the presence of magnesium ions (Kitano et.al 1975, Pentecost, 1980) and this is the case in artificial seawater and in scale closest to the steel surface (Edyvean, 1984). Magnesium is thought to retard calcite deposition by increasing its solubility. However, except at high temperatures, a large percentage (40% at 10°C) of any precipitate from a carbonate solution will still be calcite even in the presence of magnesium (Kitano, 1962).

Thus, the sequence of deposition in the artificial seawater would be that the initial high current density causes a thin layer of magnesium hydroxide and magnesite to form. This is followed by aragonite, (as the presence of magnesium will retard calcite deposition) and the mixed magnesium and calcium carbonates as dolomite and then, at lower current densities, deposition of calcite.

In the natural seawater environments the minerals are deposited in quite different proportions (Table 6). There is no aragonite or Dolomite but only magnesite and calcite and it is likely that the difference is caused by the presence of organics in the seawater. Kitano and Hood (1965) studying calcium carbonate precipitation from solutions containing organic material found that many organic acids, such as malate, lactate and pyruvate cause calcite rather than aragonite deposition even in the presence of magnesium. Several mechanisms have been proposed for this effect, including the presence of organic compounds slowing down the precipitation rate, the complexing of Mg^{2+} wih organic compounds or the selective adsorbtion of organics onto aragonitic surfaces inhibiting crystal growth (Kitano and Hood, 1965; Lippmann, 1973). Thus, in the natural seawater magnesium compounds are likely to deposit first followed by calcite, the deposition rate being slowed by the presence of dissolved organics. Finally in the high organic seawater both the current density, and hence pH is likely to be lower due to absence of oxygen and the dissolved organics will higher. Both these factors will lead to very low deposition rates. The slow reaction and organic material is likely not only to prevent aragonite from forming but also allow magnesium ions to modify the calcite precipitation to dolomite.

CONCLUSIONS

The physical and electrochemical interactions at the protected metal surface in the different environments are obviously complex and more detailed work is required on highly controlled environments to resolve the reasons for all the differences observed. However this work does show the high degree of variability of scale formation and cathodic protection behaviour in the early stages of protection.

ACKNOWLEDGEMENTS

RGJE is holder of the Sorby Research Fellowship of the Royal society.

REFERENCES

Chave,K.E. and Suess,E. (1970) Calcium carbonate saturation in seawater: Effects of dissolved organic matter. Limnol. Oceanog. 15 pp 633-637.

Edyvean, R.G.J. (1984) Interactions between microfouling and the calcareous deposit formed on cathodically protected steel in seawater. Proceedings of the 6th International Congress on Marine Corrosion and Fouling, Marine Biology Volume 469-483.

Hartt,W.H.; Culberson,C.H.; and Smith,S.W. (1984) Calcareous deposits on metallic surfaces in seawater - A critical review. Corrosion 40. 609-618.

Kitano,Y. (1962) A study of the polymorphic formation of calcium carbonate in thermal springs with an emphasis on the effect of temperature. Bull. Chem. Soc. Japan. 35. 1973-1980.

Kitano,Y and Hood,D.W. (1965) The influence of organic material on the polymorphic crystallisation of calcium carbonate. Geochim.et Cosmochim.Acta. 29. 29-41

Kitano,Y; Kanamuri,N and Yoshioka,S. (1975) In. Watabe, N and Wilbur,K.M. (eds.). The mechanisms of minerilization in invertebrates and plants. University of S.Carolina Press, Columbia S.Carolina, USA., 191-202.

Klass,H (1958) Untersuchunger uber die Dechschich lenbildung bie der kathodishen Polarisation von Stahlobeuflachen. (The formation of coatings in the cathodic polarization of steel surfaces). Archiv fur das Eisenhuttenwesen, 29. 321-328.

Lippmann,F. 1973. Sedimentary Carbonate minerals. Springer-Verlag New York, 228pp.

Marette,D.; Guillen,M.A. and Hache,A. (1963). Contribucion al estudio de la proteccion cathodica del acero sumergido en agua de mar (Contributions to the study of the cathodic protection of steels in seawater) Instituito del /hierro y del Acero (Madrid). (Contributions) 16 No.83, 21-31.

Pentecost,A. (1980) Calcification in plants. Int.Rev. of Cytology, 62. 1-27.

Thomas,C.J.; Edyvean,R.G.J. and Brook,R. (1987) Biologically enhanced corrosion-fatigue. Biofouling 1 65-77.

Wolfson,S.L. and Hartt,W.H. (1981). An. initial investigation of calcareous deposits upon cathodic steel surfaces in seawater. Corrosion 37 70-76.

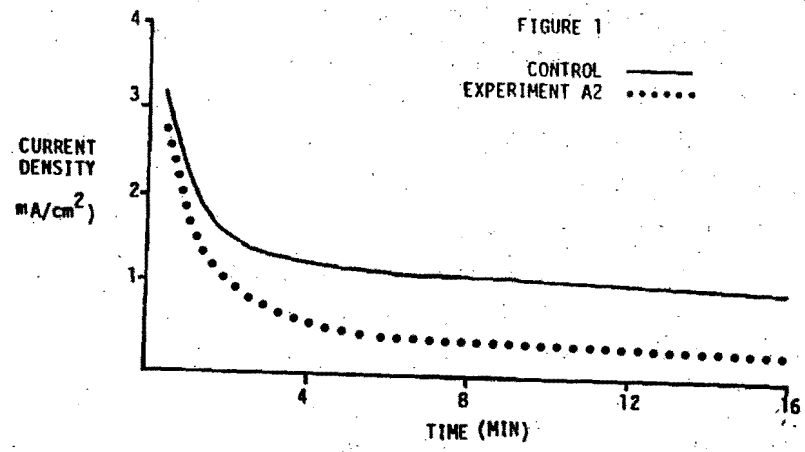

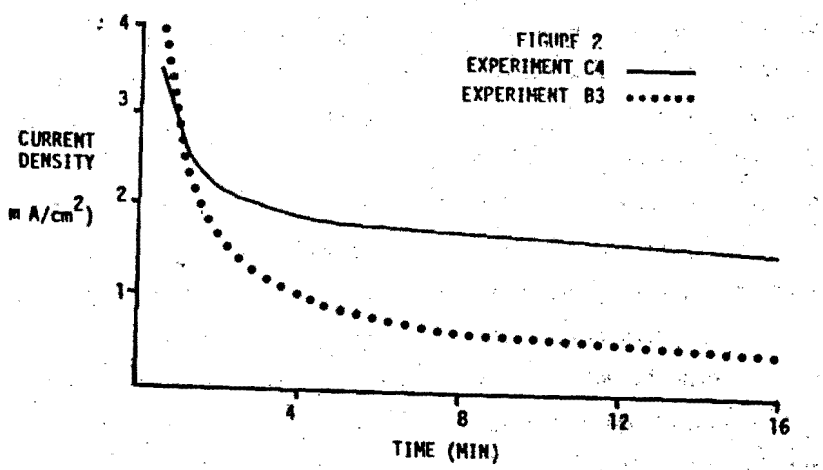

FIGURES 1 AND 2. FOR EXPERIMENTAL DETAILS SEE MATERIALS AND METHODS AND TABLES.

A CONTRIBUTION TO THE DEFINITION OF A QUALIFICATION PROCEDURE FOR APPLICATION OF STAINLESS STEELS IN SEAWATER

J.M. Krougman and F.P. IJsseling

Corrosion Laboratory, Royal Netherlands Naval College, Den Helder (The Netherlands)

A qualification procedure is described which basically consists of: three types of exposure applying micro creviced specimens in a temperature range including the service temperature and measurement of the polarisation curves in simulated crevice solutions in the same temperature range. The procedure is applied to a duplex stainless steel which was available in three product forms one of which being tested in addition in welded condition.

1. INTRODUCTION

In seawater at ambient temperature the susceptibility to crevice corrosion determines the applicability of stainless steels. From literature many test methods are known for establishing the susceptibility to crevice corrosion, most of these test methods delivering a criterion for alloy ranking (ref. 1 - 12). However, especially for critical applications, the behaviour under the actual service conditions must be known. For this reason data concerning initiation time, propagation rate and tendency to repassivation have to be obtained.

From the manifold of factors which may influence the crevice corrosion performance and the demand for data concerning actual service conditions the need to qualify stainless steels for application in seawater can be derived.

2. EXPERIMENTAL

2.1 Material

Specimens of a duplex stainless steel (25Cr5Ni2.5Mo2Cu) were available in three product forms: casting (C), bar (B) and plate (P). The chemical composition of the product forms are given in table 1. The product forms casting and bar were available in solution-treated (S) and solution-treated plus aged condition (A), plate was available in solution-treated and solution-treated plus welded condition (W).

2.2 Exposure tests

2.2.1 Galvanic coupling

The testing is performed applying samples which are provided with scratches, covered by an O-ring and mounted in a specimen holder (fig. 1). The scratched sample (anode) is short circuited with a large cathode (100x100 mm) of the same alloy, by means of a zero resistance ammeter. Both the free corrosion potential and the current between the electrodes are measured as a function of time (ref. 13). In this way apart from the initiation time,

the propagation and repassivation behaviour may be indicated. In fig. 2 the scratched surface before and after attack is shown. The tests with galvanic couples can be applied with freshly exposed cathodes as well as with pre exposed cathodes. The former represent the metal being initially exposed to seawater and the latter corresponds to a stainless surface being partly cleaned or damaged after prolonged exposure in seawater.

2.2.2 Potentiostatic exposure

The electrochemical measuring method to be used is basically the same as mentioned under pt. 2.1 keeping the scratched sample potentiostatically at 500 mV vs. SCE for three hours measuring the current flow. By increasing the temperature in steps of 15oC the exposures are performed starting at 10oC (ref. 14). Apart from a ranking according to the minimum initiation temperature an indication of the propagation is obtained.

2.3 Polarisation measurements

Three simulated crevice solutions are used: a. artificial seawater (prepared according to ASTM standard D-1141-52); b. artificial seawater with an addition of 146 gram sodium chloride per liter seawater and acidified with hydrochloric acid up to pH 2; c. artificial seawater with an addition of 263 gram sodium chloride per liter seawater and acidified with hydrochloric acid up to pH 1. The test

solutions are deoxygenated by nitrogen. The tests are performed at 10, 25 and 40oC. The measurements are carried out scanning potentiodynamically in anodic direction with a scan rate of 20 mV/min. More experimental details are reported in ref. 15. The aim of the measurements is to obtain current densities and potentials characteristic for crevice corrosion initiation.

3. RESULTS

3.1 Exposure tests

3.1.1 Galvanic coupling

3.1.1.1 Coupling to freshly exposed cathode

The cathode for these experiments was made of duplex stainless steel plate (S). The duration of the exposure was 56 days and in one case 49 days. In fig. 3 the current and the potential of the specimens are given as a function of time. It appears that casting (S) initiated crevice corrosion within 6 days and casting (A) within 3 days; bar (A) initiated within 7 days. Bar (S), plate (S) and plate (W) remained free from crevice corrosion. The mass losses, the total charges, the types of attack and the maximum penetration depths are given in table 2.

3.1.1.2 Coupling to pre exposed cathode

The cathodes for these experiments were the same as used previously for the coupling to freshly exposed cathodes. The pre exposure time was two months. The duration of the

exposure was 25 days.

In fig. 3 the current and the potential of the specimens vs. time are given. It appears that casting (S) initiated within 2 days and casting (A) within 1 day; bar (A) initiated within 1 day. Bar (S), plate (S) and plate (W) remained free from crevice corrosion.

The mass losses, the total charges, the types of attack and the maximum penetration depths are given in table 2.

3.1.2 Potentiostatic exposure tests

The specimens have been tested in duplicate at 500 mV vs. SCE in natural seawater at 10, 25 and 40oC. In fig. 4 characteristic currents of the specimens are shown. In table 3 the mass losses, the total charges, the types of attack and the maximum penetration depths of both sides of the specimens are given. It appears that the minimum temperatures at which the specimens initiated crevice corrosion are as follows: casting (S) 10oC, bar (S) 25oC, plate (S) 40oC, casting (A) 10oC, bar (A) 25oC and plate (W) 40oC.

3.1.3 Polarisation measurements

The critical current densities for passivation and breakdown potentials are given in fig. 5. The resistance against crevice corrosion being favoured by low critical current densities and high breakdown potentials, the following ranking in decreasing resistance can be

established:

- regarding critical current densities:

  plate (S) > bar (S) > casting (S)
  plate (W) > bar (A) > casting (A)

- regarding breakdown potentials:

  plate (S) > plate (W) > bar (S) > bar (A)
  > casting (S) > casting (A)

4. DISCUSSION

The results of the coupling tests applying freshly exposed cathodes and pre exposed cathodes are basically the same. The main difference, which was to be expected, is that the pre exposed cathodes decrease the initiation time of crevice corrosion. This is caused by the relatively noble potential of the pre exposed cathode shifting the potential of the scratched sample in positive direction thus stimulating initiation of crevice corrosion from the start of the exposure.

In seawater the pH in crevices spontaneously decreases to approx. 2 (ref. 16). It is postulated that critical current densities, obtained in simulated crevice solutions, higher than 10 uA/cm2 indicate depassivation hence susceptibility to crevice corrosion (ref. 17). Moreover breakdown potentials below approx. 500 mV vs. SCE, which is the highest potential stainless steel can reach in seawater (ref. 18), also indicate susceptibility

to crevice corrosion. So regarding the potential vs. time curves of the galvanic coupling exposures, the current vs. time curves of the potentiostatic measurements and the breakdown potentials in simulated crevice solutions at 25oC, it was to be expected that during the coupling exposures casting (S), casting (A) and bar (A) would initiate crevice corrosion and that bar (S), plate (S) and plate (W) would remain free from crevice corrosion.

The superior performance of plate may be attributed to a higher molybdenum and a lower sulphur content compared with casting and bar. The inferior behaviour of solution-treated plus aged product forms may be due to precipitation of deleterious phases in the microstructure during aging.

From the results obtained the following criteria for qualification at the intended service temperature may be derived: 1. no initiation of crevice corrosion, neither in the galvanic coupling exposure tests nor in the potentiostatic tests at the highest potential the alloy can reach in natural seawater; 2. in addition this behaviour should be confirmed by polarisation measurements in simulated crevice solutions, i.e. artifical seawater up to an addition of 146 g/l sodium chloride and acidified up to pH 2 indicating critical current densities lower than 10 uA/cm2 and breakdown potentials higher than 500 mV vs.

SCE. However, more research i.e. laboratory tests and long-term exposure has to be devoted to the procedure to prove the validity of the proposed qualification criteria.

5. CONCLUSIONS

From the results as discussed above the following conclusions can be derived:

1. As regards the exposure tests, applying micro creviced specimens, the differing severities of these tests deliver results which may mutually confirm, reinforce and/or complete the crevice corrosion characteristics obtained. In this respect the polarisation measurements in simulated crevice solutions may also support and/or verify the results of the exposure tests. On this basis the test procedure applied is more adequate to qualify stainless steels for application under actual seawater service condition than one single ranking test method.
2. Concerning the samples of the particular duplex stainless steel tested the following conclusions can be drawn:
   - In solution-treated and solution-treated plus welded condition only plate did not appear to be susceptible to crevice corrosion up to 25oC.
   - In solution-treated and solution-treated plus aged condition bar behaved better than casting.
   - For each product form the susceptibility to crevice

corrosion in solution-treated plus aged condition is increased compared with the solution-treated condition.

6. RECOMMENDATION

The qualification procedure applied in this investigation has been based on relatively short-term laboratory exposures applying one type of crevice geometry. It is envisaged to continue the development of a laboratory qualification procedure performing by long-term exposure in situ as well as in the laboratory. In addition the micro creviced exposure test will be adapted to enable testing of tubular products.

7. REFERENCES

1. J. Postlethwaite: Canadian Metallurgical Quarterly, 22, no. 1, p. 133 (1983).
2. F.P. IJsseling: Br. Corros. J., 15, no. 2, p. 51 (1980).
3. R.J. Brigham: Mat. Perf., Dec., p. 44 (1985).
4. P. Lau & S. Bernhardsson: Paper no. 64, NACE Intern. Corrosion Forum, Boston (1985).
5. E.L. Hibner: Mat. Perf., March, p. 37 (1985).
6. H. Kenner, B. Heubner, M.B. Rockel & E. Wallis: Werkst. u. Korr., 37, p. 183 (1986).
7. L.M. Butter & W.M.M. Huibrechts: Polyt. Tijdschrift/ Procest., 39, no. 8, p. 40 (1984).
8. R.M. Kain, T.S. Lee & J.W. Oldfield: Paper no. 60, NACE Inern. Corrosion Forum, Boston (1985).

9. R.M. Kain: Mat. Perf., Febr., p. 24 (1984).
10. J.W. Oldfield & W.H. Sutton: Br. Corros. J., 13, no. 1, p. 13 (1978).
11. J.W. Oldfield & W.H. Sutton: Br. Corros. J., 13, no. 3, p. 104 (1978).
12. J.L. Crolet, L. Séraphin & R. Tricot: Revue Metall., no. 12, p. 937 (1975).
13. J.M. Krougman: Presentation Workshop Corrosion Protection of Materials in Seawater Applications, Amsterdam, KSLA, 6-7 November 1986.
14. J.M. Krougman & F.P. IJsseling: Proc. Internat. Workshop on Electrochemical Corrosion Testing, Ferrara, 1985 (DECHEMA Monograph Vol. 101, p. 135).
15. J.M. Krougman & F.P. IJsseling: Proc. 6th Intern. Congr. on Marine Corros. and Fouling, Athens, p. 75 (1984).
16. J.L. Crolet & J.M. Defranoux: Corr. Sc., 13, p. 575 (1973).
17. J.L. Crolet, L. Séraphin & R. Tricot: Revue Metall., no. 1, p. 1 (1976).
18. A. Mollica & A. Trevis: Proc. 4th Intern. Congr. on Marine Corros. and Fouling, Juan-les-Pins, p. 351 (1976).

Table 1. Chemical composition in percentages of weight

Product form	C	Cr	Ni	Mo	Cu	S	N
Casting	0.068	25.4	5.85	2.87	2.50	0.028	0.14
Bar	0.046	25.4	6.38	2.42	1.71	0.018	0.18
Plate	0.02	25.7	5.2	3.5	1.9	0.002	0.14

Table 2. Results of galvanic coupling tests in natural seawater at 25oC

Product form & condition	Condition of cathode (1)	Mass loss (mg)	Total charge (C)	Maximum penetration depth (um)	Type of localised attack (2)
Casting (S)	f.e.	144.7	843.2	700	c, p
Bar (S)	f.e.	<0.1	0.2	<3	p
Plate (S)	f.e.	<0.1	0.2		o
Casting (A)	f.e.	270.6	1034.5	400	c, p
Bar (A)	f.e.	76.8	284.2	740	c, p
Plate (W)	f.e.	<0.1	0.2	<3	p
Casting (S)	p.e.	34.4	127.3	420	c, p
Bar (S)	p.e.	<0.1	0.3	<3	p
Plate (S)	p.e.	<0.1	0.4		o
Casting (A)	p.e.	173.1	482.0	330	c, p
Bar (A)	p.e.	18.5	52.0	280	c, p
Plate (W)	p.e.	<0.1	0.1	<3	p

(1) f.e. = freshly exposed; p.e. = pre exposed
(2) c = crevice corrosion; p = pitting; o = no localised attack

Table 3. Results of potentiostatic exposure tests in artificial seawater at 10, 25 and 40oC

Product form & condition	Temp. (oC)	Side	Mass loss (mg)	Total charge (C)	Maximum penetration depth (um)	Type of localised attack (1)
CS	10	1	<0.1	0.38	7	c, p
		2	<0.1	0.08	5	c, p
BS	10	1	<0.1	0.01	<3	p
		2	<0.1	0.01	<3	p
PS	10	1	<0.1	0.01		o
		2	<0.1	0.01		o
CA	10	1	<0.1	0.20	7	c, p
		2	<0.1	0.09	3	c, p
BA	10	1	<0.1	0.02	<3	p
		2	<0.1	0.04	<3	p
PW	10	1	<0.1	0.01	<3	p
		2	<0.1	0.01		o
CS	25	1	0.2	8.86	30	c, p
		2	<0.1	0.07	20	c, p
BS	25	1	<0.1	0.07	10	c, p
		2	<0.1	0.04	17	c, p
PS	25	1	<0.1	0.02		o
		2	<0.1	0.01		o
CA	25	1	0.3	8.98	25	c, p
		2	0.1	6.57	25	c, p
BA	25	1	<0.1	0.02	4	c, p
		2	<0.1	0.04	20	c, p
PW	25	1	<0.1	0.01	<3	p
		2	<0.1	0.01		o
CS	40	1	21.8	83.30	220	c, p
		2	2.0	11.03	185	c, p
BS	40	1	1.6	7.42	150	c, p
		2	5.4	22.47	165	c, p
PS	40	1	<0.1	0.02		o
		2	<0.1	0.03	10	c
CA	40	1	17.3	69.17	110	c, p
		2	7.4	30.70	180	c, p
BA	40	1	1.8	6.31	135	c, p
		2	6.8	27.77	185	c, p
PW	40	1	<0.1	0.05	3	p
		2	<0.1	0.13	12	p

(1) c = crevice corrosion; p = pitting; o = no localised attack

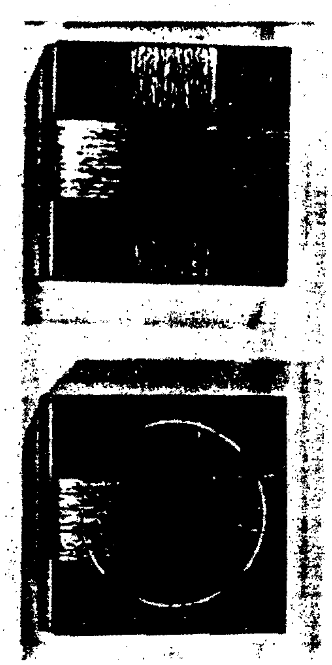

Fig. 2: Scratched surface before (left) and after (right) attack

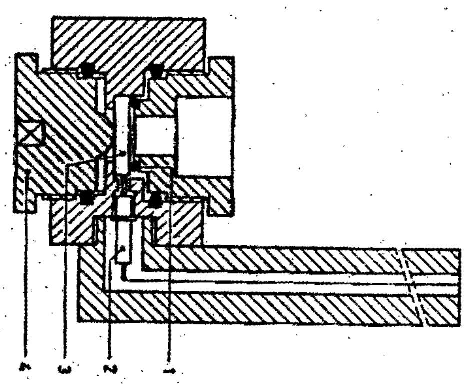

Fig. 1: Longitudinal section of holder for micro creviced specimen (1: O-ring; 2: contact wire; 3: specimen; 4: plug)

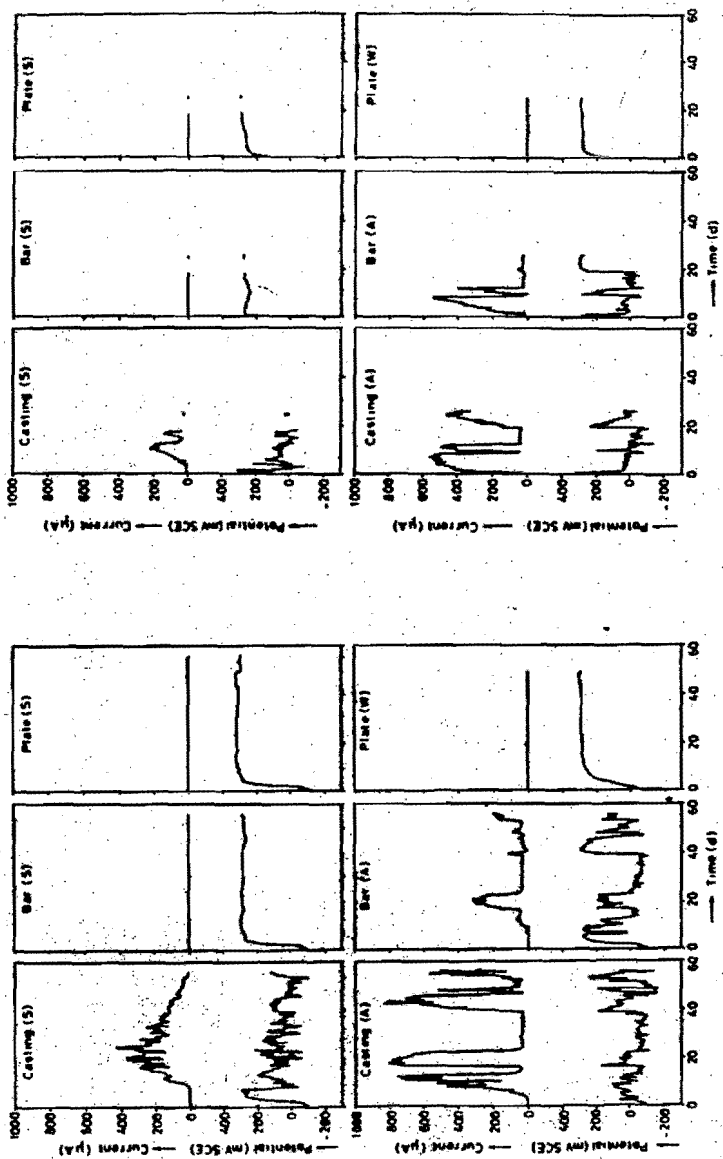

Fig. 3: Exposure tests with micro crevised specimens galvanically coupled with freshly exposed cathodes (left) and pre exposed cathodes (right) in natural seawater at 25oC

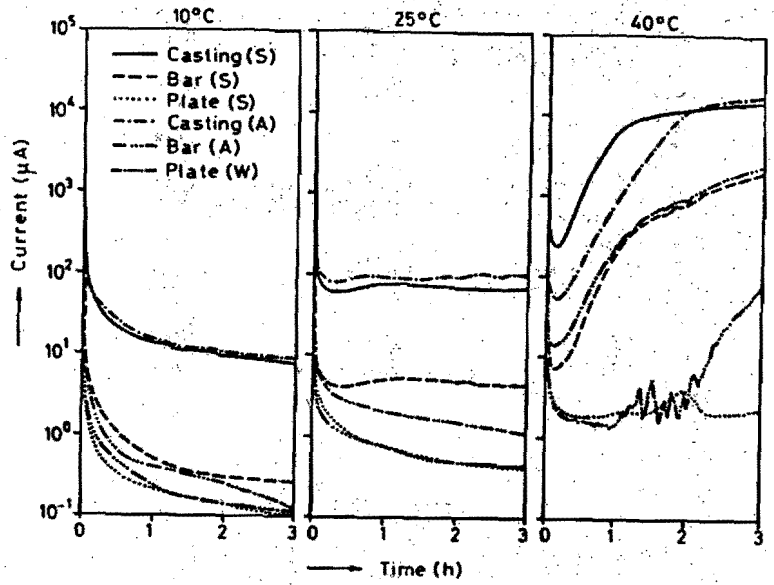

Fig. 4: Potentiostatic exposure with micro crevised specimens at 500 mV vs. SCE in natural seawater at 10, 25 and 40oC

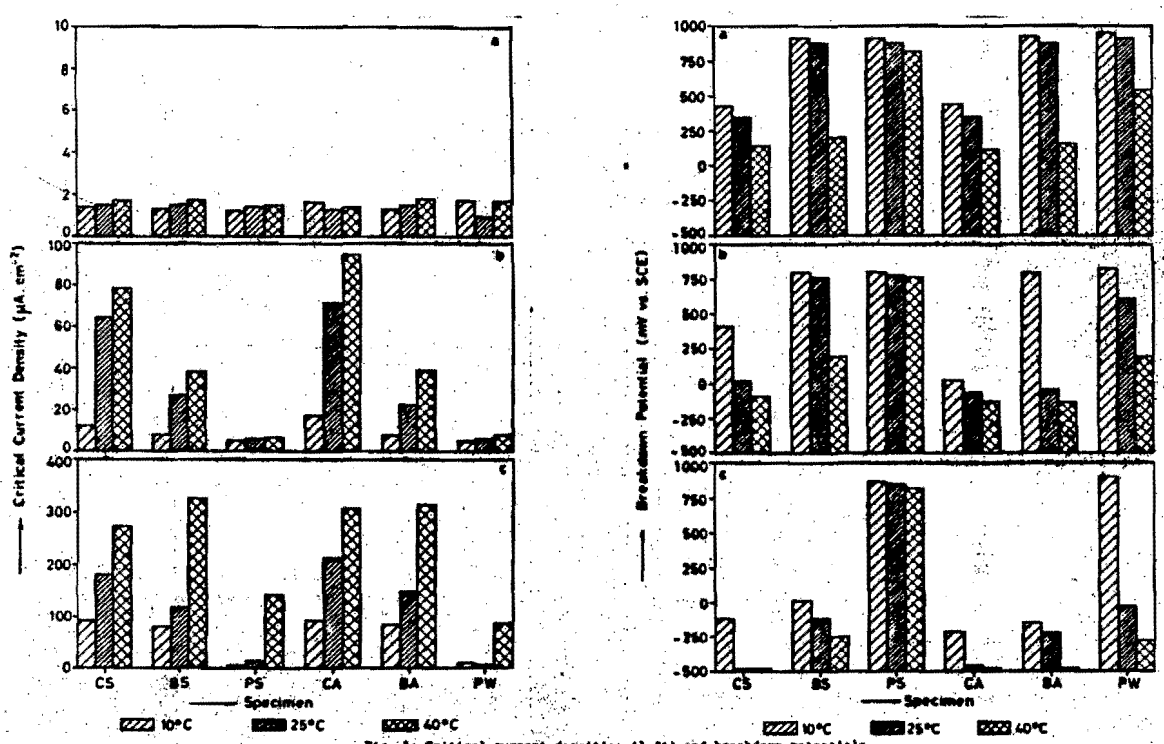

Fig. 5: Critical current densities (left) and breakdown potentials (right) obtained in simulated service solutions

THE CORROSION AND PROTECTION OF STEEL PIPE PILES IN NATURAL SEAWATER

Dr. Kiyoshi Katawaki*
Dr. Tatsuo Asama**
Kazuyuki Doi***

1. INTRODUCTION

In order to secure long-term durability of offshore steel structures, the establishment of corrosion protection technology may be said to be indispensable. Particularly, the corrosion conditions are severest at the splash and tidal zones, while maintenance and repair are difficult, and it is absolutely necessary for a corrosion protection technology which can be applied to this environment.

Therefore, as a part of the Japanese Government Ministry of Construction's project for "Development of Construction Technology for Offshore Structures", exposure tests of corrosion-protected steel piles with the objective of developing a new, long-lasting and maintenance-free corrosion protection technology were started at two locations on the Pacific Ocean coast of Japan with a 15-year schedule from 1973 to 1987 in the form of joint research of the Ministry of Construction Public Works Research Institute and the Japanese Association for Steel Pipe Piles.[1)2)3)]

This paper is a summarization of the test result for the long term period from 1973 through 1987.

---

* Dr. Kiyoshi KATAWAKI is the director of Chemistry Division, Public Works research Institute, Ministry of Construction, Japanese Government. He has engaged in the managing research activities related on the maritime structure and civil engineering materials.

** Dr. Tatsuo ASAMA is the executive director of Japanese Association for Steel Pipe Piles (JASPP). His principal achievements are on research and development of steel pile design and construction practice in civil engineering technology.

*** Mr. Kazuyuki Doi is a technical member of Japanese Association for Steel Pipe Piles. He is a senior researcher of Surface Treatment Research Lab. R&D Laboratories-II, Nippon Steel Corporation. He has engaged in research and development of corrosion protection technologies on maritime steel structures.

2. TEST MATERIAL AND TEST METHOD

(1) Exposure Test Sites and Their Corrosion Environments

As the exposure test sites for corrosion-protected steel pipe piles, two locations were selected at Chiba and at Ajigaura. Chiba is a site inside Tokyo Bay facing the Pacific Ocean where waves are quiet but there is contamination of seawater. The exposure site is 80 m offshore from a factory wharf in the city of Chiba. On the other hand, Ajigaura is a location at the sea coast of Ibaraki Prefecture facing the Pacific Ocean where waves are rough but the seawater is clean. The exposure site is 100 m from the shore line. (See Fig. 1)

Next, investigations were made of water quality of seawater in the vicinity of the exposure test sites in order to confirm the corrosive nature of the exposure environments. The results of the water quality tests are given in Table 1. According to this table, there was nothing particularly unusual, except for the facts that the chloride concerntration at Chiba was slightly lower compared with standard seawater, and that the index of water pollution NH_4^+ at Chiba was higher than that at Ajigaura.

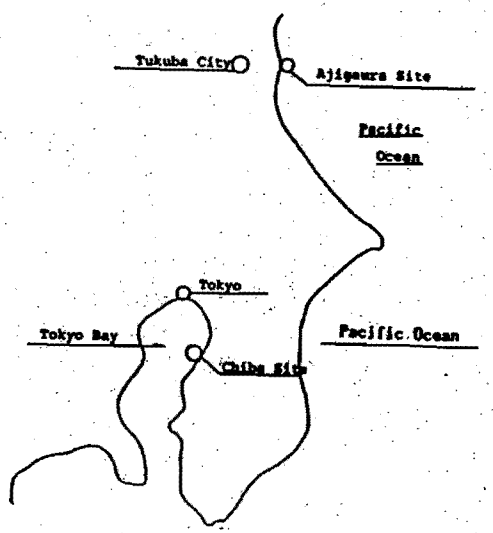

Fig. 1 Location of Exposure Test Site

TABLE 1

Chemical Analysis of Natural Seawater at Exposure Sites

Month Investigated	Water Temp. (°C)	pH	Cl^- (g/l)	SO_4^{2-} (g/l)	DO (ppm)	COD (ppm)	NH_4^+ (ppm)	NO_2^- (p4m)
Chiba:								
Feb '75 ...	8.5	8.60	17.61	2.42	8.1	-	-	-
Feb '76 ...	9.5	8.20	18.19	2.53	-	-	-	-
Oct '77 ...	19.0	7.90	18.50	2.40	3.8	-	-	-
Aug '78 ...	31.5	8.08	16.93	2.28	6.2	-	-	-
Jul '79 ...	25.9	7.67	16.35	-	5.2	-	-	-
Aug '80 ...	19.0	8.30	17.91	-	7.5	-	-	-
Jul '81 ...	26.0	8.00	17.80	-	7.2	-	-	-
Sep '82 ...	24.0	8.10	18.00	-	7.4	-	-	-
Aug '83 ...	23.3	8.40	14.60	-	5.6	7.7	0.20	1.40
Nov '84 ...	17.3	8.10	17.90	2.67	7.5	2.2	0.27	1.00
Jul '86 ...	21.3	8.20	16.40	2.29	7.3	-	-	-
Ajigaura:								
Feb '76 ...	9.2	8.20	19.32	2.65	-	-	-	-
Jul '77 ...	22.0	8.20	17.37	2.39	8.5	-	-	-
Jul '78 ...	24.0	8.25	18.64	2.49	8.5	-	-	-
Mar '80 ...	10.0	8.47	18.84	2.59	11.7	-	-	-
Jul '81 ...	23.0	8.10	18.50	-	7.5	-	-	-
Jul '82 ...	18.2	8.10	18.50	-	7.8	-	-	-
Jun '83 ...	18.0	8.10	17.90	2.54	7.8	-	-	-
Jun '84 ...	17.0	7.90	17.90	2.58	7.3	2.0	0.18	0.03
Normal ...		8.1	18.90	2.65	7-10	2	0	0
Sea Water		- 8.3						

(2) Numbers of Steel Pipe Piles and Test Pieces, and Areas Corrosion-Protected

As materials to be tested, steel pipe piles wich comprise the structural form utilized most commonly and which can serve as bases when configurations are complex were selected. The steel pipe piles used were 24 structural-use carbon steel pipe piles of 508 mm diameter and 44 m length at Chiba and 18 piles of 609 mm diameter and 16 m length at Ajigaura. Of the total number of 42 steel pipe piles, three piles for control were not corrosion-protected, while 39 were given corrosion protection coverings of 6 m at the splash-tidal zones as shown in Fig. 2. (See Photo. 1 and Photo. 2)

Also, small diameter steel pipes of 100 mm diameter and 2 m length were provided with corrosion protection coverings as shown in Fig. 3 and used as test pieces. These test pieces were exposed at the splash-tidal zones after being inflicted in advance with the 3 types of artificial defects, that is, impact defect, abraision defect and scratch defect. The total number of test pieces prepared was 100. But in this paper test results of steel pipe piles are mainly described.

(3) Corrosion Protection Systems Applied

The types of corrosion protection systems applied were selected among systems presently being mainly used, and among those new, with which long service lives might be expected, on examining corrosion resistance, applicability, economy and marketability through investigations of literature and actual performance.

The kinds of these systems were as follows:

Metal covering systems ..... 5 kinds
Paint systems ..... 7 kinds
Organic lining systems ..... 19 kinds
Inorganic lining systems ..... 2 kinds

These corrosion protection systems are listed in Table 2.

The arrangements of steel pipe piles and test pieces at Chiba and Ajigaura are shown in Fig. 4 and 5, respectively.

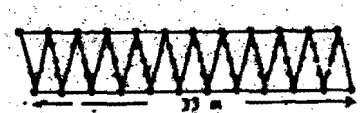

• Steel Pipe Pile (24 pcs)
• Test Piece

Fig. 4.-Arrangement at Chiba

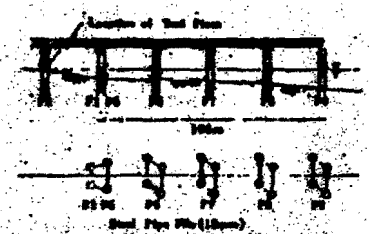

Fig. 5.-Arrangement at Ajigaura

TABLE 2

DESCRIPTION OF CORROSION-PROTECTED STEEL PIPE PILES EXPOSED AT CHIBA AND AJIGAURA

No.	Type of Covering	Exposure Test
1	Stainless steel (25 Cr-13 Ni, sheet wrap, 3 mm)	C (P, T)
2	Low-alley, corrosion-resistant steel (Cu-Cr-Al, sheet wrap, 6 mm)	C (P, T), A (P, T)
3	Monel (sheet wrap, 2 mm)	C (T)
4	Titanium (sheet clad, 0.5 mm)	C (T)
5	Flame-sprayed aluminum with seal coat (200 m)	C (P, T)
6	Flame-sprayed aluminum (100 m) + coal-tar epoxy (300 m x 2)	C (P, T)
7	Flame-sprayed alumium (100 m) + coal-tar epoxy with glass cloth (300 m x 2)	A (T)
8	Flame-sprayed alumium (100 m) + coal-tar epoxy with vinylon cloth (300 m x 2)	C (P, T), A (P)
9	Flame-sprayed zinc (100 m) + coal epoxy (300 m x 2)	C (P, T)
10	Inorganic zinc-rich paint (100 m)	C (T)
11	Inorganic zinc-rich primer (75 m) + coal-tar epoxy (300 m x 3)	C (P, T), A (P, T)
12	Inorganic zinc-rich primer (75 m) + epoxy with glass cloth (300 m x 3)	C (P, T), A (P, T)
13	Glass flake-filled polyester (1 mm and 2 mm)	C (T), A (T)
14	Polyethylene (cohesion type, extrustion process, 4 mm)	C (P, T), A (P, T)
15	Polyethlene (adhesive type, extrusion process, 4 mm)	C (T)
16	Polyethlene (fusion bonded process, 3 mm)	C (T)
17	Polyethlene heat-shrink tube (3 mm)	C (T)
18	Epoxy (fusion bonded process, 0.3 mm) + polyethylene (extrusion process, 4 mm)	C (T)
19	Epoxy resin mortar (4 mm, 5 mm)	C (P, T), A (P, T)

Photo. 1 Exposure Site off Chiba

Photo. 2 Exposure Site off Ajigaura

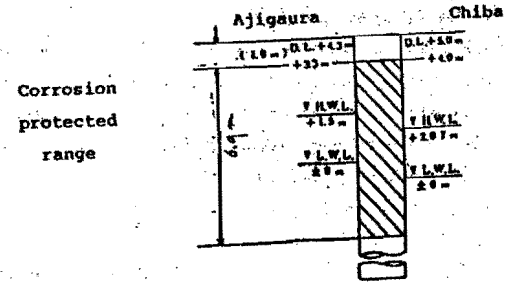

MATERIAL STK41

DIMENSION

at Chiba

ϕ508mm x t9.5mm x 44m

at Ajigaura

ϕ609.6mm x t14mm x 16m

Fig. 2 - Shape and corrosion-protected range of steel pipe pile

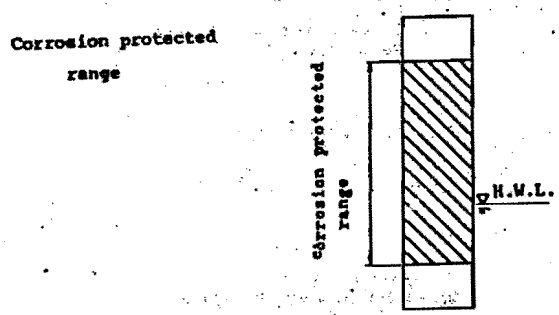

MATERIAL SGP DIMENSION

ϕ100mm x t4.5mm x 2m

Fig. 3 - Shape and corrosion protected range of test piece

Table 3 Results of Visual Inspection after 11.5 years exposure off chiba

	Type of coating	Direction	Atmos	Splash	Upper tidal	Lower tidal	Submerged
1.	Stainless steel (25Cr-13Ni sheet, 3mm)	L	9 A	9 A	9 A	9 A	9 A
		H	9	9	9	9	9
2.	Flame sprayed aluminum (200 μm)	L	9 C	9 C	0 E	0 E	0 E
		H	9	9	0	0	0
3.	Flame sprayed aluminum (100 μm) + coal-tar epoxy (100 m x 2)	L	5 D	1 D	0 D	0 E	0 E
		H	0	0	0	0	0
4.	Flame-sprayed aluminum (100 μm) + coal-tar epoxy with vinylon cloth (300 μm x 2)	L	6 C	5 C	0 D	1 D	5 C
		H	6	5	0	5	4
5.	Flame-sprayed zinc (100 μm) + coal-tar epoxy (300 μm x 2)	L	9 B	7 B	0 E	2 E	9 C
		H	9	7	0	7	8
6.	Inorganic Zinc-rich paint (75 μm) + coal-tar epoxy (300 μm x 3)	L	9 B	9 B	3 B	9 B	9 B
		H	9	9	9	9	9
7.	Inorganic Zinc-rich paint (75 μm) + epoxy (300 μm x 3)	L	9 B	5 B	7 B	8 B	9 A
		H	5	6	9	9	9
8.	Polyethelene (cohesion-type, extrusion process, 4mm)	L	9 A	9 AB	9 A	9 A	9 A
		H	9	9	9	9	9
9.	Epoxy resin mortar (4 mm)	L	0 CD	0 CD	0 C	0 C	0 C
		H	0	0	0	0	0
10.	Steel fiber reinforced concrete (100mm by casing, 50 mm by spraying	L	6 B	5 B	9 B	9 B	9 B
		H	1	6	9	9	9

(1) Direction L: Face to land (land side)
H: Face to off-shore (off-shore side)
(2) Atmos : Atmospheric zone
(3) Splash : Splash zone
(4) upper tidal : upper part of tidal zone
(5) lower tidal : lower part of tidal zone
(6) Submerged : Submerged zone
(7) A - E : Evaluation of surface appearance after removal of marine life
A : Excellent
B : Better
C : Good
D : Worse
E : Worst
(8) 0 - 9 : Rating number of rust of base steel after removal of coating (ASTM D610-68)

Table 4 Results of Visual Inspection after 10.5 years exposure off-Apigigaura

Type of coating	Atmospheric and Splash zone	Tidal zone
1. Low alloy corrosion resistant steel (6mm) wrap	All surface is covered thick rust rayer (6mm) and many rusted blister (20-50mmφ) are observed	Thick rust layers are observed around the pile, Many rust layers seem to be tight.
2. Inorgaic Zinc-rich primer (75 m) + coal-tar epoxy (300 m x 3)	Disbond of coating is observed along the spiral bead at several spot. Abrasion damages are seen at land side and rust has occured. B	At off-shore side coating disbound is observed and rusted, Condition of coating is generally good. B
3. Flame-sprayed Aluminum (100 m) + Coal-tar epoxy with glass cloth (300 m x 3)	Coating film is almost disbonded from Al layer and rusted DE	Almost all surface coating are removed from Al layer and rusted DE
4. Inorganic Zinc-rich primer (75 m) + Epoxy with glass cloth (300 m x 3)	Almost all surface are chalked. Coating disbond is observed at several spots and rusted. Condition of coating is generally good. B	No rust is observed. Coating film is generally remained at good condition. AB
5. Epoxy resin mortar (4 mm)	Many piholes are observed along the spiral bead. On all coating surface are observed spotted rusts cause of rust of base metal. Upper part of pile surface is fouled by rust flowed down from upper side. BC	Spotted rust is observed at all coating surface and obviously caused by rust of base metal, that is, steel pile. B
6. Poly-Urethane mastic (3 mm)	Coating disbond is observed around the pile. Many blisters of coating can be seen. DE	Coating disbond can be seen at all surface especially at off-shore side. DE

No.	Type of Covering	Exposure Test
20	Underwater-curing epoxy (5 mm)	C (T)
21	Glass flake-filled epoxy (2 mm)	C (T)
22	Epoxy-saturated nonwoven fabric tape (3 mm)	C (T)
23	Coal-tar epoxy mastic (14 mm)	C (T)
24	Urethane mastic (3 mm)	A (P, T)
25	Foamed polyurethane (10 mm)	C (T)
26	Asphalt mastic (10 mm)	C (T)
27	Polyurethane rubber (4 mm)	A (P, T)
28	Butyl rubber (4 mm)	C (T)
29	Cold vulcanized chloroprene sheet (5 mm)	C (T)
30	Steel fiber reinforced concrete (100 mm by casing, 50 mm by spraying)	C (T)
31	Glass fiber reinforced cement mortar (20 mm)	C (T)
32	Cement mortyar (47 mm) + polyester FRP cover (3 mm)	A (P, T)
33	Petrolatum-saturated tape (2 mm) + FRP cover (3 mm)	C (T)

C: At Chiba A: At Ajigaura P: Pipe Pile T: Test Piece

(4) Test Programs

Investigations are made on the corrosion prevention performances every year through observations of surface appearances and non-destrutive tests.

Steel pipe piles off Chiba were removed by underwater cutting about 12 m length after 11.5 years of exposure and the corrosion protection properties were investigated by destructive tests.

1) Visual Inspection

Inspection is made of the surface from a boat or a pier and the states of deterieration are recorded. Corrosion protected steel piles off Chiba were removed coverings, coatings and linings and the occurrence of rust about base steel was investigated.

2) Photography

Photographs (color) are taken from a boat or a pier of the splash-tidal zones and damaged portions, while regarding underwater portions the vicinities of the bottom edges of coverings are photographed.

3) Measurement of thicknesa of base steel

Thickness of base steel is measured by ultrasonic thickness gauge or micrometer.

4) Measurement of Adhesion of Coatings

The adhesion of coatings is measured by an adhesion, tester (pull off type). For bond with coatings an epoxy base adhesive (Araldite) is used.

5) Measurement of Electrical Resistance of Coating

The electrical resistances of the coverings are measured by the guard ring method using a paint film tester.

The method of measurement consists of attaching aluminum foil and a guard ring with electrolytic liquid paste and measuring after 18 hours have elapsed.

6) Measurement of physical properties of polyethylene

Physical properties of polythylene after 11.5 years of exposure are investigated and compared with properties before exposure.

3. TEST RESULTS

(1) Visual Inspection of Coatings and Base Steel Results of Visual inspection by surface appearance observation and photography of coatings, and occurrence of rust of base steel are summerised in Table-3 for piles off-Chiba. The results of visual inspection off-Ajigaura are listed in Table-4.

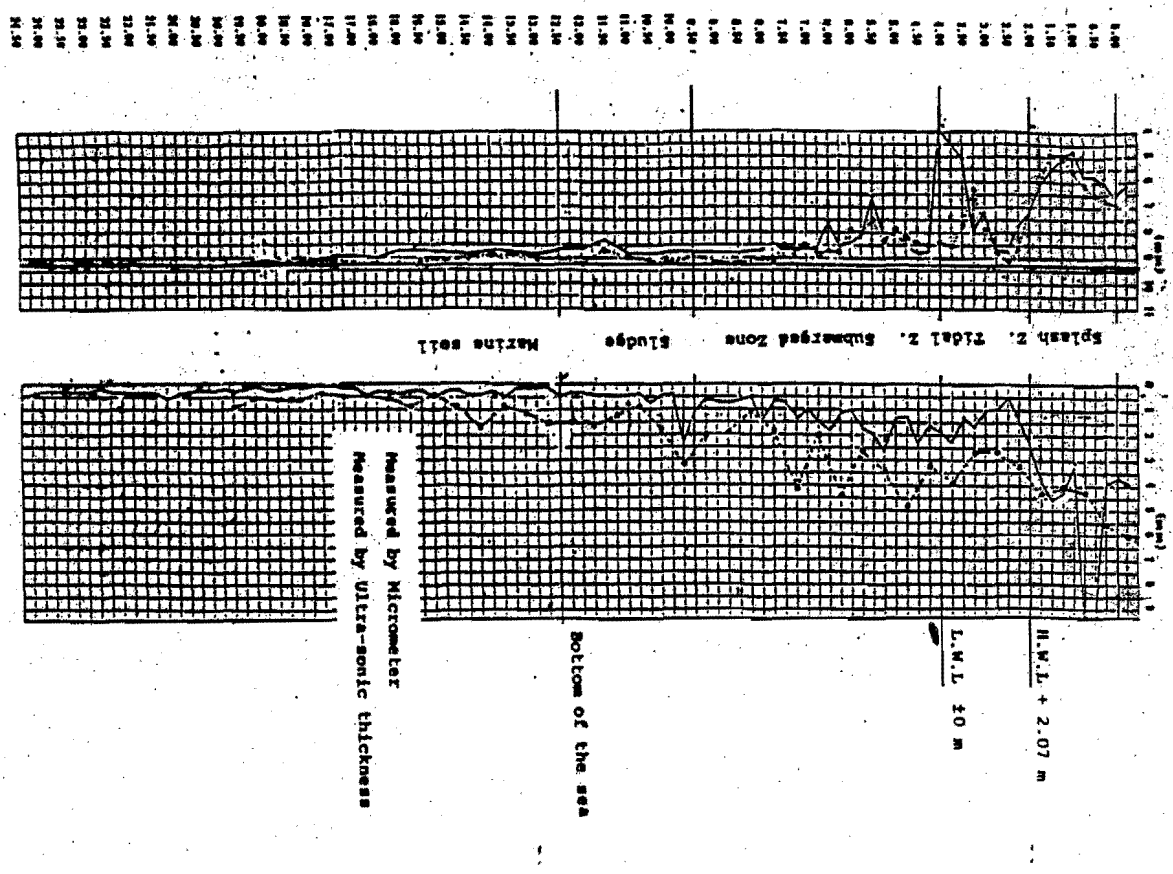

Fig. 6 Example of thickness measurement of low carbon steel pile after 11.5 years exposure off-Chiba

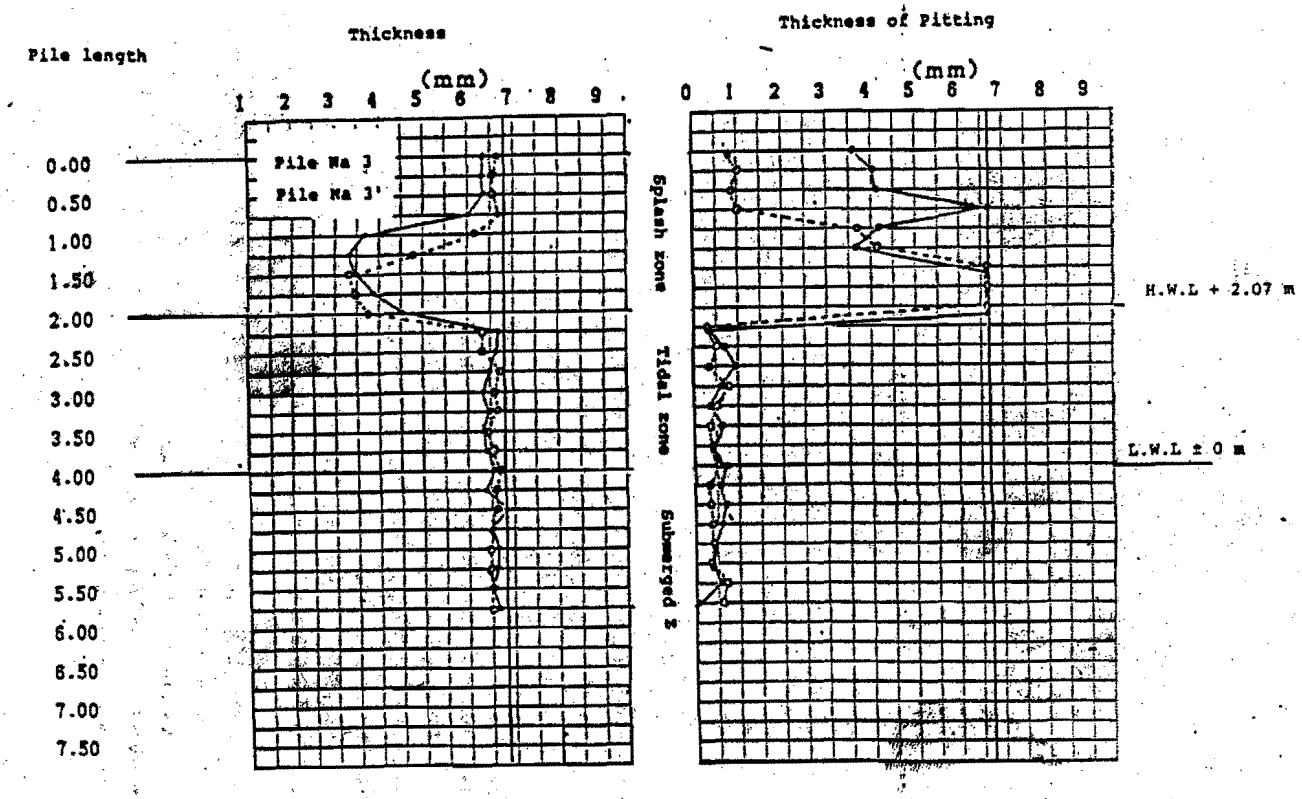

Fig. 7 Thickness of low alloy steel wrap after 11.5 years exposure off-Chiba (Initial thickness 6 mm)

Type of coating	Atmospheric and Splash zone	Tidal zone
7. Reinforced Cement Mortar lining (47 mm) + Fiber reinforced polyester cover (3 mm)	Upper part of FRP cover is destroyed and can be seen mortar lining surface. Partially steel bar is observed. B	Liming is remained excellent condition. A
8. Poly-Urethane rubber lining (4 mm)	Surface part of Coating film is scaled off (500 x 1000mm, & 200 x 200mm) at lower splash zone but no rust can be observed. AB	Coating is remained excellent condition. B
9. Polyethylene (cohesion type, extrusion process) 4 mm	Abrasion damage and fouling can be seen at surface part of coating, but no rust is observed. A	Coating is remained excellent condition. A small damage of coatng and the rust by hitting of steel chain can be seen. A

A - E : Evaluation of visual inspection at site.

A: Excellent D: Worse
B: Better E: Worst
C: Good

(2) Measurements of Thickness of Base Steel

The result of thickness measurement of non-protected low carbon steel pile is shown in Fig. 6 and for low ally steel pile is shown in Fig. 7.

The result of thickness measurement of base steel after removing stainless steel sheet wrap is shown in Fig. 8.

(3) Measurements of Adhesion and Erectrical Resistance of Coating and Lining on Steel Pipe Piles

The electrical resistance and adhesion strength of coatings were measured for steel pipe piles removed from test site off-Chiba. The results of these measurements are shown in Table 5.

(4) Measurements of Physical Properties on Polyethylene Coatings

Because polyethylene Coating is remained excellent condition after 11.5 years exposure off-Chiba, some physical properties were measured in order to investigate changes of properties before and after exposure. The results of measurements are summerized in Table 6.

Table 6 Changes of Physical properties of Polyethylene Coating (11.5 years exposure off-Chiba)

Item	Steel Pile A			Steel Pile B		
	Before Exposure	After Exposure		Before Exposure	After Exposure	
		Splash Z	Submerged		Splash Z	Submerged
Colour	bright back	brownish black	bright black	bright black	brownish black	bright black
Damage	Non	3 Small cracks	None	None	None	None
Marine Life	-	removed easily	removed easily	-	removed easily	removed easily
Under film corrosion	none	none	none	none	none	none
Peeling (kg/cm)	2.2	2.3	2.1	2.2	2.5	2.6
Melt Index (190°C)	0.37	0.25	0.26	0.14	0.15	0.14
Density (g/cm³)	0.958	0.967	0.966	0.937	0.937	0.937
Hardness (Shore D)	63	65	65	44	47	45
Tensile Strength (kg/cm²)	190	248	259	86	87	85
Breaking Point (kg/cm²)	132	152	133	120	161	137
Elongation (%)	550	246	273	550	590	520

4. Discussion and Summarization of Test Results

Steel pipe piles and test pieces given corrosion protection with various coating or wrapping materials were exposed to natural seawater and subjected to tests described in the foregoing with the objective of selecting the optimum corrosion protection method for steel structures at splash and tidal zones.

The results of comprehensive analyses on data from visual inspections (coating surface and its base metal surface), measurements of adhesion of coatings, measurements of electrical resistance of coating, and measurements of physical properties of polyethylene coatings after 11.5 years of exposure at the Chiba testsite of various corrosion protection systems are summerized as follow. The result of visual inspection evaluated at off-Ajigaura site are also summerized in this section.

(1) Stainless Steel Sheet Wrap

Although surface appearance of both steel pipe piles and test pieces present a brownish colour because of rust flowed down from upper steel member, no corrosion can be recognized. For the base steel removed stainless steel sheet, no corrosion has occurred. But galvanic corrosion has occurred between stainless steel and base steel pile (see Fig. 7). As it has been reported that no crevice corrosion can be occurred for high quality stainless sheet wrapping at splash zone[4], this wrapping system with cathodic protection in submerged zone can be expected extremely long term service life.

(2) Low-Alloy Corrosion-Resistant Steel Sheet Wrap

Corrosion has progressed for both steel piles and testpieces covered with thick layers of rust. It is recognized that the layers of rust at tidal zone are thicker and denser than that at atomospheric and splash zone. Fig. 6 shows that no macro cell corrosion has occurred near L.W.L. for low-alloy corrosion-resistant steel. But it is seen according to Fig. 5 that macro cell corrosion has occurred near L.W.L. for ordinary steel pile without corrosion protection. It is observed that local corrosion has occurred on the base steel near the edge of low alloy steel sheet.

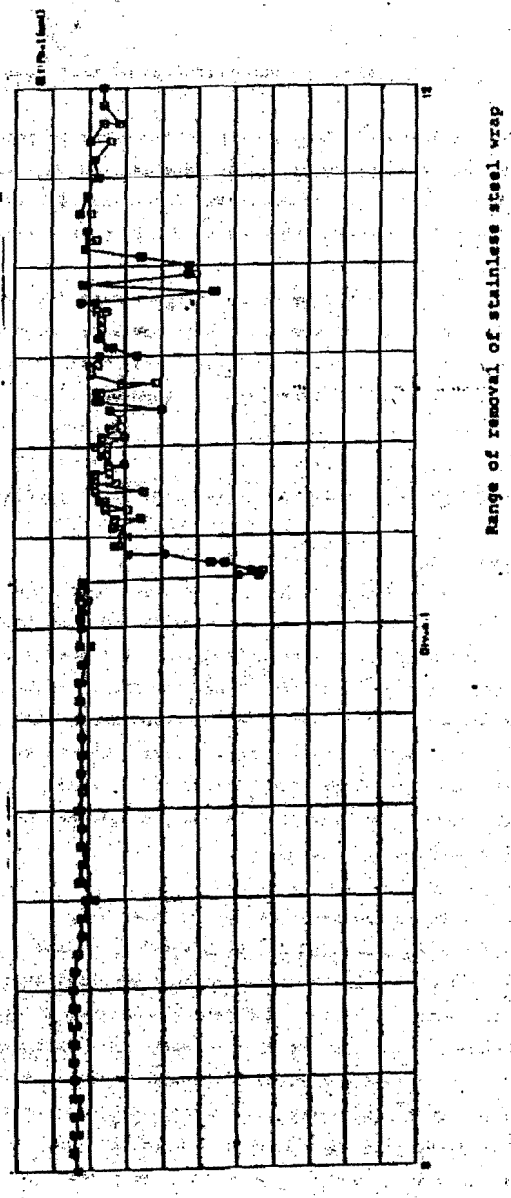

Fig. 8 Thickness measurement of low carbon steel pile after 11.5 years exposure off Chiba

Table 5 Results of Measurement of Phisical Properties on Coatings

(11.5 years exposure off-Chiba)

Type of Coating	Electrical Resistance ($\Omega \cdot cm^2$) Splash zone	Tidal upper	Zone lower	Submerged Z	Adhesion Strength (kg/cm^2) Splash zone	Tidal Upper	Zone lower	Submerged Z
2. Flame sprayed aluminum (200 μm)	-	-	-	-	70	Could not be measured because of deterieration of coatings		
3. Flame sprayed aluminum (100 μm) + coal-tar	1^{71} $X10^8$	Could not be measured			28			
4. Flame-sprayed aluminum (100 μm) + coal-tar epoxy with vinylon cloth	3.64 $X10^7$	7.96 $X10^6$	9.59 $X10^5$	8.97 $X10^5$	47	23	19	20
5. Flame-sprayed zinc (100 μm) + coal-tar epoxy (300 μ x 2)	1.07 $X10^8$	Could not be measured		700 $X10^7$	50	Could not be measured	47	48
6. Inorganic zinc-rich paint (75 μm) + coal-tar epoxy (300 μm x 3)	4.10 $X10^8$	1.91 $X10^8$	2.56 $X10^8$	2.76 $X10^9$	47	47	48	46
7. Inorganic zinc-rich paint (75 μm) + epoxy (300 μm x 3)	1.04 $X10^7$	1.12 $X10^6$	2.11 $X10^6$	1.78 $X10^6$	19	11	15	13
8. Polyethelene (cohesion-tpe, extrusion process, 4mm)	2.90 $X10^{11}$	3.05 $X10^{11}$	3.20 $X10^{11}$	3.60 $X10^{11}$	-	-	-	-
9. Epoxy resin mortar (4 mm)	2.30 $X10^5$	1.15 $X10^5$	2.28 $X10^5$	9.81 $X10^4$	11	16	15	17

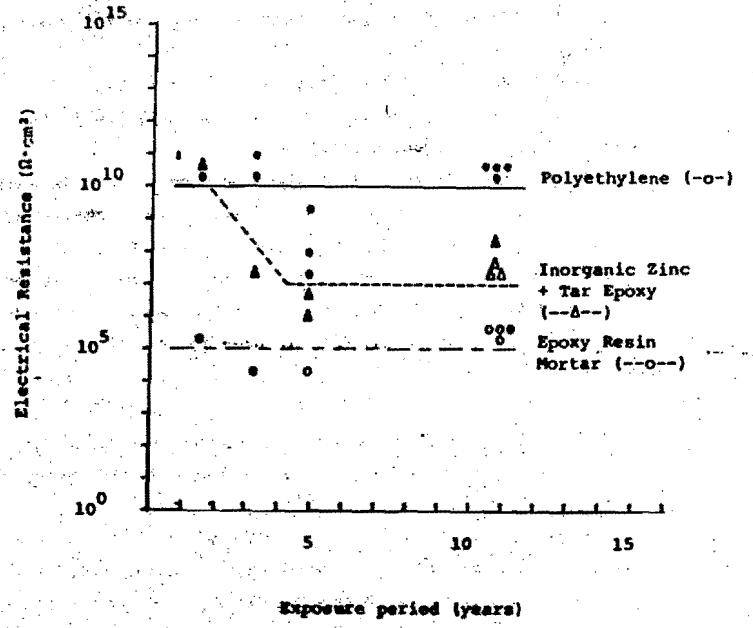

Fig. 9. Secular changes of electrical resistance (off Chiba)

For Poly-urethane mastic, coating disbond can be observed at wide range of surface by visual inspection off-Ajigaura site.

Poly-urethane rubber lining has been remained excellent condition, although small part of surface lining film is scaled off. No rust occurrence can be recognized on entire surface of lining. The reason for scaling of lining can not be explained, as the procedure of lining is mold injection method.

(8) Inorganic Lining System (Steel Fiber Reinforced Concrete without and with Protector)

Rusting due to steel fiber can be seen at a wide range of surface after removing marine lives. The cracks can be observed at upper part of the lining and they can be seen to reached to the base steel after removing the lining.

The base steel has remained good condition on the whole except the upper part of the lining. Some local corrosion like to crater can be recognized at the base steel near the lower edge of the lining.

For mortar lining with FRP protector, upper part of cover is destroyed and steel bar can be seen. But almost entire surface has been remained excellent condition by visual inspection at Ajigaura site.

With these test results, we have made the guideline of corrosion protection design at splash and tidal zone for maritime steel structure. This recommendation[6)7)], that was revised in 1988, includes the contents as follows,

1. general scope
2. corrosion protection design
   - 2.1 structure
   - 2.2 selection
   - 2.3 performance
   - 2.4 reliability
3. corrosion protection system
   - 3.1 metal lining
   - 3.2 concrete
   - 3.3 FRP
   - 3.4 organic lining
   - 3.5 coating
4. application
5. maintenance

(3) Flame-Sprayed Aluminum

It is observed about steel pipe piles that coating surface is on the whole covered with white corrosion products of aluminum at atmospheric and splash zone and covered with same corrosion products at upper tidal zone but covered with rust at lower tidal zone.

At lower tidal zone and submerged zone consumption of Aluminum has greatly progressed and rust has occurred on entire surfaces.

Adhesion of coating at splash zone remains showing high value, 70 kg/cm².

(4) Flame-Sprayed Aluminum + Coating (Coal Tar Epoxy and Coal Tar Epoxy with Vinylon Cloth)

All the surface can be seen chalking on the whole. After removing marine lives of steel pipe piles, rust can be seen almost entire surface at tidal and submerged zone and this shows that consumption of aluminum has much progressed.

Upper part of atmospheric zone has good appearance and no corrosion has occurred after removing coal-tar epoxy coating. At lower part of atmospheric zone and splash zone, rust can be observed on entire surface.

The values of adhesion strength is in the range of 19 to 47 kg/cm².

Electrical resistance of coating shows 10^7 - 10^8 Ω·cm² at splash zone and comparatively low values 10^5 Ω·cm² at tidal and submerged zone. Peeling between coal-tar epoxy with vinylon cloth can be seen at marred portion.

(5) Flame-Sprayed Zinc + Coatng (Coal-Tar Epoxy)

After removing marine lives rust can be seen in the wide range of surface at the tidal and submerged zone.

In evaluating on rusting of base steel after removing coating film, although small rust and white corrosion product can be seen, base steel is in good condition. Adhesion strength shows comparatively high values 47 - 50 kg/cm².

Electrical resistance is in the range of value 10^7 - 10^8 Ω·cm².

(6) Inorganic Zinc-Rich Primer + Coating (Coal-Tar Epoxy and Epoxy with Glass Cloth)

Chalking has on the whole progressed all surface.

Some small rust can be observed, but the base steel after removing surface coating is in good condition.

Compared with tar-epoxy system and tar-epoxy with glass cloth for adhesion strength, the value of the former is much larger than that of the latter, respectively 46 - 48 kg/cm² and 11 - 19 kg/cm².

For electrical resistance, tar-epoxy system sows larger value (10^8 - 10^9 Ω·cm²) than that of tar-epoxy with glass cloth system (10^6 - 10^7 Ω·cm²). Many pin holes can not be seen for tar-epoxy with glass cloth system but many pin holes for tar-epoxy system.

(7) Organic Lining Systems [Polyethylene (Cohesion Type, Extrusion Process), Epoxy Resin Mortar, Polyurethane Mastic, Polyurethane Rubber Liming]

Polyethylene lining is in most excellent condition same as stainless steel sheet wrap above mentioned in all evaluation, that is, visual inspection at site, surface appearance observation after removing marine lives and removing liming films. No rust has occurred all the surface of the base steel except the area of 3 small cracks. Electrical resistance of polyethylene shows highest value (10^{11} Ω·cm²) among coatings tested at off Chiba. Fig. 5 shows the secular change of electrical resistance of coatings and it can be seen that polyethylene has remained highest values of erectrical resistance, 10^{11} Ω·cm², that of inorganic zine system can be measured about 10^8 - 10^9 Ω·cm² and epoxy resin system has lowest values, 10^5 Ω·cm².

These values correspond to degree of corrosion Occurrence of base steel (See Table-2) and agree with the experimental results[5] that corrosion of base steel has occurred under the value, 10^6 Ω·cm² in immersion test.

Epoxy resin mortar can be seen rusting all the surface of the base steel by visual observation after removing the lining. Adhesion strength shows lower values at 11 - 17 kg/cm² and values of electrical resistance are lowest among coatings tested at off-Chiba (10^4 - 10^5 Ω·cm²).

Much many pin holes can be seen at the splash zone and partially at the tidal zone.

REFERENCES

(1) Annual report of exposure tests for developing protective steel pipe piles, (in Japanese) 1975, 1976, 1977, 1980, 1981, 1985, 1987.

(2) The corrosion and protection of steel pipe piles in Natural Seawater, 5th international Congress on Marine Corrosion and Fouling, 1979.

(3) M. Makita & R. Tanaka: Ocean Space Utilization '85 Proceedings of the International Symposium (2), Nihon University, P539.

(4) Y. Shimizu, S. Baichou, K. Katawaki: Proceedings of 7th Annual Meeting of Japan Association of Corrosion Control, July, '87, P93-96 (in Japanese).

(5) R.C. Bacon, J.J. Smith, F.M. Rugg: Ind. Eng. Chem. 40, 161 (1948).

(6) Tentative Guideline of corrosion protection design for maritime steel structure, 1975, PWRI.

(7) Guide line of corrosion protection design for maritime steel structure, 1988, PWRI.

The effect of the early stages of biofilm formation on the corrosion behaviour of CuNi30Fe alloy in natural sea water was studied through electrochemical experiments and superficial analysis. A comparison between electrochemical measurements performed in the laboratory with artificial solutions and with filtered sea water was also made.

EXPERIMENTAL

The working electrodes used were disks of CuNi30Fe alloy embedded in an epoxy resin which presented an exposed area of 0.38 cm^2. The chemical composition of the alloy was: Cu:67%, Ni:31.9% and Fe: 1.1%. Before being used, they were polished with several emery papers of different grits (320, 400, 600) diamond paste and finally with alumina (1 µm diam). The polished specimens were successively rinsed with acetone A.R., twice distilled water and finally air dried at room temperature. A new electrode was used for each run. A saturated calomel electrode (SCE) located in a glass tube provided with a Luggin-Haber capillary tip was used as a reference electrode. The circuit was completed with a Pt wire as counterelectrode. A conventional double wall Pyrex glass cell was employed.

Laboratory experiments were made using either natural sea water filtered with a 0.2 µm membrane of the Millipore type, or X NaCl + Y Na_2SO_4 solutions ($0 \leq X \leq 0.5$ M, $0 \leq Y \leq 0.023$ M). In all cases electrochemical measurements were carried out at 25°C. AR chemicals and twice distilled water were used to prepare the different electrolyte solutions.

Biological films were formed by exposing the metal disks of 15 mm diameter embedded in an epoxy resin (exposed area 2.35 cm^2). Previous to the exposure, the metal surface was prepared by polishing it with 320 and 600 emery papers. Exposure times varied between 5 and 49 days. Samples were located in acrylic panels like those usually employed in the study of macrofouling (3). The panels were exposed to flowing sea water (0.2 - 0.3 m/s) at the intake channel of a thermal power plant located in the vicinity of Mar del Plata harbour (38°08'17"S, 57°31'38"W) Argentina.

In the course of the present study there were variations in temperature, pH and dissolved oxygen ranging from 9.7 to 24.4°C, 7.57 to 7.68 and 2.36 to 1.37 ml/l respectively.

Microfouling observations were made using a JEOL JSM 35 CF SEM or a Philips 505 SEM. Surface deposits were also analysed by EDAX.

In order to measure open circuit potentials for CuNi30Fe alloy "in situ" -at the supply water channel in the harbour area- samples similar to those used to observed biofouling were employed. In this case each metal specimen was provided with an insulated electrical terminal connected to a Keithley 169 multimeter. In all cases a SCE placed in a glass compartment ended in a Luggin capillary was used as potential reference electrode.

RESULTS

The STPS made with CuNi30Fe alloy in deareated quiescent NaCl solution, at 0.02 V/min was published in a previous paper (4).

with clearly visible cracked areas irregularly distributed (Fig. 5). Upon film removal, a similar crack pattern could be observed . Longer exposure of the samples showed an enhanced attack, leading to deeper cracks and better defined ditches (Fig. 6). Small spheres of corrosion products could be seen. EDAX analysis of the film revealed the presence of S and higher levels of Fe than those of the base metal. At the bottom of the cracks higher levels of Cl than those found in the film were detected.

Over islands of compact film a heterogeneous deposit could be observed. This deposit consisted mainly of organic filamentous material and particulated corrosion products (Fig. 7). Isolated bacterial cells, partially covered by corrosion products, could also be seen.

When exposure time was increased, the amount of filamentous material and bacteria also increased. They usually appeared entrapped between deposits of corrosion products (Fig. 8).

CuNi30Fe samples exposed during 19 days to artificial sea water solution also showed a layered distribution of corrosion products. Nevertheless, the outer layer appears more firmly packed than those observed for metal samples exposed to natural sea water (Fig. 9).

DISCUSSION

CuNi10Fe and CuNi30Fe alloys used frequently in industrial installations employing sea water flow as coolant fluid show a complex corrosion behaviour. This complexity arises from the overlapping of two different types of corrosion processes, i.e. localized and generalized corrosion. When the formation of several layers of corrosion products takes place it is followed by a series of continuous changes of the layers which condition the future passive beahviour of the alloys. These changes depend on a wide variety of environmental factors such as temperature, dissolved oxygen, variation in the chemical composition of sea water and finally biofilm presence.

The anodic current/potential curve for CuNi30Fe alloy in deareated sea water as well as in NaCl solutions showed several coincident features with those corresponding to pure copper or pure nickel. Consequently, the peak recorded at -0.50 V -previously described as peak Aa (Fig. 1)- could be attributed to the formation of $Ni(OH)_2$, if a comparison with results corresponding to pure Ni is made. $Ni(OH)_2$ is reduced at very high cathodic potential (ca -0.88 V (5)) close to Ac peak potential (Fig. 1), thus confirming this assumption.

In buffered solutions containing chloride, three peaks can be distinguished at -0.2 V, 0.0 V and 0.1 V. They have been asigned to Cu_2O, CuCl and CuO respectively (6). Consequently, for CuNi30Fe alloy in the potential region between -0.2 V and 0.0 V, corrosion reaction should yield to Cu_2O and CuCl.

Paratacamite precipitation can be supported by some electrochemical results obtained like the decrease of the anodic peak height and the cathodic direction of potential displacement when pH was increased. At high pH values the precipitation occurred easily and the anodic peak was lower. Conversely, at high chloride concentrations, higher dissolution of copper accounted for the increase in height of the anodic peak. At 0.12 V and pH 7.5 paratacamite is stable. Consequently, the abrupt current decrease recorded near to that potential value

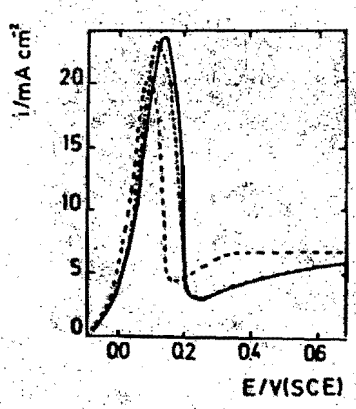

Fig. 2: Anodic polarization curves for CuNi30Fe alloy at v = 0.001 V/s in 0.5 M NaCl solution at different pH values = (—) pH = 8.0; (-.-) pH = 8.8; (---) pH = 10.5.

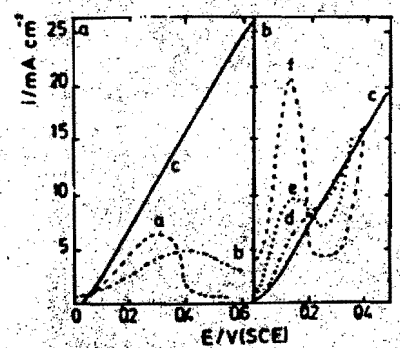

Fig. 3: Anodic polarization curves for CuNi30Fe alloy at V = 0.001 V/s in different electrolyte solutions = a) (---) 0.023 M Na_2SO_4; (-.-) 0.023 M NaCl; (——) 0.023 M Na_2SO_4 + 0.023 M NaCl. b) (-.-) 0.023 M Na_2SO_4 + 0.046 M NaCl; (...) 0.023 M Na_2SO_4 + 0.1 M NaCl; (---) 0.023 M Na_2SO_4 + 0.4 M NaCl.

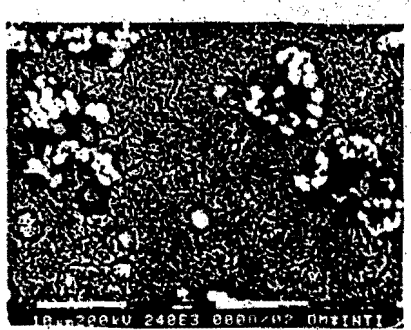

Fig. 4: SEM microphotograph corresponding to a 70/30 copper-nickel alloy sample potentiostatized at -0.12 V in 0.5 M NaCl solution during 300 s (2,400 X).

Fig. 5: SEM microphotograph corresponding to a 70/30 copper-nickel alloy sample after 7 days of immersion in natural sea water (1.010 X).

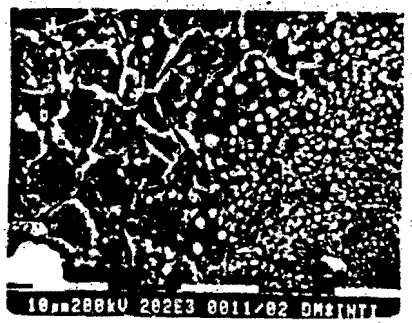

Fig. 6: SEM microphotograph corresponding to a 70/30 copper-nickel alloy sample after 35 days of immersion in natural sea water (2.020 X).

A COMPARATIVE STUDY OF THE CuNi30Fe ELECTROCHEMICAL BEHAVIOUR IN SEA WATER AND DIFFERENT CHLORIDE SALINE SOLUTIONS TO ASSES THE EFFECT OF MICROFOULING SETTLEMENT

M.F.L. de Mele*, G. Brankevich# and H.A. Videla*

* Bioelectrochemistry Section - INIFTA - Facultad de Ciencias Exactas, Universidad Nacional de La Plata - C.C. 16, Suc. 4 - (1900) La Plata - Argentina

INIDEP-DEBA - Playa Grande - C.C. 175 - (7600) Mar del Plata - Argentina

ABSTRACT

The corrosion behaviour of CuNi30Fe alloy in natural sea water and artificial solutions was studied by using different electrochemical techniques. SEM observations were used to asses the attack and microfouling settlement. EDAX analysis of the corrosion products was also made.

Relevant differences between the electrochemical responses of the alloy in the electrolyte media used could be detected.

According to the present results the protective characteristics of the complex layers that were formed on CuNi30Fe surface could be altered by the microbial adhesion on the metal surface.

INTRODUCTION

The high corrosion resistance and antifouling properties of copper-nickel alloys have led to their wide acceptance as heat exchanger constructional materials. Localized attack, due to the combined effects of corrosion and erosion (impingement attack) produced as a consequence of the removal of passive films by turbulent water flow, has been reported as one of the major causes of heat exchanger failures (1). Another frequent cause of corrosion of copper-nickel alloys in marine environments has been attributed to organic material present in polluted and almost stagnant sea water in harbour areas (2).

The corrosion behaviour of copper-nickel alloys is strongly dependent on the nature and characteristics of the passive film formed on the alloy.

In spite of the literature available in relation to the corrosion behaviour of copper-nickel alloys in laboratory experiements using artificial solutions, scarce references can be obtained on the effect of the biological activity of the microorganisms usually present in sea water. Generally speaking, this biological activity is mainly developed in biofilm formed at the metal liquid interphase.

When the record was made at a higher sweep rate (0.1 V/s) it could be noticed either in NaCl solution or in natural filtered sea water, that current increased to form a plateau Aa at -0.5 V which was followed by another plateau (Ba) (Fig.1). At higher potentials values a sharp current increase was noticeable. When a STPS was made up to an anodic limit of -0.3 V it could be seen that peak Aa was related to a cathodic peak recorded during the negative going scan at -0.88V. Other STPS run up to higher potential limits showed that the peak Ba and the following current increase Ca were related to Bc and Cc cathodic contributions. Ca is related to a current peak formation. This peak moved in the cathodic direction and its size decreased when pH increased (Fig. 2). The height of this current peak was also dependent on chloride concentration and on sweep rate.

When the potential was reversed at 0.2 V a loop was formed so that current values recorded during the negative going scan were more anodic than those corresponding to the positive scan. Similar results were obtained in the presence of oxigen.

The electrochemical behaviour of CuNi30Fe alloy at potentials higher than those corresponding to the anodic peak at 0.1 V in NaCl solutions was different from that observed in natural and artificial sea water. In the last two electrolytes a sharp increase in current at potentials of 0.35 V was observed, whereas in NaCl solution a slow increase in current was noticed. The electrochemical behaviour of the alloy in sea water could be nearly restored by adding Na_2SO_4 (0.023M) to the NaCl solution.

To analyse the effect of sulphate anions presence, different chloride/sulphate concentrations ratios were used. A broad anodic peak was recorded either in the presence of sulphate (Fig. 3, curve a) or chloride alone (Fig. 3, curve b). However, a dramatic change in the electrochemical behaviour of CuNi30Fe alloy was observed in the presence of both anions. A lineal E/i relation was recorded. At constant sulphate concentration the increase in chloride level induced the formation of a current peak. This peak, which was hardly defined at 0.046 M NaCl (curve d), became sharper and higher when the chloride concentration was increased.

Current vs time relationships were recorded at a constant potential Et, covering the potential range where the peak B formation and the initiation of the attack had occurred. When the electrode was held at potentials between -0.2 V and -0.12 V a similar electrochemical behaviour was observed. There was an abrupt current increase and decrease during the former 5 seconds and a slower decrease thereafter. Samples held at - 0.12 V showed small spheres buried in a thin layer of corrosion product (Fig. 4).

When the electrode was held at 0.1 V, a hardly defined peak was recorded. The maximum was not noticeable when the preset potential value was increased.

Open circuit vs time records obtained by means of "in situ" experiments showed potential values ranging between - 0.52 V and - 0.10 V (SCE) (Table I). The amount of the scattering in the "in situ experiences" was higher than that corresponding to laboratory measurements with artificial sea water. In the case of filtered sea water, corrosion potential values ranged between - 0.21 V and - 0.10 V.

SEM observations of CuNi30Fe specimens exposed to natural flowing

as well as the porous film observed through microscopic observation could be related to the precipitation of paratacamite.

Although the effect of chloride on the breakdown of passivity of Cu/Ni alloys is well documented, scarce information has been reported on other ions such as sulphate present in sea water. It has been written that pitting corrosion is favoured in tubes of heat exchangers exposed to waters with high sulphate content and that failures occur most rapidly in waters which also have low chloride contents. In agreement, present results showed a high dissolution rate when mixtures of NaCl and Na_2SO_4 with low chloride levels were used. Besides, a poor passivation followed by localized attack was found for high chloride/sulphate relation. Sulphate effect could eventually modify copper oxyde formation, reducing its protective characteristics and favouring the breakdown of passivity at high potentials.

SEM observations of the specimens made after five days of exposure in sea water showed that they were covered by a compact layer. Scarce groups of small spheres were detected on this layer. For longer exposure times the small spheres coalesced and formed a thick porous non adherent layer with clearly visible cracks and ditches that appeared to follow the grain boundaries (Fig. 5).

EDAX analysis made at the bottom of the cracks showed that there was a preferential dissolution of copper in the intergranular zone favoured by the presence of Cl which was at higher concentration level than in the outer film. The analysis of the film revealed the presence of S. Coincidentally, EDAX, ESCA and Auger superficial analysis of CuNi10Fe alloy showed that the outer porous layer is mainly $Cu_2(OH)_3Cl$ with some Cu_2O and Cu_2S particles. The inner layer was attributed to Cu_2O doped with Ni, Fe, S and Cl (7).

Open circuit potential values recorded during 40 days of inmersion "in situ" ranged between -0.52 and -0.10 V (Tabla I). The highest potential values were too low to justify the presence of $Cu_2(OH)_3Cl$ (paratacamite, a Cu(II) compound) which was detected on the surface of CuNi30Fe alloy (8). That compound was stable at 0.0 V, according to the corresponding potential/pH diagram. However, it must be considered that oxygen promotes Cu(I) to Cu(II) conversion and this fact should facilitate copper dissolution, Cu(II) species formation and $Cu_2(OH)_3Cl$ precipitation.

Microphotographs obtained after holding the electrode at -0.12 V in aerated and dearated quiescent solutions, showed the formation of small spheres less than 1 µm diameter, deep into a more compact layer (Fig. 4). Dobb (9) proved that when the copper-nickel specimen was covered either by a gel or in any condition of restricted diffusion, the same type of products are formed. Initially, the surface was tarnished by a thin film formation. Under diffusional restrictions this process was complicated by the nucleation of copper oxyde (Cu_2O) that precipitated on the surface. Surface analysis indicated that the nodules were almost entirely Cu_2O while NiO enriched regions occurred between them. Nodules were not found when free diffusion of ions existed. These facts explain the detection of small spheres on the metal surface in laboratory probes -in quiescent conditions- and the location of small spheres under the bottom of the cracks and ditches where the diffusion of ions was restricted.

The organic gels formed from microbial extracellular polymeric substances (EPS) could act as diffusional barriers at the solution/metal interphase influencing fluid flow regime on the surface. This could result in concentration gradients and affecting diffusional processes to and from the metal surface. Besides, spheres of Cu_2O may precipitate below EPS deposits, modifying the adhering characteristics of the inner layer.

Specimens exposed during three weeks showed that several microorganisms and filamentous material had been entrapped between corrosion products (Fig. 7 and 8). This confirmed the feasibility of a dissolution-precipitation mechanism which explains the formation of corrosion products.

TEM observations have shown that bacteria placed between the corrosion layers of copper-nickel alloys produce mucilage. This probably forms tube structures surrounding the corrosion products by the movement of bacteria between the layers (10).

Although the antifouling property of copper-nickel alloys is well documented, the protective characteristics of the complex layers that are formed on their surfaces could be distorted by the action of microorganisms. The incorporation of organic material close to the metal surface causes oxygen removal and so affects cathodic reaction control. Besides, the production of EPS by the microorganisms modifies the transport properties at the metal solution interphase generating diffusional barriers. The effect of biofilms on the morphological characteristics of the different layers of corrosion products can be noticed when a comparison between metal samples inmersed in natural sea water and artificial saline solutions is made (Fig. 8 and 9). A loose structure of the outer layer of corrosion products is obtained when biofilms are present at the metal/solution interphase. In these conditions the sloughing of the protective layers could be facilitated enhancing the risk of localized corrosion at restricted sites of the metal surface.

ACKNOWLEDGEMENT

The authors wish to thank Patricia Guiamet for her technical assistance.

REFERENCES

1. F.J. Ijsselling, J.M. Krougman and L.J.P. Drolenga, "The corrosion behaviour of the system CuNi10Fe/sea water. The protective layer of corrosion products", 5th Intern. Congress of Marine Corrosion and Fouling, Barcelona, Spanin, p. 146 (1980).
2. R. Francis, Br. Corros. J. 20(4), 167 (1985).
3. R. Bastida and G. Brankevich, "Estudios ecológicos preliminares sobre las comunidades incrustantes de puerto Quequén (Argentina)", Proceedings of 5th International Congress on Marine Corrosion and Fouling, Marine Biology, Barcelona, Spain, p. 113 (1980).
4. H.A. Videla, M.F.L. de Mele and G. Brankevich, Corrosion 87 (NACE) paper number 365 (1987).
5. L.M. Gassa, J.R. Vilche and A.J. Arvía, J. Applied Electrochem. 13 (2), 135 (1983).
6. M.R.G. de Chialvo, R.C. Salvarezza, D. Vázquez Moll and A.J. Arvía, Electrochem. Acta 30(11), 1501 (1985).
7. L.E. Eiselstein, B.C. Syrett, S.S. Wing and R.D. Caligiuri, Corros. Sci. 23(3), 223 (1983).

8. C. Kato, J.E. Castle, B.G. Ateya and H.W. Pickering, J. Electrochem. Soc. 127(9), 1897 (1980).
9. D.E. Dobb, Ph.D. Dissertation, Dept. of Chemistry, Montana State University (1984).
10. G. Blunn, Biodeterioration 6, CAB International, Farnham Royal, Slough, p. 567 (1986).

TABLE I: Open circuit potential values at different exposure times

Time/days	Open Circuit Potential/V	
	Natural sea water ("in situ" measurements)	Natural Filtered Sea Water
0	- 0.252	- 0.206
2	- 0.518	- 0.174
4	- 0.307	-
6	- 0.319	- 0.157
8	- 0.416	- 0.143
9	- 0.241	- 0.147
12	- 0.234	- 0.106
15	- 0.189	- 0.113
17	- 0.203	-
20	-	- 0.111
23	- 0.113	- 0.105
27	- 0.139	- 0.185
30	- 0.129	-
33	- 0.179	- 0.165
36	- 0.133	-
38	- 0.164	-
41	- 0.122	- 0.170

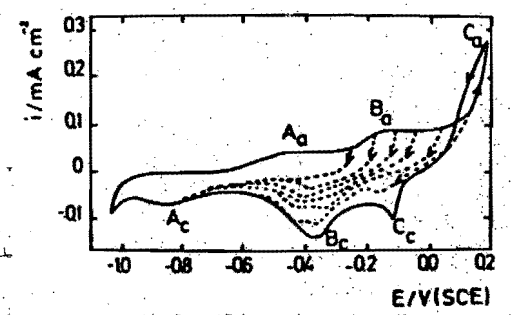

Fig. 1: STPS voltamogram run with CuNi30Fe alloy in natural filtered sea water at v = 0.1 V/s up to different anodic limits between - 0.3 V and 0.2 V.

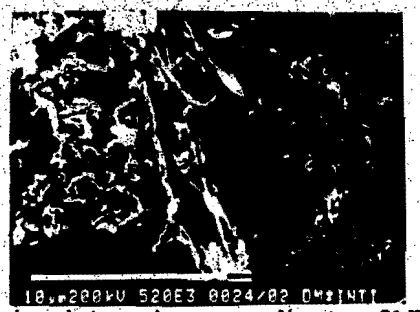

Fig. 7: SEM microphotograph corresponding to a 70/30 copper-nickel alloy sample after 21 days of immersion in natural sea water (5,200 X).

Fig. 8: SEM microphotograph corresponding to a 70/30 copper-nickel alloy sample after 35 days of immersion in natural sea water (2,980 X).

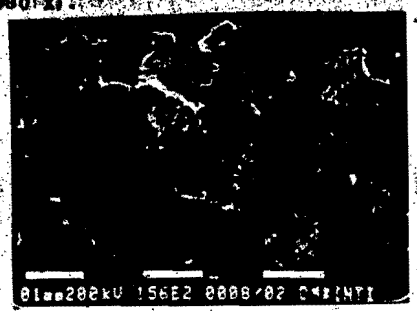

Fig. 9: SEM microphotograph corresponding to a 70/30 copper-nickel alloy sample after 19 days of immersion in artificial sea water (150 X).

7.º CONGRESO INTERNACIONAL DE CORROSIÓN MARINA E INCRUSTACIONES

7th INTERNATIONAL CONGRESS ON MARINE CORROSION AND FOULING

7ème CONGRES INTERNATIONAL DE LA CORROSION MARINE ET DES SALISSURES

UNIVERSIDAD POLITÉCNICA
Valencia, 7-11 Noviembre, 1988
ESPAÑA

SECCIÓN II

Biología marina
Marine biology
Biologie marine

The unpublished manuscripts have been reproduced as received from the authors. The Scientific Committee takes not responsability for any error or omission.

Las ponencias no han sido publicadas y están reproducidas tal y como se han recibido de sus autores. El Comité Científico no se responsabiliza de cualquier error u omisión.

SESSION II Marine Biology
Thursday 10th November

ENSAYOS BIOLOGICOS PARA LA EVALUACION DE PINTURA ANTIINCRUSTANTES
E Arias, P Suau and P Molera

PINTURAS ANTIINCRUSTANTES DE MATRIZ SOLUBLE TIPO ALTO ESPESOR
Vincente J D Rascio, Carlos A Guidice and Beatrix del Amo

APPORT DE LA BIOLUMINESCENCE DANS L'INTERPRETATION DES TESTS DE SELECTION DE BACTERICIDES SPECIFIQUES DES BACTERIES SULFATO-REDUCTRICES
Paul Auclair and Paul Couget

ETUDE DE L'INFLUENCE D'ELEMENTS "POISONS" SUR LA RESISTANCE A LA CORROSION BACTERIENNE EN MILIEU MARIN D'ACIERS INOXYDABLES
G Hernandez, C Lemaitre, J Guezennec, J Paudouard and G Beranger

ANTIFOULING PAINTS OF HIGH SEA WATER DISSOLUTION RATE
Beatiz del Amo, Carlos A Giudice and Gustavo Villoria

MODIFIED ORGANOTIN ANTIFOULANTS
C A Dooley, J P Testa Jr and P Kenis

MICROFOULING AND LEACHING FROM PAINTS
A J Mitchell and E G Bellinger

THE USE OF CALCIUM RESINATE IN THE FORMULATION OF SOLUBLE MATRIX ANTIFOULING PAINTS BASED ON CUPROUS OXIDE
Carlos A Giudice, Beatriz del Amo and Vicente J D Rascio

ADHESION OF BARNACLES AND DEVELOPMENT OF NON-TOXIC ANTIFOULANTS
Elek Lindner, Carol A Dooley and Marca Doeff

SELECTIVE ACTING ANTIFOULING ADDITIVES
Joachim Lorenz

DETERMINATION OF MINIMUM EFFECTIVE RELEASE RATES OF ANTIFOULANTS BY MEMBRANE PERFUSION
Elizabeth B Gates, William C Banta, George Loeb and Elaine Johnson

ENSAYOS BIOLÓGICOS PARA LA EVALUACIÓN DE PINTURAS ANTIINCRUSTANTES

E. Arias *, P. Suau * y P. Molera **

* Instituto de Ciencias del Mar. Paseo Nacional,s/n 08003. BARCELONA

** Departamento de Ingeniería Química y Metalurgia. Universidad de Barcelona.

RESUMEN

Este trabajo tiene como principal finalidad dar a conocer los resultados obtenidos con diferentes formulaciones sumergidas en el puerto de Palma de Mallorca.

Se efectuaron estudios sobre hidrografía, pigmentos del fitoplancton, fauna bentónica y larvas de organismos adherentes.

Las pinturas ensayadas contenían, como aglutinante acrilato de tributilestaño y copolímeros vinílicos y clorocaucho y como pigmentos tóxicos Cu_2O, TBTO, TBTF y SCNCu. En el mismo se discuten las ventajas y desventajas de las diferentes formulaciones ensayadas.

SUMMARY

Results of research on antifouling paints summerged in the harbour of Palma de Mallorca are presented in this paper.

Studies on hidrography, phytoplankton pigments macro benthos settling on PVC panels and zooplankton are also included.

Formulations of tributyltin acrylate and copolimers vynil and chlorinated rubber systems, pigmented with Cu_2O, TBTO, TBTF, SCNCu, Fe_2O_3 and ZnO and with mixtures of these toxics, were tested in a experimental raft during 12 months. The adventages and disadventages of different paints formulations are discussed.

INTRODUCCION

Los problemas ocasionados por la corrosión y el "fouling" en los cascos de las embarcaciones, por debajo de la linea de flotación, se resuelven satisfactoriamente con la aplicación de recubrimientos anticorrosivos y antiincrustantes y con una adecuada protección catódica.

Las obras sumergidas en el mar quedan recubiertas por microorganismos que, en su fase inicial, están constituidos esencialmente por bacterias, protozoos, hongos y algas, que proliferan en unas condiciones favorables del medio y, posteriormente, sirven de sustrato de fijación a las larvas de otros organismos adherentes. Los primeros intervienen en un gran número de procesos evolutivos y,con su incrustación, degradan la película de la pintura (protozoos), aceleran la corrosión de los metales (bacterias), se fijan en la línea de flotación de las embarcaciones (algas) y son la base de la incrustación en las obras sumergidas (hongos y diatomeas)(POTIN et al. 1.982). Para su eliminación se emplean pinturas en cuya composición entran a formar parte compuestos inorgánicos y orgánicos biocidas con un espectro de actividad muy amplia y con una débil to

xicidad para el organismo humano, a la vez que presentan una gran estabilidad a la luz, a la oxidación y a la acción del CO_2, SO_2 y SH_2. Estos compuestos son muy numerosos y sus grupos funcionales muy variados, utilizándose en las formulaciones aminas, amidas, compuestos de amonio cuaternario, carbamatos, fenoles, compuestos organometálicos de estaño y plomo, óxido cuproso, tiocianato de cobre, etc., etc..

Según VAN LONDEN (1.963), en una sola pintura no podían combinarse la acción anticorrosiva y antiincrustante debido a que, en la formulación de las segundas, se añadían compuestos inorgánicos de cobre y mercurio que ocasionaban la corrosión por acción electroquímica. La aparición de los compuestos orgánicos tóxicos eliminaba, en parte, este inconveniente pero como, en los primeros recubrimientos, la película debe permanecer inalterable con el tiempo y, en las segundas esto no sucede, como consecuencia de su mecanismo de acción, la preparación de una pintura que reuna ambas propiedades se hace prácticamente imposible por lo que se debe recurrir a la obtención de antiincrustantes que ejerzan una acción fundamental contra la problemática biológica pero que, al mismo tiempo, aumenten la protección contra los fenómenos físico-químicos de las aguas.

En los últimos años adquirió una amplia difusión el empleo de resinas biocidas tipo acrilato o metacrilato de trimetilestaño y tributilestaño. La forma de actuación de estas pinturas se fundamenta en la hidrólisis de la molécula de polímero, que permite disminuir la rugosidad de la superficie, la cual se renueva en contacto con el agua aumentándose, por tanto, la acción antiincrustante (TORTAROLO, 1.981).

Esta clase de pinturas ensayadas por diversos investigadores (KRONSTEIN 1981, DAWANS 1.982, PITTMAN 1.982 presentan, según ARIAS et al.(1.986) presentan una serie de ventajas, junto con una serie de inconvenientes respecto a las pinturas convencionales y a las llamadas de contacto continuo, constituidas por resinas insolubles y saponificables.

Las propiedades físicas de los polímeros de acrilato y metacrilato no son, en general, lo suficientemente satisfactorias para que los filmógenos obtenidos den un tiempo prolongado de vida activa a las pinturas antiincrustantes, salvo en el caso de que se apliquen en grandes espesores. Con el fin de remediar estos inconvenientes, DAWANS (1.982) recurre a los copolímeros de cloruro y acetato de vinilo, acrilatos o metacrilatos de alcohilo y de acronitrilo.

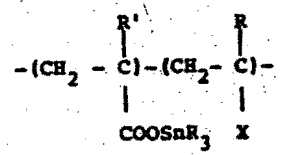

R = Alcohilo o Fenilo
R' = Hidrógeno o Metilo
X = H, Cl, C_6H_5, CN

En este trabajo se estudia el comportamiento de 32 formulaciones de pinturas antiincrustantes en 15 de las cuales se empleó acrilato de tributilestaño y en las restantes acrilato y copolímeros de cloruro de vinilo y cloro caucho. Se emplearon Cu_2O, TBTO, TBTF y SCNCu como tóxicos junto a estos tipos de ligantes.

Los polímeros biocidas fueron usados por ser biodegradables ya que en zonas fuertemente contaminadas por eu-

troficación el dióxido de tributilestaño se transforma en carbonato que, posteriormente, por la acción bacteriana o por los rayos ultravioleta se descompone, dando lugar al SnO_2 escasamente tóxico.

$$R_3SnX \xrightarrow{H_2O} (R_3Sn)_2O \xrightarrow{CO_2} (R_2Sn)_2CO_3 \xrightarrow{UV,\ microorganismos} SnO_2$$

Todos estos compuestos organometálicos de estaño, son objeto de estudio, en los momentos actuales, por su posible incidencia sobre la flora y la fauna marina pese a que, como indica DAVIES 1.982, son compuestos biodegradables.

MATERIAL Y METODOS

La investigación sobre el sistema de pinturas fué efectuado por medio de la inmersión de probetas recubiertas con una capa de 200 u de pintura antiincrustante en una balsa fondeada en el puerto de Palma de Mallorca (fig.1). Las placas se inspeccionaron regularmente prestando particular atención a la formación de ampollas y grietas, así como a la presencia de las diferentes comunidades incrustantes.

Este tipo de experiencias tienen la ventaja de que se efectúan con un control de las condiciones físico-químicas y biológicas de las aguas, lo que permite obtener una valiosa información sobre el comportamiento de las formulaciones ensayadas.

Se tomaron muestras de agua de mar para la determinación de aquellos factores ecológicos que tienen una mayor incidencia en la colonización de las probetas por el "fouling, se colocaron paneles de PVC atóxicos para obtener información del macrobentos y, por último, se hicieron pescas de zooplancton, prestando particular atención al estudio de las larvas de organismos adherentes

Las formulaciones ensayadas se exponen en el Cuadro I.

RESULTADOS

Los datos de la hidrografía y de los pigmentos del fitoplancton durante el período en el que se efectuaron las experiencias se exponen el Cuadro II.

La temperatura estuvo comprendida entre un mínimo de 13 ºC, en el mes de febrero, y un máximo de 26,6 ºC, en el mes de agosto.

La salinidad sufrió escasa variación a lo largo de todo el ciclo estudiado estando situados sus valores límites entre 35,91 y 37,82.

Los estudios de los valores hidrográficos y de nutrientes nos permiten diferenciar tres zonas en el interior del recinto portuario: Una, en donde se fondeó la balsa, fuertemente contaminada por eutroficación (estación 1); la segunda en donde la contaminación disminuye considerablemente (estación 2) y, por último, la zona correspondiente a la bocana del puerto (estación 3), en la que las aguas tienen un contenido en nutrientes menor, es normal la concentración de oxígeno y más bajo el contenido de clorofilas.

Las concentraciones de clorofilas y el contenido de oxígeno de las aguas en donde se fondeó la balsa no presentan una relación estrecha debido a que los pigmentos extraídos eran producto de material detrítico y, en consecuencia los valores del oxígeno disuelto estuvieron por debajo de los que se deberían hallar con un plancton productivo.

Si se observa en la fig. 2, el número de larvas de

Cirrípedos guarda estrecha relación con los valores registrados de clorofila a. Su concentración aumenta, en la estación 1, desde el mes de marzo hasta octubre, con la única excepción del mes de septiembre, en el que la pesca de zooplancton fue la más rica en organismos, en particular por lo que hace referencia a este tipo de larvas y a los Copépodos.

Los análisis de zooplancton (fig. 3) en las estaciones estudiadas muestra como el número más elevado de Cirrípedos se presenta en la estación 1. En las otras dos estaciones la mayor abundancia fue de Copépodos. Los Poliquetos, Ascidiados y Lamelibranquios estuvieron representados de una forma pareja en las tres estaciones.

La presencia de larvas de organismos adherentes a lo largo de todo el año se caracterizó por densidades elevadas de Cirrípedos en los meses de marzo, abril, junio, julio, septiembre y octubre y, por lo que hace referencia a los Lamelibranquios, los valores más altos se dieron en primavera y otoño, decreciendo en verano y fueron muy bajas en los restantes meses del año (figrs. 4 y 5).

DESCRIPCION DE LA COMUNIDAD INCRUSTANTE

La composición del "fouling" de las probetas testigo estuvo constituida esencialmente por cuatro tipos de organismos sesiles: Microorganismos, Algas, Cirrípedos y Serpúlidos; el resto de las incrustaciones se encontraron sólo esporádicamente y en un número muy escaso, habiéndose clasificado algunos Briozoos y Ascidiados.

La comunidad de microorganismos estuvo integrada, preferentemente, por Bacterias, Algas microscópicas, Protozoos y Copépodos. Esta comunidad se encontró durante la época invernal y fue disminuyendo a medida que se fue entrando en la primavera.

Los Cirrípedos estuvieron representados por el género Balanus del cual se encontraron las siguientes especies: B. amphitrite, B. eburneus y B. perforatus, siendo esta última la más abundante. La incrustación de estos organismos fue intensísima, en especial en el período comprendido entre los meses de mayo y octubre.

Los Serpúlidos se encontraron incrustados abundantemente entre julio y octubre, siendo la especie dominante Hydroides elegans. Esta comunidad apareció preferentemente en aquellas probetas testigo sumergidas a sólo 30 cm. de la superficie del agua.

El ciclo de los organismos incrustantes se inició con los microorganismos, en invierno, siguieron los Cirrípedos y por último por los Serpúlidos. Las experiencias fueron efectuadas, por tanto, en unas aguas con una variación específica pobre, pero de una gran intensidad en el período estival.

PINTURAS ANTIINCRUSTANTES

Todas las formulaciones se prepararon a escala de laboratorio. Las probetas utilizadas fueron de PVC protegidas con una capa de 200 μ de espesor con los recubrimientos antiincrustantes que se exponen en el Cuadro I.

El propósito fundamental de este trabajo era el desarrollo de pinturas antiincrustantes eficaces para las aguas mediterráneas españolas cuyos puertos presentan un elevado grado de contaminación por eutroficación y que, por las

condiciones físico-químicas de sus aguas, dan lugar a graves problemas de incrustación, tanto de origen vegetal como animal.

Se estudió la influencia y el tipo de tóxico, la composición química del vehículo y su comportamiento frente a los organismos adherentes presentes en las aguas del puerto.

Pigmentos utilizados

Los componentes empleados en las pinturas ensayadas fueron ZnO y Fe_2O_3 y como tóxicos SCNCu, Cu_2O, TBTO y TBTF.

El examen de los valores de fijación del "fouling" revela que las pinturas ensayadas dieron excelentes resultados, (figrs. 6 y 7) en el período de doce meses que permanecieron sumergidas en las condiciones hidrológicas y biológicas expuestas.

La lixiviación de estas pinturas fue el adecuado para evitar el macrofouling y, entre todas las formulaciones ensayadas, la que dió mejores resultados fue la número 9, en cuya composición el tóxico empleado fue el Cu_2O, y las 12, 13, 14 y 16 compuesto por Cu_2O y TBTF; Cu_2O y TBTO en la proporción 1:1 y Cu_2O, TBTF y TBTO en la proporción 1:1:1.

Vehículo

Los tres tipos de resinas empleados proporcionaron vehículos de buena resistencia, de fácil aplicación y elasticidad.

Los recubrimientos, cuyo vehículo estaba constituido

exclusivamente por acrilato de tributilestaño, fueron los que dieron mejores resultados.

Las probetas recubiertas por pinturas, cuyo vehículo estaba compuesto por acrilato de tributilestaño y por los copolímeros de vinilo y de clorocaucho presentaban su superficie recubierta, en general de forma parcial y, en algunos casos totalmente, por limos, bacterias, fitoplancton, zooplancton y otros microorganismos. Las proporción entre ambos tipos de resinas no fue, posiblemente, el más adecuado para mantener el grado de efectividad de las resinas biocidas, que, como ARIAS et al. 1,986 mantienen deben aplicarse en capas de mayor grosor con el fin de que su lixiviación sea la adecuada el mayor tiempo posible.El mecanismo de acción de este tipo de pinturas basado en la hidrólisis del acrilato de tributilestaño y en el contacto continuo y difusión en las vinílicas y en las de clorocaucho dió lugar a que se depositasen sobre la sobre la superficie de la placa la base de fijación del macrofouling.

La formación de copolímeros no dió, por el momento, los resultados perseguidos pues su comportamiento antiincrustante es ligeramente inferior debido, posiblemente, a la proporción de los tipos de resinas empleados.

AGRADECIMIENTO

Los autores agradecen a la CAYCIT la ayuda económica para la realización de este artículo.

Se dan las gracias, asimismo, a los Directores del Laboratorio del Instituto Español de Oceanografía de Palma de Mallorca por las facilidades y ayuda que nos presta

ron al concedernos autorización para utilizar sus instalaciones durante el período de tiempo que duraron estas experiencias.

BIBLIOGRAFIA

ARIAS, E., J. M. SOUSA, E. MORALES, F. VIVES y P. SUAU.- 1.986. Incrustaciones biológicas en el puerto de Villanueva y Geltrú: Ensayos para su prevención con pinturas "antifouling". Inf. Téc. Inst. Inv. Pesq., Nº 134: 1-24.

DAWANS, F. .-1.982. Les peintures marines antisalissures à base de polymères organostanniques. Rev. Inst. Fr. Pet., 37 (6): 767-807.

KRONSTEIN, M. .- 1.981. Toxic releases from applied antifouling paints. Org. Coat. Plast. Chem., 44: 363-368.

PITTMAN, Ch. Jr. y R. K. LAWYER.- 1.982. Preliminary evaluations of the biological activity of polymers with chemically bound biocides. J. Coat. Technol., 54 (690): 41-46.

POTIN, CH., A. PLEURDEAU y CM. BRUNEAU.- 1.982. Polymères à propiétés biocides. Chimie des Peintures, Nº 322: 269-282.

TORTAROLO, L..-1980. Recenti svilupi delle pitture antivegetative.Società Vernici Italiane Standard, 45 (3): 133-136.

VAN LONDEN, A. M. 1.963. A study of ship bottom paints in particular pertaining to the bahaviour and action of antifouling paints. TNO. Report 54 C.

Cuadro II

Mes	Est.	TOC	O_2	S	Fosfatos	Nitritos	Silicatos	Clor. a	Dens. Óp. $\frac{430}{665}$
XII	1	16,2	3,10	37,26	1,60	0,43	7,12	3,54	3,12
	2	16,4	5,00	37,42	0,65	0,25	2,86	2,00	3,09
	3	----	----	-----	----	----	----	----	----
I	1	13,2	4,72	36,64	0,91	0,47	10,51	3,20	2,99
	2	13,2	5,54	37,24	0	0,15	2,16	3,90	2,88
	3	----	----	-----	----	----	----	----	----
II	1	13,2	5,28	35,91	2,47	0,20	2,75	3,42	3,19
	2	13,0	5,56	37,42	1,19	0,04	2,77	1,56	3,24
	3	13,1	5,67	37,59	1,25	0,03	0,45	1,55	3,40
III	1	15,4	4,38	37,25	2,23	0,40	4,40	5,54	2,85
	2	14,7	5,71	37,48	0,69	0,02	1,05	3,90	2,87
	3	14,5	5,88	37,68	3,20	0	0,90	3,02	2,81
IV	1	16,2	4,60	37,34	1,44	0,37	2,94	5,41	3,04
	2	16,0	5,31	37,57	1,08	0,04	0,94	6,80	2,78
	3	16,0	5,52	37,83	0,48	0,08	0,06	4,13	3,00
V	1	20,4	5,07	37,53	3,20	0,23	4,35	11,66	3,23
	2	20,0	6,00	37,69	2,63	0,09	2,26	4,04	3,02
	3	20,2	6,67	37,79	2,39	0,03	1,83	1,55	3,94
VI	1	21,5	4,85	37,61	1,32	0,13	0,30	12,05	3,32
	2	21,6	5,79	37,63	0,47	0,12	0,17	4,50	3,14
	3	21,7	5,29	37,67	1,15	0,07	0,13	2,39	3,38
VII	1	26,3	4,60	37,63	2,55	0,19	2,43	21,17	3,39
	2	25,8	5,31	37,55	2,07	0,19	1,91	6,63	3,50
	3	25,8	5,52	37,73	1,40	0,07	1,82	1,81	4,03
VIII	1	26,6	3,95	37,61	0,44	0,06	5,23	22,87	2,98
	2	26,1	4,81	37,71	0,68	0	3,66	7,33	3,19
	3	26,3	5,41	37,82	0,11	0,05	3,06	3,23	3,48
IX	1	25,5	3,33	37,48	1,53	0,43	5,86	16,47	3,13
	2	26,1	4,22	37,60	0,21	0	2,38	8,56	3,11
	3	26,1	4,85	37,67	0,19	0,05	0,89	4,84	3,11

Cuadro I

Formulaciones ensayadas en el puerto de Palma de Mallorca

Nº de las Pinturas	1	2	3	4	5	6	7	8	9	10	11	12	13	14	15	16	17	18
SCNCu	18				9	9		6										
Cu_2O									18			9	9		6	15		
TBTO				18		9	9	6			18		9	9	6			15
TBTF		18	18		9		9	6		18		9		9	6		15	
Fe_2O_3									14	14	14	14	14	14	14			
ZnO	14	14	10	15	14	14	14	14								14	14	14
Disolvente	48	48	52	47	48	48	48	48	48	48	48	48	48	48	48	48	48	48
Acrilato 60 % Xilol	18	18	18	18	18	18	18	18	18	18	18	18	18	18	18	8	8	8
Vinylite 30 % Xilol																8	8	8
Clorocaucho 30% Xilol																		
Thixogel	2	2	2	2	2	2	2	2	2	2	2	2	2	2	2	2	2	2
Tricresilfosfato																5	5	5

Nº de las pinturas	19	20	21	22	23	24	25	26	27	28	29	30	31	32
SCNCu														
Cu_2O	8	8	5	15			8	8	25	10	10			
TBTO		8	5		15			8		10		20		10
TBTF	8		5			15	8				10		20	10
ZnO	14	14	14	14	14	14	14	14		10	10	14	14	14
Disolvente	48	48	48	48	48	48	48	48	50	40	40	36	36	36
Acrilato 60 % Xilol	8	8	9	9	9	9	8	8	9	9	9	9	9	9
Vinylite 30 % Xilol	8	8	8											
Clorocaucho 30 Xilol				8	8	8	8	8	9	9	9	9	9	9
Metilester carbilamina										5	5	5	5	5
Thixogel	2	2	2	2	2	2	2	2	2	2	2	2	2	2
Tricresilfosfato	4	4	5	5	5	5	4	4	5	5	5	5	5	5

Cuadro II (continuación)

X	1	23,4	3,59	37,42	2,94		0,23	7,71	21,82	3,76
	2	23,6	5,65	37,52	1,71		0,04	6,71	38,26	3,75
	3	24,8	4,29	37,72	0,26		0,07	3,27	2,00	3,69
XI	1	20,4	3,23	36,89	7,35		1,05	11,14	10,15	3,64
	2	20,7	5,10	37,44	0,57		0,22	3,62	1,48	3,66
	3	20,7	4,26	37,74	0,80		0,09	2,16		

Fig. 1.- Puerto de Palma de Mallorca en donde se efectuaron los ensayos biológicos de control de las pinturas.

Fig. 2.- Variación estacional de los Cirrípedos y de la clorofila a a lo largo del ciclo estudiado.

Fig. 3.- Composición por grupos del zooplancton en las tres estaciones.

Fig. 4.- Variación estacional de los Cirrípedos en la estación 1.

Fig. 4.- Variación estacional de los Lamelibranquios en la estación 1.

Fig. 6.- Estado de algunas probetas al finalizar las experiencias.

Fig. 7.- Estado de las probetas en cuya composición empleamos acrilato de tributilestaño y clorocaucho.

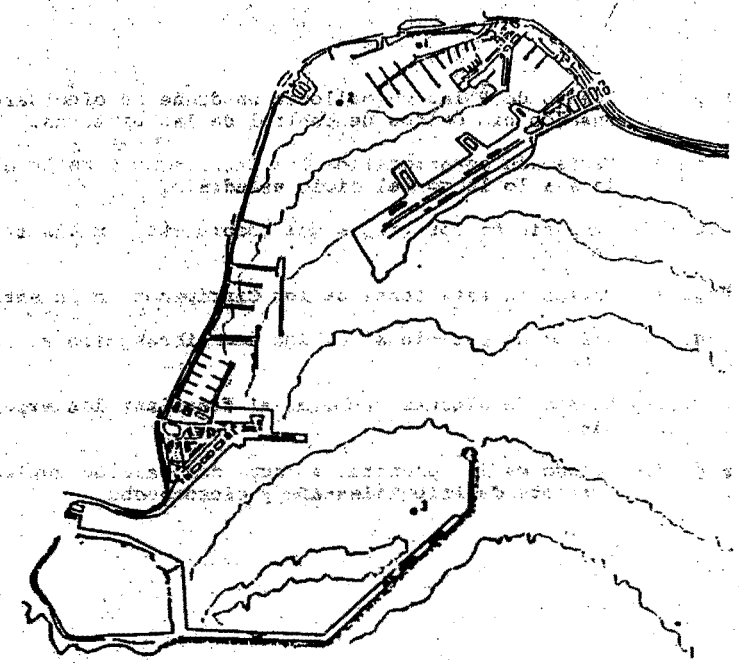

PUERTO DE PALMA DE MALLORCA

Fig. 1

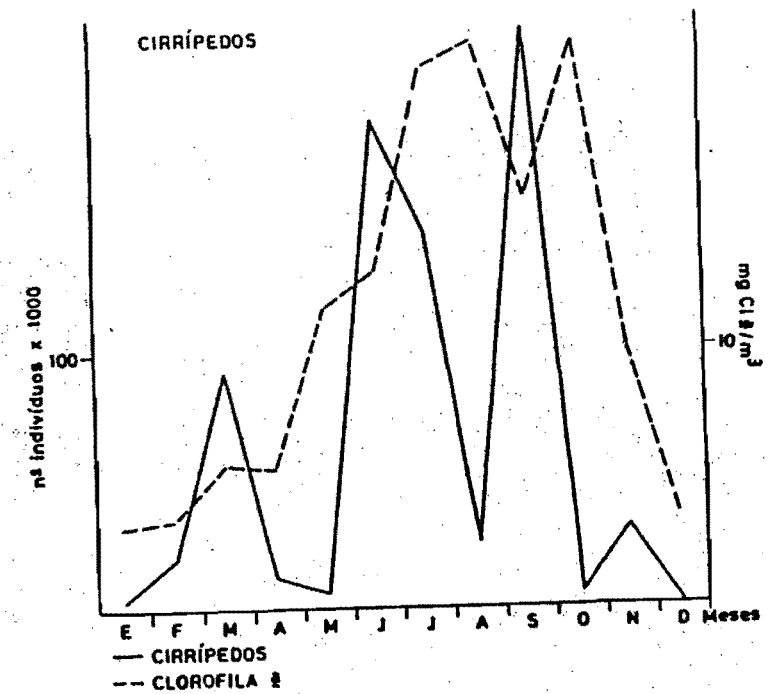

Fig. 2

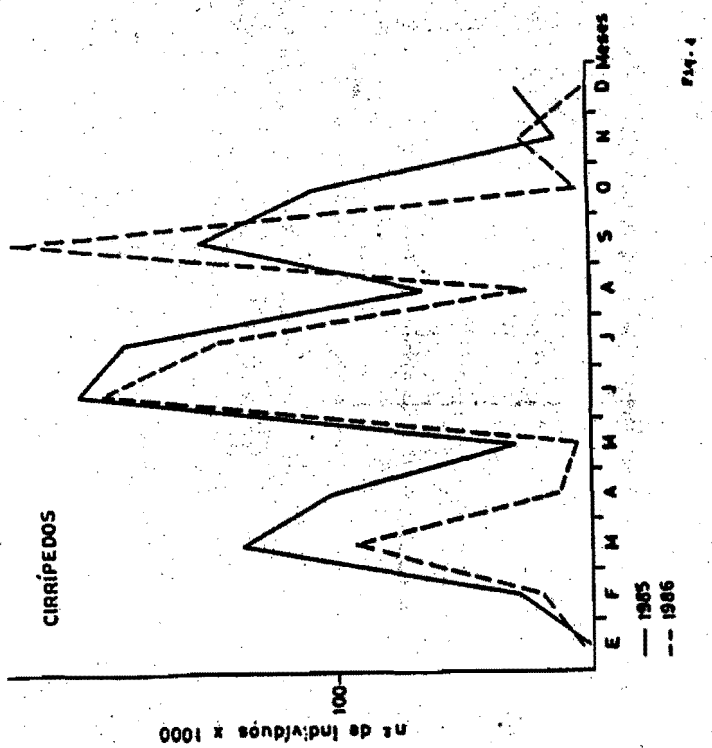
nº de individuos x 1000
100
CIRRÍPEDOS
E F M A M J J A S O N D Meses
1985
1986

Fig. 4

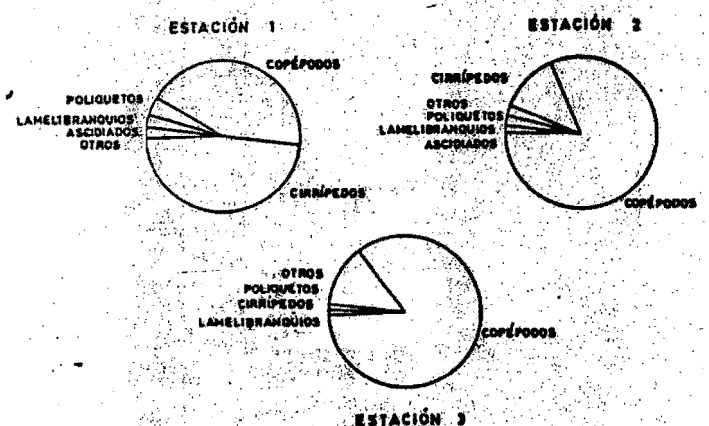
ESTACIÓN 1
COPÉPODOS
POLIQUETOS
LAMELIBRANQUIOS
ASCIDIADOS
OTROS
CIRRÍPEDOS
ESTACIÓN 2
CIRRÍPEDOS
OTROS
POLIQUETOS
LAMELIBRANQUIOS
ASCIDIADOS
COPÉPODOS
OTROS
POLIQUETOS
CIRRÍPEDOS
LAMELIBRANQUIOS
COPÉPODOS
ESTACIÓN 3

Fig. 3

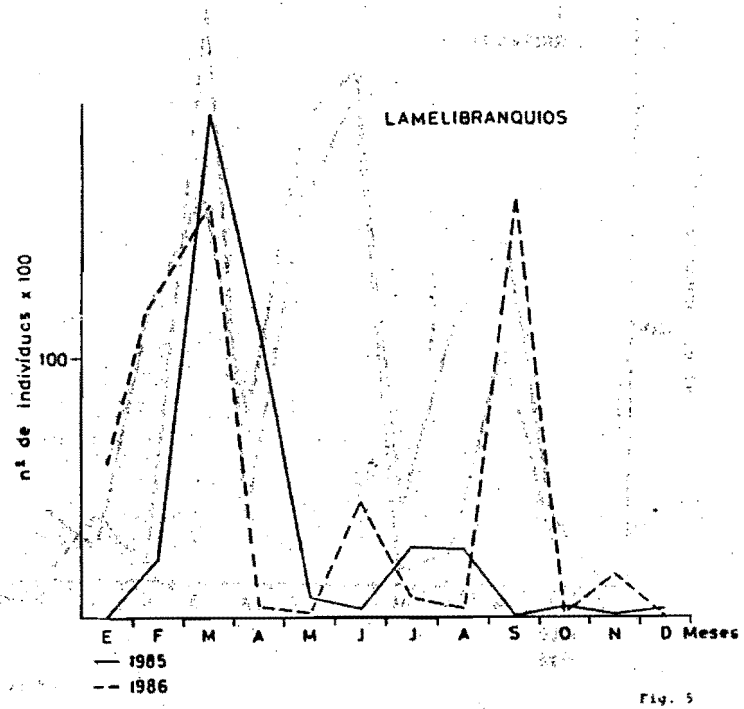

Fig. 5

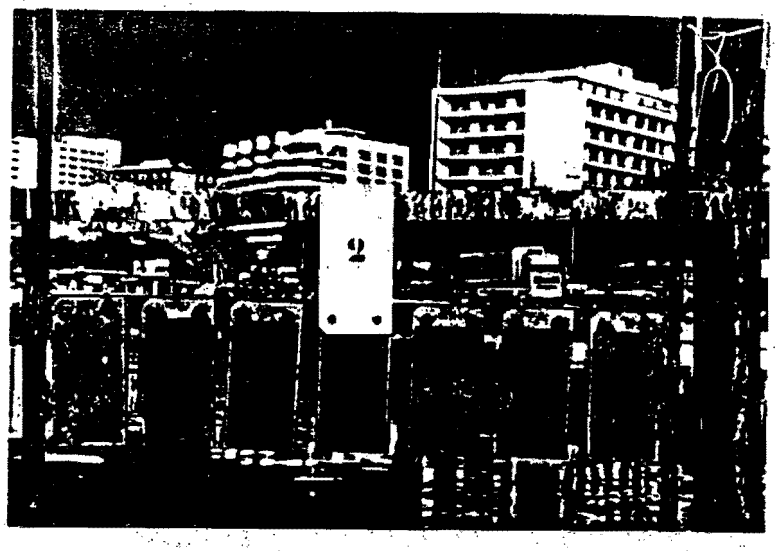

FIG. 6

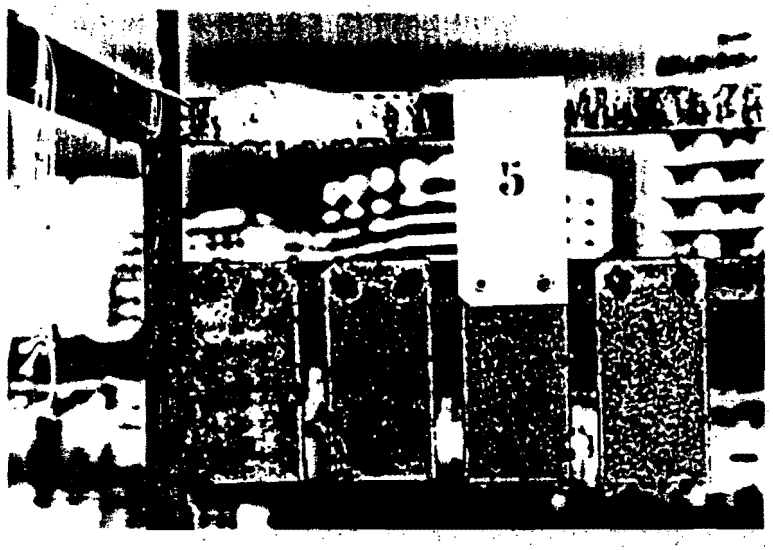

FIG. 7

PINTURAS ANTIINCRUSTANTES DE MATRIZ SOLUBLE

TIPO ALTO ESPESOR

Vicente J. D. Rascio, Carlos A. Giúdice y Beatriz del Amo

CIDEPINT - Centro de Investigación y Desarrollo en Tecnología de Pinturas (CIC-CONICET)

ABSTRACT.- Antifouling paints of the high-build type were studied. Binders were prepared with WW rosin, using chlorinated rubber grade 10 for regulating dissolution rate. Cuprous oxide was employed as toxicant and castor oil as rheological additive. Raft trials performed along 25 months permited to establish the important role of film thickness on bioactivity.

INTRODUCCION

La corrosión de las estructuras metálicas sumergidas en agua de mar y las incrustaciones biológicas que se depositan sobre las mismas obligan a encarar periódicamente la limpieza y el mantenimiento de los cascos de embarcaciones, apoyos de estructuras fuera de costa, etc.

Es un hecho conocido la influencia que ejerce la incrustación de los organismos del "fouling" sobre las condiciones operativas de los buques, alterando la continuidad del revestimiento protector, acelerando los procesos de corrosión, y provocando una merma de velocidad o un aumento de consumo de combustible por la rugosidad que producen.

La necesidad de resolver este problema de la forma más efectiva posible impulsa investigaciones a fin de obtener productos de larga vida útil, compatibles con los aspectos económicos involucrados.

Una pintura antiincrustante eficiente debe prevenir la fijación del "fouling" durante lapsos prolongados [1-6]. En un producto de tipo matriz soluble la velocidad de liberación del tóxico, que define el poder biocida, puede ser controlada tanto por el contenido de dicha sustancia en la película como también por la velocidad de disolución de la matriz. El contenido de tóxico puede ser variado entre límites muy amplios y la pintura mantendrá su efectividad si se ajusta correctamente la velocidad de disolución del ligante. De esa manera se logrará disponer sobre la superficie de la película la concentración de tóxico requerida para repeler las larvas del "fouling".

Estudios previos realizados sobre este problema [7, 8] permitieron llegar a la conclusión que pinturas eficaces y más confiables incluyen ligantes con alta velocidad de disolución en agua de mar. Sin embargo, para períodos prolongados de inmersión, la película se agota parcialmente y comienza a verificarse el proceso de fijación de organismos incrustantes.

Un aumento de la vida útil de estos productos puede lograrse aplicando un mayor espesor de película de pintura antiincrustante (p. ej. 100-120 µm) en lugar del espesor empleado habitualmente (50-60 µm). Este propósito puede obtenerse empleando mayor número de manos de un producto convencional o con una capa de pintura tixotrópica ("high-build").

La incorporación de un aditivo reológico le imparte a la pintura propiedades particulares, lo que permite lograr un producto con satisfactoria resistencia al escurrimiento durante la aplicación, que proporciona alto espesor de película por mano (y en consecuencia alto poder cubritivo), adecuada nivelación, buenas propiedades de pintabilidad y correcta adhesión.

El objetivo del presente trabajo es evaluar la influencia de diversas variables de formulación sobre el poder biocida de este tipo de pinturas, en relación con el de productos de comportamiento conocido, no tixotrópicos, estudiados previamente.

PARTE EXPERIMENTAL

Composición de las muestras

Todos los productos estudiados son de tipo matriz soluble (Tabla I). Fueron elaborados empleando resina colofonia WW como material soluble formador de película y caucho clorado grado 10 como regulador de la velocidad de disolución. En las pinturas no tixotrópicas empleadas como testigo se utilizó para dicho fin caucho clorado grado 20.

Se ensayaron las relaciones resina colofonia/caucho clorado 2/1, 1,5/1 y 1/1 en peso; con la primera de dichas relaciones se obtiene el ligante con mayor velocidad de disolución en agua de mar.

Para lograr una película de adecuadas propiedades fisicomecánicas el caucho clorado fue plastificado con parafina clorada 42 % (relación resina/plastificante 70/30 en peso).

A fin de estudiar la influencia del contenido de ligante se seleccionaron dos niveles: 24,3 y 31,8 % en peso sobre la pintura.

Como tóxico fundamental se empleó el óxido cuproso rojo, debido a su comprobada acción letal sobre los organismos incrustantes [9-11], en la proporción de 20,2 y 25,3 % sobre la pintura. Como tóxico de refuerzo se utilizó óxido de cinc (10 % en peso con respecto al tóxico fundamental).

Se empleó como aditivo reológico aceite de ricino hidrogenado estabilizado (castor oil). A cada muestra de las pinturas tipo alto espesor se le incorporó 2 % en peso de este aditivo, mientras que a las convencionales se agregó 1 %.

Preparación de las pinturas

La elaboración de las muestras se llevó a cabo en un molino de bolas de 20 litros de capacidad total, ajustando las condiciones operativas de modo de lograr una buena dispersión de los pigmentos [12,13] reduciendo al mínimo la reacción entre el ácido abiético de la resina colofonia y los compuestos de cinc, calcio y cobre (Cu^{2+}) presentes [14,15].

El aditivo reológico fue incorporado a cada una de las muestras en forma de gel, luego de finalizada la dispersión de los pigmentos. La operación se llevó a cabo en un equipo de alta velocidad, termostatizando el sistema a 40-45°C.

El gel fue preparado previamente dispersando el aditivo en xileno (15 % en peso) mediante la aplicación de un esfuerzo de corte y trabajando a 40-45°C, hasta alcanzar una estructura coloidal estable.

Ensayos de inmersión

La capacidad antiincrustante de las muestras (poder biocida) fue evaluada en el medio natural (agua de mar), empleando para tal fin una balsa experimental. Las pinturas con mayor contenido de tóxico (25,3 % en peso) fueron ensayadas también sobre la carena de una embarcación de la Armada Argentina.

Para la experiencia en balsa se utilizaron chapas de acero SAE 1010, arenadas a grado ASa 2½ (SIS 05 59 00/67). Los paneles se protegieron con una pintura anticorrosiva (120-150 µm de película seca) y un sellador (40-50 µm), ambos de eficacia comprobada en experiencias anteriores. Sobre dichas pinturas se aplicaron las diferentes muestras experimentales, con espesores de 100-120 µm en el caso de los productos tipo alto espesor (1 capa) y de 50-60 ó 100-120 µm (según el número de manos) en el de las pinturas convencionales. El tiempo de secado entre manos fue de 24 horas, dejándose transcurrir igual lapso luego de la última capa, antes de la inmersión.

La balsa fue fondeada en la Base Naval Puerto Belgrano (38°54'S y 62°06' W), zona de condiciones hidrológicas y biológicas conocidas [16-18].

Las inspecciones se realizaron a los 14, 26 y 36 meses, lapso en el cual estuvieron involucrados tres períodos de intensa actividad biológica de los organismos del "fouling" (primavera-verano).

Para el ensayo en servicio se procedió a lavar con agua a presión la carena de la embarcación seleccionada, se realizaron retoques en diversas zonas con pintura anticorrosiva y luego se aplicó una mano del sellador. Ambos productos tenían composición similar a la de los aplicados en los paneles de la balsa.

Las zonas pintadas (paneles de 16 m^2 cada uno) se dispusieron a ambos costados de la carena, desde la línea de flotación hasta las aletas antirrolido. En servicio sólo se aplicaron las formulaciones 1, 2, 5, 6, 9 y 10, tixotrópicas y convencionales. En el primer caso se utilizó soplete tipo "airless" y en el segundo soplete con aire comprimido; en ambos casos la operación estuvo a cargo de operadores expertos y el tiempo de secado fue similar al de los paneles de la balsa.

Esta experiencia en servicio se prolongó durante 25 meses, durante los cuales la embarcación navegó en mar abierto o estuvo fondeada en un lugar próximo al de la balsa experimental, lo cual aseguró similares características en cuanto a factores abióticos y "fouling".

RESULTADOS

El comportamiento de las pinturas antiincrustantes fue evaluado mediante la escala de fijación ya mencionada en anteriores publicaciones: 0, superficie exenta de "fouling"; 0-1, muy poco; 1, poco; 2, escaso; 3, regular; 4, abundante; 5, superficie completamente incrustada.

Los valores de fijación sobre los paneles de la balsa o sobre la carena de la embarcación se indican en las Tablas II y III, respectivamente.

Se consideró el valor 1 (poco) como el máximo admisible para calificar una pintura como de bioactividad aceptable (80 % de eficiencia).

En todos los casos las observaciones se completaron con registros fotográficos en color, lo que permitió comparar los resultados obtenidos en las diferentes etapas y unificar el criterio de calificación.

En el ensayo en balsa, luego de 14 meses de inmersión, los resultados obtenidos indicaron que el espesor de película había influido decisivamente en el comportamiento de las formulaciones. Las muestras tipo alto espesor y las convencionales aplicadas con espesores de 100-120 µm cumplieron con los requerimientos del ensayo (fijación 0 ó 0-1), mientras que las últimas citadas, con espesores de 50-60 µm, manifestaron un poder biocida inferior (fijación entre 0 y 2). En el caso de los productos elaborados con ligantes con una relación resina colofonia/caucho clorado 2/1 y 1,5/1 (mayor velocidad de disolución) y con el menor espesor de película se notaron zonas de completo desgaste, lo que permitió la fijación de "fouling".

Al cabo de 26 meses de inmersión la influencia del espesor de película se acentuó, con fijación sensiblemente mayor en los paneles de menor espesor y fundamentalmente en los productos con mayor velocidad de disolución (relación colofonia/caucho clorado 2/1 y 1,5/1).

Se debe remarcar que en el caso de las pinturas tipo "high-build" y en las convencionales aplicadas con el espesor más alto, en todos los casos se obtuvo un satisfactorio poder antiincrustante (0, 0-1 ó 1).

En la observación final (36 meses) de la experiencia en balsa se pudo constatar que en los paneles de pinturas convencionales con menor espesor de película, la fijación había aumentado significativamente. Las mismas pinturas, aplicadas con un espesor de película de 100-120 µm mostraron, en algunos casos, elevado poder biocida. Al respecto se deben citar en primer término las pinturas 1 y 2 (mayor relación colofonia/caucho clorado, mayor contenido de tóxico), seguidas luego por las formulaciones 5 y 6 (relación 1/1 y mayor contenido de tóxico), que también cumplieron el ensayo (fijación 0-1 ó 1).

En el ensayo en la carena del navío de la Armada, tanto en las pinturas tipo "high-build" como en las formulaciones convencionales aplicadas con espesores de película de 90 - 110 µm, se observó buen poder biocida, sin fijación o con muy poco "fouling" (0 ó 0-1) luego de 25 meses de inmersión. No se registró influencia de ninguna de las otras variables consideradas en este estudio.

CONCLUSIONES

1. En el caso de la importante influencia del espesor de película sobre la eficiencia de las pinturas, fundamentalmente en aquéllas formulaciones elaboradas con los ligantes de mayor velocidad de disolución (relaciones colofonia/caucho clorado 2/1 y 1,5/1 en peso) es necesario remarcar la trascendencia del empleo de las pinturas tipo "high-build". Estas formulaciones permitieron obtener espesores de película seca de 100 - 120 µm con una sola mano (aplicación sistema airless), lo cual representa una importante economía de mano de obra. Las pinturas formuladas resultaron aptas para la prevención de las incrustaciones biológicas por un período mínimo de 25 meses, no habiéndose continuado la experiencia por la necesidad de entrada de la embarcación a dique seco por problemas ajenos a la protección antiincrustante ó 36 meses en balsa (ensayo estático). En el caso de las muestras 1, 2, 5 y 6, de acuerdo a los espesores remanentes al final de la experiencia, cabría esperar efectiva acción tóxica durante un lapso mayor.

2. Las variables velocidad de disolución del ligante y contenido de pigmento son importantes. La primera por cuanto es factor determinante de la puesta en libertad del veneno, aspecto esencial en cuanto al poder biocida de la pintura y al lapso de mantenimiento del mismo cuando la misma protege una superficie sumergida en el mar. La cantidad de tóxico también tiene, en última instancia importancia con respecto al tiempo total de protección (un contenido de 20 % sobre la pintura significa un compromiso razonable entre calidad y economía).

3. Las pinturas tipo alto espesor formuladas presentaron buena resistencia al escurrimiento ("sagging") durante la aplicación, buen nivelado de la película y adecuadas características de pintabilidad.

AGRADECIMIENTOS

Los autores agradecen a la Comisión de Investigaciones Científicas de la Provincia de Buenos Aires (CIC), al Consejo Nacional de Investigaciones Científicas y Técnicas (CONICET), al Servicio Naval de Investigación y Desarrollo (SENID), a la Dirección de Unidades Navales de la Armada (DIUN) y al personal del Laboratorio de Talleres Generales de la Base Naval Puerto Belgrano, por el apoyo prestado para la realización de este trabajo.

BIBLIOGRAFIA

[1] Barnes, H. J.- Iron and Steel Institute, 175. London, June (1948).

[2] Bureau of Ships, Navy Department.- Marine Fouling and its Prevention. Woods Hole Oceanographic Institution, Woods Hole, Massachusets (1952).

[3] Devoluy, R., Nowacki, L. J., Fink, F. W.- Marine Technology, 4 (2), 189 (1967).

[4] van Londen, A. M.- Treatment and Protection of Ships Hulls. Fairplay Int. Shipping J., Nov. (1971).

[5] de la Court, F. H., de Vries, H. J.- Progress in Organic Coatings, 1, 375 (1973).

[6] Herbert, P. A., Bowerman, D. F., Ford, K. S.- J. Paint Technol., 47 (1), 48 (1975).

[7] Glúdice, C. A., del Amo, B., Benítez, J. C.- J. Oil Col. Chem. Assoc., 64 (1), 12 (1981).

[8] Glúdice, C. A., del Amo, B., Rascio, V., Sánchez, R.- J. Coat. Technology, 55 (697), 23 (1983).

[9] Rascio, V., Glúdice, C. A., Benítez, J. C., Presta, M.- J. Oil Col. Chem. Assoc., 61 (10), 383 (1978).

[10] Rascio, V., Glúdice, C. A., Benítez, J. C., Presta, M.- J. Oil Col. Chem. Assoc., 62 (8), 282 (1979).

[11] Glúdice, C. A., Benítez, J. C., Rascio, V.- Revista Iberoamericana de Corrosión y Protección, XV (1), 16 (1984).

[12] Glúdice, C. A., Benítez, J. C., Rascio, V., Presta, M.- J. Oil Col. Chem. Assoc., 63 (4), 153 (1980).

[13] Glúdice, C. A., Benítez, J. C., del Amo, B.- Proc. 6th Int. Congress on Marine Corrosion and Fouling, Marine Biology, 283 (1984).

[14] Glúdice, C. A., del Amo, B., Benítez, J. C.- J. Oil Col. Chem. Assoc., 64 (1), 12 (1981).

[15] Glúdice, C. A., del Amo, B., Rascio, V., Sánchez, R.- J. Coatings Technology, 55 (697), 23 (1983).

[16] Bastida, R., Spivak, E., l'Hoste, S. G., Adabbo, H. E.- Corrosión y Protección, 8 (8-9), 11 (1977).

[17] Bastida, R., l'Hoste, S. G., Spivak, E., Adabbo, H. E.- Corrosión y Protección, 8 (8-9), 33 (1977).

[18] Bastida, R., Lichtschein, V.- Corrosión y Protección, 10 (3), 7 (1979).

TABLA I

COMPOSICION DE LAS PINTURAS ANTIINCRUSTANTES

(g/100 g)

Pintura.....	1	2	3	4	5	6
Oxido cuproso rojo...	25,3	25,3	20,2	20,3	25,4	25,2
Oxido de cinc.....	2,5	2,5	2,0	2,0	2,5	2,5
Carbonato de calcio..	24,1	16,1	29,7	21,6	24,0	16,2
Colofonia WW.....	13,9	18,1	13,9	18,1	12,1	15,8
Caucho clorado (*)...	6,9	9,1	6,9	9,1	8,1	10,6
Parafina clorada 42 %..	3,5	4,6	3,5	4,6	4,0	5,3
Aditivos.....	0,3	0,4	0,3	0,3	0,5	0,4
Disolv. y diluyentes..	23,5	23,9	23,5	24,0	23,4	24,0
Relación colofonia/ caucho clorado.....	2/1	2/1	2/1	2/1	1,5/1	1,5/1

Pintura.....	7	8	9	10	11	12
Oxido cuproso rojo..	20,1	20,2	25,3	25,4	20,1	20,1
Oxido de cinc.....	2,0	2,0	2,5	2,5	2,0	2,0
Carbonato de calcio.	29,3	21,2	24,1	16,1	20,3	21,4
Colofonia WW.....	12,1	15,8	9,7	12,6	9,7	12,6
Caucho clorado (*)..	8,1	10,6	9,7	12,6	9,7	12,6
Parafina clorada 42 %	4,0	5,3	5,0	6,5	5,0	6,5
Aditivos.....	0,4	0,3	0,3	0,4	0,3	0,4
Disolv. y diluyentes	24,0	24,6	23,4	23,9	23,9	24,4
Relación colofonia/ caucho clorado.....	1,5/1	1,5/1	1/1	1/1	1/1	1/1

(*) Las pinturas antiincrustantes tipo "high-build" se elaboraron con caucho clorado grado 10 y 2,0 % de aditivo tixotrópico; las pinturas antiincrustantes convencionales se prepararon con caucho clorado grado 20 y 1,0 % de aditivo reológico.

TABLA II

FIJACION DE "FOULING" EN EL ENSAYO EN BALSA

(14, 26 y 36 meses de inmersión)

Pintura.....	1	2	3	4	5	6	7	8	9	10	11	12
Producto "high-build":												
14 meses (100-120 µm).....	0	0	0-1	0	0	0	0-1	0	0-1	0	0-1	0-1
26 meses (100-120 µm).....	0	0	0-1	1	0	0-1	1	0-1	1	0-1	1	1
36 meses(100-120 µm).....	0	0	1-2	1-2	0-1	1	3	2	2	1-2	3	2-3
Producto convencional:												
14 meses (50-60 µm).....	0-1	1-2	1	1-2	0-1	2	1	1-2	0	0-1	0-1	0-1
14 meses (100-120 µm)....	0	0	0-1	0-1	0	0	0-1	0-1	0-1	0	0	0
26 meses (50-60 µm).....	2-3	3-4	3-4	4	1-2	2-3	2-3	3-4	0-1	1	1	0-1
26 meses (100-120 µm)....	0	0	1	1	0-1	0-1	1	1	1	0	1	0
36 meses (50-60 µm).....	4-5	5	5	5	3-4	4-5	4	5	3-4	4	4-5	5
36 meses (100-120 µm)....	0-1	0	2	1-2	1	1	2-3	2	1-2	1-2	2-3	2

TABLA III

FIJACION DE "FOULING" EN LA CARENA DE UNA EMBARCACION DE LA ARMADA ARGENTINA

(25 meses de inmersión)

Pintura.....	1	2	5	6	9	10
Producto "high-build":						
Babor.....	0	0	0	0-1	0-1	0
Estribor.....	0	0	0-1	0	0	0
Producto convencional:						
Babor.....	0	0	0-1	0	0-1	0
Estribor.....	0	0-1	0	0-1	0-1	0-1

El espesor de película seca varió entre 90 y 110 µm.

SECTION II

TITLE / TITULO APPORT DE LA BIOLUMINESCENCE DANS L'INTERPRETATION DES TESTS DE SELECTION DE BACTERICIDES SPECIFIQUES DES BACTERIES SULFATO-REDUCTRICES.

NAME / NOMBRE AUCLAIR Paul ..... COUGET Paul

ORGANIZATION / ORGANIZACION SOCIETE NATIONALE ELF AQUITAINE

FRANCE.

ABSTRACT / RESUMEN .....

In the oil industry, conventional tests for selecting sulfate reducing bacteria bactericides are often affected by uneasy to analyze anomalies.

Bioluminescence used as a complementary technique in result interpretation made it possible to explain more occurately how certain bactericides operate and to establish our selection.

WORK / COMIENZO DEL TRABAJO

La corrosion bactérienne par bactéries sulfato-réductrice (SRB) est une des principales causes de la dégradation des installations d'exploitation des hydrocarbures liquides et gazeux et d'injection d'eau (particulièrement d'eau de mer). La lutte contre ces phénomènes est généralement effectuée au moyen de bactéricides. Compte-tenu des quantités utilisées et des risques encourus, le choix des additifs à utiliser est fait par sélection en laboratoire.

Toutefois, les résultats obtenus sont, souvent, entachés d'anomalies que l'utilisation de la bioluminescence, comme moyen complémentaire de contrôle, permet, en partie au moins, d'expliquer.

1 - METHODE DE SELECTION DES BACTERICIDES

Une quantité de 2 litres de milieu de culture est ensemencée par un échantillon de culture bactérienne provenant du site à étudier. Ce milieu est ensuite placé dans un récipient étanche en étuve à 37,5°C sous barbotage d'azote.

Lorsque le milieu a viré (précipité noir de SFe), il est laissé 24 ou 48 heures dans l'étuve pour atteindre le développement bactérien optimum.

La culture est alors prête pour l'étude.

Le milieu de culture utilisé pour le développement des BSR est, en principe, spécifique de ces bactéries mais il permet le développement d'autres micro-organismes.

Le test est effectué de la manière suivante :

15 cm³ de milieu viré sont introduits dans des tubes bouchés, contenant des plaquettes métalliques de 0,5 cm de large, 4 cm de long et 0,1 cm d'épaisseur. Ces tubes sont disposés en 2 séries.

a) Métal seul

15 cm³ de milieu, une plaquette métallique et une dose croissante du bactéricide à étudier (50, 200, 400 ppm). Ce test est spécifique des réseaux d'injection d'eau.

b) Métal + huile

15 cm³ de milieu, une plaquette métallique, 1 à 2 cm³ huile du site à traiter et les mêmes doses des mêmes bactéricides qu'en a). Ces tubes sont ensuite bouchés, agités et placés en étuve à 37,5°C. Ce test est spécifique des réseaux de production d'huile.

c) Interprétation

L'efficacité du bactéricide testé sera suivie en effectuant :

- des contrôles de présence de bactéries sulfato-réductrices vivantes,

- des mesures de bioluminescence (caractéristique de tout ce qui est vivant dans le milieu : BSR et autres bactéries) et ce, après des temps de contact variables avec les bactéricides (de 3 H à 7 jours).

2 - METHODES DE CONTROLE DES RESULTATS

2.1 - Par tests kits

1 cm³ du milieu à contrôler est injecté dans 10 cm³ de milieu stérile. Si des bactéries encore vivantes sont présentes, elles peuvent entamer un processus de développement en raison de la richesse en matière nutritive du milieu fourni et de la dilution du bactéricide. Cette reprise de l'activité se traduit par la précipitation de sulfure de fer de couleur noire.

2.2 - Bioluminescence

On appelle luminescence l'émission de lumière produite lors de la vesactivation d'une molécule ou d'un atome préalablement excités par une absorption d'énergie.

Dans le cas de la bioluminescence, l'énergie est apportée par un organisme vivant.

La réaction chimique est obligatoirement catalysée par une enzyme. Celle-ci n'est un catalyseur actif qu'en présence d'un activeur. On a alors la réaction :

Enzyme + Activeur + Substrat --->
Produit + Enzyme + Activeur + $h\lambda$
h = constante de Planck
λ = fréquence émise

L'intégration de la quantité de lumière émise fournit une mesure quantitative du substrat à concentration d'enzyme donnée.
L'exemple le plus connu est celui du dosage de l'adenosine triphosphate (ATP) par un système enzymatique de luciole.

La méthode consiste en un premier temps à l'extraction de cet ATP. En un deuxième temps au dosage de cet ATP extrait en rajoutant un produit qui contient de la luciférine et une enzyme : la luciférase.

On a la réaction suivante :

$$ATP + luciférine + O_2 \xrightarrow[Luciférase]{Mg^{++}} oxyluciférine + AMP + CO_2 + ppi + h\lambda$$

Lorsque tous les composés sont en excès, sauf l'ATP extrait, la quantité de photons émis est directement proportionnelle à la quantité d'ATP dégradé.

L'appareil utilisé est : Marque : BERTHOLD BIOSYS
Type : Biolumat LB 9500T
Code : BI 5106

3 - DEROULEMENT DES ESSAIS

3.1 - Souches bactériennes

Nous avons sélectionné 3 souches bactériennes pour effectuer les essais en laboratoire :

1) Une souche provenant d'une eau de mer prélevée dans le Golfe de Guinée sur le site de Kolé (offshore Camerounais).

2) Une souche provenant d'une eau douce type eau de la Saur (rivière du Sud-Ouest de la France).

3) Une souche provenant d'une eau de gisement de Gonelle (GNM8) au GABON.

Les essais sur la souche de l'eau de la Saur et sur la souche d'eau de gisement sont faits en présence d'huile non traitée, provenant du puits MTC5 (Sud-Ouest de la France).

3.2 - Bactéricides

Les bactéricides testés, au nombre de 20, sont tous des produits commerciaux provenant de 12 fournisseurs différents :

BASF (RFA)	produits	E1 et E2
CECA (FRANCE)	"	L1 L2 et L3
ENERGECO (ITALIE)	"	D
GAMLEN (USA/FRANCE)	"	J
HENKEL (RFA)	"	F
NALCO (ITALIE)	"	A1 et A2
NLTREATING (UK)	"	I
PETROLITE (USA)	"	G1 et G2
RHONE-POULENC (FRANCE)		C
SERPIC (FRANCE)	"	H1 et H2
SERVO (HOLLANDE)	"	B1 et B2
SOFRASER (FRANCE)	"	K1 et K2

3.3 - Essais réalisés

Les 20 produits à tester sont repartis dans des tubes contenant le milieu de culture (dans lequel les bactéries sont en prolifération) aux doses de 50, 200 et 400 ppm. Les mesures suivantes sont réalisées :

- après 7 jours de contact bactérie/bactéricide ensemencement de Tests-Kits pour détecter la présence de bactéries sulfato-réductrices vivantes.

- après 3 H, 24 H, 2 j, 4 j et 7 jours mesure en bioluminescence qui permet de vérifier l'action des bactéricides sur l'ensemble de micro-organismes vivants et pas seulement les BSR.

4 - RESULTATS DES ESSAIS

Afin de mieux apprécier le comportement des additifs, des essais à blanc ont été réalisés et ont donné les résultats suivants, exprimés en picogramme (10^{-12}) d'ATP :

EAU / TEMPS	MER KLM	RIVIERE SAUR	GISEMENT GNM
3 H	130 10^3	0,85 10^3	1,6 10^3
24 H	37 10^3	0,55 10^3	2,8 10^3
2 J	178 10^3	0,55 10^3	6 10^3
4 J	100 10^3	0,56 10^3	9 10^3
7 J	100 10^3	0,58 10^3	9 10^3
4 J		SANS HUILE 60 10^3	90 10^3

Les bactéries de l'eau de mer paraissent très sensibles au brusque changement de milieu. Leur nombre chute 24 H après le transfert dans la cellule d'essai. Par ailleurs, on notera les faibles valeurs d'ATP dans les essais de la SAUR et de GNM qui sont réalisés en présence d'huile, alors qu'en son absence, on retrouve des valeurs voisines de celles de l'eau de KLM. On peut donc conclure à un effet biostatique de l'huile dont les bactéries de GNM (qui "connaissent" le milieu pétrolier) s'accomodent plus facilement que celles provenant de la surface.

TABLEAU 1

ENSEMBLE DES RESULTATS (APRES 7 JOURS) EXPRIMES EN % D'ATP PAR RAPPORT AU BLANC.

	50 ppm			200 ppm			400 ppm		
	KLM	SAUR	GNM	KLM	SAUR	GNM	KLM	SAUR	GNM
A1	9	35	1*	1	10	0*	0*	5	0*
A2	0*	65	0*	0*	20	0*	0*	30	0*
B1	0*	9*	0*	0*	7*	0*	0*	16*	0*
B2	0*	80	0*	0*	20	0*	0*	25	0*
C	560	45	20	?*	20	7	13*	10	2
D	0*	9*	0*	0*	5*	0*	0*	7*	0*
E1	0*	19	0*	0*	5	0*	0*	7*	0*
E2	0*	60	0*	0*	35	0*	0*	20	1*
F	380	40	20*	13*	14	3*	0*	9*	0*
G1	35	16	0*	4	20	0*	0*	25	0*
G2	45	45	0*	50	40	0*	100	35	0*
H1	60	16*	0*	50	9*	0*	3*	2*	0*
H2	30	?	0*	0*	20	0*	0*	2*	0*
I	120	145	0*	70	80	0*	30	45	0*
J	110	9*	0*	110	5*	0*	120	5*	0*
K1	?*	14	0*	?*	7	0*	?*	7*	0*
K2	?*	10	3	?*	16	1	?*	14*	1
L1	660	40*	0*	1	5*	0*	2*	5*	0*
L2	0*	5*	0*	0*	5*	0*	0*	5*	0*
L3	0*	30	0*	0*	30	0*	0*	19	0*

* indique que les BSR sont tuées (après 7 jours).

L'ensemble des résultats obtenus, après 7 jours de contact bactérie/bactéricide est figuré dans le tableau n° 1.

4.1 - Résultats des contrôles par Tests Kits

Ces contrôles permettent d'établir un classement entre les divers produits après 7 jours de contact entre les bactéries et les bactéricides.

4.1.1 - Souche eau de mer de Kolé

Produits actifs à 50 ppm : A2 B1 E1 B2 D E2 K1 L2 L3
Produits actifs à 200 ppm : C F H2 K2
Produits actifs à 400 ppm : A1 G1 H1 L1
Produits inactifs à 400 ppm : G2, I, J

4.1.2 - Souche de la Saur

Produits actifs à 50 ppm : B1 D H1 J L1 L2
Produits actifs à 200 ppm : aucun
Produits actifs à 400 ppm : E1 F H2 K1 K2
Produits inactifs à 400 ppm : A1 A2 B2 C E2 G1 G2 I L3

Bien que la souche soit peu active, elle est beaucoup plus sélective que la première.

4.1.3 - Souche de GNM

Produits actifs à 50 ppm : A1 A2 B1 B2 D E1 E2 F G1 G2 H1 H2 I J L1 L2 L3 K1
Produits actifs à 200 ppm : aucun
Produits actifs à 400 ppm : E3
Produits inactifs à 400 ppm : C K2

La plupart des bactéricides agissent donc sur cette souche.

4.2 - Résultats des contrôles par bioluminescence

Ces contrôles ne sont pas spécifiques des BSR. Ils nous renseignent sur l'effet global du bactéricide sur les micro-organismes présents.

4.2.1 - Souche eau de Mer de KLM

Trois heures après contact avec le bactéricide, la population bactérienne a chuté de manière notable (> 90 %) pour 5 produits à 50 ppm (A2, B1, B2, E1, L1), 7 produits à 200 ppm (les mêmes plus A1 et D), 9 produits à 400 ppm (les mêmes plus C et E2).

Mais, après 24 heures, le taux d'ATP mesuré est presque dans tous les cas supérieur dans le milieu traité à celui du blanc et ce, de façon très nette. Ce phénomène n'a été observé que dans ce cas précis : voir tableau 2.

Enfin, après 2 jours de contact l'ensemble de la population a tendance à s'effondrer, sauf dans quelques cas (F G1) : voir tableau 3.

TABLEAU 2

MER KLM : % d'ATP par rapport au blanc après 24 H de contact.

	50 ppm	200 ppm	400 ppm
A1	90	80	90*
A2	75*	105*	140*
B1	120*	200*	135*
B2	115*	145*	225*
C	145	115*	125*
D	120*	85*	110*
E1	115*	190*	115*
E2	90*	165*	175*
F	225	245*	180*
G1	225	235	195*
G2	275	340	440
H1	160	170	150*
H2	45	180*	185*
i	160	125	120
j	200	230	215
K1	230*	245*	270*
K2	210	160*	185*
L1	190	125	165*
L2	160*	165*	30*
L3	240*	325*	210*

* Produit efficace après 7 jours.

TABLEAU 3

Mer KLM : % d'ATP par rapport au blanc après 2 j de contact

	50 ppm	200 ppm	400 ppm
A1	20	1	1*
A2	1*	1*	1*
B1	1*	1*	1*
B2	2*	3*	11*
C	20	16*	7*
D	5*	5*	5*
E1	5*	5*	5*
E2	5*	5*	5*
F	120	30*	20*
G1	50	35	140*
G2	2	1	1
H1	2	0	0*
H2	7	2*	1*
i	20	1	1
j	3	1	1
K1	2*	3*	2*
K2	40	3*	2*
L1	300	7	2*
L2	1*	1*	0*
L3	0*	0*	0*

* Produit efficace après 7 jours.

4.2.2 - Eau de la Saur

Les contrôles réalisés par tests-kits ont montré la sélectivité de cette eau. La bioluminescence montre que l'ensemble des micro-organismes est moins touché que dans les autres cas, même quand les BSR sont tuées (B1, D, H1, J, L1).

4.2.3 - Eau de GNM

La bioluminescence montre une action très forte sur l'ensemble des micro-organismes du milieu traité sauf sur F à 50 ppm où, bien que les BSR soient tuées, 20 % de l'ATP initial subsiste.

5 - COMPARAISON DES RESULTATS

La bioluminescence permet de mesurer l'action des additifs sur l'ensemble des micro-organismes et de suivre l'évolution de l'ensemble du système. Dans l'expérience sur l'eau de mer de KLM (voir tableau 4), tous les produits actifs vis à vis des BSR (A2, B2, D, E1, E2, L1, L2) ont un comportement identique à B1 : réduction de pratiquement 100 % du taux d'ATP après 2 jours. Tous les produits inactifs (G2, I, J) ont un comportement semblable : après une chute du taux d'ATP, la valeur remonte nettement au septième jour, et même à forte concentration de bactéricide, cette valeur peut excéder celle du blanc (sans traitement).

Les produits actifs à certaines doses et pas à d'autres (G1, H1, F, par ex.), ont un comportement hérité des deux tendances précédentes, mais dans le cas de F, où à 200 ppm on voit remonter le taux d'ATP après 7 jours, (bien que le TK soit négatif), il convient de considérer que la dose de 200 ppm est probablement proche des limites d'efficacité du produit.

Les tests-kits, par contre, ne donnent que des résultats par tout ou rien pour les seules BSR. Les quelques renseignements complémentaires obtenus concernent le temps de virage des tubes de contrôle. Par exemple, avec le produit G1, après 7 jours de contact bactérie/bactéricide, le TK de contrôle vire en 1 jour pour la dose de 50 ppm, en 7 jours pour 200 ppm et reste négatif (produit efficace sur les BSR) à 400 ppm. On considèrera qu'à 200 ppm, le G1 est plus actif (sans toutefois stériliser totalement) que le H1 pour lequel le TK de contrôle à 200 ppm vire en 2 jours.

Sous réserve d'approfondissement des travaux, la bioluminescence permet de lever l'ambiguité essentielle du mode de sélection adopté : aux fortes concentrations de bactéricides, le non virage du Test-Kit peut correspondre à la stérilisation du milieu, cas de F à 400 ppm, par ex., ou simplement, à un effet bactériostatique (bactérie vivante mais métabolisme bloqué par la dilution insuffisante du bactéricide). Les résultats obtenus en bioluminescence en F à 200 ppm et H1 à 200 ppm doivent permettre de lever cette ambiguité.

TABLEAU 4

% d'ATP résiduel par rapport au blanc

	3 H	24 H	2 J	4 J	7 J	RESULTAT DES T.K.
B1 50 ppm	2	120	1	0	0	NEGATIF
200 ppm	1	200	1	0	0	NEGATIF
400 ppm	1	135	1	0	0	NEGATIF
J 50 ppm	15	200	3	150	110	POSITIF 1 JOUR
200 ppm	30	230	1	4	110	POSITIF 2 JOURS
400 ppm	25	215	1	0	120	POSITIF 7 JOURS
F 50 ppm	55	225	120	175	380	POSITIF 1 JOUR
200 ppm	200	245	30	1	13	NEGATIF
400 ppm	45	180	20	0	0	NEGATIF
G1 50 ppm	13	225	50	400	35	POSITIF 1 JOUR
200 ppm	64	235	35	3	4	POSITIF 7 JOURS
400 ppm	40	200	140	0	0	NEGATIF
H1 50 ppm	30	160	2	50	60	POSITIF 1 JOUR
200 ppm	18	170	0	0	50	POSITIF 2 JOURS
400 ppm	25	150	0	0	3	NEGATIF

* à 50 ppm, F semble favoriser nettement l'ensemble des micro-organismes présents.

ETUDE DE L'INFLUENCE D'ELEMENTS "POISONS" SUR LA RESISTANCE A LA CORROSION BACTERIENNE EN MILIEU MARIN D'ACIERS INOXYDABLES

G.HERNANDEZ (1), C.LEMAITRE (1), J.GUEZENNEC (2), J.P.AUDOUARD (3), G. BERANGER (1)

(1) Université de Technologie, COMPIEGNE. BP 649
60206 COMPIEGNE. Cedex (France)
(2) IFREMER. Centre de BREST, BP 70 - 29263 PLOUZANE. (France)
(3) UNIREC, Centre Commun de Recherches USINOR-SACILOR, BP 50
42702 FIRMINY Cedex (France)

RESUME

Afin de lutter contre la corrosion bactérienne des aciers inoxydables en milieu marin, il a été envisagé d'ajouter dans la composition de ceux-ci des éléments chimiques considérés comme toxiques vis-à-vis des bactéries. Ce faisant, la formation du voile biologique, présent sur toute surface exposée en milieu marin, peut se trouver ralentie.

Nous avons étudié l'influence de l'addition de plusieurs éléments connus pour leurs propriétés spécifiques en ce domaine, sur la corrosion localisée d'une nuance d'acier inoxydable du type 316 L.

A l'aide de techniques électrochimiques et d'analyses fines des surfaces, nous avons comparé le comportement des nuances entre elles en eau de mer synthétique (type ASTM), puis de chaque nuance avec ou sans bactéries introduites dans ce milieu synthétique. Ces résultats sont ensuite comparés à ceux obtenus en eau de mer naturelle.

L'ensemble de ces observations permet de mettre en évidence le rôle de certains éléments "poisons" étudiés, sur le ralentissement de la formation du voile biologique à la surface des aciers inoxydables, et sur la meilleure résistance à la corrosion localisée qui en découle.

I - INTRODUCTION

De nombreuses études de corrosion microbienne en milieu marin ont été faites principalement sur des aciers doux (1-15). Sur les aciers inoxydables, le nombre de travaux publiés semble beaucoup moins important (16-22). Les études effectuées en présence de bactéries, montrent que, d'un point de vue électrochimique, des phénomènes particuliers se manifestent, notamment par une modification des potentiels (26-28) favorisant l'apparition de piqûres.

Ce phénomène a pu être attribué à la formation d'un voile biologique (23-25) dû aux microorganismes présents dans le milieu.

Il nous a semblé interessant de voir si certains éléments d'alliage, en influençant les conditions de réduction de l'oxygène, seraient susceptibles d'intervenir dans la formation de ce voile.

Dans cette étude, nous avons voulu comparer à l'aide d'essais électrochimiques et d'analyses de surface le comportement des nouvelles nuances obtenues dans des milieux contenant ou non des bactéries pour mettre en évidence le rôle spécifique joué par chacun des éléments poison considéré.

II - MATERIAUX ETUDIES

L'acier de référence est du type 316 L dont la composition est indiquée dans le tableau I.

TABLEAU I : COMPOSITION DE L'ACIER 316 L

	C	Mn	Si	S	P	Ni	Cr	Mo
Acier 316 L	0.01	1.64	.46	.005	.017	11.54	16.80	2.06

Des nuances modifiées ont été élaborées par adjonction d'éléments toxiques tels que l'arsenic, le cuivre et le sélénium. Ces nuances ont été comparées à l'acier 316 L.

L'état de surface ayant servi de référence à l'ensemble de nos échantillons correspond à celui obtenu après polissage au papier SiC jusqu'à granulométrie 600.

Dans certains cas la surface a été vieillie pendant des temps définis, soit dans l'eau de mer synthétique ASTM, soit dans l'eau de mer naturelle. Les temps de vieillissement que nous avons utilisés correspondent à :

- état fraichement poli.
- 1 semaine.
- 1 mois.

III - ESSAIS ET RESULTATS

III.1 _ Les solutions

Nous avons utilisé d'une part de l'eau de mer naturelle (à BREST) et d'autre part une solution marine synthétique du type ASTM dont la composition apparait dans le tableau II.

Afin de mieux connaître le mécanisme d'attaque et de comparer la résistance à la corrosion microbienne des aciers étudiés, nous avons mis au point un montage adapté. Des bactéries se trouvant dans des oxydes formés sur un morceau d'acier corrodé dans l'eau de mer naturelle ont été introduites dans la solution marine synthétique utilisée, comprenant un milieu propre de culture des bactéries sulfato-réductrices (29).

Les essais ont été effectués dans des conditions aérobies sur des aciers 316 L et 316 L + As puis dans des conditions anaérobies sur ces mêmes aciers afin de mettre en évidence l'effet éventuel de l'arsenic.

Tableau II : COMPOSITION DE LA SOLUTION MARINE SYNTHETIQUE DU TYPE ASTM

	Concentration g/litre.
NaCl	24.53
MgCl2	5.20
Na2SO4	4.09
CaCl2	1.16
KCl	0.695
NaHCO3	0.201
KBr	0.101
H2BO3	0.027
SrCl2	0.025
NaF	0.003

III.2 - Mesures électrochimiques

Pour les différentes études électrochimiques entreprises, nous avons utilisé l'électrode au calomel saturé (ECS) comme électrode de référence, l'électrode auxiliaire étant en platine. Différentes techniques électrochimiques ont été mises en œuvre pour caractériser le comportement des couples matériau-milieux :

- la variation du potentiel d'abandon en fonction du temps
- les courbes intensité-potentiel
- la mesure des résistances de polarisation
- les mesures d'impédance

III.2.1. Evolution du potentiel d'abandon en fonction du temps

Nous avons mesuré la variation dans le temps du potentiel libre des couples matériaux-milieu dans les différentes solutions utilisées, à partir de l'instant d'immersion.

Dans la solution marine synthétique pour les nuances modifiées de l'acier 316 L (fig.1), la comparaison des comportements dans le temps met en évidence de notables différences.

Lorsque les bactéries sont ajoutées à la solution on constate (figs. 2 et 3) une inversion de l'évolution du potentiel due à la présence d'arsenic dans l'acier 316 L.

III.2.2. Courbes de polarisation

Les courbes de polarisation ont été tracées à partir du potentiel d'abandon jusqu'à - 1000 mV pour la branche cathodique, puis vers les potentiels anodiques jusqu'à ce que le courant atteigne 1 mA/cm2, la vitesse de balayage utilisée étant de 225 mV/hr.

Dans l'eau de mer synthétique, des mesures ont été effectuées à l'aide des nuances modifiées. Les courbes de polarisation obtenues dans le sens des potentiels croissants sont représentées sur les figures 4-7. Ces courbes mettent en évidence des différences de comportement lorsque le temps de maintien en solution change.

III.2.3. Mesure de résistance de polarisation

Pour les mesures de résistance de polarisation nous avons imposé à l'électrode de travail un potentiel soumis à un balayage linéaire autour du potentiel d'abandon Eo, entre Eo ± ΔE. Toutes les mesures ont été realisées avec un ΔE = 5 mV et une vitesse de balayage de 120 mV/hr. Le tableau III montre les valeurs obtenues dans la solution synthétique sans bactéries. Lorsque des bactéries sont ajoutées (tableau IV), les variations observées sont considérables.

Tableau III : RESISTANCE DE POLARISATION DES ACIERS EN MILIEU SYNTHETIQUE.

	VIEILLISSEMENT	1 Jour	1 Semaine	1 Mois
ACIER 316L		118,181 Ω	318,195 Ω	2 500,000 Ω
316 L + Cu		1 194,117 Ω	1 500,000 Ω	454,545 Ω
316 L + Se		1 800,000 Ω	790,000 Ω	2 480,000 Ω
316 L + As		63,829 Ω	2 385,000 Ω	100,000 Ω

III.2.4. Mesures d'impédance

Chaque essai a été realisé au potentiel d'abandon préalablement mesuré puis imposé (méthode potentiostatique) et lui même perturbé par une oscillation sinusoïdale de fréquences qui varient entre 10 000 Hz et 0.001 Hz.

Les figures 8 et 9 montrent les résultats obtenus pour tous les aciers qui ont été vieillis dans l'eau de mer synthétique. En présence de bactéries, on remarque une forte diminution de l'impédance pour l'acier 316 L (fig.10), et au contraire une grande augmentation lorsque l'arsenic est présent dans l'acier (fig.11).

III.3 - Microscopie et analyses de surfaces

Pour mieux caractériser la couche passive, deux techniques d'analyse ont été utilisées : la spectroscopie à décharge luminescente (SDL) et la microscopie électronique à balayage (MEB).

La méthode d'analyse SDL n'a été utilisée que pour les aciers ayant subi un vieillissement d'un mois dans la solution marine synthétique sans bactéries. Les résultats montrent suivant les échantillons des différences. Pour chaque élément étudié on peut utiliser :

- les hauteurs de pics proportionnelles aux concentrations locales à une certaine profondeur.
- les longueurs de pics, correspondant à l'évolution de la répartition de chaque élément suivant cette même profondeur.

Lorsque la vitesse d'érosion de l'échantillon est connue, le temps d'érosion peut être directement relié à la profondeur. La répartition des différents éléments selon le temps d'érosion peut ainsi nous donner une idée de l'épaisseur de la couche passive.

De plus les aciers 316 L et 316 L + As vieillis un mois dans la solution marine avec des bactéries, (+ le milieu de culture), ont été analysés par microscopie électronique à balayage.

Pour isoler les bactéries nous avons plongé chaque acier étudié dans la solution ASTM additionnée du milieu de culture. Au bout d'un mois,le mélange a été prélevé, puis par centrifugation le résidu solide a été extrait. Celui-ci est essentiellement constitué des bactéries. Il a été ensuite deshydraté dans des solutions alcooliques successives de 30 à 100 %. Après séchage à l'air il a été introduit dans un dessicateur et finalement métallisé pour être observé au microscope électronique à balayage. De plus, l'échantillon métallique est lui-même séché sous une lampe électrique puis métallisé avant d'être analysé. Les bactéries présentes dans le milieu contenant chaque acier ont été analysées ainsi par MEB (fig.12-13).

Ces observations nous ont permis de constater que suivant les aciers, la morphologie des colonies bactériennes était différente. Il apparaît que par rapport au milieu de culture initial, la forme reste filamenteuse avec l'acier 316 L, mais avec une longueur moyenne en diminution, et elle devient globulaire en présence de l'acier qui contient de l'arsenic, il apparaît nettement que la composition de l'alliage modifie le comportement des bactéries

Tableau IV : RESISTANCE DE POLARISATION DES ACIERS 316 L et 316 + AS EN MILIEU SYNTHETIQUE AVEC DES BACTERIES

ACIER \ VIEILLISSEMENT	1 mois dans la sol. ASTM sans bactéries	1 mois dans la sol. ASTM avec des bactéries
316 L	2 500,000 Ω	24,600 Ω
316 L + As	100,000 Ω	3 852,000 Ω

IV - DISCUSSION DES RESULTATS

IV.1 - Partie électrochimique

A partir des courbes de polarisation nous pouvons observer que par rapport aux nouvelles nuances l'acier sans élément poison se distingue des autres : il est plus résistant et se comporte mieux aux potentiels fortement anodiques. Notamment, les potentiels de piqure sont légèrement déplacés. L'acier au cuivre est très actif immédiatement après polissage. Cependant, si on laisse l'alliage vieillir dans la solution, son comportement s'améliore (fig.5). Un comportement similaire s'observe avec les aciers au sélénium et à l'arsenic. Toutefois, l'amplitude de ces différences est beaucoup plus grande lorsqu'il s'agit du cuivre, cet élément tend donc à destabiliser la passivité de l'alliage, mais un temps suffisant d'immersion permet, malgré tout, la reconstruction de la couche passive.

Il apparaît qu'avec le temps d'immersion, les potentiels d'abandon augmentent pour les aciers 316 L et 316 L + Se, tandis qu'ils diminuent pour les nuances 316 L + Cu et 316 L + As (fig.1). Il semble donc d'après ce test que l'adjonction de sélénium provoque un anoblissement, tandis que l'adjonction de cuivre ou d'arsenic agissent dans l'autre sens.

Nous pouvons remarquer que les résistances de polarisation des aciers 316 L et 316 L + Se augmentent en fonction du temps, tandis que celles des aciers 316 L + Cu et 316 L + As diminuent (tableau III), ce qui confirme les différences de comportement observées ci-dessus.

Les diagrammes d'impédance montrent des différences entre les aciers après vieillissement, pour l'acier 316 L + Se, les caractéristiques du film semblent s'améliorer avec le temps d'immersion (fig. 8 et 9).

IV.2 - Analyses de surface

. Nous avons constaté que les éléments O, Cl, S, P, N, H, et C restent en surface et que l'épaisseur de la couche ainsi que la profondeur de pénétration du chlore, témoin d'une plus forte corrosion, sont plus grandes pour les aciers 316 L + Cu et 316 L + As que pour les aciers 316 L et 316 L + Se (fig.14). Ces résultats corroborent les observations effectuées grâce à l'étude de l'évolution dans le temps des potentiels et à celle de la résistance de polarisation (fig. 1 et tableau IV), à savoir que la passivité des alliages 316 au cuivre et à l'arsenic est moins bonne que celle des alliages de référence et au sélénium.

IV.3 - Etude de la corrosion microbiologique

Les résultats obtenus par des mesures de la résistance de polarisation à l'aide d'une technique potentiostatique (Tableau IV) et par la détermination de la résistance de transfert à l'aide des diagrammes d'impédance (fig. 10 et 11) permettent de constater des évolutions tout à fait similaires.

C'est ainsi que, en comparant les résistances des aciers 316 L et 316 L + As, on met en évidence l'influence de la présence d'arsenic :

- En l'absence de bactéries, cet élément diminue la tenue à la corrosion de l'acier.

- En présence des bactéries, on constate une notable amélioration.

Les observations effectuées au microscope électronique à balayage (fig. 12 et 13) montrent que l'acier sans arsenic, dans un milieu contenant des bactéries, est plus attaqué que la nuance non modifiée. L'arsenic contribue donc d'une manière favorable à la protection de l'acier lorsque la corrosion bactérienne intervient.

V - CONCLUSION

Cette étude a permis de caractériser par observation microscopique, par des méthodes électrochimiques et par des analyses de surfaces une nuance d'acier contenant ou non des éléments poisons, le milieu considéré étant dans notre cas du type ASTM.

Nous avons pu montrer que l'addition d'éléments poison à l'acier 316 L modifie son comportement électrochimique. Le sélénium modifie les caractéristiques électrochimiques dans un sens correspondant à une augmentation de la tenue à la corrosion, tandis que le cuivre et l'arsenic tendent à la diminuer. Il apparaît de plus que la présence d'arsenic dans l'alliage modifie le comportement des colonies bactériennes dans le milieu et sur l'acier lui-même.

Nous poursuivons actuellement ce travail avec pour objectif une meilleure connaissance du rôle des éléments ajoutés vis-à-vis de la corrosion microbiologique.

REMERCIEMENTS

Nous remercions M. NAVA, Mme VELUT et M. BARBOTIN du Département de Génie biologique de l'Université de Technologie de Compiègne pour leur collaboration lors de la mise en oeuvre des essais microbiologiques.

REFERENCES

1. G.H Booth, A.K. Tiller, Trans. Faraday Soc. Vol.56, p 1689 (1960)
2. G.H. Booth, A.K. Tiller, Trans. Faraday Soc. Vol.58, p 110 (1962)
3. G.H. Booth, A.K. Tiller, Trans. Faraday Soc. Vol.58, p 2510 (1962)
4. G.H. Booth, A.W. Cooper, A.K. Tiller, J. Appl. Chem. Vol.13, p 211 (1963).
5. G.H. Booth, A.W. Cooper, A.K. Tiller, J. Appl. Chem. Vol.15, p 250 (1965).
6. G.H. Booth, M. Cooper, D.S. Wakereley, Brit. Corr. J. Vol.1, p 345 (1966)
7. G.H. Booth, L. Elford, D.S. Wakereley, Brit. Corr. J. Vol.3, p 242 (1968)
8. G.H. Booth, A.K. Tiller, Corr. Sci. Vol.8, p 583 (1968)
9. R.A. King, J.D.A Miller, D.S. Wakereley, Brit. Corr. J. Vol.8, p 89 (1973)
10. R.A. King, D.A. Miller, J.S. Smith, Brit. Corr. J. Vol.8, p 137 (1973)
11. C.O. Obuekwe, D.W.E. Westlakie, J.A. Plambeck, F.D. Cook, Corrosion, Vol.37, p 461 (1981)
12. J.A. Hardy, Brit. Corr. J., Vol.4, p 190 (1983)
13. J.A. Hardy, J.L. Bown, Corrosion, Vol.40, p 650 (1984)
14. R.A. King, B.S. Skerry, D.C.A. Moore, J.F.D. Stott, Biologically Induced Corrosion, June 1985, Maryland, USA, pp 83-89 NACE
15. H.A. Videla. Biologically Induced Corrosion. Maryland, USA, pp 190-193,NACE.
16. J.W. Oldfield, W.H. Sutton, Brit. Corr. J. Vol. 15, p 31 (1980)
17. R.C. Salvarezza, H.A. Videla, Corrosion, Vol. 36, p 550 (1980)
18. A.K. Tiller, Microbial Corrosion, NPL Teddington England, March 1983, pp 104-107, Metals Society.
19. G. Kobrin, Biologically Induced Corrosion, June 1985, Maryland USA, pp 33-46, NACE
20. Silva, Tania, Silva, Silva, Biologically Induced Corrosion, June 1985, Maryland, USA, pp 76-82, NACE
21. Charles, Pugeault, Soulignal, Catelin, Eurocorr'87, Karlsruhe, RFA, pp 601-606 Dechema Ed. Frankfurt/Main (1987)
22. Holthe, Gartland, Bardal, Eurocorr'87, Karlsruhe, RFA, pp 617-623, Dechema Ed. Frankfurt/Main (1987)
23. P.F. Sanders, S. Maxwell, Microbial Corrosion, NPL Teddington England, March 1983, pp 74-83, Metals Society
24. W.A Hamilton, Ann. Rev. Microbiol. Vol. 39, p 195 (1985)
25. J.W. Costerton, G. Geesey, Biologically Induced Corrosion, June 1985, Maryland, USA, pp 223-232. NACE
26. D.J. Duquette, R.E. Ricker, Biologically Induced Corrosion, June 1985 Maryland, USA. pp 121-130, NACE
27. Alanis, Berardo, Cristofaro, Valentini, Biologically Induced Corrosion, June 1985, Maryland, USA. pp 102-108, NACE
28. S. Daumas, J. Crousier, J.P. Crousier. Métaux Corrosion Industrie, Vol.1, p 1 (1988)
29. Desulfovibrio desulfuricans Culture Media # 42 ATCC.

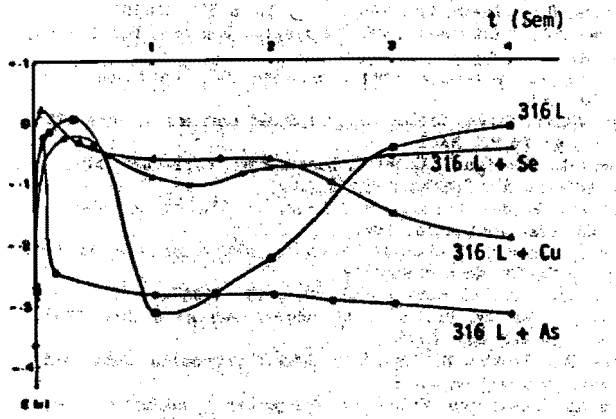

Fig 1 :

Evolution dans le temps des potentiels d'abandon.

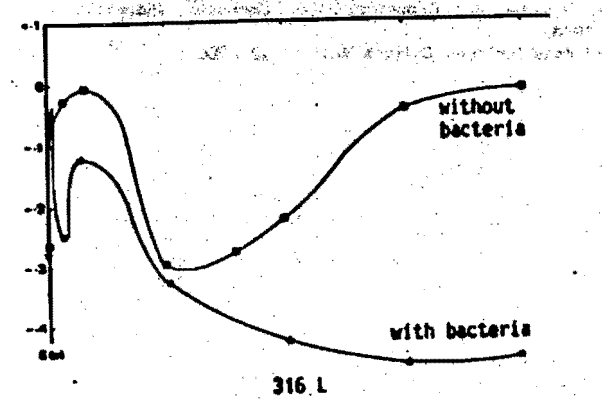

Fig 2 :

Influence des bactéries sur les potentiels d'abandon du 316 L

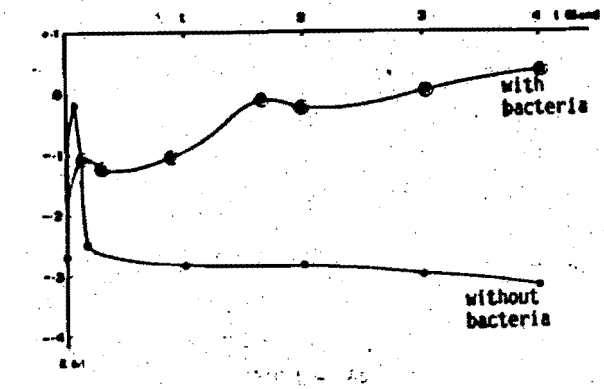

Fig 3 :

Influence des bactéries sur les potentiels d'abandon du 316 L + A_s

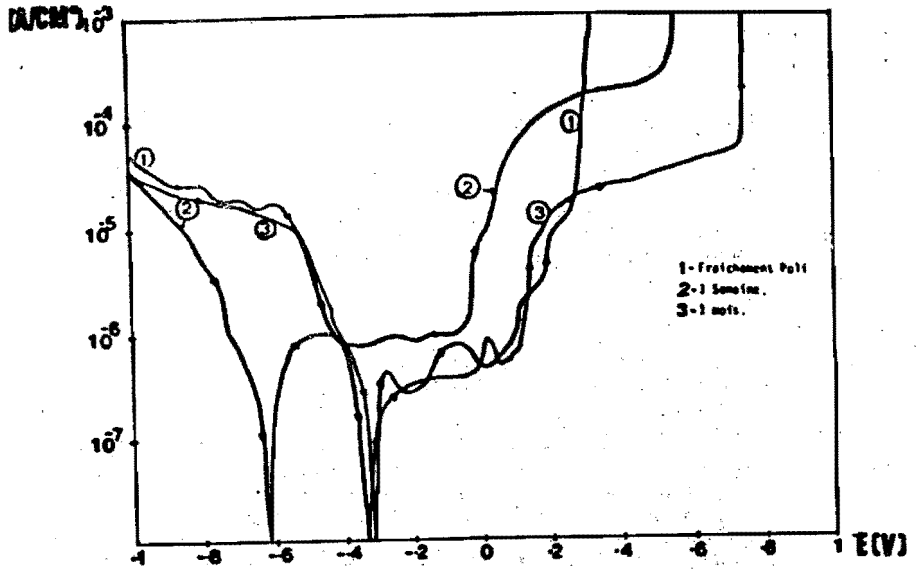

Fig 4 : Courbes de polarisation de l'acier 316 L

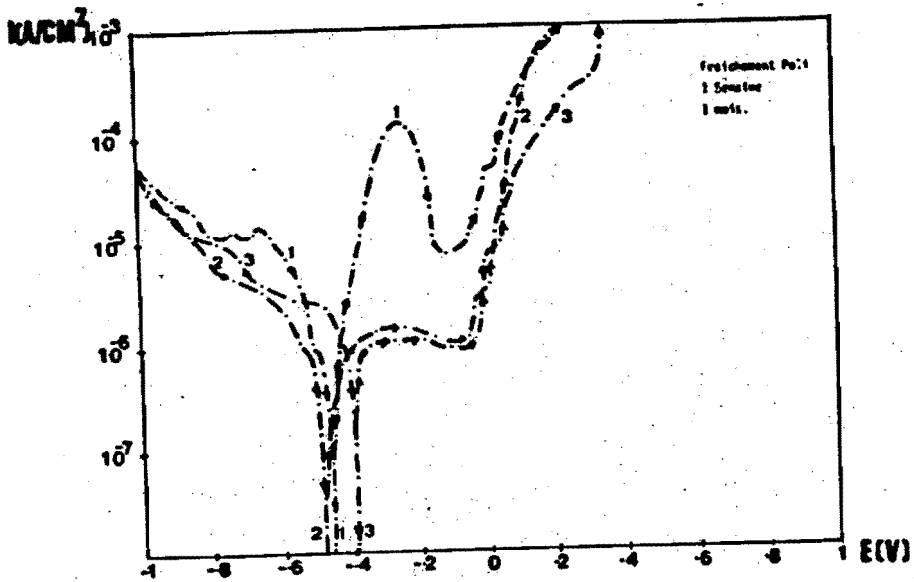

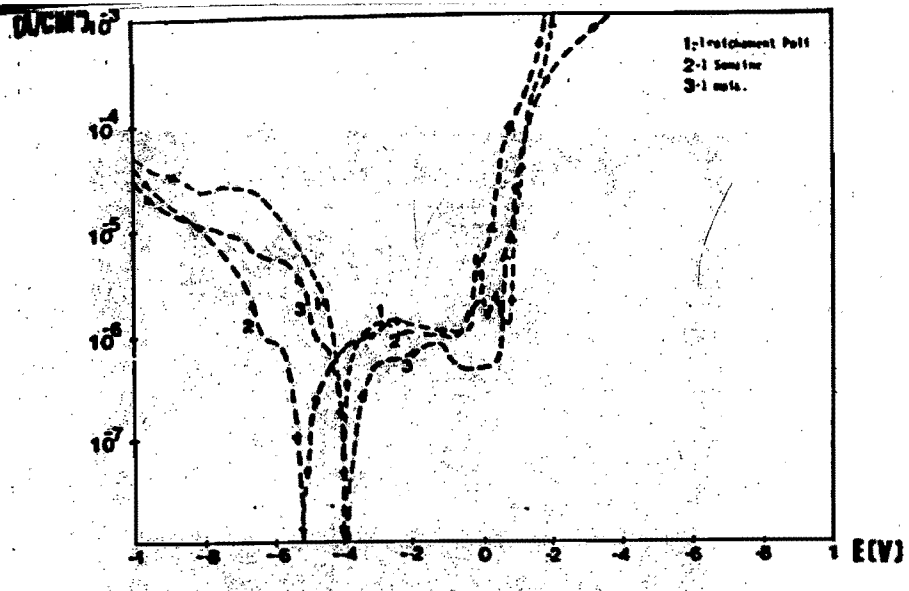

Fig 6 : Courbes de polarisation de l'acier 316 L + S_6

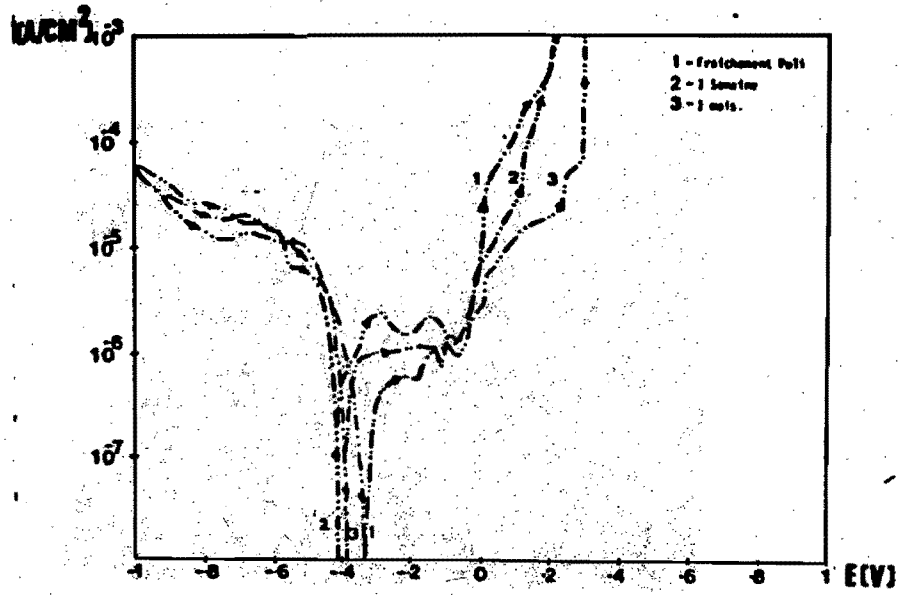

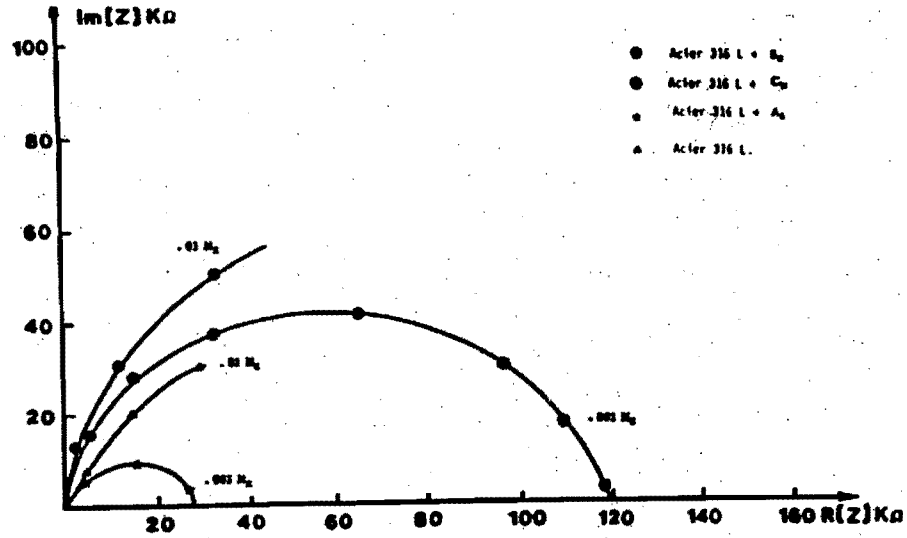

Fig 8 : Diagrammes d'impédance des aciers maintenus 1 semaine en milieu marin synthétique.

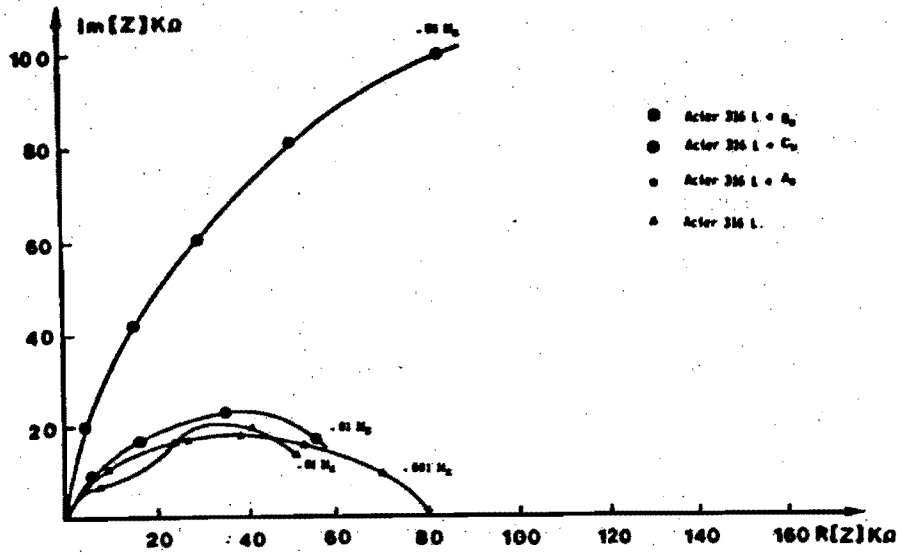

Fig 9 : Diagrammes d'impédance aprés 1 mois de maintien.

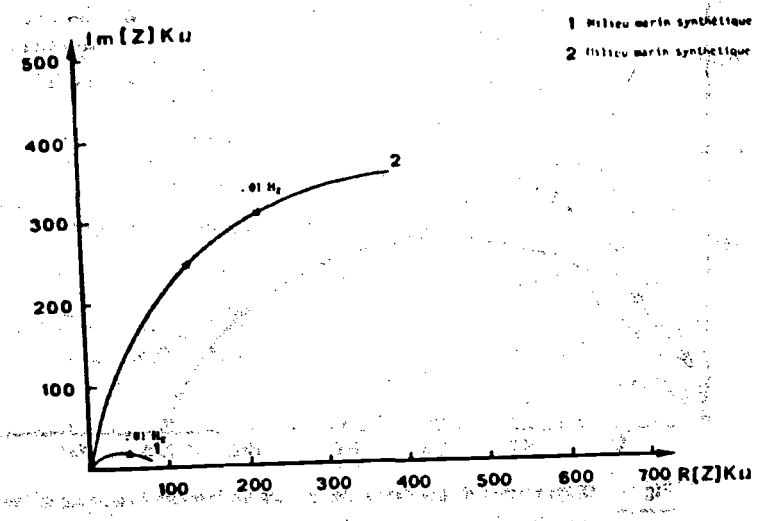

Fig 10 : Influence des bactéries sur l'impédance : Acier 316 L

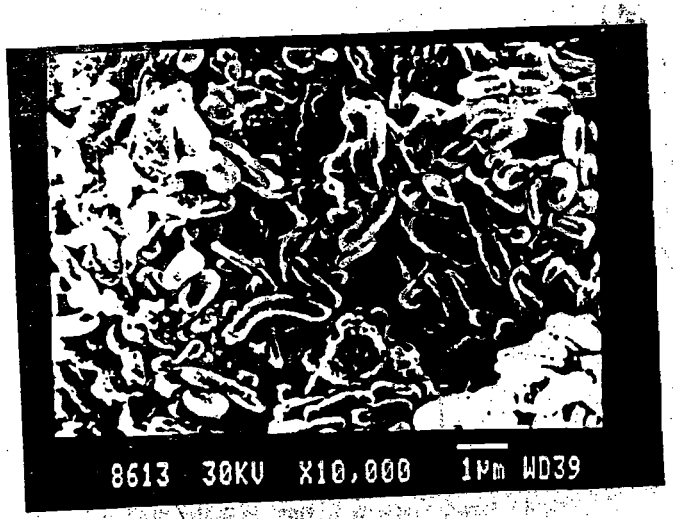

Fig 12 : Observation des bactéries prélevées dans l'electrolyte de l'acier 316 L

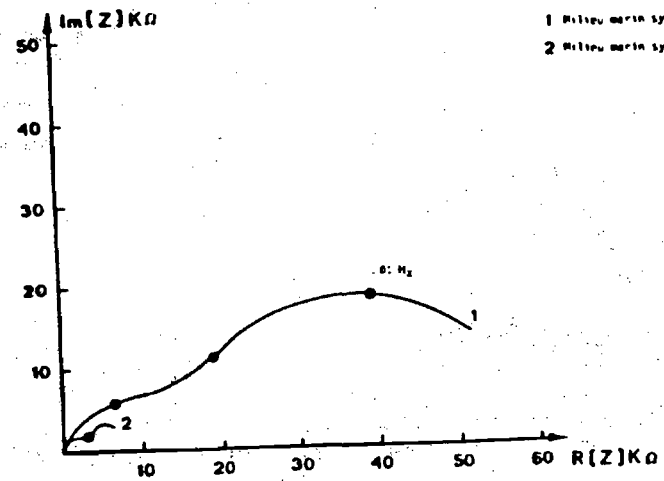

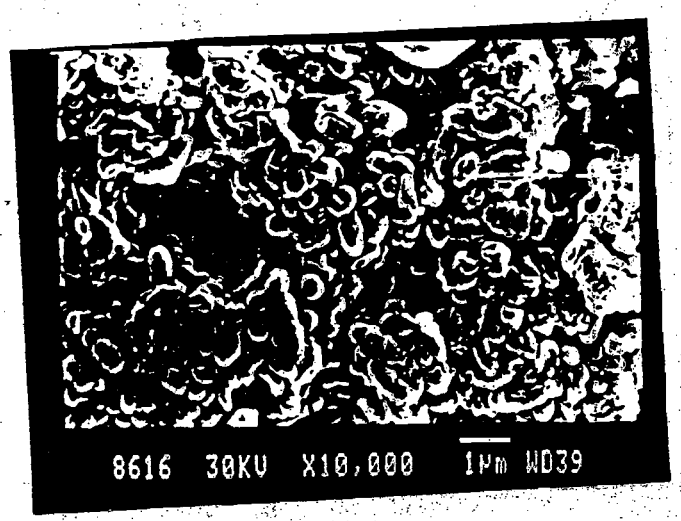

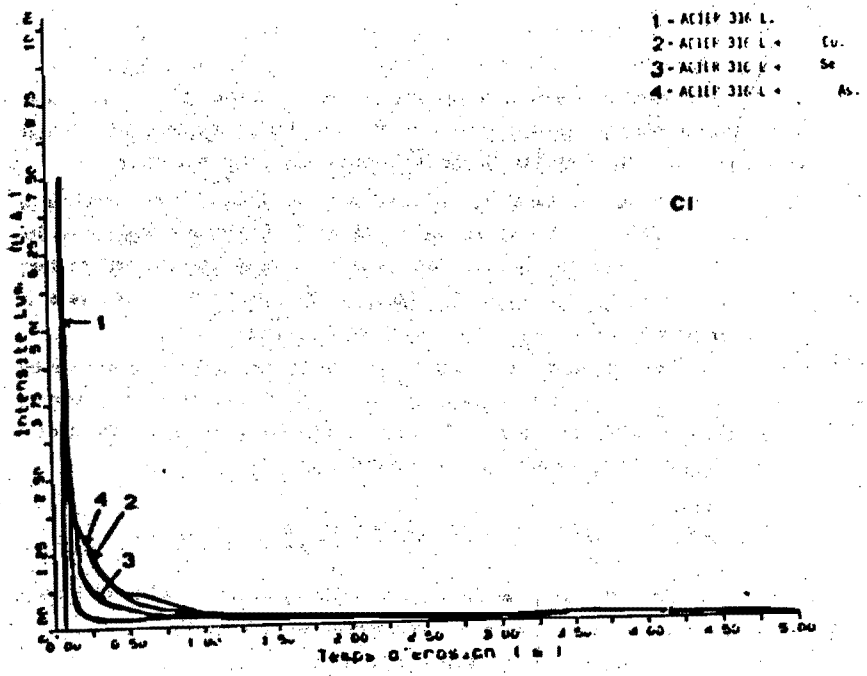

Fig 14 : Analyse SDL : pénétration du chlore dans les échantillons

ANTIFOULING PAINTS OF HIGH SEA WATER DISSOLUTION RATE

Beatriz del Amo, Carlos A. Giúdice and Gustavo Villoria

CIDEPINT - Research and Development Centre for Paint Technology
(CIC-CONICET) - Calle 52 entre 121 y 122 (1900) La Plata, Argentina

ABSTRACT.- The objective of this paper was to establish the perfomance of antifouling paints formulated with binders based on WW rosin plasticized with phenolic varnish, coal tar/tung oil (1/1 ratio, w/w) or oleic acid. Red cuprous oxide was used as toxicant in two levels.

The results obtained in laboratory tests and in raft trials (36 months) have shown that each plasticizer led to antifouling paints of different biocidal characteristics. Besides, the residual dry film thickness, the profile of copper in the film and the cuprous oxide leaching rate were in accordance with samples bioactivity.

INTRODUCTION

In soluble matrix antifouling paints, physical and chemical characteristics both of the film forming resin and of the plasticizer are factors of fundamental importance in relation with paints service behaviour; the plasticizer or co-binder has a significant influence on the binder dissolution rate and then on the toxicant release from antifouling film [1,2].

The paints based on binders of high dissolution rate and applied with 60-80 µm dry film thickness show generally a satisfactory efficiency for 12 months sea water immersion periods, but after this time an important fixation of organisms is registered fundamentally in those zones where very strong hydrodinamic flow conditions lead to a film fast exhaustion. As a consequence, paints applied with higher dry film thicknesses (120-150 µm) could have longer useful life.

In soluble matrix antifouling paints, the toxicant and the binder are simultaneously dissolved. In this form, particles of the biocidal material that were initially located inside the film make contact with sea water.

The rate at which the toxicant is released (one aspect that has a direct influence upon the efficiency of the antifouling paint) depends on its content in the film and also on binder dissolution rate. The toxicant content can be varied between very wide limits if the binder dissolution rate is adequately selected, so as to avoid fouling settlement [3,4].

The main objective of this research was to determine on experimental raft the bioactivity of antifouling paints based on soluble binders and also to correlate the above behaviour both with film dissolution rate and with toxicant leaching rate during sea water immersion test.

SAMPLES COMPOSITION AND MANUFACTURE

Experimental formulations are shown in Table I. Different binders of high dissolution rate in sea water were formulated [1].

The following variables were studied:

Component	Function	Level (%, w/w)
Red cuprous oxide	Toxicant	31.3 and 35.4
WW rosin/plasticizer	Binder	30.4
Phenolic varnish	Plasticizer	7.6
Coal tar/tung oil, 1/1 ratio	Plasticizer	5.1
Oleic acid	Plasticizer	7.6
Hydrogenated ricinic acid	Rheological additive	1.3

The characteristics of the different components were indicated in previous papers [2,5].

Samples manufacture was achieved on a laboratory scale by using a 3.3 liter jar ball mill. Operating conditions of the ball mill were specially considered for obtaining an efficient dispersion (adequate pigment particle size distribution) and for reducing the reaction between pigments and binder acidic components [6].

Paints were prepared by incorporating calcium carbonate and zinc

oxide in the vehicle. These pigments were dispersed for 24 hours and then cuprous oxide was added to the jar and dispersed for three hours.

The rheological additive employed was castor oil which was incorporated as a gel (15 % w/w) at the end of pigments dispersion; for this operation a high speed impeller working at 40-45°C temperature was used.

The above mentioned gel was previously manufactured by dissolving this substance in xylene using a high speed impeller at 40-45°C and by stirring until a stable colloidal structure was reached [7,8].

Every paint was splited up in small samples for permiting the incorporation of different organic tints. Each of them was used to apply a coat on experimental panels for allowing the qualitative evaluation of film thickness decrease during the immersion test.

LABORATORY TESTS

Adhesion and abrasion resistance

SAE 1010 steel plates were used for the tests, previously sanded to A Sa 2½ (SIS Specification 05 59 00/67), with 40 µm maximum roughness (Rm). The thickness of the plates was 1.8 mm.

Before painting the antifouling samples, the panels were protected with an anticorrosive paint of proved efficiency (30 µm dry film thickness). After 24 hours drying, antifouling paints were applied by brush, forming a 25-30 µm dry film thickness; mechanical tests were performed 24 hours after the application of the antifouling coat.

Both application of paints and laboratory tests were carried out under controlled conditions (20 ± 2°C temperature and 70 ± 5 % relative humidity).

The adhesion of coating film was evaluated by applying and removing pressure sensitive type over cuts made in the film (ASTM D 3359-78) and also by determining tensile strength (Elcometer model 106). On the other hand, abrasion resistance was evaluated with Taber Abraser (ASTM D 1044-78, 500 turns, 500 g load and abrasive CS 10).

Copper leaching rate

For this test sanded glass panels were painted with experimental samples and after 24 hours drying they were immersed in artificial sea water (ASTM D 1141-75).

The concentration of copper dissolved did not exceed in any case the 0.5 ppm value; in this way the dissolution rate was not affected.

Both initial and final concentration of copper in artificial sea water was assessed by colorimetry using sodium diethyldithiocarbamate method; it permits to determine 1 part of copper in a hundred million parts for concentration between 0.1 and 1.0 ppm [9,10].

Total copper content at different film depths

The changes of total copper content in the paint film during immersion in natural sea water were evaluated for different layers, that is at different depths. For this purpose, the film was uniformly abraded with the above Taber Abraser; different loads and abrasives were employed for obtaining the selected depths.

Both initial and remaining dry film thicknesses for different times of test were measured by using Foucault currents.

Copper content at different film depths was assessed by using the above sodium diethyldithiocarbamate method. In this case, sample was prepared by electrodepositing the copper, dissolving the copper from the electrode with nitric acid and selecting a suitable aliquot for examination.

SERVICE TRIALS

Immersion in natural sea water (raft)

In order to establish the toxic behaviour of the paints in the natural environment (sea water), a 36 months immersion test was carried out on a raft anchored at Puerto Belgrano (38°54' S; 62°06' W), an area whose hydrological and biological conditions were previously studied [11,12,13].

SAE 1010 steel plates (20 x 30 x 0.3 cm), with the same surface

treatment as that mentioned in the laboratory test, were selected for these trials. Panels were protected with an efficient anticorrosive paint (150-180 µm dry film thickness) and finally with the experimental antifouling paint; toxic dry film thicknesses of 75 ± 10 µm and 150 ± 10 µm (two and four coats, respectivily) were reached. Each coat was characterized by one different colour.

In all cases, paints were brush applied with an interval of 24 hours between coats. Drying time of the last coat prior to immersion was 48 hours. The test panels were placed vertically on the frames of the raft, at about 0.30-0.60 m under water surface.

In order to establish the bioactivity of the toxic samples, observations were made after 7, 13, 19, 24 and 36 months immersion. Photographic controls were performed in order to compare fixation with pattern records and to adjust the different values at the end of the tests.

RESULTS

Adhesion and abrasion resistance

All the paint samples showed satisfactory values of adhesion (from 5 to 8 for cutting edge blade test and from 5 to 8 $kg.cm^{-2}$ for tensile strength method) and of abrasion resistance (maximum 261.3 mg; minimum 165.4 mg). The anticorrosive paint employed had an adhesion of 14 $kg.cm^{-2}$ to the metallic substrate.

Copper leaching rate

The results of the tests made in laboratory to determine the total copper released from the paint films studied are indicated in Table II. This table displays that cuprous oxide content and the binder type and composition influenced significantly on leaching rate.

With regard to the antifouling paint thickness, this variable plays an important role only in those samples with binders of very high dissolution rate (paints 3, 4, 5 and 6). The excesive erosion of the paint films elaborated fundamentally with oleic acid, which was observed during immersion test (Table III), is the basis of the different copper leaching rate reached with two dry films thickness considered.

Copper distribution in the remaining film

The antifouling paints tested showed during immersion a significant difference in the total copper distribution (cuprous oxide, cupric oxide, metallic copper and copper complexes) as a function of film depth. Besides, a different decrease of dry film thickness was observed according to the binder type used in the paint formulation.

For instance, in the experiences carried out with 150 ± 10 µm dry film thickness, paint 2 (with phenolic varnish as plasticizer) displayed a profile of total copper content which indicates a higher film exhaustion than samples 4 and 6 (with coal tar/tung oil mixture and oleic acid, respectively), Fig. 1, 2 and 3; the above mentioned is related to the lesser decrease of dry film thickness observed in paint 2 (Tabla III).

Analogous conclusions were obtained when results corresponding to the tests made with the above samples but applied with 75 ± 10 µm dry film thickness were considered and also when values of paint 1 were compared with those of samples 3 and 5 (smaller cuprous oxide content) for both dry film thicknesses studied.

Paint bioactivity on experimental raft

The results obtained are mentioned in Table IV. The efficiency of antifouling protection was evaluated by the use of a fixation scale which ranges from 0 (surface without fouling) to 5 (completely fouled). Intermediate values of 0-1 (very rare), 1 (rare), 2 (common), 3 (very common) and 4 (abundant) were also considered. Value 1 was established as the limit of acceptance for an antifouling composition (80 % effectiveness); paints that showed protection values of 0 or 0-1 (100 and 90 % effectiveness) were considered as products of very good bioactivity.

As all antifouling paints films showed satisfactory properties in mechanical tests carried out at laboratory, different behaviour on raft allowed to conclude that both formulation variables (toxicant content and binder type) and dry film thickness (mainly for samples 3, 4, 5 and 6) influenced significantly on paint bioactivity.

Paints elaborated with phenolic varnish as plasticizer (paints 1 and

2), for two dry film thicknesses considered (75 and 150 μm), fulfilled the test requirement only for 13 months immersion (0 or 0-1 settlement values). After that period, an important fixation of fouling was registered (between 2-3 and 5 according to the immersion time considered).

Samples formulated with coal tar/tung oil mixture as plasticizer, for the two film thicknesses studied, had a good bioactivity for 24 months (0-1 or 1); only those applied with 150 μm thickness showed satisfactory efficiency during 36 months immersion (0-1 or 1).

As regards paints with oleic acid in their composition, the behaviour also depended significantly on the dry film thickness applied. These paints had a thickness decrease greater than the other samples, which led to an excessive an rapid exhaustion when they were tested with low thickness (fixation 2 or 2-3 for 19 months immersion). When the same products were applied with 150 μm dry film thickness, satisfactory antifouling characteristics were observed for 24 months (fixation 0-1 or 1); final observation (36 months) indicated an important fixation upon the above painted panels.

CONCLUSIONS

1. For long immersion periods on experimental raft, the plasticizer influenced on biocidal power of soluble matrix antifouling paints studied.

2. Both cuprous oxide contents considered led to products with different leaching rate; on this aspect it is important to point out that some paints showed an efficient bioactivity with a cuprous oxide leaching rate lesser than 10 $\mu g\ cm^{-2}\ day^{-1}$, corroborating the conclusions reached for other authors [3,4].

3. When antifouling paints based on binders of high dissolution rate are employed, the dry film thickness is a very important variable for a long immersion period.

4. Residual film thickness during sea water immersion, profile of total copper in the film and also cuprous oxide leaching rate displayed a great agreement with the bioactivity on experimental raft.

ACKNOWLEDGMENTS

The authors are grateful to CIC (Comisión de Investigaciones Científicas de la Provincia de Buenos Aires), to CONICET (Consejo nacional de Investigaciones Científicas y Técnicas) and to SENID (Servicio Naval de Investigación y Desarrollo) for their sponsorship for this research.

REFERENCES

[1] Giúdice, C.A., del Amo, B., Rascio, V.- Proc. 9th International Congress on Metallic Corrosion, Toronto, Canada, 2, 510 (1984).

[2] del Amo, B., Giúdice, C.A., Rascio, V.- J. Coat. Techn., 56 (719), 63 (1984).

[3] De la Court, F.H.- J. Oil Col. Chem. Assoc., 69 (9), 247 (1986).

[4] Partington, A.- Paint Technology, 28 (3), 24 (1964).

[5] Giúdice, C.A., del Amo, B., Rascio, V.- Proc. 6th International Congress on Marine Corrosion and Fouling, Athens, Greece, Vol. II, Marine Biology, 293 (1984).

[6] Giúdice, C.A., Benítez, J.C., Rascio, V., Presta, M.- J. Oil Col. Chem. Assoc., 63 (4), 153 (1980).

[7] Anon.- Pitture e Vernice, 56 (4), 13 (1980).

[8] Papo, A., Torriano, G.- J. Oil Col. Chem. Assoc., 63 (1), 10 (1980).

[9] Partington, A., Dunn, P.F.- J. Oil Col. Chem. Assoc., 44 (12), 869 (1961).

[10] Snell, F.D., Snell, C.- Colorimetric methods of Analysis. D. van Nostrand Co. Inc., 3rd. ed., Vol. 1, N.Y., U.S.A. (1936).

[11] Bastida, R., Spivak, E., l'Hoste, S.G., Adabbo, H.E.- Corrosión y Protección, 8 (8-9), 11 (1977).

[12] Bastida, R., l'Hoste, S.G., Spivak, E., Adabbo, H.E.- Corrosión y Protección, 8 (8-9), 33 (1977).

[13] Bastida, R., Lichstchein, V.- Corrosión y Protección, 10 (3), 7 (1979).

TABLE I

Composition of experimental paints*, % w/w

Paint	1	2	3	4	5	6
Red cuprous oxide	31.3	35.4	31.3	35.4	31.3	35.4
Zinc oxide	3.1	3.5	3.1	3.5	3.1	3.5
Natural calcium carbonate	33.9	29.4	33.9	29.4	33.9	29.4
WW rosin (gum rosin)	22.8	22.8	25.3	25.3	22.8	22.8
Phenolic varnish	7.6	7.6	--	--	--	--
Coal tar/tung oil, 1/1 ratio in weight	--	--	5.1	5.1	--	--
Oleic acid	--	--	--	--	7.6	7.6
Castor oil	1.3	1.3	1.3	1.3	1.3	1.3

(*) Solvent mixture was toluene/white spirit 1/1 ratio in weight.

TABLE II

Total copper released from film of antifouling paints, $\mu g.cm^{-2}.day^{-1}$

Paint	1	2	3	4	5	6
Film thickness: 75 ± 10 µm						
Immersion time:						
13 months	8.1	9.3	9.6	11.3	11.8	12.1
24 months	4.8	5.8	7.5	8.2	4.5	5.0
36 months	2.9	4.0	3.0	3.3	0.0	0.0
Film thickness: 150 ± 10 µm						
Immersion time:						
13 months	8.3	9.6	9.8	11.8	12.0	13.8
24 months	5.3	5.8	7.8	8.6	8.8	10.8
36 months	3.3	4.5	6.0	6.8	2.6	3.0

TABLE III

Remaining antifouling film thickness in the immersion test*

Paint	1	2	3	4	5	6
Initial film thickness: 75 ± 10 µm	78	74	79	82	73	72
Immersion time:						
7 months	63	62	56	52	45	47
13 months	53	47	50	47	20	13
19 months	40	33	28	27	0	0
24 months	32	30	19	13	0	0
36 months	14	11	0	0	0	0
Initial film thickness: 150 ± 10 µm:	152	157	148	152	147	157
Immersion time:						
7 months	135	139	127	123	116	121
13 months	123	127	119	120	91	93
19 months	118	115	97	95	71	70
24 months	112	110	90	88	58	61
36 months	91	88	65	56	23	26

* The results are the average of ten determinations made in prearranged film place.

TABLE IV

Fouling settlement in immersion test*

Paint	1	2	3	4	5	6
Dry film thickness: 75 ± 10 µm						
Immersion time:						
7 months	0	0	0	0	0	0
13 months	0-1	0	0	0	0-1	0
19 months	3-4	2	0	0-1	2-3	2
24 months	5	2-3	1	1	3-4	3
36 months	5	5	3-4	3	5	5
Dry film thickness: 150 ± 10 µm						
Immersion time:						
7 months	0	0	0	0	0	0
13 months	0-1	0	0	0	0	0
19 months	2-3	1-2	0-1	0	0	0
24 months	4-5	2-3	0-1	0	0-1	0
36 months	5	5	1	0-1	3-4	3

* Key of Table: 0, without fouling (100 % efficiency); 0-1 very rare (90 %); 1, rare (80 %); 2, common (60 %); 3, very common (40 %); 4, abundant (20 %); 5, panel completely fouled (0 %).

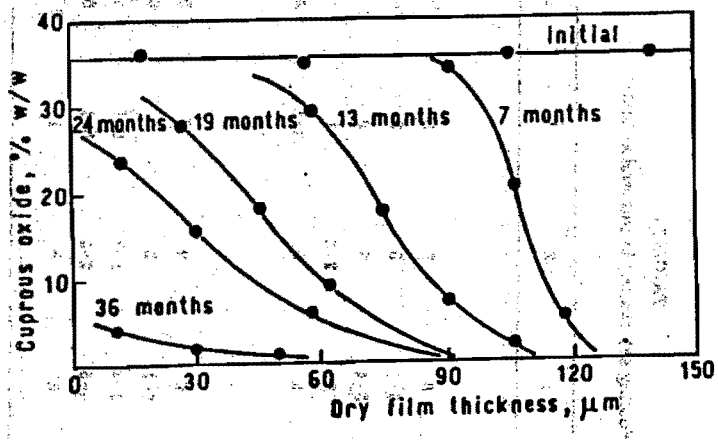

Figure 1

Change of total copper content in the dry film (150 ± 10 µm thickness), expressed as cuprous oxide; sample elaborated with phenolic varnish as plasticizer and with the highest toxicant content.

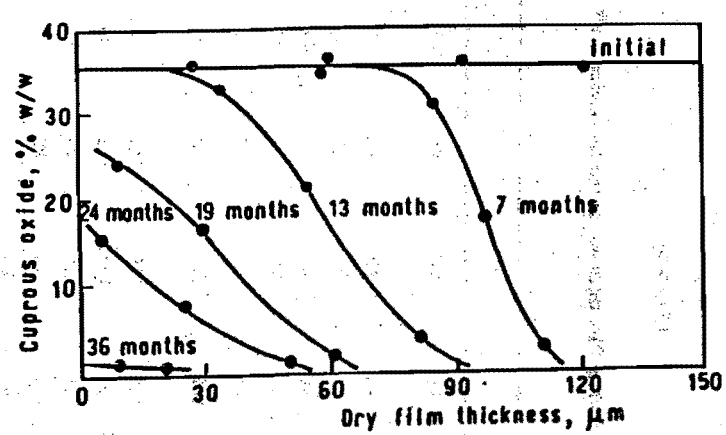

Figure 2

Change of total copper content in the dry film (150 ± 10 µm thickness), expressed as cuprous oxide; sample elaborated with coal tar/tung oil mixture as plasticizer and with the highest toxicant content.

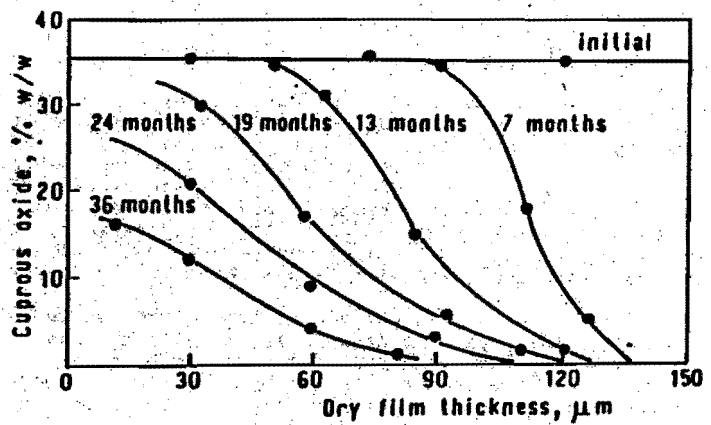

Figure 3

Change of total copper in the dry film (150 ± 10 µm thickness), expressed as cuprous oxide; sample elaborated with oleic acid as plasticizer and with highest toxicant content.

MODIFIED ORGANOTIN ANTIFOULANTS

C. A. Dooley* , J. P. Testa, Jr.** and P. Kenis*

*Naval Ocean Systems Center, **Computer Sciences Corporation

ABSTRACT

Tributenyltin bromides containing double bonds at C-1, C-2 or C-3 were synthesized. The reactivity and toxicity results indicate that the compounds with double bonds might serve as suitable and perhaps more environmentally compatible antifoulants. They exhibit degradation rates greater than and are somewhat less toxic than the tributyltin compounds currently in use.

INTRODUCTION

The use of tributyltin compounds as antifoulants for ships' hulls has become of increasing concern because of their persistence in the water column and sediments and because of the potential for bioaccumulation. It is known from literature that when ethyl and propyl groups are replaced by vinyl and allyl groups in tetraorganotins, the resulting compounds show enhanced chemical reactivity (1,2,3). In an attempt to create more reactive compounds, we synthesized organotin compounds in which butyl groups were replaced with butenyl groups. Such compounds, used as antifoulants, might be expected to degrade more quickly in the environment while retaining sufficient toxicity to target organisms.

EXPERIMENTAL

Chemicals

1-bromo-1-butene, 4-bromo-1-butene and 2-chloro-1-butene were obtained from Pfaltz & Bauer (Waterbury, CT). Resublimed magnesium chips, tetrabutyltin and tributyltin bromide were obtained from Alfa Products (Danvers, MA). All were used without further purification. Hexylmagnesium bromide (2.0M) in diethylether was obtained from Aldrich Chemical Company (Milwaukee, WI) and was used to derivatize alkenyltin halides to improve their chromatographic behavior.

Instrumentation

Retention times and mass spectra of synthesized and purchased compounds were obtained with a Hewlett-Packard Model

5890A Gas Chromatograph directly connected to a Hewlett-Packard Model 5970 Mass Selective Detector (GC/MS). Data collection and reduction was performed with a Hewlett-Packard 9000-300 Computer using Model 59970C ChemStation software. Samples were run using splitless injection onto a 12.5 m by 0.2 mm I.D. HP-1 fused silica capillary column with 0.33 um coating thickness. Helium carrier gas was used at a head pressure of 40 kPa. The oven was programmed, after an initial 2 minute hold at 50°C, to 230°C at 30 °C/min. Injector, transfer line and detector were at 250°C. Masses were scanned between 50 and 450 amu.

IR spectra were obtained of the neat compounds in AgCl cells using a Perkin-Elmer Model 1420 Ratio Recording Infrared Spectrometer.

Synthesis of Compounds

Tetra-1-butenyltin, tetra-2-butenyltin and tetra-3-butenyltin were prepared via the Grignard reaction (4,5,6,7,8). The appropriate Grignard reagent was prepared from approximately 10 g of 1-bromo-1-butene, 2-chloro-1-butene or 4-bromo-1-butene in 10 ml anhydrous tetrahydrofuran and an excess of magnesium chips. The Grignard reagent was decanted from the excess magnesium chips, then cooled to 0°C. Approximately 2 grams of anhydrous $SnCl_4$ in 10 ml of hexane was added dropwise to the stirred solution. The mixture was refluxed for four hours.

The reaction mixture was cooled to 0°C and hydrolyzed with 3% HCl. The separated organic layer was shaken with 5% aqueous KF to precipitate organotin chlorides or bromides as insoluble fluorides. The solvent and low boiling side products were then removed under vacuum at room temperature from the separated organic layer, and the residue was washed through a 22 x 1 cm Florisil column with hexane. The solvent was again removed under vacuum.

Approximately 1 g of the tetraalkenyltin was suspended in 10 ml methanol. A stoichiometric amount of bromine in methanol was added dropwise in dim light to the stirred tetrabutenyltin mixture. Monobromination of the tetraalkenyltin to form tri-1-butenyltin bromide, tri-2-butenyltin bromide and tri-3-butenyltin bromide was achieved by conducting the reaction at 0°C, -50°C and 20°C, respectively (9,10,11). Upon completion of the reaction, the solvent and low boiling side products were removed under vacuum at room temperature. The crude product was washed through a Florisil column first with hexane to recover unreacted tetraalkenyltin and then with 1:4 (v/v) ethyl acetate/hexane to selectively elute the trialkenyltin bromide. Solvent was then removed under vacuum.

Degradation Experiments

Ethanol solutions of the organotin bromides were prepared at ~1mg/ml. Aliquots of the ethanol solutions were added to filtered seawater to obtain approximately 1-5 ppm concentrations in the seawater. Solutions were either placed in 125 ml quartz tubes and exposed to sunlight over 48 hours or kept in closed 500 ml polycarbonate jars in the laboratory. 10 ml aliquots of the solutions were extracted at timed intervals with 1 ml hexane after acidification with 0.1 ml conc. HCl. Samples were analyzed directly and after derivatization with hexylmagnesium bromide by GC/MS using tetra-n-propyltin as an internal standard in the hexane extractant.

Toxicity Testing

Relative toxicity of compounds was determined using the Microtox® Toxicity Analyzer Model 2055, manufactured by Microbics Corporation, Carlsbad, CA (12,13,14). This bioassay measures the relative reduction in light output by a luminescent bacterium, Photobacterium phosphoreum NRRL B-11177 when exposed to a toxicant. The bacteria are provided in a convenient freeze-dried form by Microbics Corporation and are immediately activated by the addition of 1 ml distilled water.

For Microtox® testing, stock solutions of the compounds were prepared in 95% ethanol at ~1-2 mg/ml. Appropriate amounts of the ethanol solutions were added to 2% aqueous NaCl to achieve a workable concentration while keeping the ethanol concentration as low as possible (typically about 0.05%).

Serial dilutions of each compound for measurement are performed in the Microtox® photometer/incubator at 15 °C. Controls consist of triplicate 1 ml portions of 2% NaCl and candidate toxics are prepared in and subsequently serially diluted in 2% NaCl, with a final volume of 1 ml for each dilution. After a 5 minute period for temperature equilibration, 10 ul of rehydrated bacteria is added to each of the controls and the serial dilutions of the test compound. Measurements in the photometer are made at 5 and 15 minutes after addition of the reagent. This procedure is repeated at least four separate times for each compound to provide four independent toxicity values.

The toxicity value is expressed as an EC50 concentration, which is the concentration of a compound which caused a 50% reduction in light output. The EC50 concentrations were determined by graphic interpolation on log-log paper, plotting the gamma function against concentration. The gamma function is the ratio of the amount of light lost to the amount of light remaining. A gammma value of 1 corresponds to a 50% reduction in light, or EC50.

RESULTS AND DISCUSSION

Syntheses of the tetrabutenyltins presented no great difficulty as long as the Grignard reagent was present in large excess to assure complete alkylation. The tetrabutenyltins were all stable as neat compounds and in inert solvents. The tri-2-butenyltin bromide was so reactive with the synthesis side products that it could not be isolated. The tri-1-butenyltin bromide, and to a lesser extent, the tri-3-butenyltin bromide tended to polymerize during solvent evaporation of the crude mixture prior to column chromatography clean-up, especially if the distillation flask were warmed. Once purified, the tri-3-butenyltin and tri-1-butenyltin bromides were stable.

Progress of the reactions and purity of the products were monitored using GC/MS. Butenyltin halides were derivatized with hexylmagnesium bromide to form mixed tetraorganotin compounds. This step improved the chromatographic behavior of the halides and prevented further reaction in the crude mixtures. Where cis-trans isomers were present in the starting butenylhalides, a mixture of isomeric butenyltins were formed. These isomers could be separated by gas chromatography but not chemically.

Qualitatively the mass spectra of the tributenyltin bromides resemble that of tributyltin bromide in their fragmentation patterns. The mass spectrum of tributyltin bromide is shown in Figure 1. The mass spectra of the tributenyltin bromides are characterized by analogous clusters of tin-containing fragments with two less mass units (H atoms) per attached carbon chain than the tributyltin bromide. The differences in ion abundances that can be used to show that different compounds were indeed synthesized are summarized in Figure 2 where the major ion fragments for the triorganotin bromides are shown.

Infrared spectrometry was used to determine position of the double bond and to show that double bond position was retained after bromination of the compound and that addition of bromine across the double bond did not occur. These data are summarized in Table 1 as the vibration of C=C in alkenyltin compounds found in the literature and measured in our laboratory.

The tributenyltins exhibit considerable variation in stability and chemical reactivity. $(CH_3CH{=}CHCH_2)_3SnBr$, an allylic compound, was highly reactive and therefore transient; the compound readily underwent redistribution reactions with side products of the synthesis reactions, and so could not be isolated (16,17). The other two tributenyltin bromides were stable as neat compounds, in inert solvents and in ethanol for a reasonable length of time. Chemical reactivity appeared to follow the order allyl > vinyl > alkyl as found by other workers

(2,7,9). The $(CH_2=CHCH_2CH_2)_3SnBr$ fell between vinyl, $(CH_3CH_2CH=CH)_3SnBr$, and alkyl, $(CH_3CH_2CH_2CH_2)_3SnBr$.

In a more environmentally realistic experiment, the following results were obtained. Upon exposure to direct sunlight, seawater solutions of $(CH_3CH_2CH=CH)_3SnBr$ and $(CH_2=CHCH_2CH_2)_3SnBr$ in quartz tubes showed 80% and 100% loss of compound, respectively, after 48 hours; $(CH_3CH_2CH_2CH_2)_3SnBr$ showed a loss of only 15% over the same time period. Half-lives of 33 days, 17 days and 16 days were estimated for $(CH_3CH_2CH_2CH_2)_3SnBr$, $(CH_2=CHCH_2CH_2)_3SnBr$ and $(CH_3CH_2CH=CH)_3SnBr$ in seawater, protected from UV light and held at a constant room temperature.

Relative toxicities of the new compounds were determined by using the Microtox® Toxicity Analyzer (11). The toxicity value is expressed as an EC50, the concentration of a compound which causes a 50% reduction in light output. The results are shown in Table 2 as EC50's at 5 minutes and 15 minutes. A low EC50 indicates a more toxic compound. $(CH_3CH_2CH=CH)_3SnBr$ and $(CH_2=CHCH_2CH_2)_3SnBr$ were less toxic than $(CH_3CH_2CH_2CH_2)3SnBr$ by factors of ~3 and ~6, respectively.

SUMMARY

Tributenyltin bromides containing double bonds at C-1, C-2 or C-3 were synthesized from symmetrical tetrabutenyltins. The mass spectra of the tetra- and tri-butenyltins were obtained. Although all three tetrabutenyltin compounds were stable, only the tributenyltin bromides with double bonds at C-1 and C-3 were sufficiently stable for further studies. The tri-1-butenyltin bromide, in seawater was more stable in sunlight than the tri-3-butenyltin bromide, yet neither compound was as stable as tributyltin bromide. Stability in seawater, in the absence of UV light, was less for both the tri-1-butenyltin bromide and tri-3-butenyltin bromide than for tributyltin bromide. The relative toxicities of the tetrabutenyltins and the tributenyltins bromides were determined using a bioluminescent bacteria assay. The tetrabutenyltins exhibited greater toxicity than tetrabutyltin by up to a factor of 5. By contrast, the concentrations of tributenyltin bromides necessary to produce a toxic response were 3 to 6 times greater than for tributyltin bromide.

ACKNOWLEDGMENTS

This work was funded by the Office of Naval Research/Naval Ocean Systems Center under the Independent Research Program Element 61152N. The authors thank K. J. Meyers-Schulte for editorial advice.

REFERENCES

(1) Davies, A. G.; Smith, P. J. 1982 Comprehensive Organometallic Chemistry; Wilkinson, G.; Stone, F. G. A.; Abel, E. W., Ed.; Pergamon Press, New York, pp 519-627.

(2) Cochran, J. C.; Bayer, S. C.; Bilbo, J. T.; Brown, M. S.; Colen, L. B.; Gaspirini, F. J.; Goldsmith, D. W.; Jamin, M. D.; Neely, K. A.; Resnick, C. T.; Schwartz, G. J.; Short, W. M.; Skarda, K. R.; Spring, J. P.; Strauss, W. L. 1982 Organomet. 1: 586.

(3) Ingham, R. K.; Rosenberg, S. D.; Gilman, H. 1960 Chem. Rev. 60: 459.

(4) O'Brien, S.; Fishwick, M.; McDermott, B.; Wallbridge, M. G. H.; Wright, G. A. 1971 Inorg. Synth. 13: 73.

(5) Vijayaraghavan, K. V. 1945 J. Ind. Chem. Soc. 22:135.

(6) Rosenberg, S. D.; Gibbons, A. J., Jr.; Ramsden, H. E. 1957 J.Am. Chem. Soc. 79: 2137.

(7) Seyferth D.; Stone, F. G. A. 1957 J. Am. Chem. Soc. 79: 515.

(8) Clark, H. C.; Poller, R. C. 1970 Can J. Chem. 48: 2670.

(9) Rosenberg, S. D.; Debreczeni E.; Weinberg, E. L. 1959 J. Am Chem. Soc. 81: 972.

(10) Boue, S.; Gielen, M.;. Nasielski, J. 1968 J. Bull. Soc. Chim. Belg. 77: 43.

(11) Boue, S.; Gielen, M.; Nasielski, J.; Lieutenant, J-P.; Speielmann, R. 1969 Bull. Soc. Chim. Belg. 78: 135.

(12) DeZwart, D.; Slooff, W. 1983 Aquatic Toxicol. 4: 129.

(13) Bulich, A. A. 1982 Process Biochem. March/April: 45.

(14) Bulich A. A.; Isenberg, D. L. 1981. ISA Transactions 20: 29.

(15) Davidson, G.; Harrison, P. G.; Riley, E. M. 1973 Spectrochim. Acta 29A:1265.

(16) Peruzzo, V. 1972 J. Organomet. Chem. 40: 121.

(17) Fishwick , M.; Wallbridge, M. G. H. 1970 J. Organomet. Chem. 25: 69.

FIGURE 1

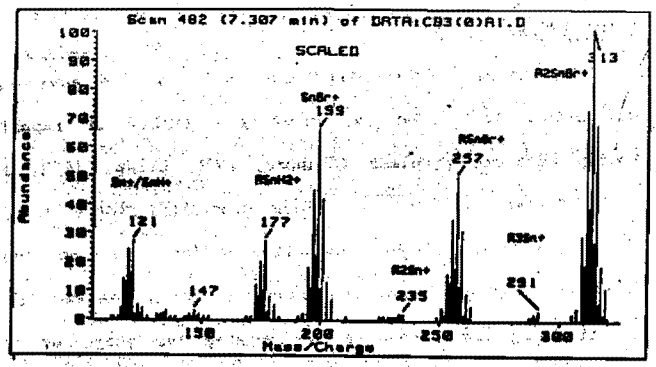

Tributyltin Bromide

FIGURE 2

MAJOR FRAGMENT IONS OF R3SnBr

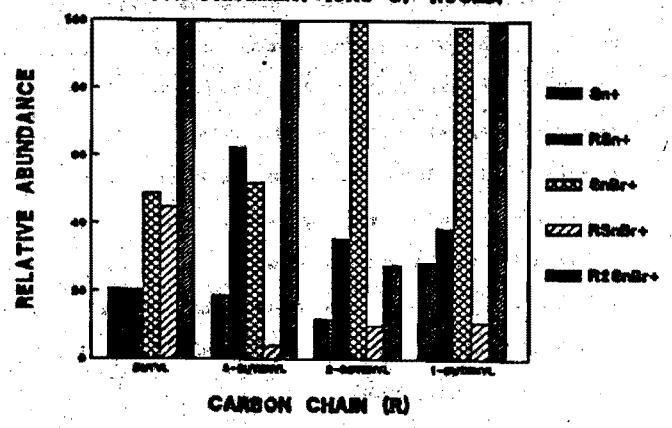

TABLE 1

IR BANDS OF ALKENYLTIN COMPOUNDS

Compound	ν (C=C) cm-1	Source
$(CH_2=CH)_2SnL_2$	1602-1588	Ref. 8
$(CH_2CH_2CH=CH)_4Sn$	1597.1	Lab
$(CH_2CH_2CH=CH)_3SnBr$	1600	Lab
$(CH_2=CHCH_2)_4Sn$	1623-1614	Ref. 8, 15
$(CH_2=CHCH_2)_4Sn$	1624.1	Lab
$(CH_2CH=CHCH_2)_2SnL_2$	1644-1638	Ref. 8
$(CH_2CH=CHCH_2)_4Sn$	1647	Lab
$(CH_2=CHCH_2CH_2)SnL_3$	1638-1635	Ref. 8
$(CH_2=CHCH_2CH_2)_4Sn$	1639.5	Lab
$(CH_2=CHCH_2CH_2)_3SnBr$	1639.5	Lab

L = ester group

TABLE 2

TOXICITY OF TRIBUTYL- AND TRIBUTENYLTIN BROMIDES

Compound	5 min EC50 (uM)	15 min EC50 (uM)
$(CH_3CH_2CH_2CH_2)_3SnBr$	0.13 ± 0.01	0.06 ± 0.02
$(CH_3CH_2CH=CH)_3SnBr$	0.82 ± 0.16	0.44 ± 0.04
$(CH_2=CHCH_2CH_2)_3SnBr$	0.44 ± 0.05	0.27 ± 0.03

MICROFOULING AND LEACHING FROM PAINTS

Mitchell,A.J. & Bellinger E.G.

Dept. Environmental Biology
University of Manchester
Oxford Road
Manchester, M13 9PL
England

Abstract

Six antifouling formulations (either Cu_2O or organotin) were exposed at Menai Strait,Anglesey for 126 days. Leaching rates were evaluated by A.A.S. and Polarography,the microfouling colonization examined SEM and the effect on toxin release assessed. A variety of bacteria were found as early colonizers. Growth of the bacterial layer encouraged silt and detritus accumulation which appeared to reduce the rate of toxin release from all paints. Cu_2O paints had better antifouling performance maintaining adequate leaching rates.

INTRODUCTION

Moving and static structures in the marine environment are susceptible to biofouling, creating a number of important and costly economic problems (Skinner, 1971; Crisp, 1973; Phillips, 1973; Christie, 1977). On ships biofouling leads to increased frictional drag and fuel consumption, whilst on oil and gas rigs it increases loading forces and corrosion. Since the removal of such fouling requires expensive dry docking for ships or underwater maintenance, antifouling paints are employed to reduce surface fouling.

The main biocidal components of antifouling paints are triorganotin compounds such as Tributyltin Oxide (TBTO), Tributyltin Fluoride (TPTF), Triphenyltin Fluoride (TPTF) and Cuprous Oxide (Cu_2O). The controlled release of such toxins results in the formation of a layer of high toxin concentration at the paint surface known as the boundary layer. The thickness of this layer depends on the leaching rate of the toxin, which in turn depends on the temperature, pH, salinity and flow rate of the seawater over the surface (de la Court, 1981; Evans, 1981). Most modern antifoulings provide effective long term protection against macrofouling, however, few prevent the growth of slime forming organisms, notably bacteria and diatoms (Corpe, 1973); Dempsey 1981 a, b; Callow, 1984).

In the present investigation six (insoluble matrix) antifoulings were exposed at the Menai Strait, Anglesey for five months. Observations were made on the development of the bifouling community on these paints and the effects this community had on

biocide leaching rate and antifouling performance.

MATERIALS AND METHODS

Six non-commercial antifouling formulations comprising 25% Cu_2O, 50% Cu_2O, Tributyltin Fluoride (TBTF), Triphenyltin Fluoride (TPTF), Tributyltin Adipate (TBTA), and Tributyltin Fumerate (TBTFum) were applied to marine plywood panels (20.2 cm x 12.5 cm and 0.6 cm depth). Each paint was applied to eight separate plates to a final dry paint thickness of 150-200 µm. All plates were exposed for five months from mid April on a raft located in the Menai Strait, Anglesey, U.K. Grid ref. O.S. sheet 114 SH 563724. In this location water flow rates of 9-12 kts are common. Representatives of each antifoulant were collected after 21, 63, 84 and 126 days (d). All plates were submerged in filtered seawater (0.22 µm) for transportation to the laboratory.

(i) LEACHING EXPERIMENTS

Leaching was carried out in rectangular plastic experimental vessels (4 l) cleaned by soaking in 10% hydrochloric acid for 24 hours and triple washed in distilled water. Each vessel was filled with 3 l of filtered (0.22 µm) seawater of known copper and tin concentration and placed onto a magnetic stirrer. One plate, representing each paint formulation at each exposure, was then clamped into position in the middle of the container. Stirring by magnetic stirrers was of equal speed in all vessels. Leaching was carried out for 24 hours at a constant temperature (10°C ± 1°C). After 24 hours the surface area of each plate exposed to the seawater and the total volume of seawater remaining in the experimental vessel was measured. Seawater controls with no experimental panels were run in parallel.

(a) Tin Analysis

Two 100 ml aliquots of leachate were removed from each experimental vessel and acidified by placing into separate 110 ml soda glass stoppered bottles containing 2 ml concentrated hydrobromic acid (G.P.R. 48-50%). This was done to facilitate subsequent analysis as trace amounts of metals, particularly butyltin and inorganic tin IV species, are known to adhere strongly in aqueous systems in the plastic or glass containers in which they are stored. All glassware was thoroughly cleaned in concentrated HCl for 24 hours and triple washed in distilled water. Acidified samples were gently shaken and allowed to stand for a minimum of 15 minutes; and then stored in a refrigerator at 4°C prior to analysis. These aliquots were then extracted according to the method described by M & T Chemicals Inc., extracting 10 ml of each sample with 200 ml of the described solvent. Extraction of the soda glass bottles followed the procedure described (M & T Chemicals Inc.) using 50 ml of solvent.

A flameless A.A. spectrophotometer (Model IL.551) with Fastac™ (Model IL.254) was used to determine tin concentrations in the extracted samples. Leaching rates for tin were then calculated.

(b) Copper Analysis

Two 100 ml aliquots of leachate were removed and acidified with 2 ml conc. HCl (ARISTAR). One extraction was undertaken by adding 10 ml of conc. HCl (ARISTAR) to the sample bottle to remove adsorbed copper. Analysis of this latter extract showed negligible amounts of adsorbed copper, therefore no further bottle extractions

were carried out.

The pH of the samples were carefully adjusted to 2.0 using either concentrated HCl (ARISTAR) or ammonia solution (ARISTAR). These were then left stirring to equilibrate for a minimum of one hour. Stock solutions of copper (1000 ppb) were also prepared for standard addition. Samples were analysed using an anodic stripping differential pulse polarographic analyser (E G and G Princeton Applied Research, Model 264) at potentials ranging from -0.8 to +0.05 volts.

(ii)SCANNING ELECTRON MICROSCOPY

A number of paint flakes approximately 5 mm^2 and 0.5-1.0 mm depth were removed from each plate. The wood was removed with the paint to prevent damage during removal and to provide support for subsequent SEM preparation. They were then fixed in 2% V/V glutaraldehyde in seawater for 20 minutes, then washed in distilled water for the same time period. They were then freeze dried for a period of 5 hours. Specimens were mounted onto 1 cm diameter stubs using silver paint and gold coated.

RESULTS

1. Leaching Rates

Results of the leaching rates from copper and tin based paints are shown in Figs. 1-2. Lower initial leaching rates were obtained at 21 d for 25% Cu_2O (27.1 μg Cu), 50% Cu_2O (24.07 μg Cu), TBTF (0.54 μg Sn) and TBTFum (2.27 μg Sn) compared with 63 d. These lower leaching rates were thought to be uncharacteristic, particularly concerning the Cu_2O paints where high fluxes of Cu_2O (40-60 μg Cu cm^2 d^{-1}) are more typical after 21 d. For the tin paints TBTF (0.54 μg Sn) and TBTFum (2.27 μg Sn) would be expected to show similar leaching rates to TBTA in the 9 μg Sn cm^2 d^{-1} range. Dry weight analysis of the six antifoulings expressed as μg Sn/Cu cm^2 d^{-1} confirmed these lower leaching results at 21 d. The method of coating, the physical nature of the paint film(s) and/or biofouling could be some of the factors responsible for these lower leaching levels. With the former, applying paint to a non-primed wood surface could have affected initial toxin release. After 63 d all paints (excepting 25% Cu_2O at 125 d) showed reductions in leaching rates with increased exposure in the field (Figs. 1-2). The extent of this decrease varied between the tin formulations despite identical toxin loadings. TBTA and TBTFum, with similar leaching rates after 653 d, were distinctly different after 126 d; TBTA showed a sharp decline from 6.24 μg Sn cm^2 d^{-1} (63 d) to 0.7 μg Sn cm^2 d^{-1} (126 d) whilst TBTFum showed a more steady decline from 6.02 μg Sn cm^2 d^{-1} (63 d) to 1.6 μg Sn cm^2 d^{-1} (126 d) (Fig. 1). 63 day TBTF was similar to TBTFum (1.67 μg Sn cm^2 d^{-1}), however no measurable leaching occurred after 84 d. For TPTF the decline occurred even sooner, giving a leaching rate of 0.07 μg Sn cm^2 d^{-1} after only 63 d (fig. 1). By the last exposure (126 d), therefore, TBTFum was the only paint with a leaching rate higher than 1.0 (1.6 μg Sn cm^2 d^{-1}), TBTF (0.35 μg Sn cm^2 d^{-1}), TPTF (0.35 μg Sn cm^2 d^{-1}) and TBTA (0.7 μg Sn cm^2 d^{-1}) all being lower.

The copper paints showed higher leaching rates than the tin throughout the 126 d exposure period; however, they also showed more fluctuations (Fig. 2). Such differences reflected the different toxin release mechanisms of the copper and tin. According

to Phillips (1973) and Evans (1981) in Cu_2O paints the toxins are in contact and as one particle leaves the paint film surface through dissolution, another is immediately exposed, resulting in high leaching rates.

In contrast, the tin antifoulant toxins are molecularly dispersed within the binder and relay diffusing through the binder maintaining a uniform concentration through the film. Toxin release into the seawater therefore results in more diffusing upwards through the film to replace it resulting in lower more consistent toxin release.

Fluctuations in the Cu_2O paints were initially evident at 63 d when the leaching rates on both copper paints increased compared to those at 21 d. 50% Cu_2O increased from 24.07 μg Cu cm^2 d^{-1} (21 d) to 66.51 μg Cu cm^2 d^{-1} (63 d), 25% Cu_2O (with a lower toxin loading) increased from 26.40 μg Cu cm^2 d^{-1} (21 d) to 34.1 μg Cu cm^2 d^{-1} (63 d). These increases could have been due to the initial high fluxes of copper (characteristic of copper antifoulants) being delayed until the 63 d exposures.

After 84 d the leaching rates of both 25% and 50% Cu_2O decreased to 24.0 and 39.57 μg Cu cm^2 d^{-1} respectively. This decline continued in 50% Cu_2O to the 126 d exposure with a final leaching rate of 28.72 μg Cu cm^2 d^{-1}. However, in 25% Cu_2O there was a marked increase in leaching after 120 d to 61.54 μg Cu cm^2 d^{-1} (Fig. 2). Dry weight analysis of 25% Cu_2O (126 d) confirmed these results.

2. Primary Biofilm Development

On all paint formulations bacteria (predominantly stalked and rod forms) were the earliest colonizers (21 d), their attachment and growth marking the beginning of biofilm development. This initial community is referred to as the 'primary biofilm'.

The primary periphytes were rod bacteria (possibly of the genera Pseudomonas, Flavobacterium, Acromobacter) (Plate 1). These secreted mucilaginous material in the form of strands, pads or sheets (Plate 3). Secondary periphytes were predominantly stalked rod bacteria colonizing the lower slime/paint layer (Plate 2). These bacteria (possibly Caulobacter, Hyphomicrobium or Saprospora) formed an extensive network of mucous strands; in some areas merging to form thicker layers of slime (Plates 4-5). In many observations these strands appeared suspended above the lower bacterial/paint layer (Plate 6). The meshed network of mucous strands and slime exudates appeared to encourage the entrainment and incorporation of silt and other debris. Both rods and stalked rods showed evidence of proliferation and growth which coupled with further bacterial colonization and incorporation of silt resulted in the biofilm developing a complex tiered structure (Plate 7).

Tertiary periphytes included ring and coccoid bacteria. Ring forms (possibly Micrecyclus) and cocci predominated at the later stages of biofilm development when the incorporation of silt, debris and other biological material was most extensive (Plate 8).

The amount of debris etc. incorporated within the biofilm appeared to increase as bacterial populations became more extensive; such inputs culminating in a mature biofilm which appeared rough, forming continuous sheets in some areas (Plates 9-10). At this stage biofilm deterioration was also evident, with

some of the slime layer cracking and peeling away (Plates 10-11). Flaking and peeling of the slime revealed lower slime layers and occasionally the paint surface, which was then open to re-colonization by bacteria (Plate 12).

Biofilm detachment could have been due to the fluid sheer stress increasing at the film surface, as a result of an increased thickness and roughness. Such detachment was reported by Characklis (1981) who stated that as the biofilm grew thicker, the fluid sheer stress at the biofilm interface generally increases. In addition, as biofilms grow thicker, the substrate, oxygen or nutrient limitation in the deeper portions is great. These limitations weaken the biofilm matrix and cause subsequent detachment.

Bacterial assemblages on 25% Cu_2O, 50% Cu_2O and TBTFum appeared to show some avoidance of active leaching areas, aggregations of bacteria surrounding - not covering - pores (Plates 13-14).

3. Secondary Biofilm Development

Various fungi, protozoa, diatoms and macrofouling organisms were recorded on toxic paints over the 126 day exposure period. Colonization by these organisms constituted the second stage of biofilm development and marked the beginning of a more diverse and complex fouling community.

In general, the earliest secondary colonizers on toxic paints were fungi and peritrichous protozoa (after 63 d). Larger fouling organisms, namely diatoms and macrofoulers, were the second group to colonize the paints (84-126 d).

(a) Fungi

In all observations fungal colonization was patchy, the hyphae forming tangled networks overlying and incorporated within the biofilm (Plate 15). These hyphal networks acted to 'stabilize' the biofilm layer and provide support for other micro/macrofouling organisms. Fungal activity was most extensive on the tin paints, nine fungal types being recorded, although none supported more than 4 different types of fungi at one time. Only one type was recorded on Cu_2O paints.

(b) Protozoa

Peritrichous protozoans (Vorticella spp.) were observed on 25 and 50% Cu_2O from 63-126 d, on TBTF from 63-84 d, and on TPTF from 84-126 d (Plate 16). Colonization was most abundant after 84 d. None were observed on TBTA or TBTFum. Peritrichs, like fungi, grew in patches comprising monospecific groups of individuals. As the exposure duration increased, cell collapse and deterioration was evident, pellicles and stalks being overgrown by bacteria (Plate 7).

(c) Diatoms

Diatoms were observed most frequently after the longest exposure period (85-126 d). They were, however, relatively few, appearing randomly dispersed across the paint surface. Most showed evidence of cell collapse and deterioration, many being overgrown by the biofilm (Plate 17). The commonest belonged to the genera Achnanthes and Navicula, the former being the most predominant. Both are predominantly surface living forms, colonizing natural surfaces such as sand grains and rocks as well as artificial submerged areas. Some of these species are characterised as resistant slime forming types. Two tin based paints, namely TBTF and TPTF, showed a higher species diversity than the Cu_2O paints.

within the latter 25% Cu_2O showed a greater number of species. In contrast TBTA and TBTFum showed little evidence of diatom colonization.

Colonization of various substrates by diatoms is well documented, most papers showing secondary development to be dominated by them (Ferguson Wood, 1949; Skerman, 1956; Cundell et al, 1977; Marszalek et al., 1979; Caron and Sieburth, 1981; Hudson and Bourget, 1981). On toxic paints exposed at the Menai Strait, diatoms were not the predominant fouling organisms; their contribution to the biofilm in terms of energy input would therefore be reduced in comparison with those quoted by Cooksey et al. (1981).

Differences in the literature regarding diatom predominance (excepting seasonal variation and surface texture effects) appeared largely due to differing environmental conditions at Menai, low recruitment of diatoms being due to exposure in deeper, faster flowing waters.

Macrofouling Organisms

Macrofoulers on toxic and non-toxic paints included four 'groups':cyprids and mature barnacles, hydroids (Tubularia sp.), crustacea (Caprella sp.) and sea slugs (Facelina auriculata and Aeolida papillosa). Barnacles (Semi-Balanus balanoides and Balanus crenatus were the earliest and most predominant macrofouling organisms on toxic paints (Plate 18). Colonization by these forms provided a more suitable substrate for the attachment of secondary colonizers such as hydroids and certain crustacea. Macrofouling was most extensive on TPTF and TBTF (64-126 d),spat fall and barnacle development being greatest on TPTF. The remaining paints, TBTFum, TBTA, 25% and 50% Cu_2O were relatively free of macrofouling forms.

DISCUSSION

(i) Influence of Biofilm on Toxin Release

All paints (excepting 25% Cu_2O 126 d) showed a reduction in toxin leacing rates as the exposure duration increased (Figs. 1-2). Tin paints in particular showed premature decreases in toxin release over the 126 d exposure period, toxin levels appearing inconsistent and well below the manufacturers' 'expected levels' for the period of exposure. Evans (1981) states that 10 μg Cu cm^2 d^{-1} and 1.2 μg Sn cm^2 d^{-1} are the critical leaching rates required to prevent macrofouling. According to these criteria TPTF showed inadequate antifouling performance after 63 d, TBTF after 84 d and TBTA after 126 d.

SEM observations on the fouling community indicated that biofilm development could be responsible for the premature decrease in biocide release. As the rate of biofilm development increased, the level of toxin release decreased. Bacteria and their mucilaginous exudates were observed on all paint formulations. The paints with higher leaching rates such as 25 and 50% Cu_2O, TBTA and TBTFum showed extensive bacterial colonization but relatively little colonization by secondary fouling organisms. All these paints, excepting 25% Cu_2O (126 d), showed reductions in the leaching rates as the exposure duration increased indicating that "primary biofilm development" could be a major contributor to much of the prematrue reductions in toxin levels.

Bacterial slime could act in two ways to reduce toxin release.

Firstly by physical blocking of the paint surface - continuous sheets of slime in certain areas encouraged entrapment of silt and detritus into the biofilm. According to Swain et al. (1982) these neutralise antifouling surfaces, making them less effective. Secondly, chelation of the antifouling toxin into the slime film could occur. Evidence is accumulating which suggests that polysaccharides similar to those secreted as adhesives by fouling bacteria can chelate metal ions (Lasik and Gordiyenko, 1977).

According to Dempsey (1981a) a reduction in antifouling efficiency could occur if the fouling bacteria broke down the toxins into non toxic metabolites. He also suggests that the breakdown of organotins may be accelerated by some fouling bacteria. Should this occur during diffusion through the fouling layer, then the concentration of toxin in the boundary layer could be reduced to ineffective levels. Korbund and Freiberger (1970) demonstrated that biofilm thickness dictates whether toxin levels are positively or negatively affected. It was found that biofilms were capable of accumulating high concentrations of toxin. In formulations employing cuprous oxide as a toxin the cuprous ions which leached from the paint were held by the slime film as various inorganic compounds. The concentration of these compounds were shown to be up to 10^3 times that of the toxin in a saturated seawater solution. It was suggested that carbon dioxide producing (aerobic) bacteria were probably responsible for these high concentrations and that these also increased the acidity of the environment. The result of this increased acidity was an increase in the rate at which copper entered solution. They demonstrated that as the slime became thicker, the available copper compounds were distributed over an increasing volume of slime. They concluded, that light slimes accumulating on toxic coatings could act to increase its antifouling effectiveness. As these slime layers became thicker they would tend to act as a barrier to toxin release, decreasing the antifouling efficiency.

Although biofilm thickness was not directly measured in this work it was observed that the earlier stages of biofilm development were dominated by loose networks of mucous strands stretched across the surface (Plates 4-6). Such slime was possibly indicative of a thin slime layer. This could have caused fluctuations in leaching rates at the earlier exposures (63 d), particularly on copper paints. As it became more extensive and denser, however, it could have acted as a barrier to toxin release (see Plates 8-10 and figs. 1-2).

Observations showed that biofilm development could eventually reduce leaching rates. It was also evident, however, that mature biofilms did deteriorate. Slime layers began to crack and peel away, in some cases exposing the underlying paint (Plate 11). If such erosion occurred over large areas it seems likely that biocide release could increase again prior to recolonization, thus resulting in periodic fluxes of toxin release. 25% Cu_2O (126 d) appeared to show such fluxes, widespread deterioration and erosion of the slime layer being accompanied by higher fluxes of Cu_2O (61.54 μg Cu cm^2 d^{-1} 126 d). If reduced toxin levels are temporary and macrofouling organisms do not attach during the period of lower toxin release, it seems feasible that good antifouling performance

could be maintained, as has been indicated by longer term field trials.

(ii) Influence of Toxins on the Biofilm

Although biofilm development did affect biocide release, observations also indicated that toxin levels affected the rate of biofilm development and the diversity of organisms comprising the fouling community. Bacteria were observed on all paint formulations. According to Banfield (1980) leaching rates of 20 μg Cu cm^2 d^{-1} are required to prevent bacterial slimes. Observations from Menai showed extensive bacterial populations on Cu_2O paints with leaching rates above 20 μg Cu cm^2 d^{-1}. The successful recruitment and growth of bacteria on toxic substrates could be attributable to:

(a) Production of mucilaginous extracellular material. Many bacteria were observed producing extensive networks of mucoid strands which suspended them above the paint film (Plates 4-5). Other bacteria secreted extensive sheets of slime (Plate 3). These methods of attachment may be strategies enabling the cells to escape the highest concentrations of toxin at the immediate surface of the paint. Slime production was more extensive on the paints with the highest biocide release, indicating that increased slime production could be a response to higher toxin levels. In addition, bacterial assemblages on formulations with higher leaching rates (25% Cu_2O, 50% Cu_2O TBTFum) showed avoidance of active leaching areas; aggregations of bacteria surrounding - not covering the pores (Plates 13-14).

(b) Chelation of antifouling toxins by extracellular material.

(c) Tolerance to toxins. Tolerance to heavy metals is a common phenomenon in microorganisms. The tolerance of fouling bacteria to cuprous oxide paints is no exception. According to Dempsey (1981a) only a limited number of bacteria have developed tolerance to copper paints. The position with regard to organotin paints is different. Organotin antifouling compounds are not effective against Gram-negative bacteria, although they are highly toxic towards Gram-positive species. (Nikaido, 1976 in Dempsey, 1981a). The majority of bacteria in the sea are Gram-negative, therefore most could colonize organotin paints.

The most toxic antifoulings tested did support other microfouling organisms, although the species diversity and abundance was greatly reduced. TBTA and TBTFum were colonized by fungi when leaching rates were relatively high (9.44 + 4.97 μg Sn cm^2 d^{-1} respectively) indicating a tolerance to tin biocides. On Cu_2O paints peritrichs were also observed. One factor allowing colonization by these latter organisms was probably avoidance of the highest toxin concentrations at the paint surface by attachment with long stalks holding them above the surface. In addition, tolerance to cuprous ions could have developed.

Diatoms were also observed at Menai, although only occasionally on the more toxic paints, Achnanthes sp. being the most frequent. Callow (1984) carried out a global study using panels coated with antifouling compositions containing either cuprous oxide, tributyltin, or both, as biocides. The most common genera encountered on these surfaces were Amphora, Achnanthes, Stauroneis, Navicula and Amphiprora. All five genera were capable of being

dominant colonizers of copper or organotin/copper paints, and showed strong resistance to copper and tin biocides.

Observations from Menai also showed that the rate of biofilm development was affected by toxin release. The rate of biofilm development could be 'measured' in terms of production of a mature primary and secondary biofilm. Such films formed a complex tiered structure including a diverse fouling community of bacteria, fungi, peritrichs, diatoms and attached macrofouling organisms. Under these criteria TPTF showed a mature biofilm after 84 d exposure; TBTF after 126 d. The remaining paints 25%, 50%, Cu_2O, TBTA and TBTFum showed no such development. All these paints showed a predominant primary fouling community. TPTF and TBTF gave zero leaching rates after only 84 d exposure. This period marked the beginning of an increase in the abundance and diversity of the fouling community. TBTA also showed low leaching after 126 d (0.70 μg Sn cm^2 d^{-1}). However, unlike TPTF and TBTF, a mature biofilm was not observed. This result was possibly due to the seasonal 'availability' of secondary fouling organisms at the 126 d exposure. Fungi and peritrichs, like cyprids, possibly undergo settlement at certain periods throughout the year. Their predominence at 63-84 d indicated extensive recruitment during this period, such recruitment possibly being reduced at the later 126 d exposure.

All of these results indicated that high toxin levels tend to apply selective pressures on colonization. Only those species which are tolerant or have strategies for avoiding toxins can survive. As the toxin concentration falls (as in TBTF and TPTF), so a greater diversity of organisms become able to foul the surface.

(iii) Antifouling Performance

According to Evans (1981) 10 μg Cu cm^2 d^{-1} and 1.2 μg Sn cm^2 d^{-1} are the critical leaching rates required to prevent macrofouling. In terms of paint performance, therefore, within the 126 d exposure period the Cu_2O paints maintained leaching rates above the critical levels required for preventing macrofouling. In contrast, tin paints which according to Evans (1970, 1971) have the potential of providing superior antifouling properties with less toxicant release over a longer period of time, did not rank high in terms of leaching performance. According to the results TPTF, TBTF and TBTA were "theoretically" ineffective against macrofouling organisms after 63, 84 and 126 d respectively. Ineffective macrofouling prevention was observed on TPTF and TBTF after 63 and 84 d respectively, Semi-Balanus balanoides, B. crenatus and Tubularia sp. being recorded. TBTA, however, remained free from macrofouling.

References

BANFIELD, T.A., (1980). Marine Finishes. Part 11. J.O.C.C.A. 69, 93-100

CALLOW, M.E., (1984). A world-wide survey of fouling on non toxic and three antifouling paint surfaces. In: Proc. Sixth Int. Congr. on Mar. Corr. and Fouling, 325-346

CARON, D.A., SIEBURTH, J.M., (1981). Disruption of the primary fouling sequence on fibre glass reinforced plastic submerged in the marine environment. Appl. and Env. Microbiol. 41, 268-273

CHARACKLIS, W.G., (1981). Fouling biofilm development: A process analysis. Biotechnology and Bioengineering. XXIII, 1923-1960

CHRISTIE, A.O., (1977). Recent developments in antifoulings. J.O.C.C.A. 60, 348-353

COOKSEY, B.,COOKSEY, K.E., MILLER, C.A., PAUL, J.H., RUBIN, R.W., WEBSTER, D.,(1981). Mar.Biod: An interdisciplinary study.

CORPE, W.A., (1973). Microfouling: The role of primary film-forming marine bacteria. In proc. 3rd Int. Cong. on Mar. Corr. and Fouling. 598-609

CRISP, D.J., (1973). Mechanism of adhesion of fouling organisms. In Proc. 3rd Int. Cong. on Mar. Corr. and fouling. 691-699

CUNDELL, A.M., SLEETER, T.D. and MITCHELL, R. (1977). Microbial populations associated with the surface of the brown algae Ascophyllum podosum. Microb. Ecol. 4, 81-91

DE LA COURT, F.H., (1981). Erosion and hydrodynamics of biofouling coatings. Mar. Biod.: An interdisciplinary study. (Eds. Costlow, J.C., Tipper, R.C.), 230-236

DEMPSEY, M.J., (1981a). Marine bacterial fouling: A scanning electron microscope study. Mar. Biol. 61, 305-315

DEMPSEY, M.J., (1981b). Colonization of antifouling paints by marine bacteria. Bot. Mar. XXIV, 185-191

EVANS, C.J., (1970). The development of organotin based antifouling paints. Tin Uses. 85, 3-7

EVANS, C.J., (1971). Organotin based antifouling paints. Corr. Prev. Control, 18, 8

EVANS, L.V., (1981). Marine algae and fouling: A review with particular reference to ship fouling. Bot. Mar. XXIV, 167-171

FERGUSON WOOD, E.J., (1949). I. The role of bacteria in the early stages of fouling. Invest. of underwater fouling. 85-91

HOBBUND, H.M. & FEHLBERGER, A. (1970). Slime films and their role in marine fouling. Ocean Engng. 1, 631-634

HUDON, C. & BOURGET, E., (1981). Initial colonization of artificial substrates: Community development and structure studied by S.E.M. Can. J. Fish. Aquat. Sci. 38, 1371-1384

LASIK, Y.A., GORDIYENKO, S.A.,(1977). Complexing of soil bacteria polysaccharides with metals. Soviet Soil Sci. 9, 192-198

M. & T. CHEMICALS INC., (1980). Private communication. Europoweg, Van Cittershaven, P.O.Box 70, NL 4380 AB Vlissingen, The Netherlands

MARSZALEK, D.S., GERCHAKOV, S.M., & UDEY, L.R., (1979). Influence of substrate composition on marine microfouling. Appl. and Env. Microbiol. 38, 987-996

NIKAIDO, H., (1976). Outer membrane of Salmonella typhimurium, transmembrane diffusion of some hydrophobic substances. Biochem. Biophys. Acta 433, 118-132

PHILLIPS, A.T., (1973). Modern trends in marine antifouling paints research. Prog. in Org. Coatings. 2, 159-192

SKERMAN, T.M., (1956). The nature and development of primary films on surfaces submerged in the sea. New Zealand Oceanographic Inst. Dept. of Scientific and Industrial Research

SKINNER, C.E., (1971). Lab. Tech. for screening potential toxicants for antifouling paints. Antifouling Symp. Ciba-Geigy. Marianburg. W. Germany

SWAIN, G.W.J., FARRAR, R.A. & HUTTON, G.P., (1982). The use of controlled copper dissolution as an antifouling system. J.Materials Sci. 17, 1079-1094

FIG.1. Leaching rates ($\mu g\ Sn\ cm^2\ d^{-1}$) from tin based antifouling paints exposed at the Menai Strait, Anglesey.

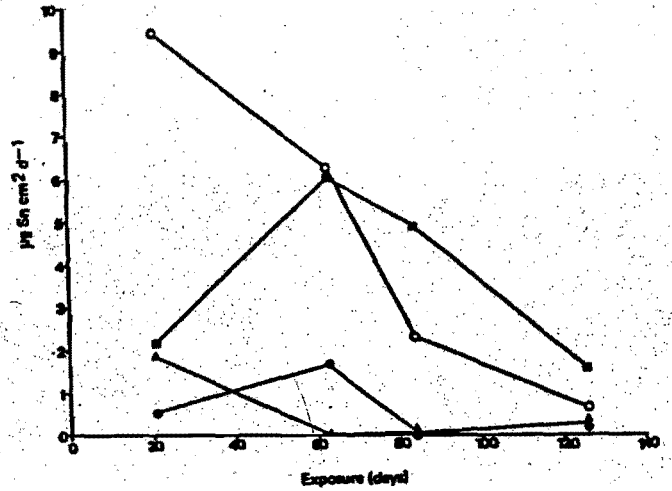

FIG.2. Leaching rates ($\mu g\ Cu\ cm^2\ d^{-1}$) of copper based antifouling paints exposed at the Menai Strait, Anglesey.

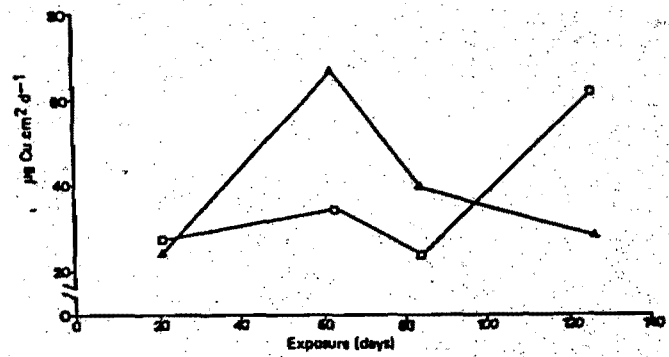

KEY

TBTF ● TBTFUM ■ 25%Cu_2O □
TPTF ▲ TBTA ○ 50%Cu_2O △

Plates 1 to 6. (1) TBTFum (21d),rod bacteria colonizing surface. Magnification X 10K
(2) TBTFum (21d), stalked bacteria attached by multiple mucous strands. Mag. X 10K
(3) 50% Cu_2O(63d), rod bacteria encapsulated in dense mucilaginous sheets. Mag.X 5K
(4) 25% Cu_2O (63d),bacterial mucilage forming sheets. Mag. X 5K
(5) 25% Cu_2O (63d),lacunate mucilage stretched across lower biofilm being colonized by rod and stalked bacteria. Mag.X 10K
(6) TBTFum (63d), stalked bacteria suspended above lower bacterial and paint layer Mag. X 5K

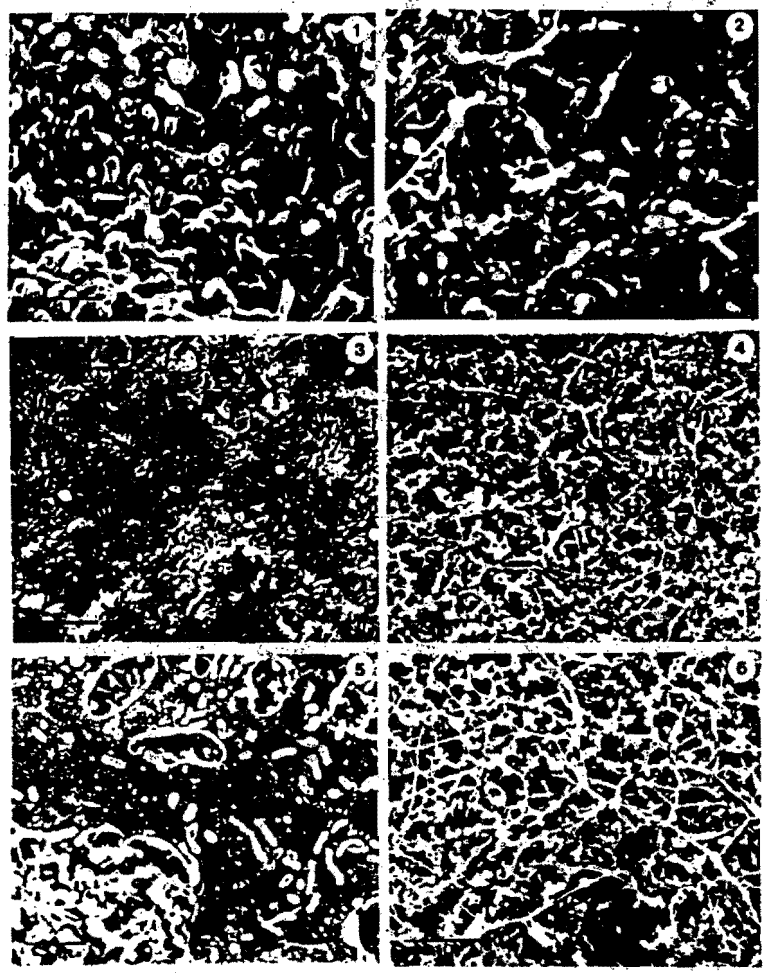

Plates 7 to 12. (7) TPTF (126d),tiered biofilm with collapsed peritrichs being incorporated into the biofilm. Mag.X 2K
(8) TPTF (126d),ring bacteria (poss. Microcyclus) and cocci colonizing debris. Mag.X 20K
(9) 25% Cu_2O (126d),rough slime layer indicative of a mature biofilm. Mag. X 500
(10) TPTF (84d),dense rough biofilm,extensive cracking and peeling. Mag. X 5K
(11) 25% Cu_2O (126d),widespread deterioration of mature biofilm. Mag. X 2K
(12) TBTFum (84d), rod and stalked bacteria recolonizing paint film. Mag.X 10K

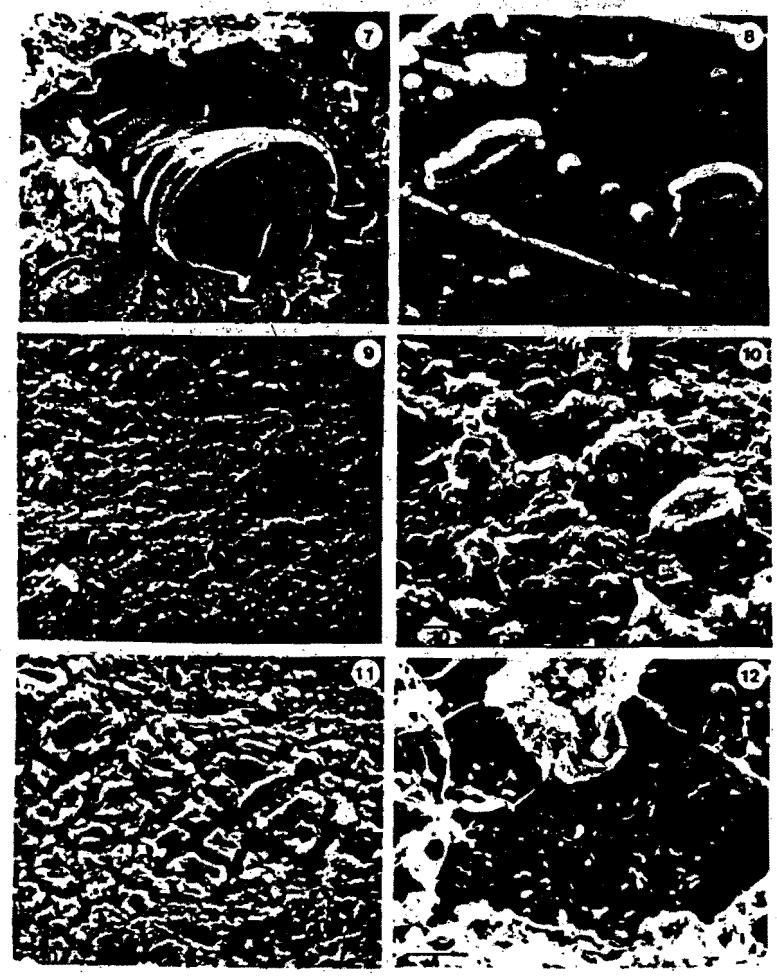

Possible evidence of active toxin avoidance. Mag, X 5K (13), 10K (14).
(15) TBTA (63d),branched fungal hyphae overlying and incorporated within biofilm.
Mag. x 100 .(16) TPTF (84d), Peritrichs (Vorticella sp.) attached to biofilm. Mag.X 5K
(17) TPTF (126d), naviculoid diatomswith evidence of cell collapse and deterioration.
Mag. X 10K . (18) TBTF (84d), Balanus crenatus with peritrichs (Vorticella sp)
colonizing shell plates. Mag. X 100

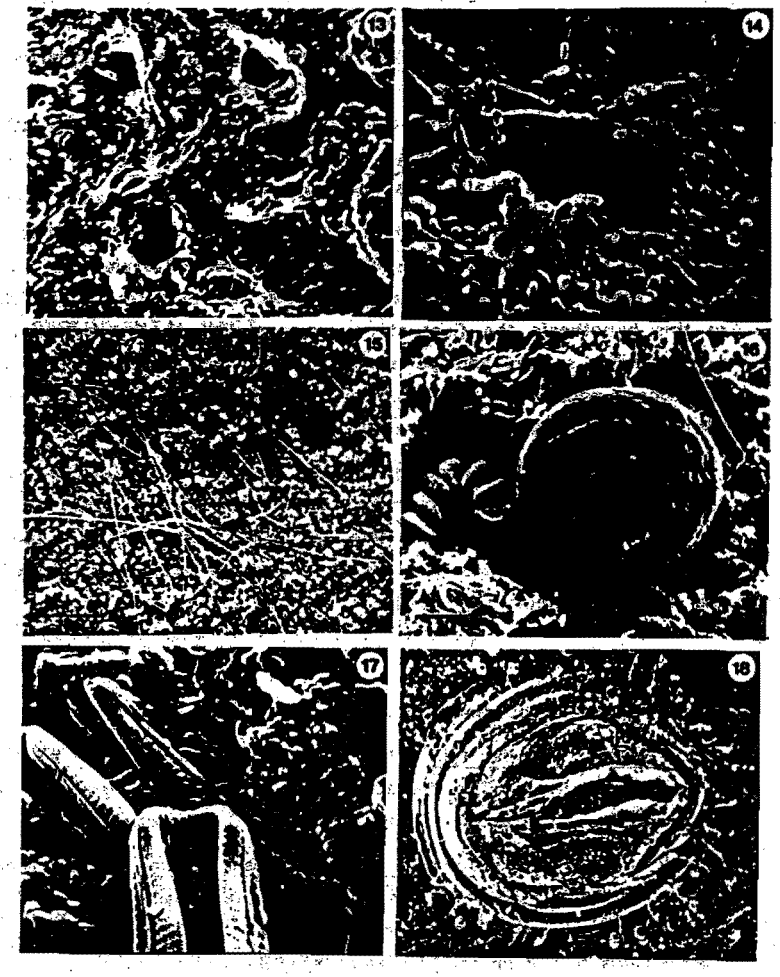

THE USE OF CALCIUM RESINATE IN THE FORMULATION OF SOLUBLE MATRIX ANTIFOULING PAINTS BASED ON CUPROUS OXIDE

Carlos A. Giúdice, Beatriz del Amo and Vicente J. D. Rascio

CIDEPINT - Research and Development Centre for Paint Technology
(CIC-CONICET)

ABSTRACT.- Antifouling paints based on calcium resinate, calcium resinate/chlorinated rubber and WW rosin/chlorinated rubber were formulated and elaborated in a laboratory scale. The experimental results of immersion raft trials (26 months) were statistically treated and later conclusions correlated with binder acid values obtained from laboratory chemical analysis.

INTRODUCTION

An efficient antifouling paint contains toxicants which are released from the film surface during sea water immersion. Thus, the settlement of fouling organisms can be controlled during long periods.

As regards soluble matrix antifouling paints, their dissolution rate is the most important variable and it influences significantly on toxicants leaching rate.

This paint type is generally based on acid resins, soluble in sea water (pH 8.0-8.2), such as WW rosin (gum rosin). The main component of the WW rosin is the abietic acid; the carboxyl group of its molecule reacts with sodium and potassium ions of sea water, giving soluble compounds (soaps), and with calcium and magnesium ions, forming resinates of lesser solubility than that of the original resin. The above mentioned reaction with divalent compounds also takes place during paint elaboration, in the pigment dispersion operation, particularly when cuprous oxide (toxicant) and calcium carbonate (extender) are used [1].

Efficient antifouling paints were developed in previous stages for immersion periods from one to three years [2, 3]. Changes in film composition (using as binder WW rosin/grade 20 chlorinated rubber) were studied and it was proved that after long immersion periods the residual resinic acid content was practically negligible; the dissolution in the steady state was a consequence of the solubilization of the alkaline resinates formed.

In the present paper it is considered the possibility that the paint may reach this steady state quickly after immersion, by using calcium resinate in the formulation, instead of rosin resin. According to this hypothesis the first stage corresponding to the formation of very soluble sodium and potassium resinates would be avoided, and its consequence, the fast toxicant loss and thickness decrease of the antifouling paint film.

Besides, this methodology would eliminate the reaction which takes place during the dispersion between the cupric oxide produced by the $Cu_2O \rightleftarrows CuO + Cu^{\circ}$ reaction [5] and the free acids of the WW rosin, which diminishes the binder dissolution rate and therefore the toxicant leaching rate [6-8].

STUDIED VARIABLES

Related to the composition

Resinous material type. The binder was prepared with WW rosin or calcium resinate. The characteristics and IR spectrograms of both substances are indicated in Table I and Fig. 1, respectively.

Resinous material/grade 20 chlorinated rubber ratio. Aiming to study the influence of this variable on film dissolution rate, three different ratios were considered: 2/1, 1/1 and 1/2. The first one corresponds to the binder of greater solubility.

Binder content. Taking into consideration that the binder content

has an important influence on the film dissolution rate [9], four different values were studied: 23.0, 27.4, 31.9 and 36.6 % w/w, expressed on the total amount of paint solids.

Related to the elaboration process

Incorporation of the raw materials to the ball mill. Cuprous oxide dispersion process was made in the presence and in the absence of the film forming material. In this way it was intended to establish the influence of this variable on the chemical reactions which take place during the dispersion [1] and its consequence on the biocidal performance.

Cuprous oxide dispersion time. In order to study the effect of this variable [10], the main toxicant used in the formulations (red cuprous oxide, commercial quality, whose characteristics are shown in Table II) was dispersed during 3 or 5 hours.

EXPERIMENTAL PART

Sample preparation

The elaborated paints composition is shown in Table III. Samples have been prepared in a ball mill of 3.3 litres capacity, whose operating conditions have been described in a previous paper [11].

A first sample series (1A to 16A paints) was prepared by dissolving calcium resinate in the solvent mixture and then, by incorporating gradually the chlorinated rubber and the plasticizer (chlorinated paraffin 42 %), under stirring.

The ball mill was loaded with the mentioned vehicle, and then zinc oxide and calcium carbonate were added. Such components were dispersed during 21 or 19 hours, according to each case. Afterwards the cuprous oxide was incorporated and the process went on till completing, in every case, a period of 24 hours (3 or 5 hours of toxicant dispersion, respectively).

With the same vehicle it was prepared a second sample series (5B to 16B paints), whose only composition difference, as regards the previous ones, was the replacement of calcium resinate by WW rosin.

Concerning the first series (1A to 16A paints), duplicates were prepared, but adding the calcium resinate after completing pigment dispersion, including the cuprous oxide. For the second series (5B to 16B paints) the same process was made, adding the WW rosin at the end of the process.

Finally, viscosity was adjusted.

Free resinic acids content

Free resinic acids content was evaluated in the binders just elaborated as well as in those extracted from paints, according to the described method in a previous paper [8]. Thus, it was intended to set the evolution of the neutralization reactions which take place during pigment dispersion.

Free resinic acids content was calculated from the respective acid values (ASTM D-1639-76) and expressed as abietic acid on the binder solids.

Immersion in the natural sea water

The paint bioactivity was evaluated by means of an experiment which was carried out (26 months immersion) on a raft anchored at Puerto Belgrano (38°58' S, 62°06' W), harbour whose hydrological and biological conditions were previously studied [12-14].

For this test, SAE 1010 steel plates were used, sanded to A Sa 2½ (SIS 05 59 00/1963), with 40 µm maximum roughness. An anticorrosive paint of high resistance was applied on these panels (dry film thickness 200 µm) and then two coats of each antifouling paint were painted (70-80 µm of dry film). In all the cases the paints were brush applied with an interval of 24 hours between coats. Drying time of the last coat prior to immersion was also 24 hours. The test panels were placed vertically on the raft frames, at about 30-60 cm under the water surface. Each sample was prepared and tested in duplicate.

RESULTS

Binders free resinic acids content

Free resinic acids content in the experimental binders is shown in Table IV; the results are expressed as abietic acid, percent by weight. The initial value for each sample and those determined after 3 and 5 hours of cuprous oxide dispersion (in the presence and in the absence of the resinous material) are also included.

Immediatly after preparation, binders based on calcium resinate presented an abiatic acid content of 10.9, 7.6 and 4.8 per cent w/w (2/1, 1/1 and 1/2 calcium resinate/chlorinated rubber ratios, respectively). These results are the expected ones taking into consideration that calcium resinate has a 18.6 % content of free acids, expressed as abietic acid.

When cuprous oxide was dispersed in the presence of calcium resinate, samples 1A to 4A showed abietic acid values ranging from 14.7 to 14.0 % for 3 hours dispersion and from 12.2 to 11.2 % for 5 hours dispersion.

On the other hand, paints 5A to 16A presented abietic acid content of 9.2 to 8.8 % (2/1 calcium resinate/chlorinated rubber ratio), 6.6 to 6.3 % (1/1 ratio) and 4.4 to 4.2 (1/2 ratio) for 3 hours toxicant dispersion. Lesser values were obtained for 5 hours.

When cuprous oxide was dispersed in the absence of the resinous material, in the case of samples formulated exclusively with calcium resinate (1A to 4A) as well as when chlorinated rubber was used as co-binder, the free resinic acids content was practically unmodified after 3 and 5 hours toxicant dispersion.

In the case of binders based on WW rosin/chlorinated rubber (2/1, 1/1 and 1/2 ratios), a high free resinic acids content was determined immediatly after preparation: respectively 48.4, 34.2 and 21.5 %. The chemical analysis of the WW rosin employed permited to establish a 17 % content of non saponifiable substances.

Referring to binders extracted from paints after cuprous oxide dispersion in the presence of WW rosin (samples 5B to 16B) it was observed a very important reduction of the acid value: 23.0 to 22.1 % (2/1 WW rosin/chlorinated rubber ratio), 16.8 to 16.1 % (1/1 ratio) and 11.0 to 10.6 % (1/2 ratio) for 3 hours toxicant dispersion; a more still significant reduction was registered when cuprous oxide was dispersed during 5 hours.

Also in the case of antifouling paints based on WW rosin, when cuprous oxide was dispersed in the absence of resinous material, it was not registered after 3 and 5 hours toxicant dispersion a considerable acid value decrease in the binders extracted from the paints.

Bioactivity of the antifouling paints

The fouling settlement values recorded on the panels in the experimental raft are shown in Tables V and VI (11 and 26 months immersion). The key to interpret the values included are indicated at the bottom of Table V. Value 0 (panel without fouling) corresponds to a paint with 100 % efficiency; 0-1 to 90 % and 1 to 80 %. The last value was considered by the authors as the minimum acceptance limit for efficient antifouling paints.

The fixation values corresponding to a period of 26 months were statistically treated with a factorial design of the type 2x2x2x3x4 (96 samples). Each sample included a duplicate [15-17].

The results of the statistical analysis considering simultaneously all the effects are shown in Table VII. It was observed a significant influence (positive Fisher test) of the main effects (resinous material type, resinous material/chlorinated rubber ratio, binder content, order of incorporation of some components and toxicant dispersion time) on bioactivity.

According to the analysis of the mean values resulting from the statistical treatment, the antifouling paints with greater bioactivity after 26 months immersion were those elaborated with calcium resinate, with a binder content of 27.4, 31.9 and 36.6 % (similar efficiency), with 2/1 resinous material/chlorinated rubber ratio and dispersing the toxicant during 3 hours in the absence of calcium resinate.

However, due to the little decrease observed in binder acid values (low advance of neutralization reactions) when cuprous oxide was dispersed in the presence or in the absence of calcium resinate, a separate statistical analysis was made taking into account the type of resinous material; the results are also indicated in Table VII.

The values obtained enabled to establish that in samples including calcium resinate in their composition (paints 1A to 16A), the variables related to the elaborating technology (incorporation order of the raw materials and toxicant dispersion time) did not show a significant influence on the bioactivity (negative Fisher test). On the other hand, composition variables (binder content and calcium resinate/chlorinated rubber ratio) influenced significantly on the paints performance.

Results of separate analysis ratified that the best efficiency of paints based on calcium resinate, after 26 months immersion (experimental raft) corresponded to those elaborated with 27.4, 31.9 and 36.6 % of binder content (similar bioactivity) and with 2/1 calcium resinate/chlorinated rubber ratio (both for 3 or 5 hours toxicant dispersion in the presence or in the absence of calcium resinate).

Referring to the formulations with binders based on WW rosin and chlorinated rubber, the separate statistical analysis showed that the effects related to the elaboration variables and the composition had a significant influence on the toxic activity.

After 26 months immersion, the highest performance corresponded to the samples elaborated with 27.4, 31.9 and 36.6 % of binder content, and with 2/1 WW rosin/chlorinated rubber ratio. With regard to the elaboration variables, the best condition was reached dispersing the toxicant during 3 hours in the absence of WW rosin.

CONCLUSIONS

1. Some antifouling paints studied showed high effectiveness in raft trials during 26 months immersion as minimum.

2. The use of calcium resinate replacing WW rosin in the formulation of soluble matrix antifouling paints based on cuprous oxide simplified markedly the elaboration technology.

The best results were obtained with paints including high soluble material content in their composition (greatest calcium resinate/chlorinated rubber ratio and larger binder content).

4. Results of the statistical analysis were in agreement with binder acid values. When pigment-binder reactions took place paints composition was modified and then the film bioactivity was reduced.

REFERENCES

[1] Giúdice, C. A., del Amo, B., Rascio, V., Sánchez, R.- J. Coat. Technol., 55, 23 (1983).

[2] Rascio, V., Giúdice, C. A., Benítez, J. C., Presta, M.- J. Oil Col. Chem. Assoc., 62, 282 (1979).

[3] Rascio, V., Giúdice, C. A., Benítez, J. C.- Proc. 8th International Congress on Metallic Corrosion, Mainz, West Germany, Vol. II, 1353 (1981).

[4] Giúdice, C. A., del Amo, B., Rascio, V., Sindoni, O.- J. Coat. Technol., 58, 45 (1986).

[5] del Amo, B., Giúdice, C. A., Rascio, V., Sindoni, O.- J. Oil Col. Chem. Assoc., 69, 178 (1986).

[6] Heslop, R. B., Robinson, P. L.- Inorganic Chemistry. Elsevier Publishing Co., Amsterdam, Holland (1962).

[7] De la Court, F. H., De Vries, H. J.- J. Oil Col. Chem. Assoc., 56, 388 (1973).

[8] Partington, A., Dunn, P. F.- Paint Technol., 26, 14 (1962).

[9] Partington, A.- Paint Technol., 28, 24 (1964).

[10] Giúdice, C. A., Benítez, J. C., Rascio, V., Presta, M.- J. Oil Col. Chem. Assoc., 63, 353 (1980).

[11] del Amo, B., Giúdice, C. A., Rascio, V.- J. Coat. Technol., 56, 63 (1984).

[12] Bastida, R., Spivak, E., L'Hoste, S. G., Adabbo, E.- Corrosión y Protección, 8, 11 (1977).

[13] Bastida, R., L'Hoste, S. G., Spivak, E., Adabbo, E.- Corrosión y Protección, 8, 33 (1977).

[14] Bastida, R., Lichtschein, V.- Corrosión y Protección, 10, 7 (1979).

[15] Li, J. R. C.- Statistical Inference. Edwards Brothers, Michigan, USA (1964).

[16] Duckworth, W. E.- Statistical Techniques in Technological Research. Mathuen and Co., Ltd., London, UK (1968).

[17] Box, G. E. P., Hunter, W. G., Stuart Hunter, J.- Statistics for Experimenters. J. Wiley and Sons, Inc., N. Y., USA (1978).

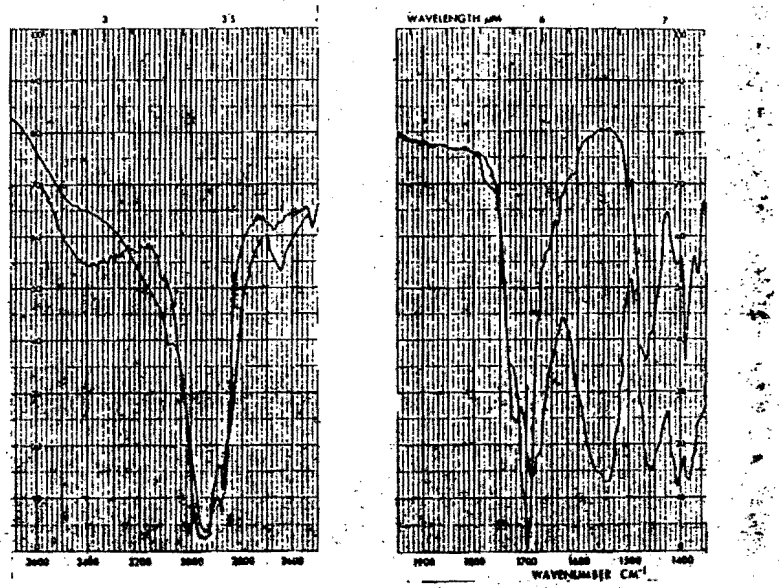

Figure 1

(a) In the wave number between 2800-3200 cm^{-1}, calcium resinate showed, in relation to WW rosin, a thinness in the absorption rank, attributable to the minimum content of abietic acid dimers. In the wave number 3400 cm^{-1}, the overtone of the present peak at 1720 cm^{-1} appeared in the curve corresponding to calcium resinate.

(b) In the wave number 1695 cm^{-1}, calcium resinate showed a lower absorption than WW rosin, since it includes in its composition a lower carbonile group content.
In the wave number 1720 cm^{-1}, only calcium resinate showed an absorption peak due to the ester carbonile group.
In the wave number 1540 cm^{-1}, only an absorption peak was appreciated for the calcium resinate corresponding to the stretching of the group

$$\left[\ R\text{-}C\begin{matrix}\nearrow O \\ \searrow O\end{matrix}\ \right]^{1-}$$

characteristic of the salts.

TABLE I

RESINOUS MATERIALS CHARACTERISTICS

	WW rosin	Calcium resinate
Density at 20°C ($g.ml^{-1}$).....	1.08	1.13
Melting point (°C).....	130	137
Acid value.....	147	35

TABLE II

COMPOSITION OF THE COMMERCIAL RED CUPROUS OXIDE

Density ($g.ml^{-1}$).....	6.10
Refraction index.....	2.70
Oil absorption (%).....	8.20
Average particle size (μ m).....	5.40
Cu^{1+} content (Cu_2O, %).....	99.84
Cu^{o} content (%).....	0.03
Cu^{2+} content (CuO, %).....	0.04

TABLE III.- SAMPLE COMPOSITION (g/100 g)*

Paint**.....	1A	2A	3A	4A
Cuprous oxide.....	36.1	34.0	31.9	29.6
Zinc oxide.....	3.6	3.4	3.2	3.0
Calcium carbonate***	36.1	34.0	31.8	29.6
Additives	1.2	1.2	1.2	1.2
Calcium resinate.....	23.0	27.4	31.9	36.6
Chlor.rubber (grade 20).	-	-	-	-
Chlorinated paraffin 42 %	-	-	-	-

Paint**.....	5A	6A	7A	8A	9A	10A
Cuprous oxide.....	36.1	36.1	36.1	34.0	34.0	34.0
Zinc oxide.....	3.6	3.6	3.6	3.4	3.4	3.4
Calcium carbonate***	36.1	36.1	36.1	34.0	34.0	34.0
Additives.....	1.2	1.2	1.2	1.2	1.2	1.2
Calcium resinate.....	13.4	9.5	6.0	16.0	11.3	7.1
Chlor.rubber (grade 20)	6.7	9.5	12.0	8.0	11.3	14.2
Chlorinated paraffin (42%)	2.9	4.0	5.0	3.4	4.8	6.1

Paint**.....	11A	12A	13A	14A	15A	16A
Cuprous oxide.....	31.9	31.9	31.9	29.6	29.6	29.6
Zinc oxide.....	3.2	3.2	3.2	3.0	3.0	3.0
Calcium carbonate***	31.8	31.8	31.8	29.6	29.6	29.6
Additives.....	1.2	1.2	1.2	1.2	1.2	1.2
Calcium resinate.....	18.6	13.1	8.3	21.4	15.1	9.5
Chlor.rubber (grade 20).	9.3	13.1	16.6	10.7	15.1	19.0
Chlorinated paraffin 42 %	4.0	5.7	7.0	4.5	6.4	8.1

* Solvent mixture: Aromasol H/Xilene, 4/1 ratio w/w; viscosity of the binder incorporated to the mill, 8 poise; adjusted final viscosity, 2.5 poise.

** Series A, included in this Table, was formulated with calcium resinate (1A to 16A); in series B (samples 5B to 16B) the mentioned compound was replaced by WW rosin.

*** Natural calcium carbonate: 46.87 CaO (corresponds to 83.57 % of $CaCO_3$).

TABLE IV.- ABIETIC ACID CONTENT IN THE EXPERIMENTAL BINDERS (% by weight)

Paint	Binders just prepared	After dispersion of Cu_2O in the presence of resinous material		After dispersion of Cu_2O in the absence of resinous material	
	Initial	3 h	5 h	3 h	5 h
1A	18.6	14.7	12.2	18.4	18.6
2A	18.6	14.5	11.9	18.8	18.3
3A	18.6	14.3	11.6	18.5	18.1
4A	18.6	14.0	11.2	18.4	18.3
5A	10.9	9.2	8.4	10.8	10.5
6A	7.6	6.6	6.3	7.3	7.2
7A	4.8	4.4	4.3	4.8	4.7
8A	10.9	9.1	8.2	10.9	10.7
9A	7.6	6.5	5.9	7.5	7.5
10A	4.8	4.3	4.2	4.8	4.8
11A	10.9	8.9	8.1	10.8	10.8
12A	7.6	6.4	5.9	7.7	7.6
13A	4.8	4.2	4.1	4.5	4.7
14A	10.9	8.8	7.4	10.9	10.7
15A	7.6	6.3	5.8	7.5	7.7
16A	4.8	4.2	4.0	4.8	4.6
5B	48.4	23.0	11.9	48.2	48.6
6B	34.2	16.8	9.0	34.5	34.0
7B	21.5	11.0	6.2	21.7	21.3
8B	48.4	22.8	11.6	48.2	48.4
9B	34.2	16.4	8.4	34.1	34.4
10B	21.5	10.9	6.0	21.7	21.3
11B	48.4	22.4	11.5	48.3	48.1
12B	34.2	16.4	8.5	34.0	34.2
13B	21.5	10.8	5.8	21.7	21.2
14B	48.4	22.1	10.5	48.3	48.4
15B	34.2	16.1	8.4	34.2	34.5
16B	21.5	10.6	5.8	21.5	21.6

Samples 1A to 16 A, formulated with calcium resinate

Samples 5B to 16B, formulated with WW rosin

TABLE V.- FOULING FIXATION, SAMPLES ELABORATED WITH CALCIUM RESINATE*

	1A	2A	3A	4A	5A	6A	7A	8A	9A	10A	11A	12A	13A	14A	15A	16A
Dispersion of cuprous oxide in the presence of calcium resinate:																
3 h dispersion:																
11 months immersion....	2	0-1	0	0	1	2	3	0	0	2	0	0	1-2	0	0	2-3
26 months immersion....	2-3	0-1	0-1	0	1-2	3	3-4	0	0-1	3	0	0-1	3	0	0-1	3-4
5 h dispersion:																
11 months immersion....	1-2	0-1	0	0	1-2	2	3	0	0-1	2-3	0	0	2-3	0	0	2
26 months immersion....	2-3	1	1	0	2	2-3	3-4	0	1	3	0	0-1	3-4	0	0-1	3
Dispersion of cuprous oxide in the absence of calcium resinate:																
3 h dispersion:																
11 months immersion....	1-2	0-1	0	0	1	1-2	2-3	0	0	2-3	0	0	2	0	0	2
26 months immersion....	3	1	0-1	0	2	2	3	0	0-1	4	0	0-1	3	0	0-1	3
5 h immersion:																
11 months immersion....	2	0	0	0	1	2	2-3	0	0-1	2-3	0	0	2-3	0	0	3
26 months immersion....	3	0-1	0-1	0	2	2-3	3	0	1	3	0	1	3	0	1	3-4

* Key of the Table:

0, panel without fixation; 0-1, very little; 1, little; 2, scarce; 3, regular; 4, abundant; 5, panel completely fouled (values were the average of fouling registers on the front and the back of the panel).

TABLE VI.- FOULING FIXATION, SAMPLES ELABORATED WITH WW ROSIN*

	5B	6B	7B	8B	9B	10B	11B	12B	13B	14B	15B	16B
Dispersion of cuprous oxide in the presence of WW rosin:												
3 h dispersion:												
11 months immersion....	0-1	1-2	3-4	0	0-1	1-2	0	0-1	1-2	0-1	0	3
26 months immersion....	1-2	3	4	0	1	3	0	1	2-3	1	0	3-4
5 h dispersion:												
11 months immersion....	3	4-5	5	1-2	2-3	5	1-2	2	4-5	0-1	2	3-4
26 months immersion....	3-4	5	5	2-3	3-4	5	2-3	3-4	5	1-2	3	5
Dispersion of cuprous oxide in the absence of WW rosin:												
3 h dispersion:												
11 months immersion....	0-1	2	2-3	0	0	1-2	0	0	2	0	0	1-2
26 months immersion....	1-2	2-3	3	0	0	2-3	0-1	0-1	2	0	0-1	2
5 h dispersion:												
11 months immersion....	0-1	2-3	2-3	0	0	0-1	0	0	1-2	0	0	1
26 months immersion....	2	3	3	0	0-1	1-2	0	0-1	2-3	0-1	0-1	2

* Key of the Table:
The same of the Table V.

TABLE VII.- STATISTICAL ANALYSIS

1. SIMULTANEOUS ANALYSIS OF ALL THE EFFECTS

Nature of the effect	Type of effect	Influence on the bioactivity
Composition variables	Type of resinous material	Significant
	Resinous material/chlorinated rubber ratio	Significant
	Binder content	Significant
Elaboration variables	Order of incorporation of the resinous material	Significant
	Dispersion time	Significant

2. SEPARATE ANALYSIS ACCORDING TO THE RESINOUS MATERIAL

Nature of the effect	Type of effect	Influence on the bioactivity
2.1 Calcium resinate:		
Composition variables	Calcium resinate/chlorinated rubber ratio	Significant
	Binder content	Significant
Elaboration variables	Order of incorporation of calcium resinate	No significant
	Dispersion time	No significant
2.2 WW rosin:		
Composition variables	WW rosin/chlorinated rubber ratio	Significant
	Binder content	Significant
Elaboration variables	Order of incorporation of WW rosin	Significant
	Dispersion time	Significant

ADHESION OF BARNACLES AND DEVELOPMENT OF NON-TOXIC ANTIFOULANTS

Elek Lindner*, Carol A. Dooley*, Marca Doeff**

*Naval Ocean Systems Center, **Computer Sciences Corporation

ABSTRACT

The attaching organs of the larval and adult forms of barnacles and the mechanism of their attachment are discussed. Histochemical, chemical and biochemical analyses indicate that the adhesive secretion of the barnacles hardens by quinone crosslinking of protein. The liquid adhesive is estimated to have a surface tension of about 12 dyne/cm. Polymers with critical surface tension less than 10 dyne/cm were synthesized and showed potential antifouling properties.

INTRODUCTION

Over 1000 different species of macroscopic invertebrates have been reported in marine fouling communities. Most of the adult fouling organisms, such as barnacles and tubeworms, are sedentary and permanently attached to the substratum. Consequently most of the adult macroscopic fouling organisms do not perform the initial attachment, rather they maintain and reinforce the attachment established by their microscopic larval forms.

In spite of the fact that the microscopic larval forms do not have enough swimming mobility to counteract strong currents and are carried to their destination by the current, most of them do not settle down on the first available substratum. They must select a location which will provide them with a continuous and adequate food supply, mates for sexual reproduction, and protection from predators, because once settled they can not change the location. This search requires sensory perception in order to identify the desired parameters and a temporary attachment mechanism to be able to leave the site in case it proves to be inadequate. Permanent attachment is made only after a satisfactory site has been located.

In this paper, the temporary attachment and the permanent settlement of the barnacles will be examined and related to the development of non toxic fouling resistant surfaces.

TEMPORARY AND PERMANENT ATTACHMENT OF FOULING ORGANISMS

During site-selection the attaching larval forms of the fouling organisms explore a large area of the substratum to evaluate acceptability. During the exploration period the larvae must maintain their hold on the substratum against water turbulence. If, however, the larva finds the site unacceptable, it should be able to leave the substratum to get into the water column and be carried by currents toward new sites.

Two major forms of temporary attachment are available in an underwater environment: suction apparatus; and secretion of a sticky mucous substance. Relatively fast moving marine organisms, such as octopus, squid, starfish, and sea urchin, use suction devices very successfully. Slower paced gastropods, sea anemones, and tunicates on the other hand, use mucous secretion for their attachment. Crisp (1972) discussed the adhesion by mucous secretion in detail and emphasized the widespread application of this type of attachment by marine organisms.

For permanent settlement those organisms with some mobility in their adult forms, such as sea anemones and tunicates, usually use mucous secretion. Those which settle for life, such as barnacles and tubeworms, use a hardened or cured adhesive cement, sometimes reinforced with calcareous deposits.

THE ATTACHMENT OF BARNACLE LARVAE

The cyprid larva is the attaching form of the barnacle and can be considered as the pupa stage of the Cirripedia (Darwin, 1851, p.19). By kicking its legs, the cyprid can propel itself rapidly through the water, while by means of its antennules, it can fasten itself to and crawl on solid substrata.

Visscher (1928) noted that "when the internal physiological conditions necessary for attachment are present .... the larvae have been observed on many occasion to walk on the substratum apparently hunting a place for attachment. This remarkable performance is accomplished by alternate attachment and release of the adhesive tips of the antennae." This walking or testing process can probably be explained by experiments of Pomerat and Weiss (1946), Weiss (1947), Gregg (1945), Crisp and Meadows (1962, 1963), Knight-Jones (1953), Crisp and Barnes (1954), and Smith (1946, 1948) that demonstrated that cyprids exhibit definite preferences for certain physical or chemical characteristics of the substratum. Darwin (1851, p. 16) observed that the attaching antennular "segment consists of a large, thin, circular, sucking disc. Also, Darwin (1851, pp. 16,33; 1854, p. 117) indicated the presence of a cementing system, suggested that the cement is secreted at the edge of the disc and observed that the antennular disc becomes cemented to

the substratum. Crisp (1967) agreed that the the "first antennae are provided with sucker-like discs" and that the cyprid "pours cement through the sucking discs to provide the initial fixation".

Saroyan, Lindner and Dooley (1968) proposed that the bell-shaped third segment of the antennule with its elastic basis may function as a suction cup. (Fig 1.) The rigid chambers of the second and third segments may be connected and an increase in the volume of the chamber of the second segment could draw in some fluid from the third antennular segment and cause the flexible circular base to be pulled inward creating vacuum.

Nott and Foster (1969) and Nott (1969) studied the internal and surface fine structure of the third antennular segment of the *Balanus balanoides* larva using transmission and scanning electron microscopy. Among the cuticular villi covering the inside of the disk perimeter, they found numerous duct openings some of which they assigned to the cement duct and others to the newly found "antennular glands". Some of these organs may function as chemoreceptors for exploring settling site.

Nott and Foster (1969) felt that the cuticular villi of the attachment disk would be disadvantageous for establishing suction cup seal, although they agreed that a viscous secretion could sufficiently improve it. Instead of the suction mechanism, they proposed that the disk acts as an adhesive pad, utilizing the villi to increase the surface area covered by a sticky secretion from the antennular glands. Measurements indicated that the temporary attachment of the cyprid larva is 2-3 times stronger than simple suction would be (Yule and Crisp 1983). Walker and Yule (1984) found a proteinaceous antennular secretion during the exploratory activity of the larva which may induce settlement of other larvae (Yule and Walker 1985).

In most cases the initial permanent attachment of the barnacle cyprid larva is reinforced by an adhesive cement (Fig. 2). Darwin (1854) and Bernard and Lane (1962) indicated that the adhesive is secreted by a pair of glands located behind the cyprid's compound eyes. These glands are 60-90 microns thick and 150 microns long, ovoid or kidney-shaped structures. Walker (1971) found two different type of cells in the glands. One type of cells produces protein, phenolic compounds and phenolase enzyme, while the other type of cells produces only protein.

CEMENTING APPARATUS OF THE ADULT BALANIDAE

The settled and attached cyprid molts its carapace and body exoskeleton and metamorphoses to its adult form. One day after metamorphosis, the barnacle (*Balanus balanoides*) is capable of producing adhesive material (Yule and Walker 1984). In the

Balanidae, the main channel of the adhesive duct network of the adult begins to grow perpendicular to the rostral-carinal axis, starting from the remains of the second antennular segment toward the perimeter of the basis. In each growing period, new vesicles form on the main channel and become the originating points of the separate duct networks (Fig. 3). Each new vesicle is larger than the former one and each duct network is more complicated than its predecessor. The end of each duct widens and forms a funnel to spread the adhesive in concentric circles around the perimeter under the growing basis. The new vesicles form around the previously existing main channel which extends toward the basis perimeter.

Near the perimeter, the main channel extension rises through the mantle tissue from the vicinity of the basis to just below the epithelium of the mantle cavity. Here, the main channel branches into numerous side channels going into different directions. The side channels connect to giant unicellular adhesive glands often more than 100 microns in diameter. The cytology and histochemistry of the adult barnacle adhesive glands have been the subject of detailed studies (Bocquet-Vedrine 1965; Lacombe 1966, 1967, 1968; Arvy and Lacombe 1968; Arvy, Lacombe, Shimony 1968; Lacombe and Liguori 1969; Walker 1970; Lindner and Dooley 1972; Lindner, Dooley, Clavell 1972). The fine structure of the gland cells is described by Lacombe (1967) and Walker (1970).

The larger the basis of the adult barnacle grows, the more adhesive is needed. In each growing cycle, new adhesive glands develop and join the existing ones and form a cluster on each side of the mantle. The individual glands of the same cluster are connected by channels with the main channel that conducts the secretion toward the basis. In each growing period a new peripheral duct network develops. The main channel connects the glands and the vesicles that are the starting points of the separate adhesive duct networks of different growing periods.

Because of the cyclic growth and molting process the adhesion process must follow the same cycle in order to adhere the newly grown outside perimeter of the basis to the substratum. Fyhn and Costlow (1976) showed that the accumulation of the adhesive gland secretion was at its maximum in the late postecdysis period of the intermolt cycle, decreased to zero during the interecdysis period, and began to increase again during the proecdysis period. This indicates that the adhesion process takes place at about half way between two consecutive moltings. The basis is cemented so firmly to the substratum by an adhesive substance that the shell will usually break when an attempt is made to detach the barnacle, although it is estimated that the tensile strength of the barnacle adhesive is about 1/10 of that of some commercial epoxies (Yule and Walker 1984). The adhesive substance is

secreted at the perimeter of the basis and spreads under it to fill any gap between basis and substratum. Due to the pressures exerted by the barnacle at the basis perimeter by contraction of the muscles connecting the basis and the shell wall plates, the gap to be filled, and hence the thickness of the adhesive layer is usually less than 5 microns.

In crowded communities, however, barnacles may develop abnormally. In such instances, a barnacle can be displaced by the neighboring specimens so that the basis is no longer in contact with the substratum. The gap between the basis and substratum is often filled with a white, opaque substance.

In the laboratory, barnacles were detached intact from smooth test panels and subsequently reattached to other smooth surfaces such as glass microscope slides. These specimens could then be kept alive indefinitely. A white, opaque substance is secreted which spreads between basis and new substratum. If the intervening space between basis and substratum is too large to be filled, thick droplets of secretion appear and hang from the basis (Fig. 4).

We believe that, initially, the adhesive is a fluid of low viscosity and solidifies within a short time after secretion from the duct system. The presence of an occasional duct filled with hardened adhesive suggests that the hardening process is not restricted to the hydrospace outside the duct system and that the adhesive is able to harden in the ducts, but is somehow removed before it can set.

The removal of the adhesive precursors from the ducts before the adhesive becomes cured may be explained by a flushing process (Saroyan, Lindner, Dooley 1969, 1970). The vesicles serve as distributing chambers and that portion of the main channel within the vesicles controls and regulates the flow of adhesive and flushing fluid. The vesicles of different ages are situated near each other and are connected by the main channel. This arrangement puts all the vesicles, the corresponding duct network and the duct ends of every duct network almost equidistant from the adhesive glands. Thus, adhesive can be secreted almost as easily through older ducts as through the newest peripheral duct system. By this mechanism the barnacle is capable of reattaching when detached and repairing damage to the base.

CHEMISTRY OF THE BARNACLE ADHESIVE

Based upon observations on other Crustacea, Yonge (1932) speculated that the secretion of the cement gland of the Cirripedia may be similar to the cuticle; and Thomas (1944) elaborated on this idea by attempting to show that the cement glands of the Cirripedia are modified tegumental glands. When

Pryor's (1940a, b) elucidated a great deal of the hardening mechanism of cuticular protein by introducing the concept of aromatic cross-linkages, several authors (Harris 1946, Pyefinch 1948, Pyefinch and Downing 1949, Knight-Jones and Crisp 1953) speculated that the barnacle adhesive could be "quinone tanned protein" - or more precisely - quinone crosslinked protein. But, with the exception of a few rather sporadic observations on its staining characteristics (Thomas 1944, Bocquet-Vedrine 1965), the adhesive secretion of the barnacles became the subject of chemical characterization only in the past twenty years.

In one of these early attempts, Lacombe (1968) indicated acid mucopolysaccharide in both the intra- and extra-cellular secretion, but Saroyan, Lindner, Dooley and Bleile (1969, 1970) showed the adhesive is proteinaceous, determined its amino acid profile, and reported results that already suggested quinone crosslinking mechanism. The subsequent results of Hillman and Nace (1970), Cook (1970), and Walker (1972), Otness and Medcalf (1972), Barnes and Blackstock (1974), and Walker and Youngson (1975), were in agreement with the proteinaceous nature of the barnacle adhesive. By histoenzymology, Arvy, Lacombe and Shimony (1968) found alkaline phosphatase activity in the cementing apparatus, and Arvy and Lacombe (1968) demonstrated succino-dehydrogenase in young cement glands.

Shimony (1971) thought that the arylsulfatase found in the mantle tissue could be associated with sulphated mucopolysaccharides in the hardening process of the adhesive. Walker (1971), on the other hand, found evidence for phenolase activity and phenolic compounds in the larval cement gland and considered this to be indicative of a quinone crosslinking mechanism for the larval attachment.

With histochemical and analytical methods, Lindner and Dooley (1973) and Lindner, Dooley and Clavell (1972) compiled evidence consistent with the general scheme of a quinone crosslinking of a proteinaceous material for the hardening mechanism of the barnacle adhesive.

$$2\ \text{PROTEIN-NH}_2 + \text{C}_6\text{H}_4\text{O}_2 \rightarrow \text{PROTEIN-NH-(C}_6\text{H}_4\text{O}_2\text{)-NH-PROTEIN}$$

The major arguments in support of this theory are: (1) the bulk of the adhesive consists of protein rich in free amino groups, which are the major functional groups in the quinone crosslinking mechanisms; (2) phenolic precursors and byproducts, such as melanin and stable free radical quinhydrone are present; and (3) most importantly, phenolase enzyme is present in the secretory glands and ducts.

A more thorough study of the mechanism is hampered by the extreme insolubility of the product. Because of these

difficulties, Lindner and Dooley (1973) selected model reactions for elucidation of the quinone crosslinking mechanism and studied its reaction kinetics. In these model studies Dooley (1971, 1973) and Lindner (1971, 1973) reacted p-benzoquinone with amines, amino acids, peptides, and crystalline proteins, and they found that the product of these reactions could be characterized by a strong absorption at 345 nm. Similar reaction products using o-dihydroxyphenol and phenolase enzyme in place of p-benzoquinone produce less intensive absorptions around 325-330 nm. The UV spectra of the mussel byssus and the barnacle adhesive show an absorption at about 325 nm, indicating that these proteinaceous substances are crosslinked by o-quinonoid bridges.

Although the basic principles of quinone crosslinking are relatively well established, namely that the free amino groups of the protein are bound to the quinonoid ring, there are a number of different routes that such a reaction can and probably does take. In the mussel (*Mytilus edulis*), for example, three different types of glands were distinguished, each believed to produce one of the three components involved in the crosslinking: the bulk of the protein, the phenolics, and the enzyme (Brown 1952, Smyth 1954). In the barnacle, however, there is only one type of adhesive gland (Saroyan, Lindner and Dooley 1968), which is believed to produce all the adhesive precursors, but without appreciable quantities of free, extractable phenolic precursors (Lindner and Dooley 1973), therefore autocrosslinking may be involved in the hardening mechanism of the barnacle adhesive. Autocrosslinking occurs between the tyrosyl residues of protein sidechains and free amino or other reactive groups of another protein molecule with the aid of the phenolase enzyme.

$$\text{PROTEIN-CH}_2\text{C}_6\text{H}_4\text{-OH} + \text{NH}_2\text{-PROTEIN} \rightarrow \text{PROTEIN-CH}_2(\text{C}_6\text{H}_3{=}\text{O})\text{-NH-PROTEIN}$$

The fact that in the o-quinone reaction the initial step that produces a monosubstituted derivative has a high limiting rate (Lindner and Dooley 1976) supports the autocrosslinking mechanism, because coupling with only one amino group of another molecule is sufficient to form an intermolecular crosslink.

NON-TOXIC NON-FOULING SURFACES

Most sessile fouling organisms secure their permanent attachment by hardened adhesive. Crosslinking, hardening or curing is an important mechanism to increase the cohesive strength of the adhesive, but the primary criterion for an adhesive is good contact with the adhering surfaces. Adhesion, spreading and wetting characteristics are governed by the surface free energies. The work of adhesion (W_{sl}), the work required to separate the liquid from a solid, is equal to the sum of surface energies the solid and the liquid ($\tau_s + \tau_l$) minus the interfacial

tension between the solid and the liquid (τ_{sl}) (Young 1805):

$$W_{sl} = \tau_s + \tau_l - \tau_{sl} \quad (1)$$

When the adhesion and the self cohesion of the liquid ($W_{ll} = 2\tau_l$) are equal

$$\tau_s - \tau_{sl} = \tau_l \quad (2)$$

When the adhesion is less than the self cohesion of the liquid, the liquid does not spread on the solid and it forms a droplet having a contact angle (θ); the larger the angle the smaller the adhesion

$$\tau_s - \tau_{sl} = \tau_l \cos\theta \quad (3)$$

and

$$W_{sl} = \tau_l (1+\cos\theta) \quad (4)$$

When the adhesion is equal to or larger than the cohesion, the angle is zero and the liquid readily spreads and wets the solid. The surface free energy of the solid τ_s and the interfacial tension τ_{sl} are difficult to determine. From studies on contact angles Zisman and his associates (Fox and Zisman 1952, Zisman 1964) concluded that when the cosine of the contact angles of various liquids on a solid is plotted against the surface tension of the liquids, the value where the contact angle is zero ($\cos\theta = 1$), called the critical surface tension of the solid (τ_c), is relatively easy to calculate and is a fair approximation of the surface free energy of the solid τ_s. By definition

$$\tau_c = \tau_l \quad (5)$$

and only those solids are non-wetting which have lower critical surface tension than the liquid. As an example, water (τ=72.8 dynes/cm) wets glass (τ_c=200 dynes/cm) but not poly-tetrafluoroethylene (PTFE) (τ_c=18 dynes/cm).

It is difficult to obtain liquid adhesive for surface tension measurements because the adhesive of barnacles and mussels harden within minutes after secretion. However, the surface tension of the liquid barnacle adhesive can be estimated from the curvature (radius) of solidified droplets (Fig. 4). The surface tension of the droplet is equal with its weight divided by the radius of the surface area of the end of the tube from which it is falling off (Harkins and Brown 1919):

$$\tau = ((4/3)\pi R^3(D-d)g)/r \quad (6)$$

where R = radius of droplet
D = density of droplet (1.340029, measured by CsCl flotation)
d = density of surrounding medium (sea water 1.025)
g = gravitational constant (980.6 cm/sec²)
r = radius of the tube end

If the surface from which the droplet hangs is larger than the droplet, then R = r and

$$\tau = (4/3)\pi R^2(D-d)g = 11.67 \text{ dyne/cm} \qquad (7)$$

Because the surface tension of the liquid barnacle adhesive is lower than the critical surface tension of PTFE, barnacles attach to it. To prevent barnacle attachment, coatings with surface free energies lower than 12 dyne/cm are needed. Zisman and his coworkers (Hare, Shafrin, Zisman 1954, Zisman 1964) showed that adsorbed monolayers of long chain perfluorinated alcohols have critical surface tensions as low as 6 dyne/cm.

We synthesized polymers with perfluorinated sidechains that have critical surface energies as low as 8.3 dyne/cm. Some of these polymers showed remarkable antifouling properties. After two month exposure, the uncoated surfaces of the panel were heavily fouled, but the circular and small rectangular areas coated with these polymers were not only free of barnacles, but free of algae and slime-film as well (Fig. 5). It is interesting to note that the barnacle population immediately around the coated area is much denser than farther away. This indicates that the barnacle larvae explored the coated area but could not attach and when they reached the edge of coated surface, settled at the first uncoated place where finally they could attach. After three months (Fig. 6) the coated areas were still relatively free of fouling.

CONCLUSION

These experiments clearly demonstrate the feasibility of developing non-toxic low surface energy antifouling coatings. These new antifoulants work because they have a non-wetting low-energy surface which resists the attachment of the organisms. The low surface energy antifoulants release no toxic material into the environment, therefore no environmental hazard is created. While toxic antifoulants are specific against certain types of fouling, the low energy surfaces prevent any kind of attachment and provide universal protection. More importantly, there is no depletion of the active substance in the low surface energy coating; rather its efficiency is based upon a physical surface phenomenon, ensuring long effective life.

REFERENCES

Arvy, L. and D. Lacombe. 1968. Activités enzymatiqus traceuses dans (l' appareil cementaire) des Balanidae (Crustacea, Cirripedia). C. R. Acad. Sci. Paris 267: 1326-1328.

Arvy, L., D. Lacombe and T. Shimony. 1968. Studies on the biology of barnacles; alkaline phosphatase activity histochemically detectable in the cement apparatus of the Balanidae (Crustacea, Cirripedia). Amer. Zool. 8: 817.

Barnes, H. and J. Blackstock. 1974. The biochemical composition of the cement of a pedunculate cirripede. J. Exp. Mar. Biol. Eco. 16: 87-91.

Bernard, F. J. and C. E. Lane. 1962. Early settlement and metamorphosis of the barnacle *Balanus amphitrite* niveus. J. Morphol. 110:19-40.

Bocquet-Védrine, J. 1965. Etude du tégument et de la mue chez le cirripéde opercule *Elminius modestus* Darwin. Arch. Zool. Exp. Gén. 105: 30-76.

Brown, C. H. 1952. Some structural proteins of *Mytilus edulis*. Quart. J. Micr Sci. 93: 487.

Cook, M. Composition of mussel and barnacle deposits at the attachment interface. In: Adhesion in biological systems. pp. 139-150. Ed. by R. S. Manley. New York: Academic Press. 1970.

Crisp, D. J. 1967. Barnacles. Science J. 3: 69-74.

Crisp, D. J. Mechanism of adhesion of fouling organisms. In: Proceedings of the Third International Congress on Marine Corrosion and Fouling. pp. 691-699. Maryland: National Bureau of Standards. 1972.

Crisp, D. J. and J. Barnes. 1954. The orientation and distribution of barnacles at settlement with particular reference to surface contour. J. Anim. Ecol. 26: 142-162.

Crisp, D. J. and P. S. Meadows. 1962. Chemical basis of gregariousness in cirripedes. Proc. Roy. Soc. (London) B156: 500-520.

Crisp, D. J. and P. S. Meadows. 1963. Adsorbed layers; the stimulus to settlement in barnacles. Proc. Roy. Soc. (Londnon) B158: 364-389.

Darwin, C. A monograph on the subclass cirripedia-the Lepadidae. London: Ray Society. 1851.

Darwin, C. A monograph on the subclass cirripedia-the Balanidae. London: Ray Society. 1854.

Dooley, C. A. 1971. Model reactions on the crosslinking of some natural proteins. Presented at the 7th Western Regional Meeting, A. C. S., Anaheim, Ca.

Dooley, C. a. 1973. Studies on the possible reaction mechanisms between quinones and amino compounds. Presented at the 1973 Pacific Conference on Chemistry and Spectroscopy, San Diego, Ca.

Fyhn, U. E. H. and J. D. Costlow, 1976. A histochemical study of the cement secretion during the intermolt cycle in barnacles. Biol. Bull. 150: 47-56.

Gregg, J. H. 1945. Background illumination as a factor in the attachment of barnacle cyprids. Biol. Bull. 88(1): 41-49.

Hare, E.F., E.G. Shafrin, and W.A. Zisman, 1954. Properties of films of adsorbed fluorinated acids. J. Phys. Chem. 58: 236.

Harkins, W. D., Brown, 1919. J. A. C. S. p499.

Harris, J. E. 1946. Report on antifouling research 1942-44. J. Iron Steel Inst. 154: 297-333.

Hillman, R. E. and P. F. Nace. Histochemistry of barnacle cyprid adhesive formation. In: Adhesion in biological systems. pp. 113-139. Ed. by R. S. Manley. New York: Academic Press. 1970.

Knight-Jones, E. W. 1953. Laboratory experiments on the gregariousness during settling in *Balanus balanoides* and other barnacles. J. Exptl. Biol. 30: 584-589.

Knight-Jones, E. W. and D. J. Crisp. 1953. Gregariousness in barnacles in relation to the fouling of ships and to antifouling research. Nature 171: 1109-1110.

Lacombe, D. 1966. Glandulas de cimento e seus canais em *Balanus tintinnabulum* (Cirripedia-Balanidae). Publcoes Inst. Pesq. mar. Rio de Janeiro 32: 1-39.

Lacombe D. 1967. Histoquimica e histofotometria das glandulas de cimento de *Balanus tintinnabulum* (Balanidae-Cirripedia). Publcoes Inst. Pesq. mar.Rio de Janeiro 011: 1-29.

Lacombe, D. 1968. Histologia, histoquimica e ultra estructura das glandulas de cimento e seus canais em *Balanus tintinnabulum*. Publicacao do Instituto de Pesquisas da Marinha No. 017: 1-22

Lacombe,D. and V. R. Liguori. 1969. Comparative histological studies of the cement apparatus of *Lepas anatifera* and *Balanus tintinnabulum*. Biol. Bull. 137: 170-180.

Lindner, E. 1971. Chemical and enzymatic degradation of some natural crosslinked proteins. Presented at the 7th Western Regional Meeting, A. C. S. Anaheim, Ca.

Lindner, E. 1973. Kinetic studies on reactions between quinones and amino compounds. Presented at the 1973 Pacific Conference on Chemistry and Spectroscopy, San Diego, Ca.

Lindner, E. and C. A. Dooley. Chemical bonding in cirriped adhesive. In: Proceedings of the Third International Congress on Marine Corosion and Fouling. pp. 653-673. Maryland: National Bureau of Standards. 1973.

Lindner, E. and C. A. Dooley. Physical and chemical mechanisms of barnacle attachment. In: Proceedings of the third international biodegredation symposium. pp. 456-494. Ed. by J. M. Sharpley and A. M. Kaplan. London :Applied Science Publishers Ltd. 1976.

Lindner, E., C. A. Dooley and C. Clavell. The chemistry of barnacle cement as related to future antifouling techniques. In: Proceedings of the fourth internaval conference on marine corrosion. pp. 358-391. Washington D. C.: Naval Research Lab. 1972.

Nott, J. A. 1969. Settlement of barnacle larvae: surface structure of the antennular attachment disc by scanning electron microscopy. Mar. Biol. 2: 248-251.

Nott, J. A. and B. A. Foster. 1969. On the structure of the antennular attachment organ of the cypris larva of *Balanus balanoides* (L) Phil. Trans. Roy. Soc. B256: 115-134.

Otness, J. S. and D. G. Medcalf. 1972. Chemical and physical characterization of barnacle cement. Comp. Biochem. Physiol. 43B: 443-449.

Pomerat, C. M. and C. M. Weiss. 1946. The influence of texture and composition of surface on the attachment of sedentary marine organisms. Biol. Bull. 91: 57-65.

Pryor, M. G. M. 1940a. On the hardening of the ootheca of *Blatta orientalis*. Proc. Roy. Soc. (London) B128: 378-393.

Pryor, M. G. M. 1940b. On the hardening of the cuticle of insects. Proc. Roy. Soc. (London) B128: 393-407.

Pyefinch, K. A. 1948. Notes on the biology of cirripedes. J. Mar. Biol. Assoc. U. K., 27: 464-503.

Pyefinch, K. A. and F. S. Downing. 1949. Notes on the general biology of *Tubularia larynx* Ellis and Solander. J. Mar. Biol. Assoc. U. K. 28: 21-43.

Saroyan, J. R., E. Lindner and C. A. Dooley. 1968. Attachment mechanism of barnacles. In: Proceedings of the 2nd International Congress on Marine Corrosion and Fouling. pp. 495-512. Athens: Technical Chambers of Greece. 1968.

Saroyan, J. R., E. Lindner, and C. A. Dooley. 1970. Repair and reattachment in the Balanidae as related to their cementing mechanism. Biol. Bull. 139: 333-350.

Saroyan, J. R., E. Lindner, C. A. Dooley, and H. R. Bleile. 1969. Barnacle cement: the key to second generation antifouling coatings. In: Proc. of 158th Meeting A. C. S., Org. Coat. Plast. Chem. 29: 62-82.

Saroyan, J. R., E. Lindner, C. A. Dooley, and H. R. Bleile. 1970. Barnacle cement: the key to second generation antifouling coatings. I. & E. C. Prod. Res. Dev. 9: 122-133.

Shimony, T. B. 1971. Biochemical and histochemical studies of the enzyme arylsulphatase in the mantle of the barnacle *Balanus eburneus*, Gould. Diss. Abstr. 32B: 3788-3789.

Smith, F. D. R. 1946. Effect of water currents upon the attachment and growth of barnacles. Biol. Bull. 90: 51-70.

Smith, F. D. W. 1948. Surface illumination and barnacle attachment. Biol. Bull. 94: 33-39.

Smyth, D. J. 1954. A technique for the demonstration of polyphenol oxidase and its application to egg-shell formation in Helminths and byssus formation in *Mytilus*. Quart. J. Micr. Sci. 95: 139-152.

Thomas, H. J. 1944. Tegumental glands in the Cirripedia Thoracica. Quart. J. Micr. Sci. 84: 257-282.

Visscher, J. P. 1928. Reaction of the cyprid larvae of the barnacles at he time of attachment. Biol. Bull. 54: 327-335.

Walker, G. 1970. The histology, histochemistry and ultrastructure of the cement apparatus of three adult sessile barnacles, *Elminius modestus*, *Balanus balanoides* and *Balanus hameri*. Mar. Biol. 7: 239-248.

Walker, G. 1971. A study of the cement apparatus of the cypris larva of the barnacle *Balanus balanoides*. Mar. Biol. 9: 205-212.

Walker, G. 1972. The biochemical composition of the cement of two barnacle species, *Balanus hameri* and *Balanus crenatus*. J. Mar. Biol. Assoc. U. K. 52: 429-435.

Walker, G., Youngson, A. 1975. The biochemical composition of *Lepas anatifera* (L) cement (Crustacea: Cirripedia). J. Mar. Biol. Assoc. U. K. 55: 703-707.

Walker, G., Yule, A. B. 1984. Temporary adhesion of the barnacle cyprid: the existence of an antennular adhesive secretion. J. Mar. Biol. Assoc. U. K. 64: 679-686

Weiss, C. M. 1947. The effect of illumination and stage of tide on the attachment of barnacle cyprids. Biol. Bull. 93: 240-249.

Yonge, C. M. 1932. On the nature and permeability of chitin. I. The chitin lining the foregut of decapod crustacea and the functionof the tegumental glands. Proc. Roy. Soc. (London) B111: 298-329.

Young, T., 1805. Phil. Trans. Roy. Soc. (London) 95:65

Yule, A. B., Crisp, D. J. 1983. Adhesion of cypris larvae of the barnacle, *Balanus balanoides*, to clean and arthropodin treated surfaces. J. Mar. Biol. Assoc. U. K. 63:261-271.

Yule, A. B., Walker, G. 1984. The adhesion of the barnacle, *Balanus balanoides*, to slate surfaces. J. Mar. Biol. Assoc. U. K. 64:147-156.

Yule, A. B., Walker, G. 1985. Settlement of *Balanus balanoides*: the effect of cyprid antennular secretion. J. Mar. Biol. Assoc. U. K. 65:707-712.

Zisman, W.A., 1964. Relation of the equilibrium contact angle to liquid and solid constitution. In: Contact Angle, Wettability and Adhesion, ACS Advances in Chemistry, No. 43, p. 1-51.

Figure 1. Cyprid antennule.

Figure 2. Cyprid adhesive patch.

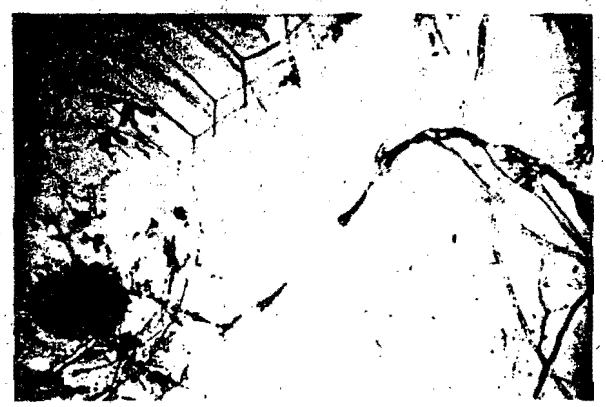

Figure 3. Cementing system of barnacle.

Figure 4. Adhesive droplets on barnacle base.

low surface energy coating

Figure 5. Two months exposure.

Figure 6. Three months exposure.

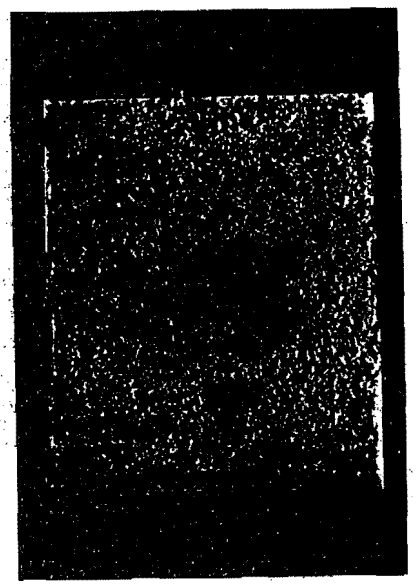

SELECTIVE ACTING ANTIFOULING ADDITIVES

Joachim Lorenz

CIBA-GEIGY MARIENBERG GMBH

D-6140 Bensheim 1
Germany

Comparison of leaching rates of biocides out of antifouling paints and data received in the lab leads to the definition of a minimum killing concentration against algae. Based on this an effective algicide would allow to reduce the amount of metal containing biocides in antifouling paints. Research work with herbicides and fungicides resulted in a triazine which enables protection from algae fouling at low use concentrations. The new product has good environmental compatibility.

Introduction

Observations about unexpected high activity of TBTO to non-target organisms created uncertainty in the ongoing development of antifouling paints. To remember the facts Table 1 presents four figures out of the many available (1).

To draw a consequence from this seems relatively simple for politicians: Prohibition of the use of TBTO - at least for a certain part of antifouling paints. It is by far less simple for ship owners or - more clearly - for the antifouling paint industry. Therefore, this industry tries to develop new antifouling paints away from existing approved formulations. New antifouling paints are required which allow best possible preservation of the maritime environment without loosing the well-known parameters like perfect protection from any kind of fouling, long lasting effectivity, most positive influence on surface quality and safe handling.

Neither a substitute for TBTO nor a new technology is available immediately. The question was raised "Antifouling - how to proceed" (2).

Fundamentals

Two groups of organisms are responsible for fouling: animals and algae. Both cause fouling by following more or less the same process which can be divided in three steps.

1. The free swimming organisms meet by chance any surface by hydrodynamic and electrostatic forces.

2. They excrete a glue and adhere to the surface.

3. They undergo a metamorphosis and develop to adults.

The question arises whether we can influence any of the three steps mentioned.

The most elegant way would be to prevent the first step, the very first attachment. We hardly can influence or change the basic hydrodynamic forces. We only have the possibility of changing the electrostatic conditions of the surface on a ship bottom. Ongoing work looks promising in principle but obviously needs some further polishing and time to come into practical use (3).

The second step is more complex. Algae adhere by an adhesive resulting from various types of glycoproteines or polysaccharides (4) whereas animals like Barnacles adhere by developing a polypeptide (5).

The build-up of an adhesive layer is obviously an enzymatically controlled step. Such a process has to be influenced within seconds or even parts of seconds. As a consequence, an active product preventing the cementation processes has indeed to be the total antifouling paint surface itself. Any transportation of active molecules out of the paint to the surface would be too slow. Furthermore, such a product has to be multi-functional in so far as it has to interrupt different enzymatic processes. All this sounds rather unlikely to our today's knowledge.

Some more time is allowed for an active product to influence the third step. Algae fix between less than 1 hour and a few hours (6). Barnacles need 24 to 48 hours (7). This is the important time interval between first attachment and firm fixation. Chemicals are required which influence this part of the life cycle of the organisms. In other words, we have to continue with products which we are used to call biocides.

While searching for a new and acceptable biocide it would be better to consider first what we know about the traditionally used and proven biocides.

Discussion

Callow (8) published an examination of fouling organisms studied on 34 in-service ships (Table 2).

Obviously the addition of organotin to copper is advantageous with reference to Barnacles and Enteromorpha in contrast to Amphora. This coincides with toxicity data published by Phillip (9) for antifouling toxines (Table 3). These data show an activity of TBT which is about 10 times higher than of Cu_2O.

Table 3 contains another interesting result. If we consider the highest figure to be relevant, both compounds - Cu_2O and TBT - require five times the "antibarnacle concentration" to become effective against algae.

This seems to be supported by leaching rate results from antifouling paints. Phillip (10) reports effectivity of TBTO at a "leaching rate of 0.8 - 1.2 $\mu g/cm^2/day$ as sufficient to prevent the attachment of all marine organisms except diatomes and algae". Naess (11) mentions 1 $\mu g/cm^2/day$ against animals and 2.3 $\mu g/cm^2/day$ against algae spores. Banfield (12) gives a value of 1 and 5 $\mu g/cm^2/day$ against animal and all fouling respectively. This clearly indicates that TBTO has higher activity against animals than against algae.

But this seems not to come out from lab results. For the most important fouling algae, Enteromorpha and Ectocárpus, Skinner (13) reports inhibition concentrations for TBTO of 0.35 and 0.6 ppm respectively. We found in our lab MIC-values for TBTO of 0.1 ppm for Enteromorpha intestinales and 0.5 ppm for Ectocarpus siliculosus.

When we chose in our lab Artemia salina as a model organism for Barnacles we received activity of TBTO at 0.2 - 0.3 ppm. This is quite good compared to Phillip's

0.1 - 1 ppm against Barnacles. Callow (14) received with TBTO values of <0,1 against Elminius modestus.

According to these values the activity against animals and algae should be expected to be in the same range.

The discrepancy between activity experienced from leaching rate and lab tests is simply due to the fact of comparing incomparable values. The 0.2 - 0.3 ppm against Artemia means from the test: Killing of Artemia is obtained after 24 hours at a level of 0.3 ppm TBTO and after 48 hours at a level of 0.2 ppm TBTO. 24 to 48 hours is the time which Barnacles need to fix and develop.

In contrast to that algae need between less than 1 and 5 hours to perform the corresponding steps in their development.

Therefore, a killing concentration for algae has to be found as well. This minimum killing concentration (MKC) has to be defined for a reasonable short time within the maximum of 5 hours of algae fixation and development.

Experimental Work

For the test Enteromorpha plants as such were used. The reason was that settled spores of Enteromorpha are reported to be more resistant than swimming spores (15), that additional attachment is accomplished by the production of large numbers of rhizoidal filaments during erect shoot development in Enteromorpha (16) and that regrowth starting from Enteromorpha plants is heavy (17).

We chose an influence time of 4 hours exposing Enteromorpha to a certain concentration of the product under test. After 4 hours the plant was removed from the test solution, carefully washed with seawater and replaced in fresh seawater containing nutrient for further 6 to 8 weeks. Recovery or dying out after this time was recorded. The received MKC_4 values are given in Table 4.

This table now gives the explanation why against algae fouling a higher amount of the biocide in question is required than for preventing animal fouling. Hence, it supports the findings from leaching rates reported above.

Table 4 is the key to the better enviromental acceptance of antifouling paints as well. If we change our mentality from 'all effects by one product' to a combination of selectively acting products we should be able to reduce the environmental impact drastically. The reduction of copper or TBT is possible without loosing effectivity against the growth of animals. The arising lack of protection against weed growth needs an effective algicide.

"Effective" means a killing activity against algae at a level comparable to that of cuprous oxide or TBTO against Barnacles. If such a product only interrupts photosynthesis it even would be harmless to marine animals.

Without any doubt Enteromorpha is the most important seaweed fouling organism to combat. But it is not the only one. Other chlorophyceae as well as phaeophyceae, diatomes and further algae strains have to be expected.

Therefore, we can expect satisfying application in antifouling only if a product offers activity against the broadest possible spectrum of algae.

To find a suitable algicide and to minimize the amount of work, we tested first the minimum inhibition concentration on an algae agar against the fresh water algae given in Table 5 and in liquid culture against Enteromorpha. 19 products were selected for the test. Most of them are well-known herbicides, some known fungicides. The tested concentration was between 0.03 ppm and 10 ppm for the fresh water algae but for Enteromorpha 0.5 ppm exclusively. The results are given in Table 6.

There are only a few products with a real broad spectrum effectivity at concentrations lower than 10 ppm against the fresh water algae and/or MIC of 0.5 ppm against Enteromorpha. The group of triazines looked particularly promising. Chlorothalonil and the Quinone A 24 were selected for a next series due to the MIC of 0.5 ppm against Enteromorpha, Diuron and the Diphenyl-ether DP 300 in spite of Enteromorpha MIC >5 ppm due to their good broad spectrum against the other algae. To the triazines tested in the first series some more were added for series 2. The results are shown in Table 7.

In addition to the MIC against fresh water algae, the MIC against Enteromorpha was now examined in more detail. The MKC_4 against Enteromorpha was tested at 0.5, 2 and 5 ppm.

The water solubility of the products is also included in Table 7. A long lasting effectivity could not be received from a product with high water solubility. Such a compound would be lost out of the antifouling paint within a short time.

Conclusion

The results given in Table 7 are quite interesting. Inhibition concentration against Enteromorpha is with some products promisingly low. But surprisingly the minimum killing concentration is not at all in parallel. Only two of the products exhibit killing activity against Enteromorpha at concentrations lower than 5 ppm.

The Triazine 1051 was found to be by far the best product. The minimum inhibition concentration against all tested algae is 0.3 ppm or less. This is also the case with further algae strains (Table 8). The killing concentration (4 hours) against Enteromorpha of 0.5 ppm is in the focused range. The water solubility of 7 ppm is a favoured value as well.

Being sucessful from the biological point of view the crucial question after all is the environmental impact which this product might have. The Triazine 1051 is a typical representative of its chemical group. It influences photosynthesis but has no activity against non-photosynthesising organism. Tests with a variety of aquatic organisms were performed. Some of the results are included in Table 9, showing excellent values in comparison to those repeated from Table 1.

Table 9 further includes the figures given already in Table 4. It demonstrates the possibility of reducing the amount of metal containing biocides. They now can be used at the low possible level which prevents animal growth only. The higher concentration required in the past to prevent algae fouling can now be substituted by the low amount of Triazine 1051.

All the work reported was performed only thanks to the assistance of my co-workers, especially Dr. Reinhard Grade, Mrs. Waltraud Pfeifer and Miss Barbara Roose.

Table 1

The effect of tributyltin against some aquatic organisms (1)

Shrimp Larvae	96 h	LC 50	1.5 ppb
Eastern Oyster Larvae	48 h	EC 50	0.9 ppb
Rainbow Trout	96 h	LC 50	6.9 ppb
Daphnia Magna	48 h	LC 50	1.67ppb

Table 2

Incidence of fouling organisms on "in-service" ships* (8)

Organism	Copper+	Organotin/Copper++
Barnacles	8	1
Enteromorpha	11	4
Ectocarpus	5	6
Other macro-algae	5	2
Amphora	5	18
Other diatoms	10	12

*Fouling samples from a total of 34 ships were examined

+ 11 ships ++ 23 ships

Table 3

Comparative toxicity data (9)

Metal Compound	Algae ppm	Barnacles ppm
Cu_2O	1 - 50	1 - 10
R_3SnX	0.01 - 5	0.1 - 1

Table 4

Toxicity data from laboratory test [in ppm]

	Cu	TBTO
Barnacles $MKC_{48/24}$	0.1 - 0.25 (Cu_2O) (14) 0.5 - > 1.0 (CuCl)(14)	0.05 - < 0.1 (14)
Artemia $MKC_{48/24}$	0.3 - 0.5 (Cu_2O)	0.2 - 0.3
Enteromorpha MKC_4	45 (CuCl)	2.0

MKC_4 = Minimum killing concentration after 4 hours exposition

$MKC_{48/24}$ = Minimum killing concentration after 48 and 24 hours respectively

Table 5

Algae strains used for agar incorporation test

a Oscillatoria geminata
b Nostoc ellipsosporum
c Phormidium foreolarum
d Synechococcus leopoliensis (Anacystis nidulans)
e Chlorella vulgaris
f Chlorella protothecoides (Chlorella pyrenoidosa)
g Scenedesmus obliquus
h Klebsormidum subtilissimum (Ulothrix subtilissima)
i Tribonema aequale
k Haematococcus lacustris

Table 6 Minimum Inhibition Concentration (in ppm)

	a	b	c	d	e	f	g	h	i	k	Ent.
Chlorothalonil	1	1	10	0,3	>10	1	10	1	1		0,5
2.4-D	>10	>10	>10	>10	>10	>10	>10	>10	>10	>10	>0,5
Diuron	0,3	0,3	0,1	0,1	3	1	0,3	1	0,3	0,1	>0,5
Propanil	3	3	1	1	10	10	3	3	1	1	>0,5
Alachlor	>10	>10	>10	>10	>10	>10	>10	>10	>10	>10	>0,5
Propachlor	>10	3	>10	>10	>10	>10	>10	>10	>10	3	>0,5
EPTC	>10	>10	1	>10	>10	>10	>10	>10	>10	>10	>0,5
Zineb	10	3	3	3	3	3	3	10	3	3	>0,5
Trifluralin	>10	>10	>10	>10	>10	>10	>10	>10	>10	>10	>0,5
Benzalkonium	1	3	3		1		1	1	1		>0,5
Dichlofluanid	3	3	3	1	3	10	>10	1	3		>0,5
Captan	10	3	10	3	>10	>10	>10	3	3		0,5
Simazine	1	0,3		1	1	>10	>10	1	1		0,5
Atrazine	0,3	0,3	3	3	>10	3	0,3	3	3		0,5
Ametryne	0,3	0,3	3	0,3	3	0,3	0,03	3	0,3		0,5
Terbutryne	0,3	0,3	0,3	0,3	3	0,3	0,03	3	0,3		0,5
Quinone A 24	0,1	0,3	0,3	0,3	1	1	0,3	0,1	1		0,5
Acifluorfen	>10	>10	>10	>10	>10	>10	>10	>10	>10	>10	>0,5
Diphenylether DP 300	0,3	0,3	0,3	0,3	0,3	0,3	0,3	0,3	0,3		>0,5

Table 7

Comparison of Algicides (all values are ppm)

	Minimum Inhibition Conc. (for strains see Table 5)									Enteromorpha		water solub.
	a	b	c	d	e	f	g	h	i	MTC	MKC_4	
 Chlorothalonil	1	1	10	0,3	>10	1	10	1	1	0,5	>5	0,6
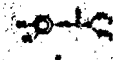 Diuron	0,3	0,3	0,1	0,1	3	1	0,3	1	0,3	>0,5	>5	42
 Quinone A 24	0,1	0,3	0,3	0,3	1	1	0,3	0,1	1	0,05	>5	<100
 Diphenylether DP300	0,3	0,3	0,3	0,3	0,3	0,3	0,3	0,3	0,3	>0,5	5	10
 Simazine	1	0,3	1	1	>30	>30	0,3	1	1	0,5	>5	5
 Atrazine	0,3	0,3	1	3	40	3	0,3	3	3	0,025	>5	33
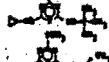 Triazine 1049	0,03	0,03	0,3	0,3	3	0,3	0,03	3	0,03	0,1	5	n.t.
 Ametryne	0,3	0,03	3	0,3	3	0,3	0,03	3	0,3	0,025	5	158
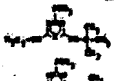 Terbutryne	0,3	0,3	0,3	0,3	3	0,3	0,03	3	0,3	0,025	2-5	58
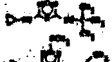 Triazine 1051	0,03	0,03	0,03	0,03	0,3	0,03	0,03	0,3	0,03	0,01	0,5	7
 Triazine 1052	0,03	0,03	0,3	0,03	0,3	0,3	0,03	0,3	0,03	0,025	>5	n.t.
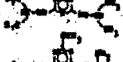 Prometryne	0,3	0,3	>10	3	>10	3	0,3	10	3	0,5	>5	48
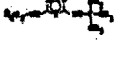 Terbutos	10	0,3	10	3	>10	3	3	3	3	>0,5	>5	130

Table 8

MIC values in ppm of the Triazine 1051

on algae agar		in liquid culture	
Achnanthes	0.3	Achnanthes	0.1
Amphora	0.3	Amphora	0.01
Pinnularia	0.3	Ectocarpus	0.05
		Cladophora	0.1

Table 9

Comparison of metal containing and metal free antifouling biocides

			Cu	TBTO	Triazine 1051
Barnacles $MKC_{48/24}$			0.1 - 0.25 ppm (Cu_2O) (14) 0.5 - >1.0 ppm (CuCl) (14)	0.05 - <0.1 ppm (14)	not active
Artemia $MKC_{48/24}$			0.3 - 0.5 ppm (Cu_2O)	0.2 - 0.3 ppm	not active
Enteromorpha MKC_4			45 ppm (CuCl)	2.0 ppm	0.5 ppm
Shrimp Larvae	96 h	LC 50		1.5 ppb (1)	400 ppb
Eastern Oyster Larvae	48 h	EC 50		0.9 ppb (1)	3200 ppb
Rainbow Trout	96 h	LC 50		6.9 ppb (1)	860 ppb
Daphnia Magna	48 h	LC 50		1.67 ppb (1)	66000 ppb

Bibliography

(1) "Organotin in Antifouling Paints - Environmental considerations" Pollution Paper No. 25, Her Majesty's Stationery Office, London (1986).

(2) Symposium "Antifouling - How to Proceed" TNO Paint Res. Institute (1987).

(3) Furtado, S. E. J., Proc. Symp. "Antifouling - How to Proceed?", TNO Paint Res. Inst. (1987).

(4) Callow, M.E., Pitchers, R.A., Milne, A. in Evans and Hoagland, "Algal Biofouling" Elsevier (1986).

(5) Lindner, E., Dooley, C.A., Proc. 4th Int. Congr. Mar. Corr. and Fouling, 393 (1976).

(6) van London, A.M., Antifouling Symp. 1971, CIBA-GEIGY Marienberg GmbH (1973).

(7) Kühl, H., Proc. 2nd Int. Congr. Mar. Corr. and Fouling, (1968), and personal communication.

(8) Callow, M.E. in Evans and Hoagland, "Algal Biofouling" Elsevier (1986).

(9) Phillip, A.T., Australien OCCA Proceedings and News, 17 (July 1973).

(10) Phillip, A.T., Progr. in Organic Coatings, 2, 159 (1973/74).

(11) Ness,E., NTNF rapport SK. 30.14752 (1983).

(12) Banfield, T.A., JOCCA, 63, 93 (1980).

(13) Skinner, C.E., Antifouling Symposium 1971, CIBA-GEIGY Marienberg GmbH (1973).

(14) Callow, M.E., personal communication

(15) Christie, A.O., Proc. Int. Congr. Mar. Corr. Foul., 3, 674 (1972).

(16) Fletcher, R.L., Proc. 4th Int. Congr. Mar. Corr. and Fouling, 169 (1976).

(17) Moss, B., Marsland, A., Proc. Imas, 10 (1976).

DETERMINATION OF MINIMUM EFFECTIVE RELEASE RATES OF ANTIFOULANTS BY MEMBRANE PERFUSION

ELIZABETH B. GATES AND WILLIAM C. BANTA
THE AMERICAN UNIVERSITY

GEORGE LOEB
DAVID TAYLOR RESEARCH CENTER

ELAINE JOHNSON
La PLATA HIGH SCHOOL

ABSTRACT

Antifouling (AF) coatings prevent biofouling by releasing bioactive compounds over a number of years. Because biocides are also toxic to non-target organisms, environmental damage may result from excessive release rates. Known fluxes of tributyltin (TBT) biocide were released through a microporous membrane in flowing seawater to determine minimum release rates of biocides which will prevent significant growth of a test organism.

INTRODUCTION

Antifouling paints containing tributyltin (TBT) as the active biocide are the most effective coatings to maintain a smooth hull. A large fraction of world shipping uses these paints. Concern over environmental insult resulting from high localized concentrations of this powerful biocide in marinas and harbors has led to state and federal legislation regulating the use of these paints (U.S. Congress, 1987). An EPA method has recently been chosen to limit release rates of AF paints used on large vessels, while use of organotin paints will not be permitted on vessels shorter than 25 meters.

Although it is not known how rapidly TBT must be

released to be effective against foulers, there is evidence that current AF paint release rates are several times higher than necessary to prevent significant fouling (Schatzberg, 1987). It is important to determine the optimum release rate of TBT and other biocides because lower release rates may reduce environmental insult without decreasing the effectiveness of AF coatings.

This paper reports an efficient, inexpensive method to measure the effect of precisely controlled release of a biocide from an inert surface, and to test the response of fouling organisms to that situation without formulating a paint. We varied the flux of TBT biocide to estimate the minimum effective release rate to suppress peritrich protozoan colonization.

MATERIALS AND METHODS

Test cells were made from a modified 47 mm Swin-Lok™ polycarbonate filter holder (Nucleopore, cat.# 420410) by removing the central 4 cm of the filter cap with a grinding tool, converting the cap into a ring. The test surface was a circular polycarbonate membrane, 47 mm in diameter (Nucleopore, 0.2 um pore size, cat.# 111106), held in place by the modified filter holder. The edge of the membrane was sealed with an O-ring in the filter holder, exposing only the central area (41 mm diameter) of the membrane to seawater.

Test cells were suspended in a flowing seawater system (Fig. 1). Seawater pumped from the Severn River Estuary entered from the bottom of an experimental tank at 1-2 L/min, and passed through a baffle system consisting of 1) a 10 cm bed of rock with an average diameter of about 3 cm, 2) a plankton net to direct gas bubbles away from the filters, and 3) a horizontal 30 cm circular plexiglass plate perforated by 30 holes, each 5 mm in diameter. Cells were mounted on an inclined rectangular plexiglass plate provided with slots to hold the test cells. Water entered the bottom of the inner tank, passed through the baffle system, and overflowed. The tank was covered with aluminum foil to reduce algal growth and prevent the possibility of light causing an uneven distribution of organisms in the tank.

A 0.0697 mmolar stock solution of tributyltin chloride (TBTCl) was prepared from the 95% oil by dissolving 0.0161 g TBTCl in 250 ml methyl alcohol. This stock solution was stored in the dark at 4C until use. Test solutions were prepared from the stock solution by serial dilution using filtered (Millipore, 5 um pore size), pasteurized (30 min, 60C) seawater to yield the desired TBT concentrations in a 1% methanol solution. Control solutions were also 1% methanol in filtered pasteurized seawater.

All components of the system contacting TBT

solution were composed of either polycarbonate, fluorinated ethylene propylene (FEP) Teflon, or TBT-saturated glass; these materials do not absorb significant quantities of TBT (Valkirs et al., 1985; and Blair, et al., 1986).

Flux through the filters was controlled by delivering the toxic solution at a constant hydrostatic head through a capillary tube (Accu-Glass, length 2.5 cm; ID, 0.11 mm cat.# 670-451). A constant hydrostatic head was produced by placing the solutions in a 100 ml glass burette in which a Marriott tube was fitted (Fig. 2). Actual flow rates were determined by measuring the volume of solution delivered by the burette.

It was necessary to pasteurize (30 min, 60C) and filter (Millipore 047 000) the seawater used to make up TBT and control solutions to prevent clogging the capillary.

Each experimental run included four flowing test cells containing various concentrations of TBT solution and three controls (two flowing and one non-flowing) containing 1% methanol in seawater. Test cells were exposed approximately 24 hr. After exposure, membranes were fixed 1-7 days in a 5% unbuffered formalin in filtered seawater. They were then stained 5 min in acetocarmine, rinsed with distilled water, placed on a 75 x 50 mm slide with five drops of immersion oil, and dried

2 hr under vacuum at 40C. A 48 x 60 mm #1 coverslip was applied and peritrichs were counted at 100X total magnification.

On each membrane 141 fields (area 1.99 mm^2) were counted (21% of the exposed membrane).

RESULTS

There was no detectable variation in flow rate during runs for test cells whose flows were not interrupted by plugging of the capillary tube. Data from burettes which did not flow properly were discarded.

There was no significant variation in peritrich densities between flowing and non-flowing test cells or between position in the tank (one-way ANOVA, $p < 0.05$, $F(.05[2,13])=0.77$. Counts from still and flowing test cells were therefore lumped.

Salinity during the study period ranged from 8-10 ppt, oxygen concentrations were near saturation, about 6 ml/L, and water temperatures ranged from 6-24C, decreasing throughout the test period. The water in the Annapolis Harbor area contains from <10 to 31 ng/L TBT (Batiuk, 1987), presumably released from antifouling paints on vessels in the area.

Significant biofilms were present on control filters after 21 hours. The predominant organisms in our preparations were species of ciliated peritrich

protozoans: Carchesium sp., Zoothamnium sp., and possibly Pseudocarchesium sp. (Curds et al., 1983). Other organisms including bacteria, protozoans, and a few diatoms were present. Many organisms not irreversibly attached to the substratum were probably lost in preparation of filter membranes for counting. We saw no evidence of significant loss of peritrichs by stalk breakage.

Peritrich densities varied widely on control filters from run to run. Therefore proportional reduction in peritrich densities from controls exposed at the same time is considered the significant quantity in these experiments.

Mean peritrich densities relative to controls versus TBT flux are plotted (Fig. 3). Equations for the estimation of X from Y (inverse prediction) are then applied (Sokal, 1969) to estimate the flux of TBT necessary to reduce peritrich populations by 100%. A 95% confidence interval of $L_1 = 1.83$, $L_2 = 3.08$ about the most probable value of 2.4 $ug/cm^2/day$ is shown.

Fluxes greater than about 3.1 $ug/cm^2/day$ suppressed peritrich growth altogether, and were therefore excluded from the statistical analysis. One extreme point (flux 3.74) did not meet Chauvenet's criterion (Daniels et al., 1949), and was not used in the analysis.

DISCUSSION AND CONCLUSIONS

The membrane perfusion method can be used to deliver known quantities of dissolved bioactive substances independent of other paint components. Using the data obtained in this way can lead to a rapid identification of the optimum quantity of biocides, and may reduce the number of steps needed to formulate a paint.

We estimate that the minimum release rate of TBT alone which is effective in preventing growth of peritrich protozoans is about 2.4 ug/cm^2/day. Release rates of paints in this range would probably only provide marginal control of peritrich colonization. TBT paints are unlikely to be an environmentally acceptable method for controlling resistant slime organisms such as these.

The method may be applied to the quantitative study of any dissolved bioactive compound released from a surface; bioactive compounds can be tested alone or in combination with other biocides. For example, we are now using the method to test various anti-microbial agents for AF activity.

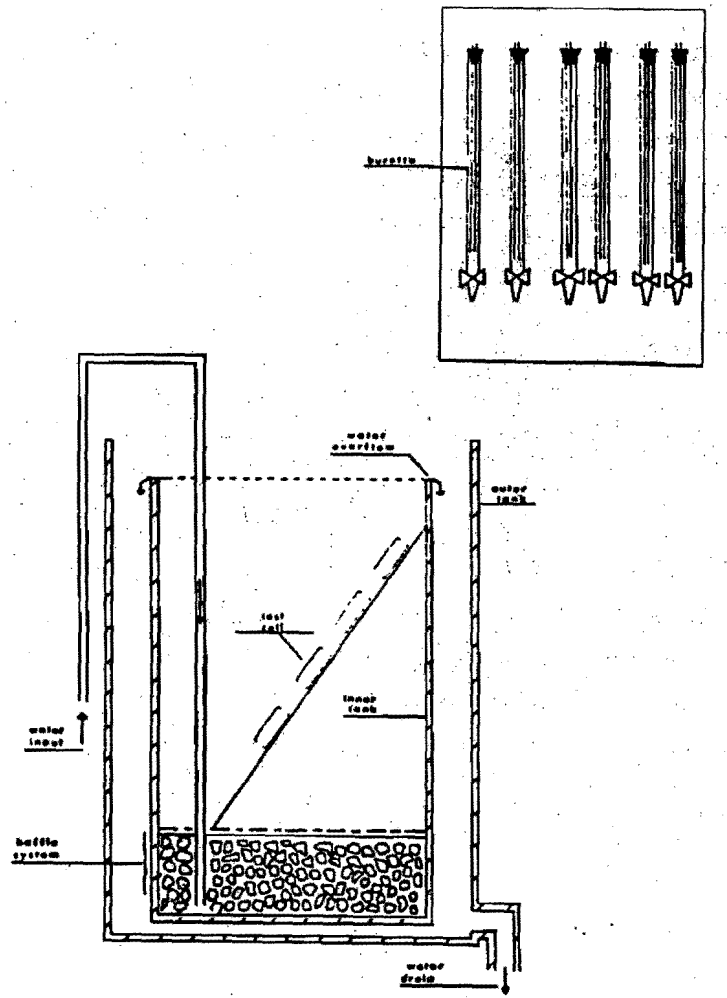

Fig. 1. Diagram of flowing seawater system and burette/test cell delivery system.

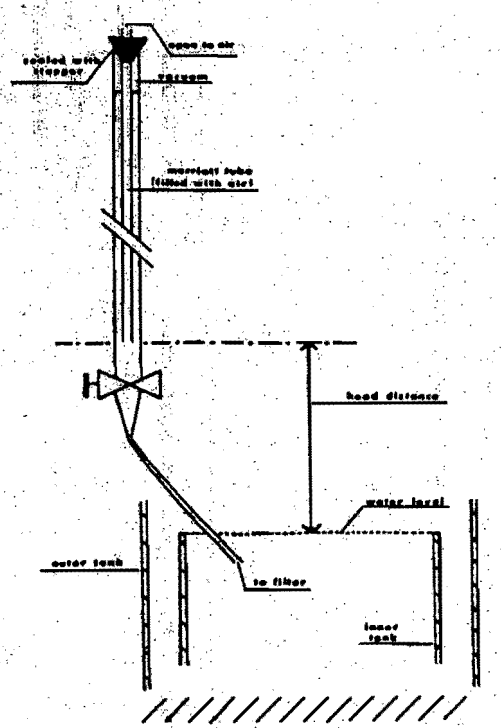

Fig. 2. Marriott bottle. Constant rate of delivery is a function of head distance.

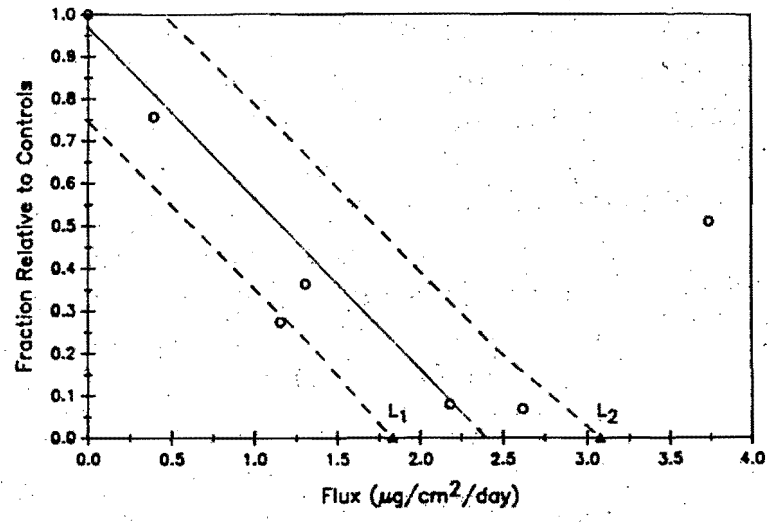

Fig. 3. Peritrich densities (fraction from controls) vs flux (ug/cm^2/day). 95% confidence limits shown by dashed line. L_1 and L_2 indicate limits on the flux axis.

REFERENCE LIST

Batiuk, Richard. 1987. Survey of tributyltin and dibutyltin concentrations at selected harbors in Chesapeake Bay- final report. Washington, D.C.: U.S. Environmental Protection Agency, Office of Pesticides and Toxic Substances. CBP/TRS 14/87.

Blair, W.R., G.J. Olson, and F.E. Brinckman. 1986. An International butyltin measurement methods intercomparison: Sample preparation and results analyses. Gaithersburg, MD: Office of Naval Research, National Bureau of Standards. NBSIR, 86-3321.

Curds, Colin R., A. Michael Gates, and David Roberts. 1983. British and other freshwater ciliated protozoa. Cambridge University Press, London.

Daniels, Farrington, Joseph H. Mathews, John W. Williams, Paul Bender, George W. Murphy, Robert A. Alberty. 1949. Experimental physical chemistry. McGraw-Hill Book Company, Inc., New York, New York.

Schatzberg, Paul. 1987. Organotin antifouling hull paints and the U.S. Navy: A Historical Perspective. In Oceans

'87 Proceedings: Organotin Symposium in Halifax, Canada, September 28- October 1, 1987. by the Marine Technology Society: 5 vols. IEEE, Inc., 1324-1333.

Sokal, Robert R., and F. James Rohlf. 1969. Biometry. San Francisco: W. H. Freeman and Company.

U.S. Congress. Senate. 1987. Organotin antifouling paint control act of 1987. Ammendment of H.R. 2210. 100th Cong., 2nd sess. Congressional record. (18 April), vol. 134, no. 49.

Valkirs, A.O., P.F. Seligman, G. Vafa, P.M. Stang, V. Homer, and S.H. Lieberman. 1985. Speciation of butyltins and methyltins in seawater and marine sediments by hydride derivatization and atomic absorption detection. Naval Ocean Systems Center, Technical Report 1037, San Diego, California.